Department of Chemical Engineering

Faculty of Engineering and the Built Environment

University of Cape Town

THE RELATIONSHIP BETWEEN ENTHALPY OF IMMERSION, AND ITS DERIVED WETTABILITY PARAMETERS, TO FLOTATION RESPONSE

By

Jestos Taguta

2018

A thesis submitted to the University of Cape Town as fulfilment of the requirement for the degree of **Doctor of Philosophy in Chemical Engineering**

CENTRE FOR MINERALS RESEARCH

Declaration

I hereby declare that this thesis is my own work in design and execution and has not been submitted for any degree at any institution. I understand the meaning of plagiarism and all the work in this thesis is my own work, except for the material contained herein that has been duly acknowledged.

Signature: Signed by candidate

Jestos Taguta

Date: 19 October 2018

Acknowledgements

I would like to firstly acknowledge the grace of God that enabled me to finish my doctoral studies. Indeed, the following verse by Apostle Paul applies to me:

"But by the grace of God I am what I am: and his grace which was bestowed upon me was not in vain; but I laboured more abundantly than they all: yet not I, but the grace of God which was with me" 1 Cor 15 vs 10.

Special acknowledgement to my supervisors, Dr Belinda McFadzean and Professor Cyril O'Connor for your support, supervision and guidance throughout my PhD candidature. Your invaluable insight and great expertise made this thesis a success. Thank you for your patience throughout the PhD process.

I would also like to acknowledge the love of my wife, Julieth for being a great friend and pillar of strength to me. You were always there for me, even in difficult times. My beloved sons, Tadiwanaishe, Simbarashe and Jayden, you are such a great blessing and you give me a reason to smile every day.

I dedicate this thesis to my parents, Jealous Simbararashe and Lucia for teaching me to work hard and dream big in life. Thank you very much for your support!

Thanks to the Centre for Minerals Research (CMR) staff, students and colleagues for the support given to me throughout my studies. Indeed, CMR had become a second home to me.

List of Publications and Conferences

1. The relationship between the flotation behaviour of a mineral and its surface energy properties using calorimetry.
   Jestos Taguta, Belinda McFadzean & Cyril O'Connor
   Paper under review, *Minerals Engineering.*
2. The relationship between enthalpy of immersion and flotation response.
   Jestos Taguta, Belinda McFadzean & Cyril O'Connor
   Colloids and Surfaces A: Physicochemical and Engineering Aspects, 558 (2018) 263-270.
3. Investigating the interaction of thiol collectors and collector mixtures with sulphide minerals using thermochemistry and microflotation.
   Jestos Taguta, Belinda McFadzean & Cyril O'Connor
   Minerals Engineering, 119 (2018) 99-104.
4. The effect of alkyl chain length and ligand type on the enthalpy of adsorption and floatability of sulphide minerals.
   Jestos Taguta, Belinda McFadzean & Cyril O'Connor
   Minerals Engineering, 110 (2017) 145-152.
5. Relating the enthalpy of immersion to mineral surface hydrophobicity
   Jestos Taguta, Belinda McFadzean & Cyril O'Connor
   Proceedings of the International Mineral Processing Congress (IMPC 2018), 15-21 September 2018, Moscow, Russia.
6. Design and modification of collectors for sulphide minerals: Computational and experimental study.
   Peace P. Mkhonto, Jestos Taguta, Belinda McFadzean, Xingrong Zhang and Phuti E. Ngoepe
   Proceedings of the International Mineral Processing Congress (IMPC 2018), 15-21 September 2018, Moscow, Russia.
7. The enthalpy of immersion as an indicator of mineral surface wettability
   Jestos Taguta, Belinda McFadzean & Cyril O'Connor
   Proceedings of International Conference on Flotation 2017, November 13-16, Cape Town, South Africa (plus oral presentation).

8. Relating enthalpies of adsorption of thiol collectors and collector mixtures on base metal sulfide minerals to their floatability.
   Jestos Taguta, Belinda McFadzean & Cyril O'Connor
   Proceedings of the XXVIII International Mineral Processing Congress, September 11-15, 2016, Canada (plus oral presentation).
9. The effect of alkyl chain length and ligand type on the enthalpy of adsorption and floatability of sulphide minerals.
   Jestos Taguta, Belinda McFadzean & Cyril O'Connor
   Proceedings of International Conference on Flotation 2015, November 15-19, 2015, Cape Town, South Africa (plus oral presentation).
10. The effect of alkyl chain length and ligand type on the enthalpy of adsorption and floatability of sulphide minerals.
    Jestos Taguta, Belinda McFadzean, Cyril O'Connor
    SAIMM Mineral Processing 15, August 2015, Cape Town, South Africa (plus oral presentation).
11. The thermochemical behaviour of thiol collectors with sulphide minerals.
    Jestos Taguta, Belinda McFadzean, Cyril O'Connor
    SAIMM Mineral Processing 13, August 2014, Cape Town, South Africa (plus oral presentation).

Synopsis

The wettability of mineral surfaces plays an important role in the flotation process. A wettable mineral is hydrophilic while a non-wettable mineral is hydrophobic. In the flotation process, sufficiently hydrophobic particles are collected by rising air bubbles and they report to the concentrate. On the other hand, hydrophilic particles do not attach to the air bubbles and they report to the tailings.

Some of the conventional methods used to characterise mineral surface wettability include contact angle, inverse gas chromatography (iGC), time of flight secondary ion mass spectrometry (ToF-SIMS) and induction time measurements. The measurement of contact angles on flat, smooth and ideal surfaces is relatively simple, straight forward and well-described, but the measurement of powder contact angles is not so straight forward. The iGC technique is a gas phase technique while ToF-SIMS exposes the particles under high vacuum compared to an aqueous environment in real flotation systems. This thesis has investigated the use of the enthalpy of immersion as an indicator of the wettability of mineral surfaces. The enthalpy of immersion is the heat change arising from the replacement of the solid-gas interface with the solid-liquid interface when a solid surface is immersed in a liquid. Although immersion calorimetry has been established as a reliable means of determining the wettability of solid surfaces, it has found only limited applications in flotation research where wettability of mineral ores is a key variable.

In this study, precision solution calorimetry was employed to measure the enthalpies of immersion of different minerals in water. The Washburn method and a microflotation system were used to measure the corresponding powder contact angles and the flotation responses of the same minerals respectively. Two mineral systems were investigated in this study, viz: different pure minerals in their natural form as well as collector-coated sulphide minerals. Furthermore, to assess whether the enthalpy of immersion is able to differentiate between the amounts of minerals of different wettabilities in a mineral mixture, a synthetic ore comprising of different proportions of a sulphide mineral (realgar) and a silicate gangue mineral(albite) was also investigated. The surface energetics of different minerals and the synthetic ore were also characterised by measuring the enthalpies of immersion in different probe liquids

and applying the van Oss-Chaudhury-Good (VOCG) model. The VOCG model is reported to give consistent results in terms of surface energetics of surfaces.

It has been found that the enthalpy of immersion technique was capable of distinguishing differences in the wettabilities of different minerals and these differences were explained in terms of the solid state properties of the minerals. The enthalpy of immersion method was also able to assess the changes in the surface chemical properties of the galena and realgar surfaces resulting from collector adsorption. The magnitude of the enthalpy of immersion was inversely related to the surface coverage of potassium amyl xanthate on both galena and realgar. The enthalpy of immersion measurements correlated well with powder contact angle measurements, but, most importantly, the enthalpy of immersion measurements were found to be more reproducible and sensitive than the contact angle measurements. It has also been shown that the enthalpy of immersion is a more widely applicable measure of the hydrophobicity of mineral particles typical of those used in the flotation process as opposed to the contact angle. It is therefore concluded that the enthalpy of immersion is a superior indicator of the extent to which minerals are hydrophobic or hydrophilic either in their natural form or after treatment with a collector.

Furthermore, it was found that there was a strong inverse relationship between the enthalpy of immersion of the minerals studied and their flotation response. The strong inverse relationship has potential to be used in pulp phase flotation models, although this was not the focus of this thesis. In addition, a value, termed the critical enthalpy of immersion (CEI), was observed above which no flotation occurred. The CEI was in the region of -200 mJ/m^2. At values less exothermic than the CEI, the flotation response was found to be inversely related to the enthalpy of immersion. At values more exothermic, viz. more negative, than the CEI, no flotation occurs. The significance of this finding is that for any mineral whose flotation behaviour is unknown, the measurement of the enthalpy of immersion appears to be able to predict the flotation response of the mineral. The variance in the inverse relationship between enthalpy of immersion and rate of flotation was reduced when the data was normalized with respect to particle density which was the only variable in the flotation studies in terms of particle-bubble encounter efficiency. These results have shown that the

enthalpy of immersion is an excellent indicator of both the natural mineral hydrophobicity and of the extent to which collectors render a mineral hydrophobic.

The relative strength of the acid-base sites was shown to depend on the mineral type. The surface energetics obtained in this study were consistent with the hydrophobic-hydrophilic nature of these minerals. The basic, polar components as well as the total surface energy decreased in the following order: silicates > metallic sulphide minerals and talc. It was observed that the higher the total surface energy, the lower the hydrophobicity of the mineral. The acid-base characteristics of the minerals, measured by solution calorimetry, can give a detailed insight into the surface energies of different mineral types and may be useful in optimising processing strategies. Using the surface energetics, two important parameters were calculated, viz: the interfacial free energy of interaction between mineral particles and bubbles immersed in water *(ΔG_{pwb})* as well as the work of adhesion for water *(W_{adh}).* Interestingly, and not surprisingly, the trends in both of these parameters coincided with the trend in the enthalpies of immersion of the different minerals in water. Critical values of ΔG_{pwb} and W_{adh} parameters in the region of 200 mJ/m² and 320 mJ/m² respectively were observed above which no flotation occurs. At values less than the critical values, both parameters were inversely related to the flotation response.

The enthalpy of immersion was able to differentiate between the amounts of minerals of different wettabilities in a mineral mixture. The enthalpy of immersion became increasingly exothermic as the percentage of albite in the realgar-albite mixtures increased. The experimentally determined enthalpies of immersion in water were in excellent agreement with the weighted enthalpies of immersion for the realgar-albite mixtures. The weighted enthalpies of immersion of the synthetic ore were calculated based on the specific surface areas of both realgar and albite. Therefore, it is possible to calculate the enthalpy of immersion of a synthetic ore (mineral mixtures) from the knowledge of the proportion and the enthalpy of immersion in water of the individual minerals comprising the synthetic ore. The surface energetics of the synthetic ore showed that there is a relationship between the mass recovery and the calculated relative surface polarity, based on the individual polar and total surface energies. As the relative surface polarity increases, there is a significant decrease in the mass

recovery after a relative surface polarity of about 0.4. Thus, the enthalpy of immersion has the potential to be used to predict the wettability and the floatability potential of mineral mixtures. It is proposed that this work should be extended to other mineral mixtures, with careful measurement and calculation of the surface energetics of these mixtures. Thus, this work presents an opportunity for further study to investigate the use of the enthalpy of immersion to characterise the wettability of real ores.

Table of Contents

List of Figures

List of Tables

Nomenclature

h_i	The enthalpy change during immersion process (mJ/m^2)
h_{pred}	Predicted enthalpy of immersion (mJ/m^2)
H	Surface energy or surface enthalpy (mJ/m^2)
U	Internal energy (J)
A	Interfacial surface area (m^2)
V	System volume (m^3)
P	Pressure (Pa)
T	Temperature (K)
ΔG_s	Gibbs free energy of the system (mJ/m^2)
ΔG_{int}	Interfacial energy of interaction (mJ/m^2)
ΔG_{pwb}	Interfacial energy of interaction between particles and bubbles immersed in water (mJ/m^2)
H^T	Total surface energy (mJ/m^2)
H^{LW}	Liftshitz-Van der Waals component of surface energy (mJ/m^2)
H^{AB}	Lewis acid/base component or polar component of surface energy (mJ/m^2)
H^+	Acidic component of the surface energy (mJ/m^2)
H^-	Basic component of the surface energy (mJ/m^2)
W_{adh}	Work of adhesion (mJ/m^2)
K	Hydrophobicity force constant (J)

k	First-order flotation rate constant (min^{-1})
k_{rsp}	Relative surface polarity of a given mineral (%)
Q	Volumetric gas flow rate (m^3/s)
k_a	Attachment rate constant (min^{-1})
E_{coll}	Collection efficiency (fractional)
E_c	Collision efficiency (fractional)
E_a	Attachment efficiency (fractional)
E_d	Detachment efficiency (fractional)
h	Cell height (m)
d_b	Bubble diameter (m)
d_p	Particle diameter (m)
V_R	Reference volume (m^3)
R	Measured terminal recovery (%)
R_{max}	Maximum possible recovery (%)
t	Flotation time (min)
C	Constant of the solid bed structure for Washburn method
SE	Standard deviation of the sampling distribution of the mean

Greek letters

θ	Contact angle induced between a mineral particle and the air bubble (°)
θ_c	Cassie contact angle (°)
η	Viscosity of the liquid (Pa)
Υ	Surface tension (dyne/cm)
μ	Micrometre (= 10^{-6} m)
ρ	Liquid density (kg/m^3)
ρ_p	Mineral or particle density (kg/m^3)
Υ_c	Critical surface tension of wetting of a solid (dyne/cm)

Subscripts

l	Liquid
v	Vapour
s	Solid
sv	Solid-vapour interface
sl	Solid-liquid interface
lv	Liquid-volume interface
s/a	Solid-air interface
s/w	Solid-liquid interface
w/a	Liquid-air interface

Parameters

n, c	Empirical constants

Abbreviations

SIBX	Sodium Isobutyl Xanthate
PAX	Potassium Amyl Xanthate
KCl	Potassium Chloride
CEI	Critical Enthalpy of Immersion
XRD	X-ray Diffraction
XPS	X-ray Photoelectron Spectroscopy
FTIR	Fourier transform infra-red spectroscopy
UV-VIS	Ultraviolet-Visible Spectroscopy
ToF-SIMS	Time of Flight Secondary Ion Mass Spectroscopy
UCT	University of Cape Town
PGM	Platinum Group Minerals
BMS	Base Metal Sulphides
BET	Brunauer–Emmett–Teller (surnames of the authors of the gas adsorption surface area estimation technique).
TL	Test Liquid for Washburn method
PWL	Perfectly Wetting Liquid for Washburn method

CHAPTER 1

1 INTRODUCTION AND LITERATURE REVIEW

1.1 SCOPE OF THESIS

Wettability is one of the most important surface properties of materials. Knowledge of the wetting properties of surfaces is crucial in a number of processes, including:

- The mineral flotation process
- The pharmaceutical industry
- The catalysis industry
- The oil and chemical industry
- Powder technology

A significant amount of research has been conducted to understand the role of hydrophobicity in biological, chemical and physical processes. This thesis will focus on the wettability phenomenon in mineral processing, specifically froth flotation. The wettability of mineral surfaces is a central component in the flotation process. Wettability affects sub-processes in both the pulp and froth phases, namely bubble-particle attachment and froth stability. The separation efficiency is to a large extent controlled by the relative wettabilities of the mineral particles in the pulp zone. A better understanding of the factors which affect the wettability of the mineral surfaces will thus help improve the efficiency of the separation of valuable minerals from gangue.

The scope of this thesis is to characterise the hydrophobicity/wettability of mineral surfaces and correlate this to the floatability of the minerals. The focus is on developing a methodology to characterise the wettability of the mineral surface itself using the enthalpy of immersion and then to determine the extent to which these values are related to various chemical environments such as the presence of surfactants and in turn to their hydrophobicity as indicated by their attachment to bubbles in a relatively quiescent regime typical of a microflotation cell. In the absence of a collector this will determine the natural hydrophobicity but after treatment of minerals with collectors prior to immersion in water the effect collectors have on the wettability can also be studied.

For the development of the methodology, a model system with well-controlled surface properties was used. For this purpose, galena and realgar mineral samples whose surfaces were modified to different degrees of hydrophobicity using a potassium amyl xanthate collector were investigated. Furthermore, different pure minerals (metallic sulphide, elemental, silicate and phyllosilicate minerals) were investigated. For the present purposes, this study focussed on the fundamental study of the surface properties of pure minerals and mixtures of such minerals. It should be emphasised that, although the behaviour of real mineral mixtures is a long-term goal of this research, it is not the central focus of this thesis. The study of mineral mixtures represents a preliminary scoping study since the main focus remains on the single mineral studies. The complex froth flotation process is governed by many inter-related variables such as machine-dependent, operational and chemistry variables. The scope of this work is depicted diagrammatically in Figure 1-1.

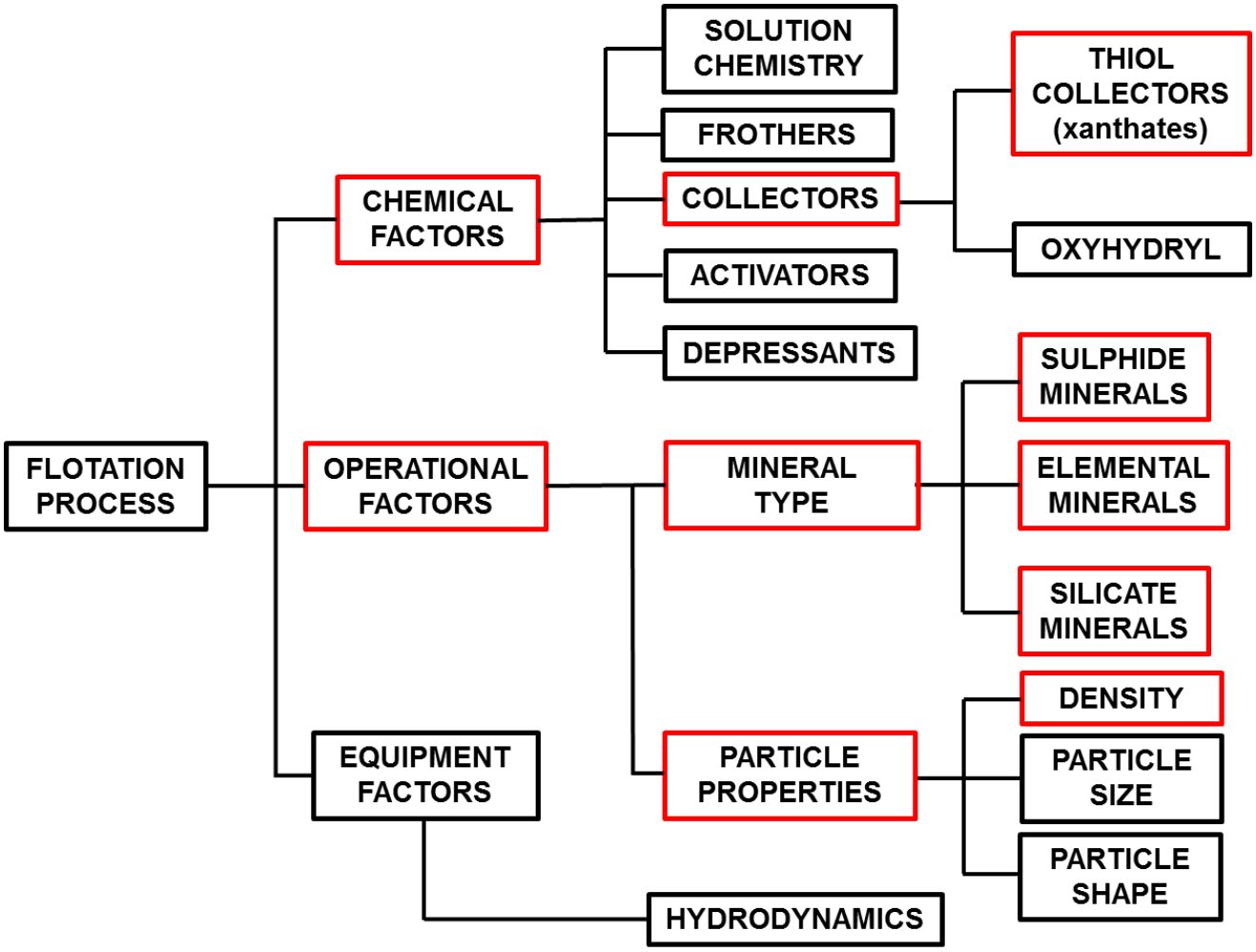

Figure 1-1: Scope of the thesis.

1.2 THEORY OF THE FLOTATION PROCESS

Froth flotation is a complex mineral beneficiation process in which the separation of valuable minerals from gangue is based on wettability differences of the particles in the pulp. Flotation is arguably one of the most important unit operations in the mineral beneficiation chain. In excess of 2000 million tonnes of over 100 different mineral species are recovered annually through the process of flotation. About 400 million tons of sulphide ore is treated annually by flotation processes worldwide (Fuerstenau 2005; Kohad and Mines 1998). The flotation process has been used for more than a century in mineral beneficiation to separate valuable minerals from gangue minerals based on wettability differences of the particles in the pulp.

Froth flotation is a combination of two distinct zones, viz: the pulp and froth zones. Mineral recovery takes place in the pulp zone while separation of the value mineral from gangue mineral takes place in the froth zone. The pulp comprises of particles of different degrees of wettabilities in an agitated slurry. Upon the introduction of air, the partially or incompletely wetted particles attach to air bubbles forming stable particle-bubble agglomerates which rise to the surface and report to the froth phase. In the froth phase, separation is achieved by allowing the drainage of the entrained material back into the pulp zone. The particles that are completely wetted remain in the pulp and report to the tailings. Thus, wettability plays a central role in the flotation process. Hydrophobic particles are required for stable particle-bubble aggregates to be formed. A hydrophilic surface is completely wetted while a hydrophobic surface is at most only partially wetted. The extent of wetting of a flat surface is depicted schematically in Figure 1-2 in terms of contact angles. Thus, hydrophilic surfaces have small contact angles, while hydrophobic surfaces have large contact angles, as shown in Figure 1-2.

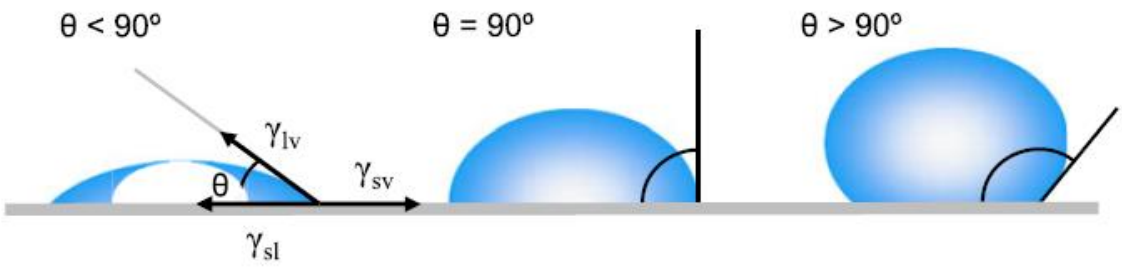

Figure 1-2: A schematic of the extent of wetting of a water droplet on a flat surface (Gharabaghi & Aghazadeh, 2014).

The froth flotation process involves the addition of different chemical reagents such as collectors, depressants and frothers into the flotation cell. These reagents are dispersed using an impeller. Collectors render the valuable mineral surface hydrophobic while depressants suppress the flotation of naturally hydrophobic gangue. Frothers aid in the formation of bubbles and in the stabilisation of the froth. The flotation process is schematically depicted in Figure 1-3.

Particles can be recovered either by true flotation or by entrainment. True flotation is when hydrophobic particles are carried by air bubbles into the froth zone. Thus, true flotation is selective as it only favours the hydrophobic particles. Entrainment is when particles are carried by water into the froth phase. Consequently, entrainment is unselective as it collects even the unwanted gangue mineral particles into the froth phase. Entrainment is undesirable as it increases the recovery of the non-value minerals and hence adversely lowers the concentrate grades. Therefore, the main goal in froth flotation is to maximise true flotation while minimising entrainment.

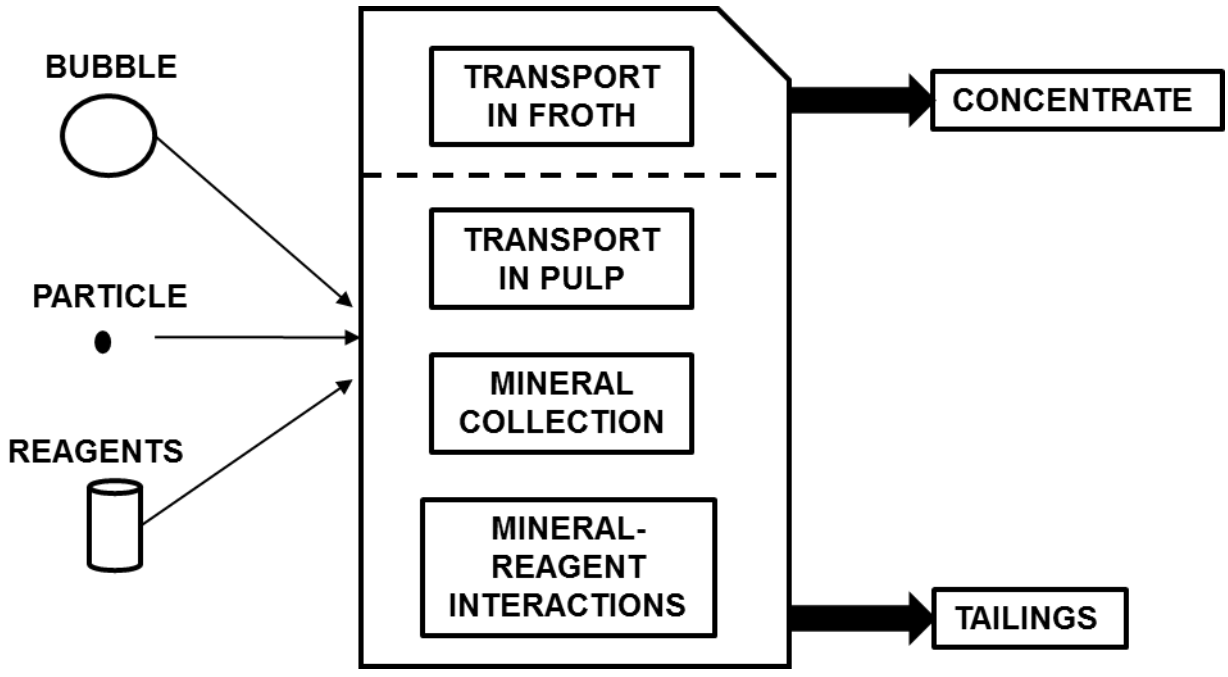

Figure 1-3: Schematic of the process of froth flotation.

1.2.1 Flotation thermodynamics

The thermodynamic criterion for bubble-particle attachment in flotation is given by equation 1-1:

$$\Delta G_s = \Upsilon_{sv} - \Upsilon_{lv} - \Upsilon_{sl} = \Upsilon_{lv}(cos\theta - 1) < 0 \qquad \textit{Equation 1-1}$$

where ΔG_s = the change in the Gibbs free energy of the system (J/m^2);

Υ = the surface tension (Nm^{-1});

θ = the contact angle (°) defined as the angle formed between the mineral surface and the bubble;

s,v,l denote the solid, vapour and liquid phases.

Equation 1-1 gives information on whether the attachment of a particle to a bubble is thermodynamically feasible. The criteria for spontaneous bubble-particle attachment is that the Gibbs free energy change is less than zero ($\Delta G < 0$) and this can only happen when $\theta > 0$ ($\cos\theta < 1$). The more negative the value of ΔG, the greater the probability of bubble-particle attachment and subsequent flotation occurring. Equation 1-1 thus shows that mineral surface hydrophobicity has a very important role in the bubble-particle attachment sub-process. The Gibbs free energy is dependent on the interfacial tensions of the solid, liquid and vapour phase. The interfacial tensions can be manipulated by the addition of collectors into the pulp. Collector adsorption lowers the surface tension of a given mineral surface, thus increasing the contact angle. Therefore, increasing the hydrophobicity (contact angle) of a mineral surface renders the value of ΔG more negative thereby promoting bubble-particle attachment. Flotation thermodynamics is limited in that it is equilibrium based but froth flotation is a dynamic process strongly influenced by many other kinetic parameters which mitigate against bubble-particle attachment.

1.2.2 Flotation kinetics

Flotation thermodynamics provides information on the feasibility of the flotation process without any indication of the rate of the flotation process. According to Rao (1982), the contact angle is an indicator but not a measure of flotation performance. This is because the flotation process is influenced by many other parameters than the thermodynamic criteria. Klimpel (1984) developed a model for computing the first-order flotation rate constant from the recovery-time data using equation 1.2. The basis for the model is that the flotation process is divided into two distinct regimes, viz: a rate-controlled and an equilibrium-controlled process. The constants k and R_{max} are the respective descriptors for these two processes.

$$R = R_{max}(1 - e^{-kt}) \qquad \textit{Equation 1-2}$$

where t = flotation time (min);

k = first-order flotation rate constant (min^{-1});

R = recovery at time t (%);

R_{max} = maximum possible recovery of the mineral at infinite time (%).

The flotation rate constant is a function of many variables as shown in equation 1.3 (Blake & Ralston, 1985a).

$$k = \frac{3Q.E_{coll}.h}{2d_b V_R} \qquad \textit{Equation 1-3}$$

where Q = volumetric gas flow rate;

E_{coll} = collection efficiency;

h = cell height;

d_b = diameter of rising bubble;

V_R = reference volume.

By maintaining the gas flow rate, cell height, bubble diameter and reference volume constant, any change in the first-order flotation rate constant is attributed to the changes in the efficiency of the particle collection process. It is therefore necessary to review the sub-processes affecting the particle collection process.

1.2.3 The sub-processes of flotation

The overall froth flotation process is a combination of many interdependent sub-processes, all of which are required for a mineral particle to report to the flotation concentrate. These sub-processes are collector-mineral interactions, particle collection and particle recovery in the froth phase. This thesis focuses on the first 2 sub-processes taking place in the pulp phase. Because the froth phase, critically important as it is, is outside the scope of this thesis, it is not discussed in detail.

1.2.3.1 Collector-mineral interactions

In most cases, collectors are added into the pulp to render the valuable mineral particles sufficiently hydrophobic. This is a pre-requisite for the formation of stable bubble-particle aggregates.

1.2.3.2 Particle collection

Key sub-processes in the collection of particles by bubbles in the pulp are bubble-particle collision, attachment and detachment (Dai et al., 1998; Duan et al, 2003). These sub-processes are schematically depicted in Figure 1-4.

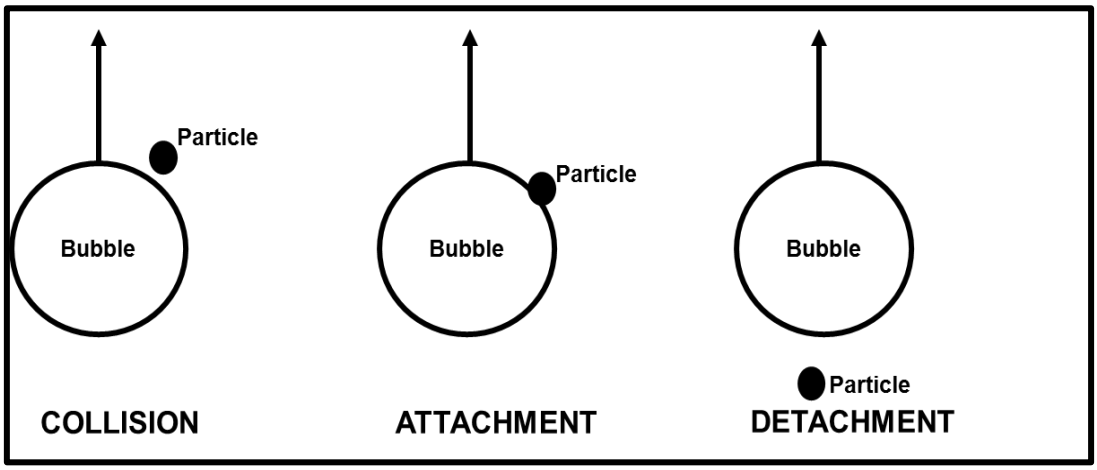

Figure 1-4: Schematic of the sub-processes of particle collection by a bubble in the pulp phase.

1.2.3.2.1 Bubble-particle collision

Collision between a mineral particle and an air bubble is obviously essential in the flotation process as it is a precursor to particle-bubble attachment. Factors affecting collision include particle and bubble size, particle momentum, etc.

1.2.3.2.2 Bubble-particle attachment

After collision, subsequent attachment of the particle and bubble takes place. Thinning and rupturing of the thin film separating the colliding bubble and particle is a requirement for bubble-particle attachment to occur. Not all the particles colliding with the bubble result in flotation as some particles might not have sufficient hydrophobicity to form stable bubble-particle aggregates.

1.2.3.2.3 Bubble-particle detachment

The particle may get detached from the bubble due to considerable disruptive, turbulent forces in the pulp. Detachment is dominant in turbulent systems due to the presence of external shear forces.

1.2.3.3 Particle recovery in the froth phase

This involves the transport of particles from the pulp phase into the froth phase. As mentioned earlier, true flotation and entrainment are responsible for the recovery of particles into the froth phase. There is also the possibility of particles elutriating back into the pulp phase.

1.2.4 Mathematical description of the flotation process

The efficiency of particle collection by air bubbles, called collection efficiency, E_{coll}, is a product of the efficiencies of the three sub-processes according to equation 1-4 (Dooby & Finch, 1987; Ralston, 1999):

$$E_{coll} = E_c . E_a . E_d \qquad \textit{Equation 1-4}$$

where E_c = the collision efficiency;

E_a = the attachment efficiency;

E_d = the detachment efficiency.

Collision efficiency is defined as the ratio of the number of particles encountering a bubble to the number of particles approaching the bubble in a flow tube of equivalent diameter. It is controlled by hydrodynamic forces in the flotation systems e.g. bubble size, superficial gas rate, energy input.

Attachment efficiency is defined as the fraction of the particles colliding with the bubble that remain attached to it. It is controlled by mineral surface hydrophobicity as well as the hydrodynamic forces.

Detachment efficiency is defined as the fraction of attached particles detaching from the bubbles. It is controlled by the hydrodynamic forces in the pulp as well as the mineral surface hydrophobicity (stability of the particle-bubble aggregates).

1.2.5 Flotation in quiescent system

A quiescent system is characterised by very low energy input and consequently low external stresses. A microflotation system is an example of a quiescent system. The low particle velocity in a quiescent system ensures negligible hydrodynamic interaction such that the effect of surface forces can be investigated. Detachment is assumed negligible (thus E_d = 1) in a quiescent system and the collection efficiency may be expressed using equation 1-5:

$$E_{coll} = E_c . E_a \qquad \text{Equation 1-5}$$

Equation 1-5 implies that all particles colliding and attaching to bubbles will report to the concentrate in a quiescent system.

If hydrodynamic factors and particle properties (size, shape and density) are maintained constant, the collision efficiency, E_c is constant. Thus, any changes in flotation response are attributed to changes in mineral surface hydrophobicity in the case of a single mineral (with constant particle density). In the case of different mineral types, the effect of particle density on particle-bubble interaction must be considered (Section 1.3.4).

1.3 FACTORS AFFECTING THE FLOTATION PROCESS

The factors affecting the flotation process can be divided into three groups namely, chemistry, operational and machine related factors as depicted diagrammatically in Figure 1-5. These factors are so inter-related that careful experimental design is required to investigate the effect of any particular component.

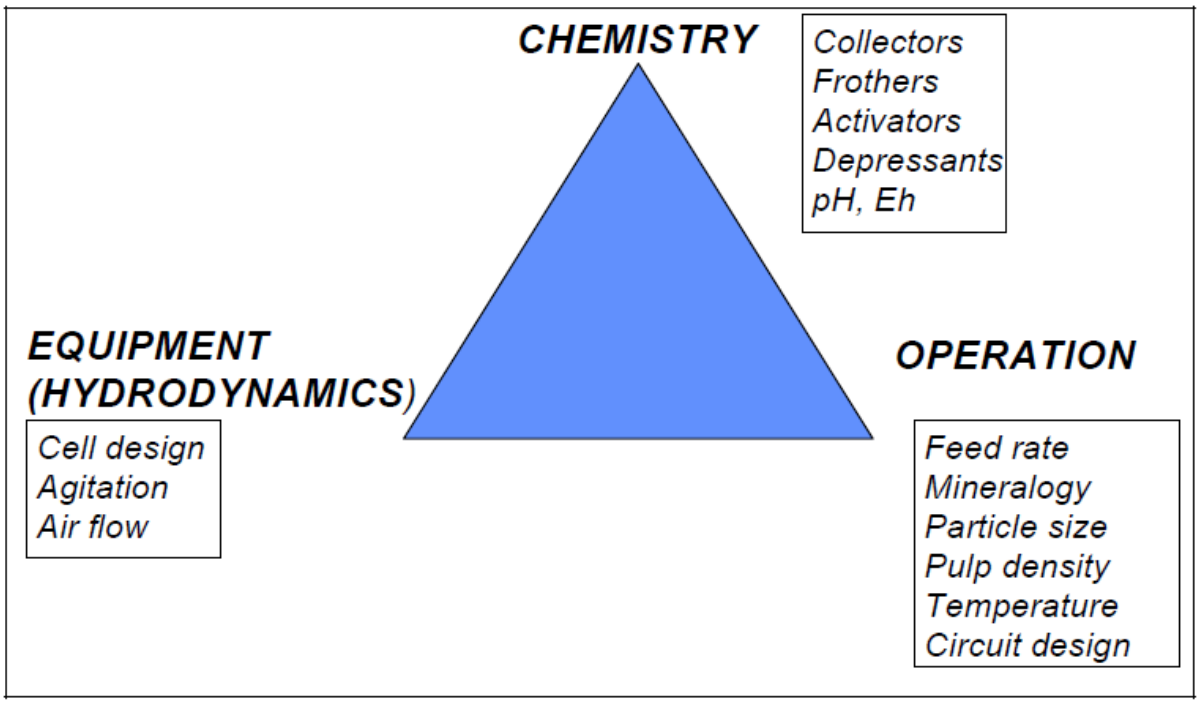

Figure 1-5: Triangular representation of the factors affecting the flotation process (Klimpel, 1984).

Although the machine related factors are important in the flotation process, they are beyond the focus of this thesis and are therefore not discussed in detail.

Hydrophobicity may be natural (inherent) and is thus dependent on the crystal structure of the mineral (Gaudin, 1957). This thesis has investigated the use of the enthalpy of immersion as a surface characterisation tool to determine mineral surface hydrophobicity / wettability. The wettability of different minerals as indicated by the enthalpy of immersion values were related to hydrophobicity as indicated by the extent of particle-bubble interaction in a quiescent system typical of a microflotation cell. While the enthalpy of immersion is driven by surface forces only, particle-bubble interaction is driven by both surface forces and particle density in a quiescent system. The fact that different minerals have different densities makes particle density an important parameter in this investigation. Therefore, this investigation focussed on two factors, viz: mineral type and particle density. Hydrophobicity may also be conferred onto a mineral surface using a collector. Therefore, with regards to chemistry factors, the hydrophobicity of mineral samples treated using xanthate collectors was also investigated. Due to the focus of this thesis, the effects of mineral type, hydrophobicity and particle density on froth flotation will be extensively discussed in the following sections.

1.3.1 The natural hydrophobicity/hydrophilicity of minerals

Minerals are classified into 2 groups, viz: non-polar and polar minerals according to their surface characteristics (Wills and Napier-Munn, 2006). The non-polar minerals have covalently bonded molecules held together by weak van der Waals forces which do not readily interact with water. Thus, such minerals are naturally or inherently hydrophobic and they cannot be completely wetted by water. Examples of the naturally hydrophobic minerals include graphite, diamond, sulphur, molybdenite, stibnite, realgar, orpiment, talc, coals, etc. These minerals can be floated naturally without any surface treatment such as using flotation collectors. On the other hand, the polar minerals have strong ionic bonding which make them readily interact with water. Examples of the hydrophilic minerals are the oxides and the silicate minerals. Thus such minerals are hydrophilic and require surface treatment before they can be floated. Gaudin (1957) also classified minerals according to their crystalline structures. The crystalline structure dictates the surface characteristics and ultimately the wetting behaviour of the minerals as discussed in Section 1.3.1.1.

The natural hydrophobicity can either be conserved or disrupted during comminution depending on which bonds are ruptured during cleavage. When cleavage occurs by rupturing of the interatomic bonds, the resultant surface is strongly hydrated by polar water molecules. This gives rise to some degree of hydrophilicity in the mineral. On the other hand, when cleavage occurs by the rupturing of the bonds between the groups of atoms (weak van der Waals bonds), the resultant surface is predominantly hydrophobic and is not easily wetted by water. Oxidation of these naturally hydrophobic minerals introduces oxygen to the mineral surface. Oxygen readily interacts with water via hydrogen bonding, thus oxidation induces hydrophilicity onto the naturally hydrophobic minerals.

Ozcan (1992) also classified minerals according to their critical surface tension, γ_c. The critical surface tension of wetting, γ_c is defined as that value of surface tension below which liquid wets the surface completely by spreading spontaneously. The lower the critical surface tension, the more hydrophobic the mineral is. On the contrary, the higher the critical surface tension, the more hydrophilic the mineral is. The minerals were classified as follows:

a) Naturally hydrophobic minerals with $26 \leq \gamma_c < 35$ dyne/cm. These minerals include sulphur, talc, graphite, orpiment and realgar and can be floated without a flotation collector;
b) Moderately hydrophobic minerals with $35 \leq \gamma_c < 49$ dyne/cm. These minerals include galena, sphalerite, chalcocite, chalcopyrite and stibnite;
c) Hydrophilic minerals with $\gamma_c = 72$ dyne/cm. These minerals cannot be floated without collectors. These minerals include apatite, calcite, fluorite and highly oxidised coal.

The reason for the natural floatability of sulphide minerals has also been widely researched. The formation of elemental sulphur at the surface, which is classified as being naturally hydrophobic, is generally accepted as the reason for the natural floatability of sulphide minerals. Gardner and Woods (1979) using electrochemical measurements, confirmed that elemental sulphur was responsible for the natural hydrophobicity of sulphide minerals. This was substantiated by Yoon and Luttrell (1984) who detected the presence of elemental sulphur on sulphide mineral surfaces

using spectrometric methods. Furthermore, Acres (2010) in a synchrotron study has in fact shown that there is elemental sulphur present on chalcopyrite .

1.3.1.1 Effect of mineral type on wettability

The wettability of minerals depends on the nature of the mineral and its crystalline structure (Gaudin, 1957). This thesis has investigated different mineral types, viz: metallic sulphides, elemental, silicate and phyllosilicate minerals. The apparent relationship between crystal structures and wettability of the different minerals is briefly discussed in the following section.

1.3.1.1.1 Metallic sulphide minerals

The metallic sulphide minerals investigated in this thesis are galena, realgar and orpiment.

a) Galena (PbS_2)

Galena has a cubic, rock-salt type structure with Pb^{2+} and S^{2-} ions in the place of Na and Cl^- ions respectively. It has a co-ordination number of 6. Its crystal structure is shown in Figure 1-6. The bonding in galena is predominantly covalent. The covalent molecules in galena are held together by van der Waals forces. It is therefore expected that galena does not readily interact with water. Galena has been classified as a moderately hydrophobic mineral (Ozcan, 1992; Wills and Napier-Munn, 2006).

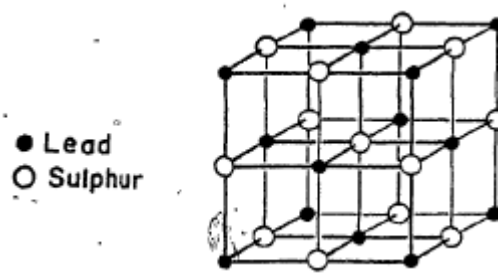

Figure 1-6: Crystal structure of galena (Kelebek, 1984).

b) Realgar (As_4S_4)

Realgar consists of puckered ring molecules (As_4S_4) in which four sulphur and four arsenic atoms are bound together by covalent bonds. Its crystal structure is shown in Figure 1-7. The ring molecules are held together by weak van der Waals forces and thus minimal interaction is expected between realgar and water. Realgar has been

classified as a naturally hydrophobic mineral which is floatable without a collector (Ozcan, 1992).

Figure 1-7: Crystal structure of realgar (Kelebek, 1984).

c) Orpiment (As_2S_3)

Orpiment consists superimposed As_2S_3 layers in which each arsenic atom is bonded to three sulphur atoms and each sulphur atom is bonded to two arsenic atoms. Its crystal structure is shown in Figure 1-8. The layers are held together in weak van der Waals forces. Thus, minimal interaction is expected between orpiment and water. Similar to realgar, orpiment has been classified as a naturally hydrophobic mineral which is floatable without a collector (Ozcan, 1992).

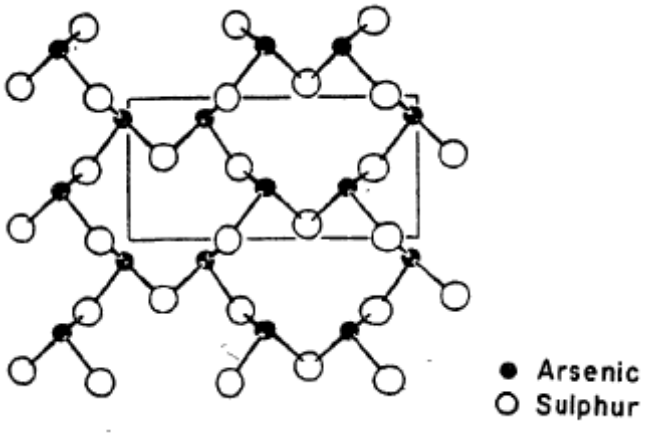

Figure 1-8: Crystal structure of orpiment (Kelebek, 1984).

1.3.1.1.2 Elemental minerals

Graphite is the only elemental mineral investigated in this study.

a) Graphite (C)

Graphite is one of the allotropes of carbon in which each carbon atom is covalently bonded to three other carbon atoms and these atoms are arranged in hexagonal layers that can slide past one another. Its crystal structure is shown in Figure 1-9. Each layer

is considered as a giant molecule and the layers are held together only by weak van der Waals forces. Therefore, graphite is expected not to readily interact with water. Graphite is also reported to be hydrophobic (Morcos, 1970). However, it must be noted that chances are high that graphite can oxidise during grinding and this may result in a lower than expected enthalpy of immersion in water.

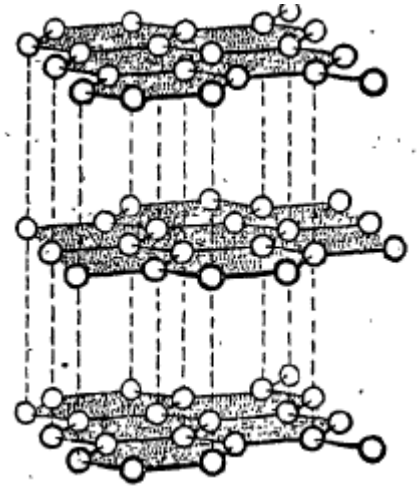

Figure 1-9: Crystal structure of graphite (Kelebek, 1984).

1.3.1.1.3 Phyllosilicate minerals

a) Talc ($3MgO.4SiO_2.H_2O$)

Talc is a 2:1 layered silicate mineral with a structure of an octahedral layer (brucite or gibbsite layer) sandwiched by two silica tetrahedral layers as shown in Figure 1-10. As a result, talc is an anisotropic mineral comprising of edges and basal cleavage planes. The two silica tetrahedral layers have negative charges and the octahedral gibbsite layer has a neutralising positive charge. Thus talc comprises of sheets which are electrically neutral and van der Waals forces hold the trilayer sheets together. There is no tetrahedral substitution of silicon by aluminiun or magnesium which could affect the polarity of the talc. Because of the low substitution and low polarity, talc is naturally hydrophobic (Yan et al., 2011; Yin et al., 2012). Therefore talc is expected to have minimal interaction with water. Furthermore, talc has been classified as a naturally hydrophobic mineral (Ozcan, 1992).

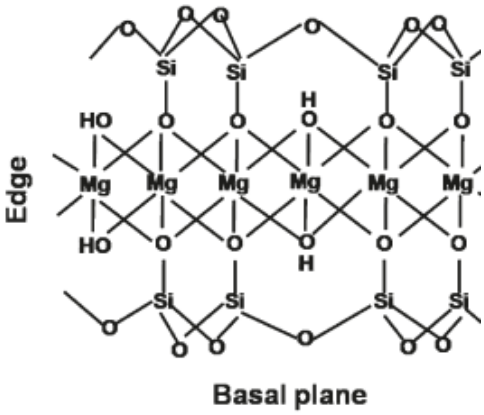

Figure 1-10: Crystal structure of talc (Yan et al., 2011).

1.3.1.1.4 Silicate minerals

The silicate minerals investigated in this study are mica, albite and wollastonite.

a) Mica

The structure of mica is similar to that of talc and its crystal structure is shown in Figure 1-11. The only difference is that unlike talc, mica undergoes various degrees of lattice substitution whereby Al^{3+} substitute for the Si^{4+} in the tetrahedral layers. Consequently, the tetrahedral layer carries a negative charge which is usually neutralised by potassium ions. However, the ion exchange capacity of mica is low as the potassium ions are fixed. When mica is cleaved during grinding, it is assumed that the surface carries a constant negative charge the magnitude of which depends on the degree of lattice substitution (Yin et al., 2012). It follows that mica sheets are held together by ionic inter-layer bonds which readily interact with water. Freshly cleaved mica was reported to be hydrophilic, having a contact angle of 10° (Bryant et al, 2006).

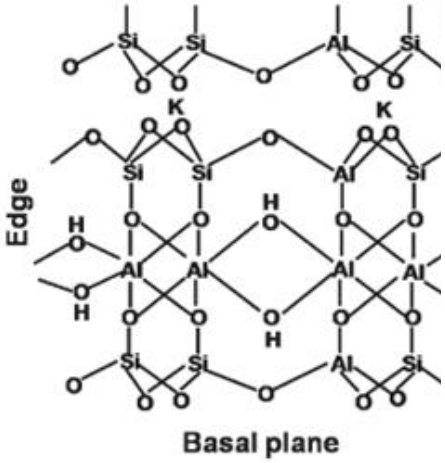

Figure 1-11: Crystal structure of mica (Yan et al., 2011).

b) Wollastonite ($CaSiO_3$)

Wollastonite is a natural calcium meta-silicate in which the Si-O tetrahedra group into chains. Prabhakar et al, (2005) investigated the dissolution of wollastonite by monitoring the changes of pH with time when wollstonite is conditioned in water and their results are depicted diagrammatically in Figure 1-12. Dissolution tests showed that slurry pH changes quickly in the initial stages before reaching equilibrium at pH 9.5 within a minute, irrespective of the initial solution pH. Prabhakar et al, (2005) observed that dissolution was more pronounced for finer size fractions.

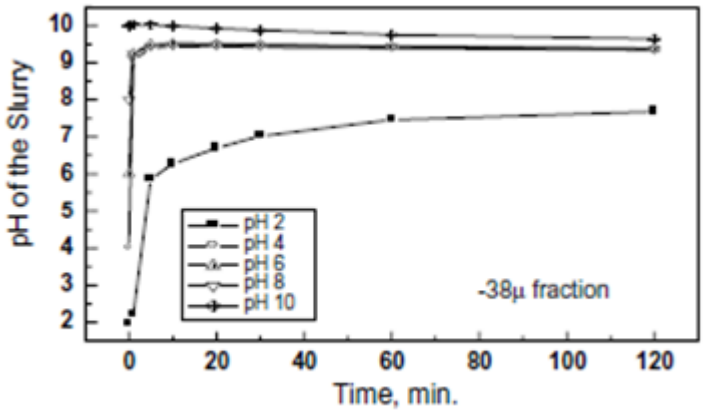

Figure 1-12: Changes in pH of the slurry with time when wollastonite is conditioned in water (Prabhakar et al, 2005).

The same phenomenon was observed by other researchers (Bailey & Reesman, 1971; Rimstidt & Dove, 1986). This was attributed to the exchange of protons from the

aqeous media with calcium ions on the wollastonite surface. To substantiate this, Prabhakar et al (2005) went further to conduct a chemical analysis of filtrate to quantify the relative amounts of Ca^{2+} and Si^{4+} released into the solution. Their results are summarised in Table 1-1.

Table 1-1: Chemical analyses of filtrate at pH 8 for the -38 µm size fraction.

Time (min)	Ca (mg/L)	Si (mg/L)
5	4.16	0.763
10	4.97	1.030
20	5.24	1.290
30	5.43	1.560
60	6.16	2.380
120	7.59	4.24

The rate of the release of calcium was found to be higher than that of silicon, thus wollastonite undergoes incongruent dissolution. Calcium dissolution leaves behind a negative lattice and active SiOH and SiO^- sites. Auger electron spectroscopic analysis has shown that the exposed atoms on the cleavage surfaces of wollastonite are mainly Si and O and few calcium atoms. The resultant silica rich surface readilly interacts strongly with water. This is consistent with the result that natural wollastonite was found to have a contact angle of 11° (Hou et al., 2013).

c) Albite, $4(Na(AlSi_3O_8))$ and Diopside, $4(Ca(Mg,Fe^{2+})AlFe^{3+}Ti(Si,Al)_2O_6$

Albite and diopside are chain silicate minerals in which the Si-O tetrahedra group into chains. Albite was reported to undergo incongruent initial dissolution (Chou and Wollast, 1984; Blum and Lagasa, 1991; Wollast and Chou, 1992; Shmulovich et al, 2001). The same behaviour was observed for diopside (Shmulovich et al, 2001). Similar to wollastonite, incongruent dissolution leaves behind a silica-rich surface which is hydrophilic. Therefore, both albite and diopside are expected to readily interact with water.

1.3.1.2 Partial ionic character of covalent bonds

Although the metal-sulphur bonds in the sulphide minerals are predominantly covalent, the bonds also have some intrinsic partial ionic character. This is attributed to the

differences in the electronegativity between the sulphur and the various metal atoms in the sulphide minerals. The unequal sharing of electrons polarises the metal-sulphur bond thereby inducing a certain degree of ionic character. This partial ionic character has an effect on the wettability of the sulphide minerals with the extent of wettability depending on the magnitude of the difference in the electronegativity between the sulphur and the metallic atom. According to Pauling (1960) the partial ionic character of a single bond between atoms A and B with electronegativities X_A and X_B respectively is estimated by equation 1-6.

$$Partial\ ionic\ charge = 1 - e^{-0.25(X_A - X_B)^2} \qquad \textit{Equation 1-6}$$

Using the electronegativity values from Pauling (1960) and equation 1-6, the percentage partial ionic character of the sulphide minerals investigated in this study are shown in Table 1-2.

Table 1-2: The percentage of partial ionic character of the covalent bonds of minerals investigated in this study.

Bond	Magnitude of (X_A-X_B)	Partial Ionic Character (%)
As-S	0.05	6.1
Pb-S	0.7	11.5
C-C	0	0
Si-O	1.7	51.4

The effect of the differences in the metallic ion on the percentage partial ionic character of the different sulphide minerals is clearly evident from Table 1-2. The partial ionic character of the Pb-S bond in galena is twice that of the As-S bond in arsenic sulphides. Therefore, galena is expected to be more wettable than the arsenic sulphides. This is consistent with Ozcan (1992) who concluded that realgar and orpiment are more hydrophobic than galena. The elemental graphite has no partial ionic charge and thus is expected to have no interaction with water. However, chances of oxidation are high during the grinding. The oxidation products may cause the graphite to have some interaction with water. The degree of interaction depends on the degree of oxidation. The Si-O bond in the silicate minerals has a very high partial ionic character compared to the metal-sulphur bonds in sulphide minerals. Therefore,

silicate minerals are expected to interact more readily with water compared to the sulphide minerals. It is generally accepted that the silicate minerals are hydrophilic.

1.3.2 Induced hydrophobicity

Collectors are added into the pulp to render the valuable mineral surface hydrophobic. A collector is a hetero-polar reagent comprising of the polar reactive group and the non-polar hydrocarbon chain. The polar reactive head group reacts with the mineral surface and the non-polar hydrocarbon chain imparts hydrophobicity, as shown in Figure 1-13.

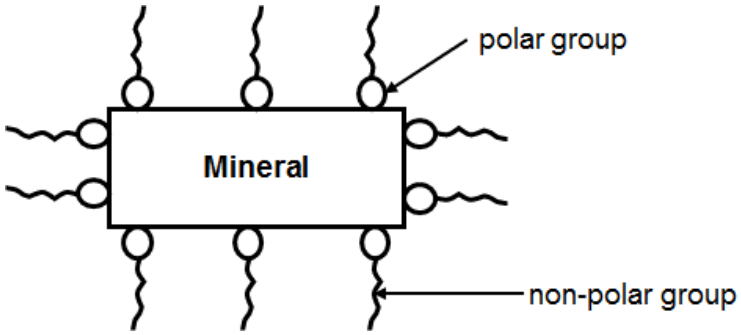

Figure 1-13: Schematic of collector adsorption on a mineral surface (Wills and Napier-Munn 2006).

Collectors have been shown to increase the contact angle of mineral surfaces (Wark and Wark 1932). It has been established that the longer the alkyl chain length, the stronger the induced hydrophobicity (Wark and Wark, 1932; Rao, 1982; Ackerman et al., 1987; Fuerstenau, 2005; Taguta et al, 2017). Thiol collectors are extensively used in the flotation of base metal sulphides (BMS) and the platinum group minerals (PGM). The most common thiol collectors are the xanthates, dithiocarbamates and the dithiophosphates. The interaction between sulphide minerals and thiol collectors is reported to follow a mixed potential model (Alison et al. 1972; Finkelstein and Goold 1972; Rao 1982). Sulphide minerals being semi-conductors, catalyse the anodic oxidation of thiol collector anions. The anodic oxidation of the collector is coupled with the cathodic reduction of dissolved oxygen in the pulp. This thesis was particularly interested in hydrophobicity, either natural or induced, and a detailed description of the mechanisms whereby thiol collectors interact with sulphide minerals was outside the scope of this study.

1.3.3 The role of particle hydrophobicity on flotation

1.3.3.1 Effect of particle hydrophobicity on the pulp phase

1.3.3.1.1 Flotation response

Mineral surface hydrophobicity is central to the sub-process of bubble-particle attachment in flotation. The collector surface coverage and contact angle have been used as a conventional measure and indicator of hydrophobicity (Wark and Wark, 1932; Rao, 1982; Prestidge and Ralston, 1996; Prestidge and Ralston, 1996; Bulatovic, 2007). Many researchers have investigated the effect of hydrophobicity on the flotation response of different minerals. Blake & Ralston (1985), in their study of the interrelationship between particle size, surface coverage and flotation response for methylated quartz system, found that for a given particle size, a critical surface coverage of a hydrophobising agent is required before flotation occurs. Their results are depicted diagrammatically in Figure 1-14.

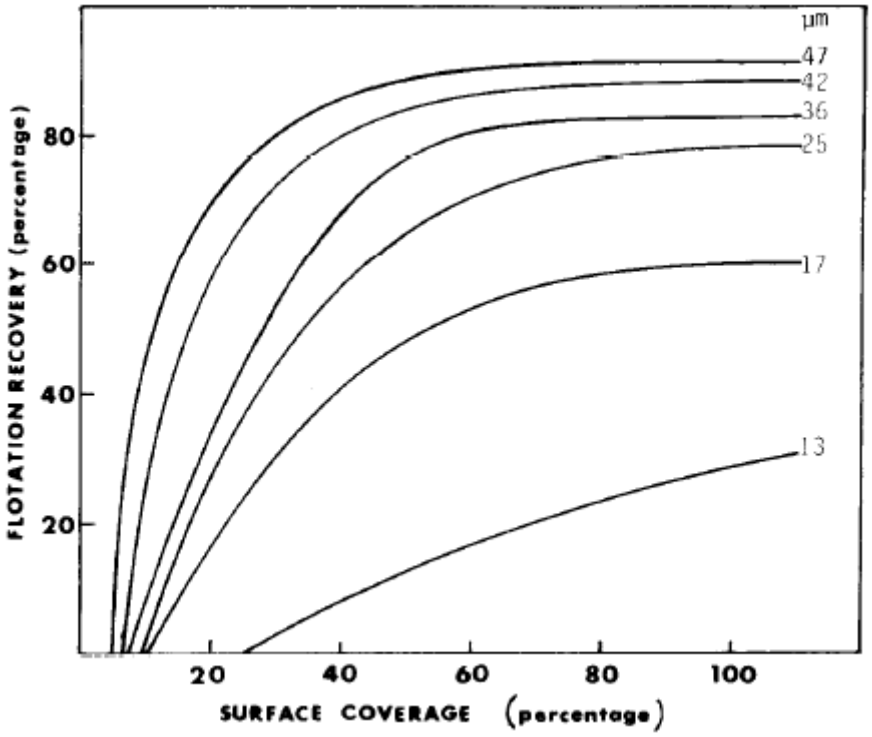

Figure 1-14: The flotation recovery of quartz as a function of the surface coverage of trimethylsilyl groups for different particle sizes (Blake & Ralston, 1985a).

The same conclusion was made by Crawford & Ralston (1988). Similarly, Prestidge & Ralston (1996), in their study of the effect of particle size and collector surface coverage on contact angle and floatability, concluded that the contact angle and floatability are influenced by particle hydrophobicity as quantified by surface coverage

of a collector. They also found that for any particular size range of galena particles, there is a critical contact angle above which the flotation response significantly increases.

1.3.3.1.2 Attachment efficiency

The increase in flotation response with increasing particle hydrophobicity (contact angle) can be attributed to increased attachment efficiency. Shi et al. (2014), using atomic force microscopy observed that bare, hydrophilic mica particles showed no interaction with air bubbles in water. However, hydrophobised mica particles showed interaction with air bubbles. Dai et al (1999) found that attachment efficiency increases as particle contact angle increases. Their results are depicted in Figure 1-15.

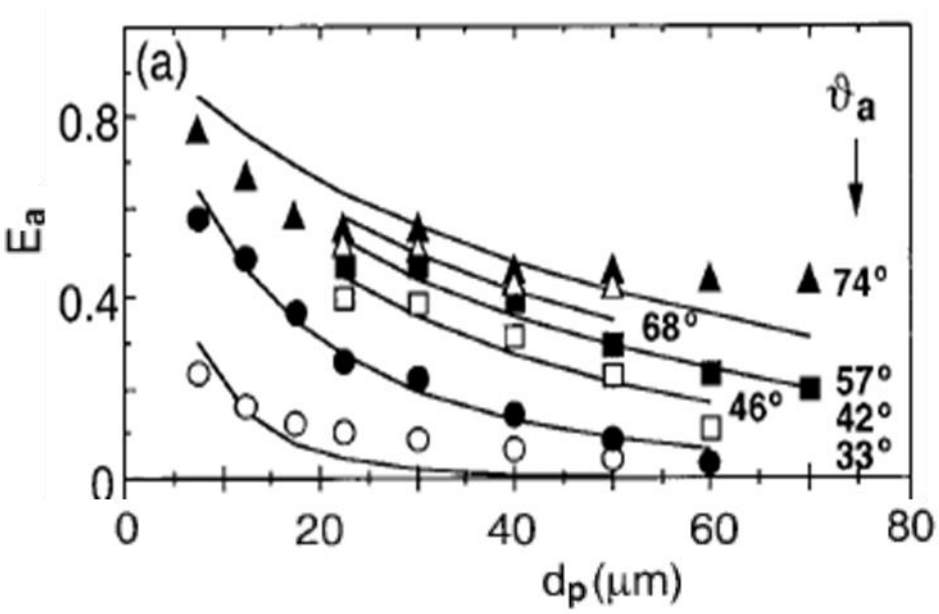

Figure 1-15: Variation of the attachment efficiency as a function of particle size and particle contact angle (Dai et al, 1999).

It is clear from Figure 1-15 that for a given particle size, an increase in particle contact angle results in a corresponding increase in attachment efficiency. Hewitt et al (1995) also reported similar findings. The increase in attachment efficiency with increasing particle hydrophobicity can be attributed to increased hydrophobic forces of attraction between the particle and the bubble as well as reduced induction time.

1.3.3.1.3 Nanobubbles and hydrophobic interactions

According to the extended Derjaguin, Landau, Verwey, and Overbeek (DLVO) theory, there are three surface forces in froth flotation which are important to the adhesion of

a particle to an air bubble, viz: the electrostatic forces, the van der Waals and the hydrophobic forces. Electrostatic forces are so weak that the particle can easily get detached from the bubble. Furthermore, bubble-particle adhesion is only possible if the particle and the bubble are oppositely charged. However, in many flotation systems the particle and bubble are both negatively charged. The particle and bubble repel one another. As a result, the electrostatic forces are not the ones responsible for the rupturing of the wetting film. Similarly to electrostatic forces, the van der Waals forces are repulsive in wetting films (Laskowski & Kitchener, 1969) and thus cannot be responsible for bubble-particle adhesion. The attraction between the negatively charged particle and bubble in flotation systems has been attributed to two phenomena, viz: the occurrence of nanobubbles and the hydrophobic force. Nanobubbles are small gas layers that form on hydrophobic surfaces and are several tens of nanometres thick (Ralston et al, 2001; Mishchuk et al, 2002; Krasowska et al, 2009; Zhang et al., 2009; Hammer et al., 2010; Peng et al, 2013). Several researchers assert that these nanobubbles are necessary for the formation of a bubble-particle aggregate in flotation cells (Nguyen et al., 2003; Schubert, 2005; Zhang et al., 2009; Peng et al, 2013). However, it is argued that even in the absence of nanobubbles, attraction between a particle and a bubble still occurs through the hydrophobic force. The hydrophobic force is widely accepted as the one that is responsible for the rupturing of the wetting film in the flotation process (Laskowski & Kitchener, 1969; Yoon & Mao, 1996; Ralston et al, 2001; Li & Yoon, 2013). The hydrophobic forces were found to be strongly attractive (Rabinovich & Yoon, 1994). The hydrophobic forces of attraction and the subsequent adhesion between hydrophobic particles have been shown to increase with the contact angle of mineral particles (Rabinovich and Yoon, 1994; Fielden et al, 1996; Yoon and Mao, 1996; Yoon, 2000). The effect of the advancing contact angle on the hydrophobic force constant, K is shown in Figure 1-16. The hydrophobic force constant, K is a constant representing the magnitude of the hydrophobic force in a wetting film. The more hydrophobic a mineral particle is, the greater its ability to destabilise the wetting film and consequently the more stable the particle-bubble aggregate.

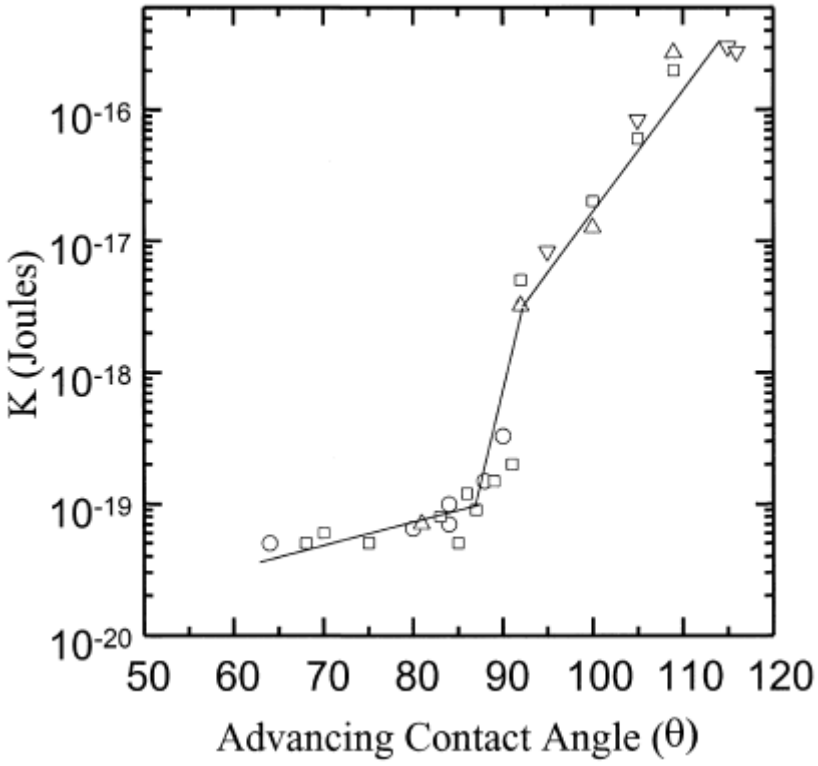

Figure 1-16: Variation of the hydrophobic force constant with advancing contact angle (Yoon, 2000).

1.3.3.1.4 Effect of collector addition on the hydrophobic force

Collectors are chemical reagents added into the pulp to render the valuable mineral surface hydrophobic. Pan et al (2012) investigated the role of collector on the kinetics of wetting film thinning for pure untreated gold and for gold treated with a xanthate collector. They concluded that the collector not only improves the kinetics of film thinning but also destabilises the films so that they can rupture expeditiously forming bubble-particle aggregates. They went further to conclude that the collector creates the hydrophobic force that can overcome the repulsive van der Waals and electrostatic forces present in wetting films. A similar finding was made by Xing et al (2017). Wang et al (2013) measured the surface forces between gold surfaces treated with a xanthate collector using atomic force microscopy. They observed that both the contact angle and the hydrophobic force increased with increasing collector concentration (that is increasing hydrophobicity).

1.3.3.1.5 Induction time

The induction time, defined as the time taken for the liquid film separating the bubble from the particle to thin, rupture and form the three phase line of contact, is strongly dependent on mineral surface hydrophobicity (Yoon, 2000). Yoon and Yordan (1991) found that the induction time decreases with increasing collector concentration for the quartz-amine system at pH 6 and their results are depicted diagrammatically in Figure 1-17.

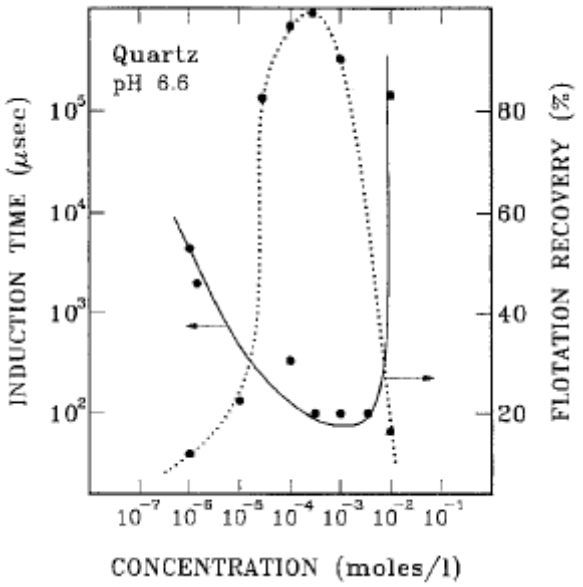

Figure 1-17: Effect of amine (collector) concentration on induction time and the flotation recovery of quartz at pH 6.6 (Yoon & Yordan, 1991).

This was attributed to increasing adsorption density of collector at the quartz surface with increasing collector concentration, rendering the quartz surface increasingly hydrophobic. Increasingly hydrophobic particles destabilise the wetting film separating the particle from the bubble, thus promoting bubble-particle interaction. It is also clear from Figure 1-17 that the induction time and the flotation recovery are inversely related, that is, the lower the induction time the higher the flotation recoveries. Similarly, Dai et al (1999) found that the induction time decreases with an increase in particle contact angle. The same observations were made by Krasowska et al (2006) on teflon studies as well as Crawford and Ralston (1988) for the methylated quartz system.

1.3.3.2 Effect of hydrophobicity on the froth phase

It was found that increasing the hydrophobicity of particles increased both the flow rate of particles entering the froth as well as recovery of particles across the froth for contact angles up to 63° (Schwarz & Grano, 2005). Schwarz & Grano (2005), in their investigation on the effect of hydrophobicity on particle and water transport across a flotation froth, concluded that there exists a critical contact angle, dependent on particle size and shape, above which there is reduction in particle recovery in the froth phase. This is attributed to significant bubble coalescence within the froth phase, reducing the bubble surface area and translating to a decrease in the froth carrying capacity. Ata et al. (2002) concluded that the collection of particles in the froth phase is influenced by particle hydrophobicity as well as the surface area available for attachment in the froth. Similarly, Ata et al. (2003) concluded that maximum froth stability is attained when froth contains particles with moderate hydrophobicity. The presence of strongly hydrophobic particles result in rapid bubble coalescence compared to the case of moderately hydrophobic particles while the presence of weakly hydrophobic particles resulted in the slowest bubble coalescence (Ata et al, 2003). The same finding was reinforced by Johansson & Pugh (1992) who found that strongly hydrophobic particles destabilised the froth while hydrophilic particles did not have an effect on the froth properties. In summary, these researchers agree that particle hydrophobicity has a significant influence on the behaviour of the froth phase. As mentioned earlier, the froth phase factors are outside the scope of this thesis.

1.3.4 Effect of particle density on flotation

Particle density has been reported to have a significant effect on the floatability of minerals, with an influence on both the collision and attachment efficiencies (Sutherland, 1948; Pyke et al, 2003; Shi and Fornasiero, 2003; Pyke, 2004; Nguyen et al, 2006; Nguyen and Nguyen, 2009; Safari and Deglon, 2018). Pyke (2004) concluded that an increase in particle density results in an increase in the first-order flotation rate constant with his results shown in Figure 1-18.

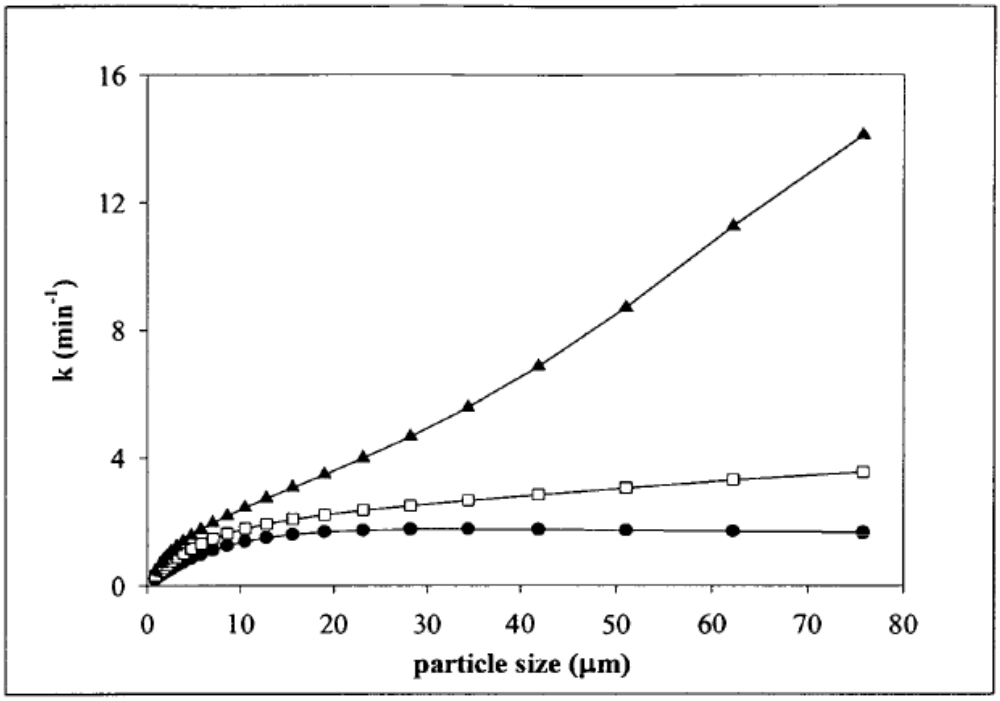

Figure 1-18: Effect of density on the calculated flotation rate constant at constant contact angle of 60° (constant hydrodynamic factors). Dots – 2.65 g/cm^3; Squares – 4.1 g/cm^3; Triangles – 7.4 g/cm^3 (Pyke, 2004).

The increased flotation rate constants were attributed to increased collision and attachment efficiencies due to increased momentum as density increases. The effect of particle density on the collision and attachment efficiency is summarised in Figure 1-18.

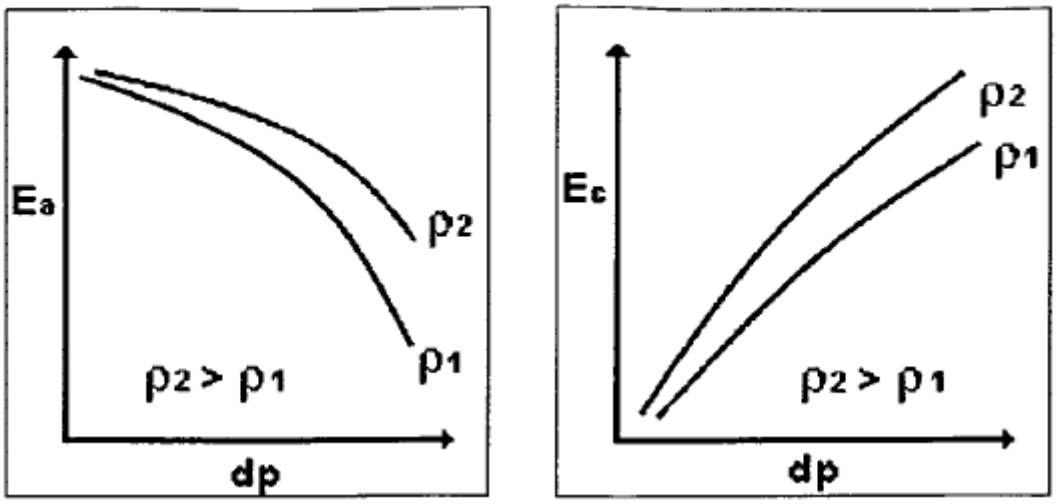

Figure 1-19: Effect of density on collision and attachment efficiency (Pyke, 2004).

With increasing particle density and a corresponding increase in inertial forces, the inertial deposition of a particle onto a bubble becomes increasingly stronger leading to increased collision efficiency. This was shown by Nguyen and Nguyen (2009) using computational modelling for intermediate and coarse particle sizes. Furthermore, more dense particles experience a higher attachment efficiency than less dense particles (Pyke, 2004). This has been attributed to the increase in the angle of tangency as particle density increases for intermediate and coarse particle sizes (Nguyen & Nguyen, 2009).

1.4 CHARACTERISING THE WETTABILITY OF SOLID SURFACES

There are many methods to determine the wettability of both surfaces and powders. The most common methods are time of flight secondary ion mass spectroscopy, contact angle, induction time measurements and the enthalpy of immersion. The contact angle and the enthalpy of immersion are the ones that are more comprehensively discussed in the following sections.

1.4.1 Time of flight secondary ion mass spectroscopy

Time of Flight Secondary Ion Mass Spectroscopy (ToF-SIMS) is a surface science technique based on collecting and analysing the secondary ions that are removed from the surface after bombardment with an ion beam. A number of researchers have studied a possible correlation between the contact angle and the surface analysis by ToF-SIMS (Duan et al, 2003; Brito E Abreu and Skinner, 2011a, 2011b). However, this technique does not simulate real flotation conditions and it is also not conducted in real time. The signal intensities can be affected by the concentration of the ions species on the mineral surface, sputter yield of species, matrix mix and the beam conditions (Chehreh Chelgani & Hart, 2014). Also, the question arises of the state of the particle under high vacuum compared to an aqueous environment.

1.4.2 Induction time measurements

The induction time, defined as the time taken for the liquid film separating the bubble from the particle to thin, rupture and form the three phase line of contact, is an indicator of mineral surface wettability (Yoon & Yordan, 1991; Dai et al, 1999; Yoon, 2000). Yoon and Yordan (1991) found that the induction time decreases with increasing hydrophobicity of quartz surface (Section 1.3.3.1.5). Similar findings were made by Dai (1999), Krasowska et al (2006) and Crawford and Ralston (1988).

1.4.3 Atomic force spectroscopy

Atomic force spectroscopy has been widely used in measuring the surfaces forces between the sharp tip of a cantilever and a given mineral surface. The force measurements can be conducted in any medium of interest, e.g. in pure water or water at different pH and ionic strengths. Force distance curves are used to show the interaction force between an AFM tip and the mineral surface. The total surface force, F^{total} based on the extended DVLO theory is given by equation 1-7.

$$F^{total} = F^{hydrophobic} + F^{vdw} + F^{edl} \qquad \textit{Equation 1-7}$$

where F^{vdw}, F^{edl} and $F^{hydrophobic}$ are the van der Waals, electrical double layer and hydrophobic forces respectively.

F^{edl} can be eliminated by conducting the force measurements at a pH close to the point of zero charge of the tip such that only F^{vdw} and $F^{hydrophobic}$ can be considered. The relative sizes of the forces are the basis for deciding whether F^{vdw} or $F^{hydrophobic}$ is a dominant force. The AFM has the advantage that it can make force measurements on a targeted local point on the surface as opposed to other techniques which can only measure the integral properties of particle surfaces.

1.4.4 Contact angle

The contact angle has been used as a quantitative measure of the wettability of a solid by a liquid phase. It is defined as the angle induced between air and a mineral particle in a liquid phase. If the angle is greater than 90°, the liquid is non-wetting, whereas if the angle is less than 90°, the liquid is wetting. A value of 0°contact angle signifies complete wetting. The contact angle has been a subject of intensive research for more than a century (Chau et al., 2009). The contact angle has been extensively used by many researchers as a conventional measure of hydrophobicity (Wark and Wark, 1932; Rao, 1982; Prestidge and Ralston, 1996; Prestidge and Ralston, 1996; Bulatovic, 2007, Drelich et al, 2017). Wark and Wark (1932) investigated the effect of different collector addition on the contact angle induced on various mineral surfaces.

1.4.4.1 Contact angles on flat surfaces

The measurement of the contact angle on a flat surface is straight-forward and well described. The concept of contact angle is easily understood in the measurement on a smooth, flat and ideal surface. The attachment of the air bubble to the mineral

particle is determined by the interfacial energies between the solid, liquid and gas phases shown in Figure 1-20.

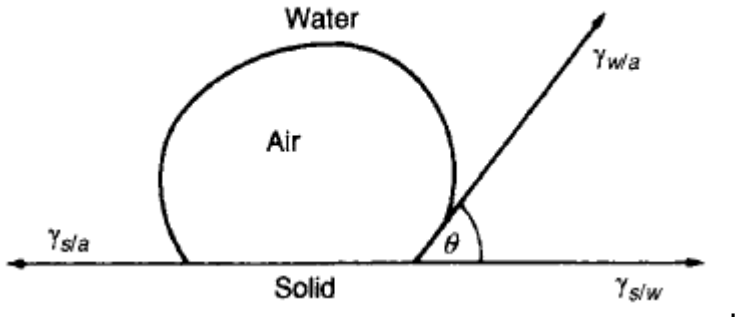

Figure 1-20: Contact angle between particle and air bubble in the liquid phase (Wills and Napier-Munn 2006).

At equilibrium the contact angle, Θ, in terms of the interfacial energies (forces) at the solid/water/air interface is given by the Young - Dupre Equation as shown in equation 1-8:

$$Y_{w/a}cos\Theta = Y_{s/a} - Y_{s/w} \qquad \textit{Equation 1-8}$$

where $Y_{w/a}$, $Y_{s/a}$, $Y_{s/w}$ are the surface energies of the water/air interface, solid/air interface and solid/water interface respectively. *Θ* is the contact angle between the mineral surface and the bubble.

However, the flat surface represents an idealised system whereas most surfaces are heterogeneous. The apparent contact angle on a heterogeneous surface is related to the ideal contact angle by the Cassie equation given in equation 1.9:

$$cos\theta_c = f_1 cos\theta_1 + f_2 cos\theta_2 \qquad \textit{Equation 1-9}$$

where f_1 and f_2 are the fractions of the surface with contact angles θ_1 and θ_2 respectively; θ_c is the Cassie contact angle.

1.4.4.2 Contact angles on powders

The measurement of the contact angle on powders is not as simple, straight forward and well-described as that on surfaces (Buckton, 1990). Although it is difficult to measure the contact angle to characterise the wettability of powders, techniques have been developed to determine the contact angles on such powders. Powders also

represent a system which is closer to reality. The commonly used techniques are the Washburn, the Bartell, the compressed disc and the Wilhelmy gravitational method. The Washburn and Bartell methods are the oldest direct techniques used to determine the contact angles on powders (Washburn, 1921; Bartell & Merrill, 1931). The compressed disc and Wilhelmy gravitational techniques are indirect methods with the limitation that they use compressed powders in which the surface properties of the powders may be altered during compaction due to plastic deformation. Thus the contact angle measured on compressed powders may not be representative of the original powders (Buckton, 1990).

Both the Washburn and the Bartell techniques are based on the same principle of liquid penetration, except that the Washburn method is dynamic while the Bartell method is static. The Washburn method is based on measuring the rate at which the liquid is drawn into the bed of powder (Washburn, 1921) while the Bartell method is based on measuring the pressure to be exerted on the liquid--gas interphase in the packed bed to prevent further penetration of the liquid (Bartell & Merrill, 1931). The principle is to measure the rate of penetration of a liquid that is known to perfectly wet the particles into a loosely packed bed of powder. The rate of penetration of the test liquid (for which the contact angle is being measured) is also measured. The contact angle, Θ, is then calculated using the formula shown in equation 1-10:

$$cos\theta = \left[\frac{\eta}{CY\rho^2}\right]\left[\frac{m^2}{t}\right] \qquad \textit{Equation 1-10}$$

where t = time after contact;

η = viscosity of the liquid;

C = constant of the solid bed structure;

ρ = density of the liquid;

Y = surface tension of the liquid;

m = mass of liquid absorbed on solid.

1.4.4.3 Limitations of the contact angle

Despite the contact angle having been extensively studied and widely used for more than a century (Chibowski and Perea-Carpio, 2002; Kumar and Prabhu, 2007; Chau

et al., 2009, Drelich et al 2017), using the contact angle as an indication of wettability has limitations:

a. It is not a fundamental physical quantity since it is inferred from the surface energies;
b. It is difficult to obtain meaningful and reproducible contact angle values of powders. This is because there are a number of parameters that are difficult to control – surface roughness, chemical heterogeneity, particle size & shape (Denoyel et al, 2004; Gharabaghi and Aghazadeh, 2014).
c. The deriving theory of the Washburn and Bartell techniques assumes a bundle of parallel capillaries with constant radius. This, however, is an over-simplification of the tortuous path travelled by the liquid in the bed (Spagnolo et al, 1996). This assumption demands that the bed is, and remains, homogenous throughout the wetting process. However, this is difficult to achieve in practice since wetting changes the surface properties of the particles, thereby altering the particle-particle interactions;
d. It is difficult to prove if the contact angle induced by the completely wetting liquid is actually zero (Spagnolo et al, 1996);
e. It is difficult to measure the contact angle for very hydrophobic particles with large contact angles using pure water using the Washburn method (Buckton, 1990; Spagnolo et al, 1996). It is difficult to get water to penetrate the packed bed. An external pressure has to be applied to force the water to penetrate the bed and at large pressure differences, channelling occurs and thus destabilises the packed bed. Some authors have resorted to using binary mixtures (e.g. alcohol / water mixtures) to decrease the contact angles and then extrapolate back to determine the contact angle induced by water. However, the bed is still unstable and the experiments become tedious and time-consuming.

Due to the shortcomings listed above, it is difficult to get reliable, meaningful and reproducible contact angle data on mineral powders.

1.4.5 The enthalpy of immersion

Another way to study wettability is by conducting calorimetric experiments where it is possible to measure state functions such as internal energy or the enthalpy of immersion associated with the wetting process (Denoyel et al, 2004). The enthalpy of

immersion is the heat absorbed or released when a clean, powdered solid in a vacuum is immersed in a liquid phase (Spagnolo et al, 1996). The immersion process is depicted diagrammatically in Figure 1-21.

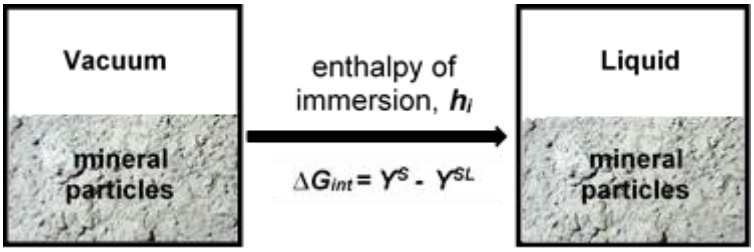

Figure 1-21: Schematic of the immersion process.

The replacement of the solid-gas interface with the solid-liquid interface is associated with a decrease in the Gibbs energy. This process releases heat, the magnitude of which depends on the area of interaction at the interface and the intensity of the interaction between the liquid molecules and the surface of the solid (Goncharuk, 2015)**.** Thus, the enthalpy of immersion is a direct measure of the surface energy. Immersion calorimetry has been useful in characterising the surface characteristics of solid surfaces. It also follows that enthalpy of immersion has potential to characterise the wettability of the mineral surface. The advantage of characterising the surface energy using the enthalpy of immersion is that the enthalpy of immersion is readily measured in a calorimetric experiment and has the advantage of being measured at ambient conditions typical of those prevailing in a real flotation system. The interaction of water with a mineral surface (in this case iron hydroxide) is depicted schematically in Figure 1-22. If the mineral surface is hydrophilic, the measured enthalpy of immersion is more exothermic. On the contrary, if the mineral surface is hydrophobic, the enthalpy of immersion is less exothermic.

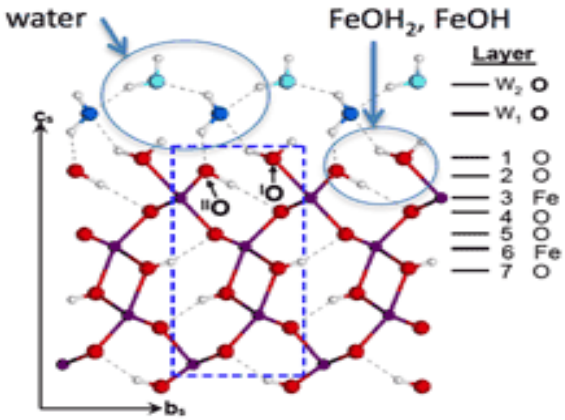

Figure 1-22: A schematic of a hydrated mineral surface.

Enthalpy of immersion has been measured for a variety of systems. For example, Malandrini et al. (1997) quoted the enthalpies of immersion of polytetrafluoroethylene (PTFE) and quartz in water and the h_i values are shown in Table 1-3.

Table 1-3: Enthalpy of immersion, h_i of PTFE and quartz in water (Malandrini et al, 1997)

Material	h_i (mJ/m²)	Wettability
PTFE	-6	hydrophobic
Quartz	-365	hydrophilic

It is clear from Table 1-3 that the enthalpy of immersion of quartz is more exothermic than that of PTFE, implying that quartz interacts more strongly with water than PTFE. This is intuitively correct since it is generally agreed that quartz is hydrophilic while PTFE is well known to be hydrophobic. Thus, the relative h_i values indicate the relative wettabilities of the surfaces.

1.4.5.1 Previous studies on the enthalpy of immersion

The enthalpy of immersion is an established method in characterising the wettability of various materials. Some of the studies involving the enthalpy of immersion have been mentioned in Section 1.5.4.1 where teflon, graphon, graphite and griseofulvin were investigated (Young et al., 1954; Chessick et al, 1956; Hansford et al, 1980). Furthermore, the enthalpy of immersion measurements have been used in the following areas.

a) Estimation of surface areas as well as hydrophobic and hydrophilic sites

The enthalpy of immersion as directly measured by calorimetry has been applied in studying various fluid-solid interactions (Groszek, 1958, 1998; Templer, 1972), including the estimation of the surface areas of minerals (Allen & Patel, 1968; Ticknor & Saluja, 1990). The enthalpy of immersion has also been used to quantify the hydrophobic and hydrophilic sites in a variety of carbonaceous and mineral solids of different hydrophobicities (Partyka, 1993). The surface areas of the hydrophilic and hydrophobic sites were found to be related to the heats of displacement of 1-butanol from n-heptane and water solutions, respectively. Similar studies to quantify the surface areas of the hydrophilic and hydrophobic sites were conducted by many researchers (Nakamoto & Takahashi, 1982; Bolis et al., 1991; Yildirim, 2001).

b) Silica studies

The surface properties of silica have been extensively investigated because of its widespread use as a catalyst support, adsorbent, etc. Yan et al. (2000) studied the enthalpies of immersion of silanised fumed silica nanospheres and they found that the enthalpy of immersion in water decreased with increasing hydrophobicity of the silica nanospheres. Similarly, Goncharuk (2015) found that the enthalpy of immersion of silanised silica decreased almost linearly with increasing coverage (hydrophobicity) in polar liquids. This is because the concentration of OH^- decreased with increasing trimethylsilyl (TMS) coverage, thus the magnitude of interaction with polar molecules and OH^- decreases with increasing TMS coverage. However, the enthalpies of immersion in non-polar liquids were almost constant and these are attributed to van der Waals forces of attraction. Spagnolo et al. (1996) measured the enthalpy of immersion of three fluorinated carbons using a water / 1-propanol mixture. They observed that the enthalpy of immersion decreased with increasing hydrophobicity (fluorine content).

The variation of the enthalpy of immersion of silica with heat treatment was studied by (Young & Bursh 1960). It was concluded that the enthalpy of immersion of silica in water depends on evacuation temperature and thermal pre-treatment of the powder. Similar findings were made by Makrides and Hackerman (1952).

c) Zeolite studies

Zeolites are mainly used as commercial adsorbents and catalysts. Enthalpy of immersion measurements have also been useful in characterising the nature of zeolites. Nakamoto & Takahashi (1982) investigated the adsorption of various probe liquids on a series of zeolites in which the SiO_2/Al_2O_3 ratio was varied. They found that the hydrophobicity of the zeolites decreased with increasing SiO_2/Al_2O_3. Tsutsumi & Takahashi (1969) investigated the electrostatic field strengths of Na- and Ca-substituted Y zeolites using enthalpy of immersion measurements of various organic liquids. The probe liquid's dipole moment affected the enthalpy of immersion when the solid had an electrostatic field on its surface.

d) Carbon black and charcoal studies

Adsorbent carbons and charcoal have also been investigated using the enthalpy of immersion because their surface properties can readily be altered through oxidation. Kraus (1955) measured the enthalpy of immersion of nine carbon blacks in water, methanol and n-hexane. The enthalpy of immersion in water and methanol increased linearly with oxygen content. This is because the more the oxygen content, the more the hydrogen bonds formed in polar liquids and hence the more exothermic the enthalpy of immersion. However, the enthalpy of immersion in n-hexane was constant across the whole spectrum of the carbon blacks and this is attributed to dispersive forces of attraction between the carbon black surface and the non-polar liquids. Similar findings were made by Puri et al. (1953), when investigating the enthalpy of immersion of charcoal as a function of its oxygen complexes.

e) Coal studies

The effects of coal rank, surface oxidation state, moisture content, and petrographic constituents on the wetting characteristics and surface properties were investigated using the enthalpies of immersion of six coals in water, methanol and surfactant solutions (Melkus et al, 1987). Furthermore, different coal samples of different oxygen contents were characterised by measuring the heats of methanol adsorption on the coal surfaces (Wang et al., 1998). It was found that the heat of adsorption of methanol depends on coal hydrophilicity and not on particle size distribution and quantity of inorganic impurities on coal surface. Methanol interacts with the polar (hydrophilic) sites via hydrogen bonding. The higher the number of the hydrophilic sites, the greater

the magnitude of interaction with the molecules of methanol. This results in a higher value of the measured heat of methanol adsorption. An interesting finding by Melkus et al. (1987) was that the trends in the enthalpies of immersion of the different coals (for varying coal rank, lithotypes and oxidation) coincided with the trends reported for the floatability of the different coals. This work was successful only in as far as distinguishing or ranking the different types of coal is concerned. However, the authors did not explicitly establish the relationship between the enthalpy of immersion and floatability – which is the key objective of this thesis. Furthermore, it would have been more informative to quantify the surface energy and its components as well as correlate this to floatability.

f) Minerals

The enthalpy of immersion technique has been applied in the mineral processing field only to a limited extent. Zimmerman et al. (1987) described a new calorimetric vessel for enthalpy of immersion studies and the vessel was tested by measuring the enthalpies of CaF_2 in water and enthalpies of immersion of different minerals in water. Their results agreed with previously published data. They suggested that the enthalpy of immersion as measured by precision calorimetry can provide a reliable approach to investigate the flotation process. However, no flotation work was conducted in their study. The present investigation seeks to build on their study by correlating the enthalpy of immersion of different minerals in water and the floatability of these minerals.

1.4.5.2 Advantages of the enthalpy of immersion measurements

The enthalpy of immersion method has a number of advantages when compared to other wettability characterisation methods. Some of the advantages are listed below:

1. The advancement of calorimeters over the last few decades has resulted in enthalpy of immersion measurements that are reliable and accurate, with the enthalpies of immersion measured to the microwatt range. Due to high sensitivity, the enthalpy of immersion measurements have been used to determine a difference in wetting between solids whose contact angles are reported to be near to zero. For example, the contact angles of SiO_2, CaF_2 and TiO_2 against water are approximately zero while their enthalpies of immersion differ significantly, viz -165; -463 and -550 mJ/m^2 respectively (Arai, 1996). This

is an example of how the enthalpy of immersion measurements using modern instruments is a much more sensitive indicator of wettability than the contact angle.

2. Sample preparations for enthalpy of immersion measurements are relatively easier when compared to other conventional methods of determining wettability (Spagnolo et al, 1996). This results in more reproducible data, with higher experimental success than the Washburn and Bartell methods.
3. The experiments can be readily carried out in a calorimeter at conditions typical of those prevailing in real flotation processes.
4. The enthalpy of immersion can be used to characterise the wettability of composite particles or mineral mixtures (Zettlemoyer, 1968). In contrast, the measurement of the contact angles for mixtures of minerals of different hydrophobicities is a challenge.
5. The enthalpy of immersion is not vulnerable to challenges such as contact angle hysteresis, surface roughness or drop size as is the case with the compressed pellet method (Spagnolo et al, 1996).

1.5 ENTHALPY OF IMMERSION, GIBBS ENERGY CHANGE, CONTACT ANGLE AND FLOATABILITY

1.5.1 The interfacial Gibbs energy vs wettability

The characteristics of the mineral surface dictate the surface energy and ultimately the wettability of the surface. Thus, the extent of wetting of a particular surface can be inferred by determining the energy of the surface.

When the interfacial energy of interaction (ΔG_{int}) between particles of a particular material in water is relatively high, the interaction of the material with water dominates and the surface of the material is hydrophilic. However, when ΔG_{int} is relatively lower, the polar cohesive attraction between the water molecules dominates and the material is hydrophobic (van Oss & Giese, 1995). The magnitude of the interfacial Gibbs energy is a quantitative measure of wettability (hydrophobicity / hydrophilicity) (van Oss & Giese, 1995). Van Oss and Giese (1995) reported some ΔG_{int} values for a number of solids in water and these are shown in Table 1-4.

Table 1-4: Values of the interfacial energy of interaction, ΔG_{int} for different solids in water at 20°C.

Material	ΔG_{int} (mJ/m²)
Teflon	-102
Talc	-49.5
Muscovite	+43.4
Glass	+45.3

It is clear from Table 1-4 that the ΔG_{int} of teflon and talc was less than zero while that of muscovite and glass was greater than zero. The ΔG_{int} values show that muscovite and glass interact more strongly with water than teflon and talc. This is consistent with the known hydrophobic-hydrophilic nature of these materials. Talc is well known to be hydrophobic (Yan et al., 2011; Yin et al., 2012). Teflon is also well known to be hydrophobic. On the other hand, muscovite is well known to be hydrophilic (Bryant, Bowman & Buckley, 2006; Yin et al., 2012). Glass, mainly made of silica, is also well known to be hydrophilic. Thus, the relative ΔG_{int} values indicate the relative wettabilities of the surfaces.

1.5.2 Enthalpy of immersion vs interfacial Gibbs energy change

When a solid is suspended over a liquid in a closed vessel, the solid surface is in equilibrium with the liquid vapour. If the solid is immersed into the liquid, the energy change, ΔG_{int} accompanying this process is given by equation 1-11:

$$\Delta G_{int} = \Upsilon_{sl} - \Upsilon_{sv} \qquad \textit{Equation 1-11}$$

where Υ_{sv} = the interfacial tension at the solid/vapour interface;

Υ_{sl} = the interfacial tension at the solid/liquid interface.

When a solid is immersed into a liquid without being exposed to the vapour of the wetting liquid, the energy change, ΔG_{int} is given by equation 1-12:

$$\Delta G_{int} = \Upsilon_{sl} - \Upsilon_{s} \qquad \textit{Equation 1-12}$$

where Υ_{s} = the interfacial tension at the interface between the solid in equilibrium with its own vapour.

The change in the enthalpy of immersion, h_i is given by equation 1-13:

$$h_i = \Delta G_{int} - T\frac{d(\Delta G_i)}{dT} \qquad \textit{Equation 1-13}$$

where T = temperature.

Substituting equation 1-12 into equation 1-13 yields equation 1-14:

$$h_i = \Delta G_{int} - T\frac{dY_{sl} - dY_s}{dT} \qquad \textit{Equation 1-14}$$

The physical implication of equation 1-14 is that the immersion process, which is associated with changes in the interfacial Gibbs energy, can be directly and readily quantified by measuring the enthalpy of immersion. Furthermore, each solid will have a characteristic enthalpy of immersion depending not only the surface characteristics of the solid but also on the magnitude of solid-liquid interactions at the interface. For very hydrophobic solids, there is very little interaction between the solid and the liquid (van der Waals forces). For low energy surfaces, $\frac{d(Y_i)}{dT}$ is assumed to be constant (-0.07 ±0.02 mJ/m².K) (Spagnolo et al, 1996). Spagnolo et al. (1996) in their calculation of the contact angle using the enthalpy of immersion, assumed that the solid/liquid surface tension is independent of temperature. However, this is an over-simplification because it is established that surface tension changes with temperature. The experimentally measured enthalpy of immersion should be a direct indicator of the wettability of a given solid.

1.5.3 Contact angle vs floatability

The relationship between contact angle and floatability has been intensively studied and is well established in literature. The effect of hydrophobicity as quantified by the contact angle has already been discussed in Section 1.3. There has been some definitive work on relating the contact angle induced on mineral surfaces to their flotation performances in the pulp phase (Prestidge & Ralston 1996; Crawford 1986; Crawford & Ralston 1988). All these researchers had a common finding that for any particular particle size range, a critical contact angle must be achieved before flotation takes place. Above the critical contact angle, the flotation recoveries increase significantly with contact angle. Muganda et al. (2011a) and Muganda et al. (2011b) took this concept further and developed a model relating maximum recovery as

observed in a standard batch flotation cell and critical contact angle to particle size for chalcopyrite particles.

1.5.4 Enthalpy of immersion vs contact angle

Combining the Young's equation (equation 1-8), the change in the interfacial Gibbs energy (equation 1-12) and equation 1-14, it is possible to relate the enthalpy of immersion to the contact angle through equation 1-15:

$$-h_i = T\Upsilon_{lv}\frac{dcos\theta}{dT} - \left(\Upsilon_{lv} - T\frac{d\Upsilon_{lv}}{dT}\right)cos\theta \qquad \textit{Equation 1-15}$$

where h_i = the enthalpy of immersion (mJ/m^2);

T = absolute temperature (K);

Θ = contact angle (°);

Υ_{lv} = liquid-vapour interfacial tension (mJ/m^2).

This is a well-established theoretical relationship between the enthalpy of immersion and the contact angle (Adamson and Ling, 1964; Melrose, 1965; Arai, 1996; Spagnolo et al, 1996; Denoyel, Beurroies and Lefevre, 2004; Douillard and Zajac, 2006). Equation 1-15 shows that it should be possible to determine the contact angle values from the enthalpy of immersion if γ_{lv}, $\delta\gamma_{lv}/\delta T$ and $\delta cos\theta/\delta T$ are known. The first two are usually available from literature. However, the temperature dependence of contact angle needs to be determined experimentally. This somewhat defeats the purpose since, in order to determine the enthalpy of immersion, the contact angles need to be measured. These contact angles can be measured in a variety of ways with certain assumptions being made for each one: firstly, polished surfaces can be used, assuming that the temperature coefficient remains the same when the mineral is pulverised; secondly, contact angles of pressed pellets can be measured, assuming that the temperature coefficient remains the same for loose powders; and thirdly the capillary rise technique can be used assuming that the temperature coefficients of the equilibrium and advancing contact angles are the same.

Instead of calculating the contact angle, Neumann (1974) used equation 1-15 to calculate the enthalpy of immersion of teflon in alkanes from the measurement of the contact angle and liquid-vapour surface tension as a function of temperature. Directly

measured enthalpies of immersion and enthalpies of immersion calculated using equation 1-15 were compared and they were found to be in agreement.

Equation 1-15 shows that there is a relationship between the enthalpy of immersion and the contact angle. Thus, it is proposed in this thesis that the enthalpy of immersion is an alternative surface characterisation tool for determining of mineral surface wettability. For a particular mineral, the parameters $\delta\gamma_M/\delta T$ and $\delta\cos\theta/\delta T$ are constants at a constant temperature. The $\delta\gamma_M/\delta T$ for various test liquids at 20°C are available in literature. For example, the contact angle has been shown to linearly decrease as temperature increases for the crystalline naphthalene-water system (Jones and Adamson, 1968) and their results are shown in Figure 1-23. Similar results were reported by Park and Aluru (2009) in titanium dioxide using molecular dynamics simulation.

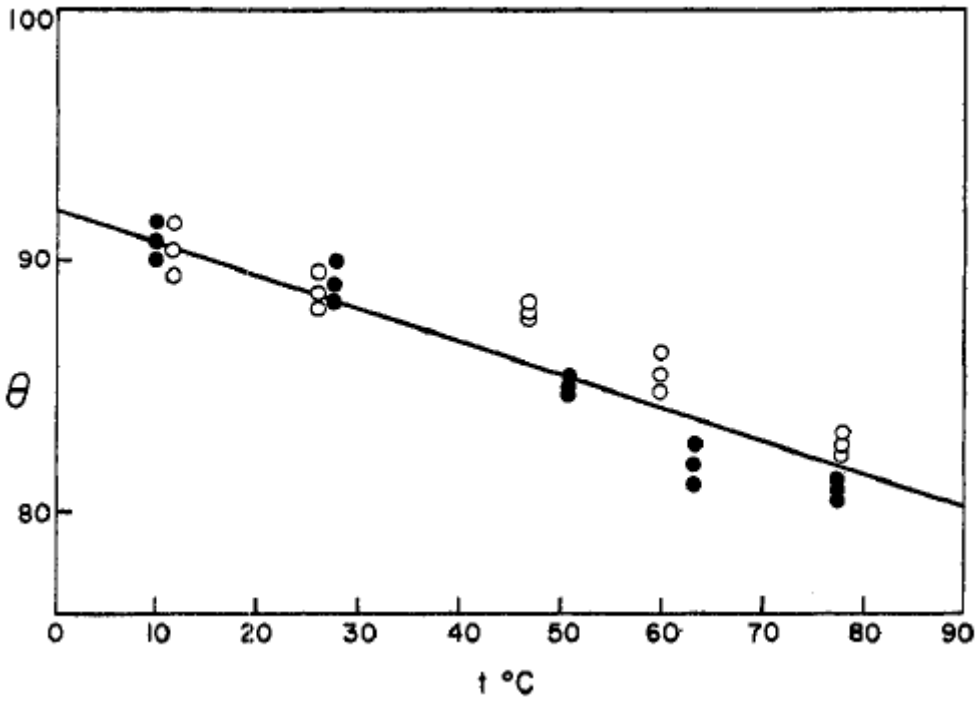

Figure 1-23: The variation of contact angle with temperature for the crystalline naphthalene-water system (Jones & Adamson, 1968).

Therefore, it can be assumed that $\delta\cos\theta/\delta T$ is constant at a constant temperature. Hence equation 1-15 reduces to the general equation of a straight line of the form:

$$y = mx + c \qquad \textit{Equation 1-16}$$

where *x* & *y* = coordinate system in the x-y plane;

m = the gradient of the straight line;

c = the y-intercept.

This analysis is suggestive of an inverse linear relationship between the enthalpy of immersion and the cosine of the contact angle. A comparison of equation 1-15 and 1-16 shows that a plot of the enthalpy of immersion (y-axis) against the cosine of the contact angle (x-axis) is a straight line with the following parameters:

$$\mathrm{m} = \left(\mathrm{Y_{lv}} - \mathrm{T}\frac{\mathrm{dY_{lv}}}{\mathrm{dT}}\right)$$

$$\mathrm{c} = \mathrm{TY_{lv}}\frac{\mathrm{d}\cos\Theta}{\mathrm{dT}}$$

1.5.4.1 Predicted vs experimental contact angle

Contact angle calculated using the enthalpy of immersion (Θ_{pred}) is based purely on the thermodynamics of the system, without any assumptions, while directly measured contact angles (Θ_{exp}) using the Washburn and Bartell methods are based on assumptions as discussed in Section 1.4.4.3. Provided that the mineral surface area is known and that the mineral powder is completely degassed before the immersion process, the contact angle value determined from the enthalpy of immersion data (Θ_{pred}) should be more accurate than values determined using the traditional methods.

Spagnolo et al. (1996) made certain simplifying assumptions in order to approximate the contact angle from the enthalpy of immersion for hydrophobic surfaces. Their simplified relationship between the contact angle and enthalpy of immersion is as follows:

$$cos\theta = \frac{-0.07T - h_i}{\mathrm{Y}_{lv}} \qquad \textit{Equation 1-17}$$

where h_i = the enthalpy of immersion (mJ/m^2);

T is temperature (K);

Y_{lv} is the interfacial tension at the liquid/vapour interface (mJ/m^2).

A number of researchers compared the predicted contact angle (Θ_{pred}) using equation 1-17 and the contact angle measured using the Washburn methods (Θ_{exp}). Their results are summarised in Table 1-5.

Table 1-5: Comparison between predicted and directly measured contact angles for different materials.

Material	Enthalpy of immersion, h_i (mJ/m²)	Predicted contact angle (°)	Directly measured contact angles (°)	References
Teflon	-6	102	110	(Chessick et al, 1956)
Graphon	-32	81	81	(Young et al., 1954)
Griseofulvin	-5.7	102	101.9	(Hansford et al, 1980)
Graphite	-47.5	68	86	(Arai, 1996)

Table 1-5 shows that the discrepancies between the predicted and the directly measured is small for hydrophobic surfaces (teflon, graphon and griseofulvin) but becomes larger for more hydrophilic surfaces (graphite). Furthermore, a closer scrutiny of equation 1-17 shows that it cannot be applied in cases where the enthalpy of immersion is more exothermic than -50 mJ/m², otherwise the cosine of the contact angle becomes undefined ($|\cos\Theta| < 1$). Thus equation 1-17 is only valid for hydrophobic surfaces having very low surface tensions and cannot be applied for hydrophilic surfaces which produce more exothermic enthalpies of immersion.

1.5.5 The enthalpy of immersion vs floatability

It has been shown beyond any doubt that the contact angle is related to the floatability of the minerals and, since it was shown in Section 1.5.4 that contact angle is related to the enthalpy of immersion, then it follows that there ought to be a relationship between enthalpy of immersion and floatability. There has been limited work conducted to investigate the relationship between the enthalpy of immersion and floatability. As far as can be ascertained, only two researchers have applied enthalpy of immersion to a mineral processing context. Melkus et al. (1987), using enthalpy of immersion measurements, distinguished six different coals (of varying coal rank, lithotypes and oxidation). They reported that the trends in the enthalpies of immersion

were the same as the trends in the floatability of the different coals. It must be emphasised that their objective was just to distinguish or rank the different coals. An explicit relationship between the enthalpy of immersion and the floatability was thus not established.

Yildirim (2001) compared the directly measured contact angles (flat surfaces and powders) to the indirectly measured contact angles using the enthalpy of immersion on talc. The author concluded the enthalpy of immersion decreased as contact angle increased. He measured the enthalpy of immersion, heat of adsorption and contact angle on anatase as a function of the surface coverage of the hydroxamate collector. It was found that the enthalpy of immersion decreased with increasing hydrophobicity (collector surface coverage). Again, the study was not explicit in establishing the relationship between the enthalpy of immersion and floatability. Thus, a model system with well-defined levels of hydrophobicity is required when investigating the relationship between the enthalpy of immersion and the pulp phenomena.

This thesis introduces the concept of using the enthalpy of immersion as an indicator of mineral surface hydrophobicity. Both the enthalpy of immersion and the contact angle measurements are thermodynamic equilibrium values which dictate whether or not flotation will take place. On the other hand, floatability is defined as the ability of a mineral particle to attach to an air bubble in the flotation cell. Floatability, or the extent to which a particle will report to the froth phase, is a function of surface properties of the mineral, particle size, particle density, hydrodynamic conditions, energy dissipation and the pulp environment. Unlike hydrophobicity which is a thermodynamic parameter, floatability includes both thermodynamic and kinetic aspects of the flotation process.

If the hydrodynamics is maintained constant and the environment is quiescent in the microflotation process, the collision efficiency can be regarded as constant (Section 1.2.5). Thus, different flotation responses (recoveries and kinetics) imply different hydrophobicities of particles in the pulp. The microflotation technique, which is a modified Hallimond tube, is used in this study to determine the microflotation response in this work (Section 3.9) at constant cell dynamics and bubble properties. At constant cell dynamics and bubble properties, the measured floatability is an indicator of mineral surface hydrophobicity. The microflotation technique can thus be considered to be a hydrophobicity meter.

1.6 CHARACTERISING THE SURFACE ENERGY OF SOLIDS

The surface energies and their components (dispersive and polar fractions) dictate not only the nature (hydrophobic or hydrophilic) of a surface but also the magnitude of interaction between two interacting surfaces. Froth flotation depends strongly on the differences in the surface energies of the valuable and gangue mineral solids present in the pulp. The higher the surface energy, the more hydrophilic is the mineral surface. On the contrary, the lower the surface energy, the more hydrophobic is the mineral surface. Because the surface energies of solids are not directly measurable, the surface energies of solids are limited in literature (Sun & Berg, 2002).

Ali et al. (2013) determined the surface energies of quartz and galena using inverse gas chromatography. They went further to determine corresponding microflotation recoveries of the two minerals. They found that quartz which had a higher surface energy compared to galena would interact more strongly with water making it more hydrophilic than galena. Microflotation tests confirmed this finding as evidenced by the lower quartz collectorless recovery compared to that of galena (6.94% and 27.63% respectively).

1.6.1 Surface energies of solid surfaces

The surface free energy of a solid is thermodynamically defined as the work required to reversibly create a unit area of a surface. Due to cleavage, there are fewer bonds between molecules on a solid surface compared to the bulk molecules. The resultant excess energy on the solid surface is called the surface free energy. The surface energy of solids is the summation of the non-polar (Liftshitz-Van der Waals forces) component and the polar (acid-base) component. The non-polar and polar components can be referred to as the non-specific and specific components respectively.

1.6.1.1 Theories on surface energies and models

For the flotation process, which depends on the interfacial interactions between mineral particles and water, the characterisation of the surface energy and its dispersive and polar components is very important. However, the surface energy of solids is difficult to measure directly due to the immobility of the molecules in the solid phase. A number of indirect mathematical models or methods have been developed to calculate the surface energies of solids, viz: inverse gas chromatography (iGC),

Equation of State (EOS), Zisman, Fowkes/ OWRK, Owens and Wendt, Wu as well as the van Oss, Chaudhury and Good approaches.

1.6.1.1.1 Inverse gas chromatography (iGC)

Inverse gas chromatography (iGC) is a versatile and powerful technique for characterizing physicochemical properties of materials, including surface energy and surface heterogeneity. iGC requires the use of a series of alkane homologues to obtain the dispersion component of the surface energy. Then a polar liquid is used to obtain the polar component. In this method, a known volume of a vapour is passed through a column containing particles under investigation. The fundamental data obtained from the iGC is a plot of detector signal as a function of retention time. The retention time refers to the time the probe molecules require to generate a peak as a result of interactions with the stationary phase. The elution peak obtained gives information on the surface properties of the material. The Schultz et al (1987) approach is commonly used to calculate the non-polar component of the surface energy based on equation 1-18.

$$RTlnV_N = N_A a 2\sqrt{\Upsilon_s^d \Upsilon_l^d} + C \qquad \textit{Equation 1-18}$$

where R = molar gas constant (J mol^{-1} K^{-1});

T = absolute temperature (K);

V_N = net retention volume (mlg^{-1});

N_A = Avogadro's constant (mol^{-1});

a = the cross-sectional area of the probe molecule (m^2);

Υ_s^d & Υ_l^d = dispersive components of surface free energy of the solid and probe molecule (mJm^{-2}), respectively.

The constant C depends on the chosen reference. The plot of $RTLnV_N$ against Υ_l^d for a series of n-alkanes is a straight line whose gradient is the Υ_s^d. The polar component of the surface energy, Υ_s^p is also calculated from the same plot as the distance from the points representing the polar liquids to the straight line. Using two probe liquids, the acidic and basic components are then calculated based on the VOCG model as shown in equation 1-19.

$$\Upsilon_s^p = 2N_A a\left[\sqrt{\Upsilon_s^+\Upsilon_l^-} + \sqrt{\Upsilon_s^-\Upsilon_l^+}\right] \qquad \textit{Equation 1-19}$$

A number of researchers have employed iGC to characterise the surface energies of mineral particle surfaces (Ali et al., 2013; Mohammadi-Jam and Waters, 2014; Mohammadi-Jam et al, 2014; Rudolph and Hartmann, 2017). The disadvantage of the iGC technique is that it is a gas phase technique where measurement takes place on dried powders whereas flotation occurs as a result of particle bubble interactions in a pulp.

1.6.1.1.2 Neumann model

The Neumann formula shown in equation 1-20 is the most common form of the Equation of State (EQS) (Kwok & Neumann, 1999) used to calculate surface energy.

$$cos\theta = -1 + 2\sqrt{\frac{\Upsilon_s}{\Upsilon_l}}[1 - \beta(\Upsilon_l - \Upsilon_s)^2] \qquad \textit{Equation 1-20}$$

where Θ, Υ_s, Υ_l are the contact angle, surface energies of the solid and liquid respectively. The coefficient β= 0.0001247 $(mJ/m^2)^{-2}$ and is determined experimentally by measuring the contact angles for different polymeric solids using a large number of liquids (Kwok & Neumann, 1999).

The major controversy with this theory is whether β is a universal constant which applies to all materials or just a quantity obtained as a result of the iterative procedures applied. This model ignores the concept of partitioning the surface energy into the non-polar and polar components. This is the only theory that requires the use of one probe liquid to calculate the surface energy of the solid.

1.6.1.1.3 Zisman plot

The Zisman plot is used to determine the critical surface tension of wetting, Υ_c which is defined as that value of surface tension below which liquid wets the surface completely by spreading spontaneously (Fox & Zisman, 1952a,b). The relationship between Υ_c and the natural wettability of minerals has been discussed in Section 1.3.1. The method involves measuring the contact angles formed between low energy solids and various homologous series of liquids. An adhesion tension diagram is then plotted with the cosine of the contact angle on the y-axis and the liquid surface tension on the x-axis. A straight line is fitted to the measurement points and the critical surface tension is obtained by extrapolation to cos Θ = 1. It must be noted that the critical

surface tension, Υ_c is different from the surface energy of the solid, Υ_s. Thus, Υ_c is not divided into non-polar and polar components. The application of the Zisman method is rare because of insufficient theoretical justification and time-consuming investigation procedures.

1.6.1.1.4 The Fowkes/ OWRK method

Fowkes (1964, 1968, 1972) assumed that the total surface energy of any solid and liquid may be expressed as a sum of independent components, associated with specific interactions and is given by equation 1-21.

$$\Upsilon_s = \Upsilon_s^d + \Upsilon_s^p + \Upsilon_s^h + \Upsilon_s^i + \Upsilon_s^{ab} + \Upsilon_s^o \qquad \textit{Equation 1-21}$$

where Υ_s^d, Υ_s^p, Υ_s^h, Υ_s^i, Υ_s^{ab} are dispersion, polar, hydrogen, induction, acid-base components respectively while Υ_s^o are all remaining interactions. Fowkes's theory is based on 2 fundamental assumptions, viz: the surface energies corresponding to each intermolecular interaction are additive and that the work of adhesion between two phases is the geometric mean of the corresponding energies of the two phases. Fowkes mainly focussed on low energy, two phase systems (solid or liquid) in which the dispersion interactions were dominant. For such systems, Fowkes calculated the surface energy of the solid-liquid interface using equation 1-22. The major limitation of this equation is that it is limited to dispersion forces only.

$$\Upsilon_{sl} = \Upsilon_s + \Upsilon_l - 2\left(\sqrt{\Upsilon_s^d \Upsilon_l^d}\right) \qquad \textit{Equation 1-22}$$

1.6.1.1.5 Owen and Wendt

Owens & Wendt (1969) furthered the idea of Fowkes by asserting that all the components on the right side of the Fowkes equation (equation 1-21) except Υ_s^d can be considered to be polar, Υ_s^p. As a result, equation 1-23 was obtained:

$$\Upsilon_{sl} = \Upsilon_s + \Upsilon_l - 2\left[\sqrt{\Upsilon_s^d \Upsilon_l^d} + \sqrt{\Upsilon_s^p \Upsilon_l^p}\right] \qquad \textit{Equation 1-23}$$

1.6.1.1.6 Wu

Wu (1971, 1973) accepted the approach of Owen and Wendt but used the harmonic mean instead of the geometric mean. Consequently, equation 1-24 was obtained.

$$\Upsilon_{sl} = \Upsilon_s + \Upsilon_l - 4\left[\frac{\Upsilon_s^d \Upsilon_l^d}{(\Upsilon_s^d + \Upsilon_l^d)} + \frac{\Upsilon_s^p \Upsilon_l^p}{(\Upsilon_s^p + \Upsilon_l^p)}\right] \qquad \textit{Equation 1-24}$$

1.6.1.1.7 The van Oss-Chaudhury-Good (VOCG) model

Van Oss, Chaudhury and Good (1988) developed the latest model for calculating the surface energy of solids. According to the VOCG model, surface tensions of solids and liquids can be further categorised into two additive components, viz: Liftshitz-Van der Waals component and the Lewis acid/base components. Accordingly, the total surface energy of the solid is given by equation 1-25.

$$\Upsilon_s = \Upsilon_s^{LW} + 2\sqrt{\Upsilon_s^+ \Upsilon_s^-} \qquad \textit{Equation 1-25}$$

The major assumptions of the VOCG model are that:

1. van der Waals (or dispersive forces) do not interact with polar forces;
2. Acidic forces interact only with basic forces.

Equation 1-26 represents the VOCG approach:

$$\Upsilon_{sl} = \Upsilon_s + \Upsilon_l - 2\left[\sqrt{\Upsilon_s^{LW} \Upsilon_l^{LW}} + \sqrt{\Upsilon_s^+ \Upsilon_l^-} + \sqrt{\Upsilon_s^- \Upsilon_l^+}\right] \qquad \textit{Equation 1-26}$$

where Υ^+, Υ^- are the acidic and basic components respectively.

The VOCG model developed by van Oss et al (1988) has been useful in characterising the surface energetics of solids using the contact angle as an input parameter (Jańczuk et al., 1992, 1993; Raichur et al, 2001; Swarna et al, 2003; Prabhakar et al, 2005).

1.6.1.2 Critical analysis of the surface energy models

The comparison of the surface energy values obtained from the different methods is complicated by the fact that each individual method is premised on different assumptions. This means that for a given material, the surface energy values evaluated using different methods and different probe liquids will be different.

It is clear that all the approaches or methods for calculating surface energy are premised on measuring the contact angle with the exception of the iGC. The fact that contact angle measurements are at the heart of all the methods of determining the surface energies makes these methods unreliable. The limitations of the using contact angle as an indicator of wettability have been extensively reviewed in Section 1.4.4.3.

This thesis seeks to use the enthalpy of immersion measurements to characterise the surface energetics of different minerals.

The VOCG approach has the advantage that it can give more detailed information about mineral surfaces, especially the acid-base interactions. Sharma & Hanumantha Rao (2002) reported that this approach not only gives the most consistent results but also provides information about a particular surface. The major limitation of the application of the VOCG model is that in some cases, the roots of the acidic and basic components are negative (Della Volpe & Siboni, 1997; Volpe & Siboni, 2000). However, this limitation can be ignored by working with the negative roots and the obtained results can be useful for the direct comparison of the surface energetics of different minerals (Volpe & Siboni, 2000). It is important to note that the values of the surface energy and its components calculated using the different methods are relative and not absolute. This is because the magnitude of the surface energetics depend strongly on the choice of the three probe liquids chosen for the experiments (Della Volpe & Siboni, 1997; Volpe & Siboni, 2000). Though the VOCG approach has been used with the iGC method, the iGC is a gas phase technique and therefore the results obtained from iGC fall short to describe the real situation since industrial flotation occurs in aqueous phase. This study seeks use the enthalpy of immersion (as opposed to the contact angle) as an input parameter into the VOCG model.

1.6.2 Calculating surface energies from the enthalpies of immersion

The enthalpy of immersion method has potential to characterise the surface energy (and components) of minerals and a number of researchers have used the enthalpy of immersion method to characterise the surface energy and its components of solids (Douillard et al., 1994, 1995, 2002, 2007; Salles et al, 2006). Although the relevant interactions are the same for the enthalpy of immersion and all the other methods presented in Section 1.6.1.1, the enthalpy of immersion in water as a single value, has proved to be a robust measure of mineral surface wettability/hydrophobicity (Taguta, et al, 2018). This is not the case with all the other methods in which the non-polar and

polar components must be evaluated in order to characterise the wettability of mineral surfaces.

1.6.2.1 Thermodynamic relations

For every interface, a derivative (denoted H_{ij}) of the surface energy is linked to the surface tension by the equation 1-27 (Douillard et al., 2007):

$$\left(\frac{\delta U}{\delta A}\right)_{T,V',V''} = H_{sl} = \Upsilon_{sl} - T\left(\frac{\delta \Upsilon_{sl}}{\delta T}\right)_{T,P} \qquad \textit{Equation 1-27}$$

where H_{sl} = usually regarded as the "surface energy" or the "surface enthalpy";

U = internal energy;

A = the interfacial surface area;

Υ = the surface tension;

T = temperature;

V = volume;

P = pressure.

The enthalpy of immersion per unit area is given by substituting (1-12) and (1-27) into (1-13):

$$h_i = (\Upsilon_s^o - \Upsilon_{sl}) - T\left(\frac{\delta(\Upsilon_s^o - \Upsilon_{sl})}{\delta T}\right)$$

$$= H_s^o - H_{sl} \qquad \textit{Equation 1-28}$$

From equation 1-28 it follows that the enthalpy of immersion depends on the nature of both the mineral and the wetting liquid. H_s^o is a surface enthalpy of the solid surface and depends on the nature of the mineral surface while H_{sl} is the surface enthalpy of the solid-liquid interface which depends on the nature of both the solid and the wetting liquid. For low energy surfaces (hydrophobic minerals) the interaction between the solid and a polar liquid is mainly repulsive and therefore the solid-liquid enthalpy is very high. This translates to less exothermic enthalpy of immersion. However, for a high energy surface (hydrophilic minerals), hydrogen bonds are formed. The stronger

interaction between the polar solid and the polar liquid implies a very low solid-liquid enthalpy. This translates into a more exothermic enthalpy of immersion.

The surface enthalpy of the interface formed between two pure phases can be obtained from the surface enthalpy (interphase-vacuum) of the separated phases 1 and 2, and is given by equation 1-29:

$$H_{sl} = H_s + H_l - f(H_s, H_l) \qquad \textit{Equation 1-29}$$

where *f* is an averaging function (arithmetic, geometric, etc.).

1.6.2.2 VOCG model extended to the enthalpy of immersion

The VOCG model has been theoretically extended to calculate the surface energy and its components from the enthalpy of immersion measurements (Douillard et al., 1994, 1995, 2002, 2007; Salles et al, 2006). Therefore, the enthalpy of immersion measurements can be used as an input into the VOCG model to characterise the surface energetics of a given solid.

By applying the VOCG approach and its laws of exclusion, equation 1-29 becomes:

$$H_{sl} = H_s^o + H_l - 2\left[\left(\sqrt{H_s^{LW} H_l^{LW}}\right) + \left(\sqrt{H_s^+ H_l^-}\right) + \left(\sqrt{H_s^- H_l^+}\right)\right] \qquad \textit{Equation 1-30}$$

Substituting equation 1-28 into equation 1-30, we get equation 1-31:

$$-h_i = -H_l + 2\left[\left(\sqrt{H_s^{LW} H_l^{LW}}\right) + \left(\sqrt{H_s^+ H_l^-}\right) + \left(\sqrt{H_s^- H_l^+}\right)\right] \qquad \textit{Equation 1-31}$$

Equation 1-31 can be used to compute the surface energy components of a particular mineral surface which are:

a) the Liftshitz-Van der Waals component of the surface energy, H_s^{LW};
b) the acidic component of the surface energy, H_s^+;
c) the basic component of the surface energy, H_s^-.

This is achieved by measuring the enthalpies of immersion of a given mineral in 3 different probe liquids, preferably one non-polar liquid as well as 2 polar liquids. The probe liquids should be well characterised in terms of their enthalpic components, i.e. the Liftshitz-Van der Waals and polar enthalpic components of each probe liquid

should be known. The following procedure is used to calculate the surface energy components:

1. Calculating the Liftshitz-Van der Waals component (H_s^{LW}).

The non-polar liquid only has the Liftshitz-Van der Waals component, H_L^{LW}. Therefore, the non-polar liquid interacts with the mineral surface only via the Liftshitz-Van der Waals forces. The acid and base components (H_l^+ and H_l^-) are equal to zero for the non-polar liquid. Thus, the second 2 terms on the right-hand side of equation 1-31 are equal to zero. The Liftshitz-Van der Waals component (H_s^{LW}) of the minerals is calculated by direct substitution into equation 1-31. It must be noted that the H_L^{LW} and H_L of n-hexane, the non-polar liquid used in this study, are known terms from the literature and are shown in Table 3-2 under Section 3.5.1.

2. Calculating the acidic (H_s^+) and basic (H_s^-).

Having calculated H_s^{LW}, only two unknowns remain, viz: H_s^+ and H_s^-. The polar liquids have both the Liftshitz-Van der Waals component as well as the polar components. Therefore, enthalpies of immersion of the mineral powder in the 2 polar solvents are a result of both the Liftshitz-Van der Waals and the polar interactions. Substitution in equation 1-31 results in 2 equations with 2 unknowns. These two equations can be solved simultaneously to obtain H_s^+ and H_s^-. It must be noted that the H_L^{LW}, H_L, H_L^+ and H_L^- of water and formamide, the 2 polar solvents used in this study, are known terms from the literature and are shown in Table 3-2 under Section 3.5.1.

The polar component of the mineral surface, H_S^{AB} is calculated from H_s^+ and H_s^- as shown in equation 1-32:

$$H_s^{AB} = \sqrt{(H_s^+ H_s^-)} \qquad \textit{Equation 1-32}$$

The total surface energy of the mineral surface, H_s^T is a summation of the Liftshitz-Van der Waals component, H_s^{LW} and the polar component, H_S^{AB} as shown in equation 1-33:

$$H_s^T = H_s^{LW} + H_s^{AB} \qquad \textit{Equation 1-33}$$

1.6.3 Important wettability parameters derived from the enthalpy of immersion

1.6.3.1 Relative surface polarity of mineral surfaces

Mineral surfaces are heterogeneous, that is they consist of a number of chemically different sites. Some sites are polar while some are non-polar. It is possible to characterise the relative surface polarity of different minerals using their surface energy components. The ratio of the polar component of the surface energy to the total surface energy has been used by some researchers as an indicator of relative surface polarity (hydrophilicity) of a given surface (Ho et al., 2010; Ali et al., 2013). The relative surface polarity, k_{rsp} is calculated as shown in equation 1-34:

$$k_{rsp} = \frac{H_S^{AB}}{H_S^T} \qquad \textit{Equation 1-34}$$

1.6.3.2 Energy of interaction of particles and bubbles immersed in water

Since the flotation process involves particle-bubble interactions in water, it is the interfacial free energy of particles and bubbles immersed in water, ΔG_{pwb} that is fundamental and relevant to the flotation studies. ΔG_{pwb} gives information on whether the attachment of a particle to a bubble in water is thermodynamically feasible. If $\Delta G_{pwb} < 0$, bubble-particle attachment occurs spontaneously. The more negative the ΔG_{pwb}, the stronger the hydrophobic force and consequently the greater the probability of bubble-particle attachment in water. This should translate to improved flotation response in a quiescent system where particle-bubble detachment is negligible. According to van Oss (2003), ΔG_{pwb} is calculated according to equation 1-35.

$$\Delta G_{pwb} = \left(\sqrt{H_p^{LW}} - \sqrt{H_b^{LW}}\right)^2 - \left(\sqrt{H_p^{LW}} - \sqrt{H_w^{LW}}\right)^2 - \left(\sqrt{H_b^{LW}} - \sqrt{H_w^{LW}}\right)^2 +$$

$$2\left[\sqrt{H_w^+}\left(\sqrt{H_p^-} + \sqrt{H_b^-} - \sqrt{H_w^-}\right) + \sqrt{H_w^-}\left(\sqrt{H_p^+} + \sqrt{H_b^+} - \sqrt{H_w^+}\right) - \sqrt{H_p^+ H_b^-} - \sqrt{H_p^- H_b^+}\right]$$

Equation 1-35

where the subscripts *p, w* and *b* represent particle, water and bubble respectively.

It must be noted that the H_W^{LW}, H_w^+ and H_W^- are known terms from the literature and are shown in Table 3-2 under Section 3.5.1. Air bubbles are super hydrophobic and the H_b^{LW}, H_b^+ and H_b^- terms are all equal to zero (van Oss et al, 2005). It is expected that the ΔG_{pwb} parameter is indirectly related to the flotation response because the more hydrophobic the particle is, the less the energy of interaction between the particle

and the bubble. On the contrary, the less hydrophobic the particle is, the higher the energy of interaction between the particle and the bubble. There is limited work conducted to investigate the relationship between the ΔG_{pwb} parameter and the microflotation response in literature. Using inverse gas chromatography (iGC), Rudolph and Hartmann (2017) found that the magnitude of the energy of interaction between a particle and a bubble was indirectly related to the microflotation recovery especially for the small fraction of high energetic site on apatite, magnetite and quartz. One of the objectives of this thesis was therefore to investigate the relationship between the ΔG_{pwb} parameter and the microflotation response.

1.6.3.3 Work of adhesion

The work of adhesion, W_{adh} is defined as the difference in interfacial energy between adhering and individual phases, such as a liquid on a solid. The work of adhesion gives an indication of the strength of a bond formed between two materials. The higher the work of adhesion, the stronger the bond. On the contrary, the lower the work of adhesion, the weaker the bond. In the context of solid-liquid interactions, the work of adhesion is an indication of the affinity of a given liquid for a particular solid. The work of adhesion is related to the contact angle through equation 1-36.

$$W_{adh} = \Upsilon_{lv}(1 + cos\theta) \qquad \textit{Equation 1-36}$$

where Θ = contact angle formed between the solid mineral surface and air;

W_{adh} = the work of adhesion

This relationship has been developed in the 19th century and has been extensively reviewed in Surface Chemistry of Froth Flotation, volume 2, pg. 356 by (Rao & Leja, 2004b). Equation 1-36 implies that any changes in hydrophobicity (contact angle) translates to a corresponding change in the work of adhesion at constant temperature. There has been some definitive work on relating the contact angle induced on mineral surfaces to their flotation performances in the pulp phase (e.g. Prestidge & Ralston 1996; Crawford 1986; Crawford & Ralston 1988). It follows that there should be a relationship between the work of adhesion and floatability. However, there is limited work conducted to investigate this relationship. One of the objectives of this thesis is to explore the relationship between the work of adhesion and the flotation response.

The work of adhesion is directly related to the surface energetics of the solid surface and it can alternatively be calculated from the surface energies by equation 1-37 (Ali et al., 2013):

$$W_{adh} = 2\left[\left(\sqrt{H_s^{LW} H_l^{LW}}\right) + \left(\sqrt{H_s^{+} H_l^{-}}\right) + \left(\sqrt{H_s^{-} H_l^{+}}\right)\right] \qquad \textit{Equation 1-37}$$

Substituting equation 1-37 into equation 1-31 gives equation 1-38 which was used to calculate the work of adhesion in this study.

$$W_{adh} = -h_i + H_l \qquad \textit{Equation 1-38}$$

In the flotation context, it is the work of adhesion of water that is of interest. The higher the work of adhesion, the stronger the affinity the mineral surface has for water and consequently the less floatable the mineral.

1.7 SUMMARY AND GAP ANALYSIS

The literature review has shown that mineral surface hydrophobicity is central to the flotation process. Hydrophobicity is known to influence both the pulp phase and froth phase processes. With regards to the pulp phase, it has been established that for a given particle size, a critical hydrophobicity is required before flotation occurs. Above the critical hydrophobicity, the flotation response significantly increases. The reason for the increase in attachment efficiency with increasing particle hydrophobicity has been attributed to increased hydrophobic forces of attraction between the particle and the bubble as well as reduced induction time. The more hydrophobic a mineral particle is, the greater its ability to destabilise the wetting film and consequently the more stable the particle-bubble aggregate. It has also been found that the induction time decreases with an increase in particle contact angle (hydrophobicity). Hydrophobicity may be inherent or be induced by a collector. The addition of collector has been shown to improve the kinetics of film thinning and destabilise the films so that they can rupture expeditiously forming bubble-particle aggregates. It was further concluded that the collector creates the hydrophobic force that can overcome the repulsive van der Waals and electrostatic forces present in wetting films.

With regards to the froth phase, froth stability has been shown to increase with increasing particle hydrophobicity. Maximum froth stability has been shown to be

attained when froth contains particles of moderate hydrophobicity. Strongly hydrophobic particles result in rapid bubble coalescence and thus destabilise the froth.

Particle wettability has been characterised using inverse gas chromatography (iGC), time of flight secondary ion mass spectroscopy (ToF-SIMS), induction time measurements and the contact angle. However, the methods have their limitations. The iGC and ToF-SIMS do not simulate real flotation conditions as the iGC is a gas phase technique while ToF-SIMS studies the mineral particles under very high vacuum. The contact angle is straight-forward and well-understood in the context of flat, smooth and ideal surfaces. However, the mineral is encountered in the form of powder in real flotation systems. The Washburn method uses powders but has been shown it is difficult to get reliable, meaningful and reproducible contact angle data using this method.

This thesis has investigated the use of the enthalpy of immersion as a surface characterisation tool for mineral surface hydrophobicity. The enthalpy of immersion is the enthalpy change as a result of replacing the solid-gas interface with the solid-liquid interface during the immersion process. The enthalpy of immersion is easily measurable in a solution calorimeter experiment at conditions typical of those prevailing in real flotation conditions. The literature review has shown that the enthalpy of immersion is an established method in characterising the wettability of various materials in different fields. Some of the fields include estimation of surface areas, silica studies, zeolites, and carbon black and charcoal studies. Despite being an established surface characterisation tool, the enthalpy of immersion has been applied only to a limited extent in the mineral processing field. Although there is abundant literature relating flotation recovery to contact angle, the relationship between the enthalpy of immersion and floatability has not been investigated to any significant extent. Thus, a major objective of this research is to investigate the use of the enthalpy of immersion as a surface characterisation tool to determine mineral hydrophobicity and then to relate this to flotation performance.

It has also been shown in the literature review that the enthalpy of immersion measurements can be input into the VOCG model to characterise the surface energetics of different minerals. The characterisation of the mineral surface energetics is very important since the efficiency of the flotation process depends on the

differences in surface energies of the valuable minerals and gangue minerals. Furthermore, the interfacial energy of interaction between particles and bubbles immersed in water as well as the work of adhesion which are fundamental parameters in wettability studies, can be calculated using the surface energy components of different minerals. This thesis has thus also investigated the use the enthalpy of immersion measurements to systematically characterise the surface energetics, the interfacial energy of interaction between particles and bubbles immersed in water as well as work of adhesion of minerals of different types (metallic sulphides, elemental, silicate and phyllosilicate minerals).

1.8 HYPOTHESES

1. The enthalpy of immersion is an indicator of the hydrophobicity of a given mineral because the enthalpy of immersion is a direct measure of the heat absorbed or produced when water interacts with the surface of the mineral. This is, in turn directly related to wettability of the mineral through interactions involving, for example, hydrogen bonding. Provided that factors related to the cell hydrodynamics (e.g. bubble size, superficial gas velocity and energy dissipation) are maintained constant, the enthalpy of immersion would thus provide an indication of the extent to which the mineral particle will attach to a bubble in a microflotation cell and hence be recovered in such a cell.
2. The enthalpy of immersion can be used to characterise the surface energetics of different minerals. This is because the chemically different sites present in on a mineral surface will interact differently with probe liquids of different polarities. Using the enthalpy of immersion, the application of the van Oss-Chaudhury-Good (VOCG) model then allows the calculation of the surface energetics of the minerals.

CHAPTER 2

2 RESEARCH OBJECTIVES

2.1 OVERALL THESIS OBJECTIVES

The main objective of this work was to investigate the use of the enthalpy of immersion to characterise mineral surface hydrophobicity and to relate this to the flotation performance in a microflotation cell. As an intermediate step, the enthalpy of immersion values of different minerals in water were compared to the corresponding powder contact angle values. This intermediate step is important in order to confirm that the enthalpy of immersion is related to the more accepted, and better known, measure of mineral surface wettability. It will then be shown that the enthalpy of immersion is in fact a much more sensitive and more widely applicable measure of hydrophobicity of mineral particles typical of those used in the flotation process.

2.1.1 Specific objectives

The specific objectives of this thesis were:

1. To measure and compare the enthalpies of immersion in water, contact angles and the flotation response as indicated by the first-order flotation rate constant for the different pure minerals and xanthate-coated sulphide minerals at different percentage surface coverages. The relationships between the enthalpy of immersion, contact angle and flotation response were then investigated.
2. To compare the enthalpies of immersion of different pure minerals in different probe liquids.
3. To compare the surface energetics, the interfacial energy of interaction between particles and bubbles immersed in water and work of adhesion of different minerals using different probe liquids.
4. To investigate the relationship between the surface energetics, the interfacial energy of interaction between particles and bubbles immersed in water, work of adhesion, contact angle and flotation response.

2.2 KEY QUESTIONS

The major key question driving this work was:

"What is the relationship between the enthalpy of immersion and microflotation performance?"

Other key questions which will help answering the major key question were:

1. Do differences in mineral types have any effect on the magnitude of the enthalpies of immersion in water, contact angle and microflotation response?
2. Is immersion calorimetry capable of assessing the changes in the physicochemical properties of mineral surfaces as a result of collector adsorption?
3. Do differences in the polarity of wetting liquids have any effect on the magnitude of the enthalpies of immersion for the same mineral?
4. What is the relationship between the enthalpy of immersion and the contact angle?
5. Will different minerals producing the same enthalpies of immersion produce similar microflotation recoveries as well as flotation kinetics?
6. Is it possible to characterise the surface energetics, the interfacial energy of interaction between particles and bubbles immersed in water and work of adhesion using the enthalpy of immersion measurements?
7. Is it possible to distinguish minerals according their surface energetics, the interfacial energy of interaction between particles and bubbles immersed in water and work of adhesion?
8. What is the relationship between the surface energetics, the interfacial energy of interaction between particles and bubbles immersed in water, work of adhesion, contact angle and flotation response?

2.3 RESEARCH APPROACH

Solution calorimetry was employed in this work to measure the enthalpies of immersion of different minerals in different probe liquids. Solution calorimetry is the measurement of the heat of solution of a solid immersed in a liquid. The Washburn method and the microflotation technique were also employed to measure the powder

contact angles and the flotation response of different minerals, respectively. The microflotation technique provides a low energy, quiescent system which allows the investigation of the effects surface properties on the flotation process since it essentially measures the overall effectiveness of the bubble-particle attachment. Different mineral types were chosen in this study, viz: metallic sulphides, elemental silicate and phyllosilicate minerals. Potassium amyl xanthate was also used to confer hydrophobicity onto sulphide minerals. For solution calorimetry, different wetting liquids were used, viz: water, n-hexane and formamide. This work was organised into four phases with each phase designed to answer specific research questions.

2.3.1 Phase 1 - Model systems

Relationship between the enthalpy of immersion, contact angle and microflotation response using model systems.

The first set of experiments included the following:

a. Measuring the enthalpies of immersion of xanthate-coated galena and realgar at different surface coverages;
b. Measuring the contact angles for xanthate-coated galena and realgar at different surface coverages;
c. Measure the corresponding microflotation response;
d. Determine the relationship between the enthalpy of immersion and contact angle;
e. Determine the relationship between contact angle and microflotation response;
f. Determine the relationship between the enthalpy of immersion and microflotation response.

Key questions:

1. *Is immersion calorimetry capable of assessing the changes in the physicochemical properties of mineral surfaces as a result of collector adsorption?*
2. *What is the relationship between the enthalpy of immersion, contact angle and microflotation response?*

2.3.2 Phase 2 - Different pure minerals

Relationship between the enthalpy of immersion, contact angle and microflotation response using pure minerals.

The steps (a – f) above were repeated using different pure mineral types, viz: metallic sulphides, elemental, silicate and phyllosilicate minerals. It is expected that the minerals will have different enthalpies of immersion, contact angles and different microflotation response because they have different surface properties.

Key questions:

1. *Do differences in mineral types have any effect on the magnitude of the enthalpies of immersion in water, contact angle and microflotation response?*
2. *Will the relationship between h_i, contact angle and microflotation response for the model system be sustained for different pure minerals?*
3. *Will different minerals producing the same enthalpies of immersion produce similar microflotation response?*

2.3.3 Phase 3 - Enthalpy of immersion in different probe liquids and characterisation of the surface energetics of different minerals

Relationship between the surface energetics, work of adhesion, contact angle and microflotation response.

The following experiments were undertaken:

a. Measure the enthalpies of immersion of different pure minerals in water, n-hexane and formamide;
b. Calculate the surface energy (and its components), the interfacial energy of interaction between particles and bubbles immersed in water, the work of adhesion of different minerals against different probe liquids;
c. Determine the relationship between the surface energetics, the interfacial energy of interaction between particles and bubbles immersed in water, work of adhesion, contact angle and the microflotation response.

Key questions:

1. *Is it possible to characterise the surface energetics, the interfacial energy of interaction between particles and bubbles immersed in water, and work of adhesion using the enthalpy of immersion measurements?*
2. *Is it possible to distinguish minerals according to their surface energetics, the interfacial energy of interaction between particles and bubbles in water, and work of adhesion?*

2.3.4 Phase 4 - Mineral mixtures

Relationship between the enthalpy of immersion and the mineral composition of binary mineral mixtures

The following experiments were undertaken:

a) Measure the enthalpies of immersion of binary mineral mixtures with varying mineral composition.
b) Measure the enthalpies of immersion of binary mineral mixtures with varying mineral composition in water, n-hexane and formamide;
c) Calculate the surface energy (and its components) and the work of adhesion of binary mineral mixtures with varying mineral composition against different probe liquids.

Key questions:

1. *What is the effect of mineral composition on the enthalpy of immersion for binary mineral mixtures?*
2. *What is the effect of mineral composition on the surface energetics of binary mineral mixtures?*

CHAPTER 3

3 EXPERIMENTAL DESIGN

3.1 INTRODUCTION

This chapter describes how the enthalpies of immersion, the powder contact angles and the microflotation response of different minerals were determined using solution calorimetry, the Washburn method and the microflotation technique, respectively. The relationships between the enthalpy of immersion, the corresponding contact angle and microflotation experiments was then investigated. The experimental procedure is schematically summarised in Figure 3-1.

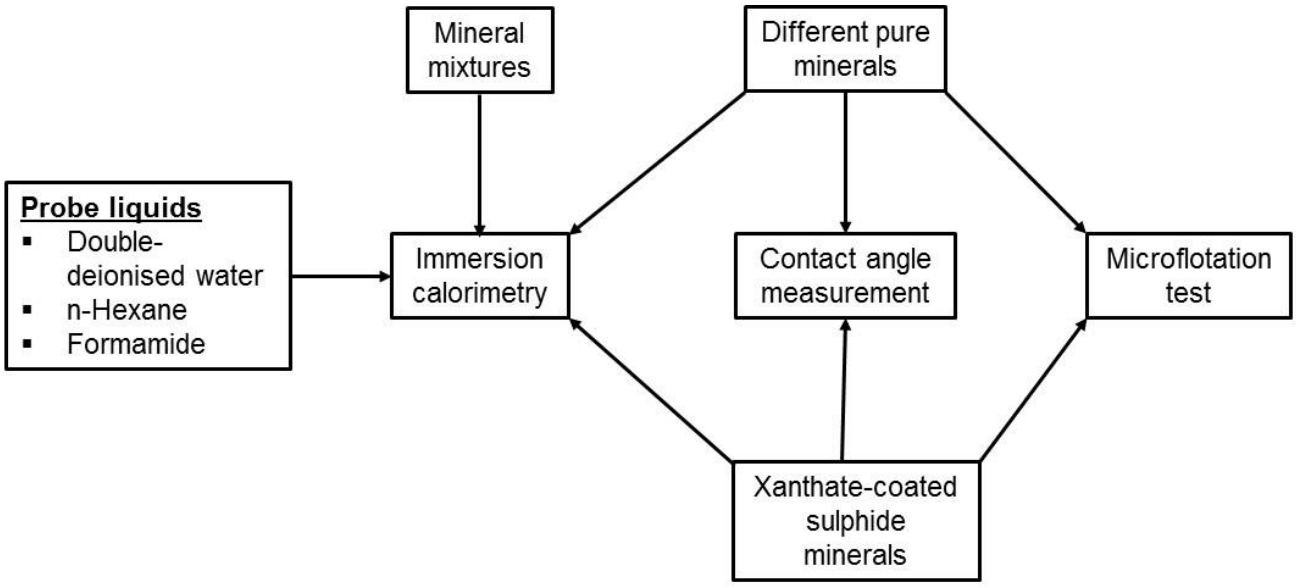

Figure 3-1: Schematic of the experimental programme.

3.2 ORGANISATION OF THE TEST WORK

The experimental work was organised in the following order:

- Received mineral samples of different types, viz: metallic sulphides, elemental, silicate and phyllosilicate minerals.
- Preparation and handling of the different minerals.
- Mineralogical analysis of the mineral sample using X-ray diffraction (XRD) using the Rietveld method.

- Preliminary solution calorimetry experiments to ensure that the calorimeter was operating correctly and to establish optimum calorimeter settings to measure the enthalpies of immersion in this study.
- Blank tests to determine the heats produced during breaking the ampoules.
- Preparation of the model systems, viz: galena and realgar samples whose surfaces have been pre-treated to different degrees of hydrophobicities using different dosages of sodium amyl xanthate.
- Enthalpy of immersion measurements for all the different pure minerals and model system using double deionised water as the wetting liquid.
- Contact angle measurements for all the different pure minerals and model systems.
- Collectorless flotation of the different pure minerals to determine the natural hydrophobicities of the minerals.
- Flotation of the model system by re-suspending the hydrophobised galena and realgar particles.
- Enthalpy of immersion measurements for all the different pure minerals in n-hexane and formamide.

3.3 MATERIALS

To meet the objective of this study, different mineral types were required. Different minerals have different crystalline structures and hence different extents of wettability as well as different subsequent flotation behaviours as previously discussed in Section 1.3.1.1. The minerals were carefully chosen to cover a variety of mineral types as follows:

1. Metallic sulphide minerals – galena, realgar and orpiment;
2. Elemental minerals – graphite;
3. Phyllosilicate minerals – talc
4. Silicate minerals – mica, albite, wollastonite and diopside.

Table 3-1 shows the 9 minerals that were investigated in this thesis. Realgar and orpiment were received from Perth Industrials. The rest of the minerals were received from Wards Natural Resources, New York. The minerals were received as chunks of up to 150 mm in diameter. The mineralogical composition of all the minerals was determined using X-ray diffraction (XRD) using the Rietveld method and the results

are shown in Table 3-1. Full XRD results are shown in Appendix A. It is clear from Table 3-1 that the majority of the minerals were extremely pure except talc which was found to contain 12.2% dolomite and 3.3% quartz. This was taken into account when interpreting the results obtained for talc.

3.4 MINERAL PREPARATION AND HANDLING

Size reduction of all the different mineral samples was achieved by means of manual grinding using a ceramic mortar and pestle. This method of grinding was preferred as it does not introduce metallic ions which would alter the surface properties of the mineral surfaces. Representative mineral samples were obtained by splitting the mineral powder into 10 samples.

The Brunauer–Emmett–Teller (BET) technique was used to determine the specific surface areas of the mineral powders and the results are shown in Table 3-1. The samples were dried at 90°C before the measurement of nitrogen adsorption. Higher operating temperatures lead to the oxidation of sulphide minerals as discussed in Section 3.7.6.

The particle densities of the different minerals were quoted from Battey and Pring (1997).

After grinding, all the mineral samples were immediately purged under nitrogen in order to exclude moisture that would affect the solution calorimetry experiments. All metallic sulphide mineral samples were immediately stored under N_2 at -30 °C to minimise surface oxidation. Furthermore, all the mineral samples were evacuated in a vacuum oven at a pressure of 100 mBar and temperature of 40°C over a period of 4 days to drive off moisture prior to the enthalpy of immersion measurements. Preliminary investigations showed that a constant mass of mineral sample was achieved after 4 days in the vacuum oven. This implies that all pre-adsorbed moisture has been driven off.

Although extensive precautions were taken to minimise the mineral surface oxidation of the sulphide minerals, it is important to note that any surface oxidation would not affect the relationship between the enthalpy of immersion and the subsequent microflotation response since each of the sulfide mineral samples for the enthalpy of immersion measurements and microflotation tests were exposed to the same

environmental conditions prior to the experiments. In other words, it is assumed that surface properties of each particular mineral were maintained constant in all the experiments.

Table 3-1: XRD results, BET specific surface areas and particle densities for different minerals.

Sample	Expected Mineral	Chemical Formula	Mineralogical Composition (%)	BET Specific Surface Area (m^2/g)	Mineral density (g/cm^3)
1	Galena	PbS	100	0.7747	7.58
2	Realgar	As_4S_4	100	4.8117	3.48
3	Orpiment	As_2S_3	100	4.2607	3.49
4	Talc	$3MgO.4SiO_2.H_2O$	84.5	19.5136	2.90
5	Graphite	C	100	7.1236	2.16
6	Albite	$4(Na(AlSi_3O_8))$	98.5	5.7863	3.26
7	Diopside	$4(Ca(Mg,Fe^{2+})AlFe^{3+}Ti(Si,Al)_2O_6$	100	4.7511	3.26
8	Wollastonite	$2(Ca_3(Si_3O_9))$	100	4.2762	2.90
9	Mica	$KAl_2(AlSi_3O_{10})(OH)_2$	100	24.0038	2.90

3.5 REAGENTS

Double deionised water at a pH of 6.5 was used in all experiments.

3.5.1 Probe liquids

One of the objectives of this thesis was to determine and compare the surface energetics of different pure minerals using the enthalpy of immersion measurements. As highlighted in Section 1.6.2, this requires the use of three probe liquids of different polarities as wetting liquids. Water, n-hexane and formamide were chosen in this study as they are the most widely used probe liquids in such experiments. The water used is in the form of double deionised water at a pH of 6.5. Formamide and n-hexane were received from Sigma Aldrich (Pty) Limited with purities of ≥ 99.5% and ≥ 97% respectively. Both n-hexane and formamide were dried over molecular sieves (3 A° porosity) prior to the experiments in order to remove water. The probe liquids need to be well-characterised in terms of their enthalpic components and these are shown in Table 3-2 (Douillard et al., 2007).

Table 3-2: The surface energy components and chemical structures of the different probe liquids used in this study.

	Water	**n-hexane**	**Formamide**
Non-polar term, H_l^{LW} (mJ/m^2)	36	48.4	55.2
Acidic term, H_i^+ (mJ/m^2)	41	0	3.23
Basic term, H_i^- (mJ/m^2)	41	0	56
Surface enthalpy, H_l (mJ/m^2)	118	48.4	82.1
Chemical structure	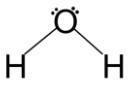	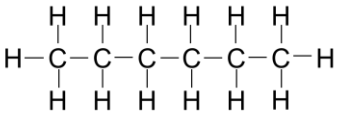	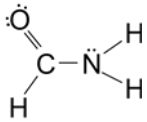

3.5.2 Characteristics of the probe liquids

Table 3-2 shows that the three probe liquids have different enthalpic components and are therefore expected to interact differently with a particular mineral. It must be emphasised that the major reason behind the determination of the enthalpies of immersion in different probe liquids was to characterise the surface energetics of the

different minerals using the VOCG model. Therefore, little attention will be devoted to an in-depth investigation of the molecular-level interactions between the different probe liquids and the different mineral surfaces.

It is clear from Table 3-2 that water is amphoteric, with a balance of the acidic and basic components. Thus, water is self-associated containing both the basic oxygen and the acidic hydrogens. Therefore, water interacts with both non-polar and polar components (both basic and acidic) of the mineral surfaces. The measured enthalpies of immersion of minerals in water is the net sum (average) of the contributions from the non-polar and polar sites on the mineral surface. A more negative enthalpy of immersion in water is an indication of a more polar mineral surface. On the contrary, a less negative enthalpy of in water is an indication of a less polar mineral surface. A mineral with a higher proportion of polar sites than hydrophobic sites (pre-dominantly hydrophilic) is expected to interact more exothermically with water than a predominantly hydrophobic mineral surface. The values of the enthalpy of immersion in water are valuable for the comparison of the overall polarity of different minerals. The use of water as a probe liquid provides knowledge of the hydration enthalpies, which is of considerable interest when assessing the wettability (hydrophilicity or hydrophobicity) of mineral powder. This is because water is used as a medium in the process of froth flotation.

It is clear from Table 3-2 that n-hexane has only the non-polar component and has no acidic and basic component. Therefore n-hexane will interact with the non-polar components of the mineral surface only, and hence the enthalpy of immersion of n-hexane is a characteristic of the non-polar sites on the mineral surface.

Although formamide is amphoteric as water, formamide is mostly basic. Formamide interacts with the non-polar sites as well as the polar sites. However, the enthalpy of immersion of a particular mineral in formamide is an indication of the acidity of the mineral surface because of the relatively high basicity of formamide. This is because the basic component of formamide will interact only with the acidic component of the mineral surface. The acidic component of the mineral surface comprises of the acidic protons, electron acceptor sites, and hydrogen from neutral or weakly acidic hydroxyls. Thus, the more exothermic the enthalpy of immersion of minerals in formamide, the more acidic the mineral surface. On the contrary, the less exothermic the enthalpy of

immersion of minerals in formamide, the less acidic the mineral surface. Therefore, formamide is used to detect the acidic sites on the mineral surface.

3.5.3 Collector

In order to assess the relationship between the enthalpy of immersion and the hydrophobicity of collector-coated minerals, sulphide mineral samples whose surfaces were treated to different but known degrees of hydrophobicity using thiol collectors were considered appropriate. Thiol collectors continue to dominate in the base metal sulphide (BMS) and platinum group mineral (PGM) flotation industry. Thiol collectors are hetero-polar molecules consisting of the reactive head group and a hydrophobic alkyl chain. It has been established that an increase in the hydrocarbon chain length of a collector results in a decrease in the solubility of the hydrophobic species formed (Hamilton and Woods, 1979; Kim et al, 2000). This is independent of whether a metal thiolate or a dithiolate is formed as the hydrophobic species. Therefore, potassium amyl xanthate (PAX) with 5 carbons in its hydrocarbon chain length was chosen as the hydrophobising agent as it can create a very hydrophobic surface at higher dosages. The potassium amyl xanthate (PAX) was supplied by Senmin (Pty) Limited in powder form with a purity of 99.2%.

3.6 MODEL SYSTEM

A model system with well-controlled hydrophobicity is required for the proof of concept in order to assess the relationship between the enthalpy of immersion and the hydrophobicity of collector-coated minerals. This is especially important for the proof of concept. A system is needed where the mineral surface can be modified to different and accurately known levels of hydrophobicity by varying the degree of collector surface coverage. The galena / amyl xanthate (PAX) system was considered a perfect model system for this purpose. Galena is a simple monatomic mineral that has been widely studied in fundamental flotation research (Ralston, 1994; Prestidge and Ralston, 1996; Grano et al, 1997). It has been classified as a moderately hydrophobic mineral (Ozcan, 1992; Wills and Napier-Munn, 2006). Mineral surfaces are reported to be heterogeneous, consisting of hydrophobic and hydrophilic sites. A hydrophobic mineral is predominantly hydrophobic having a higher proportion of hydrophobic sites. On the contrary, a hydrophilic mineral is predominantly hydrophilic having a higher proportion of hydrophilic sites. The collector molecules displace the OH-groups from

the hydrophilic sites on the galena surface after the introduction of the collector. The hydrophobic hydrocarbon chain length extends into the liquid phase, thereby rendering the galena surface hydrophobic. The degree of hydrophobicity depends on the surface coverage which also depends on the concentration of the collector solution. Untreated galena has a higher concentration of OH-groups and as the surface coverage of the PAX collector increases, the galena surface will become increasingly hydrophobic. In order to investigate whether the relationship between the enthalpy of immersion and the hydrophobicity of collector-coated minerals is mineral specific, the realgar-amyl xanthate system was also investigated in this thesis.

3.6.1 Surface modification procedure

Molar dosages of PAX were added to the galena samples in a controlled manner so as to achieve different approximate degrees of surface coverages, viz: 0%, 16%, 25%, 50%, 75% and 100%. The PAX surface coverages were calculated based on the active content of PAX and also on the BET specific surface areas shown in Table 3-1. It is assumed that the cross-sectional head area of PAX to be 28.8 Å (Grano et al, 1997).

10 g of freshly ground mineral powder was weighed and prepared into a 100 mL slurry. The slurry was deslimed by sonicating for cycles of 30 seconds followed by decanting until a clear supernatant was obtained. A collector solution of PAX was prepared in such a way that 0.5 mL of the solution contained the number of moles of collector equivalent to a particular surface coverage. The 0.5 mL of the collector solution was pipetted into the mineral slurry and conditioning was allowed for 8 minutes with stirring at 200 rpm. After conditioning, the mineral particles were allowed to settle, and the supernatant was decanted out. This was followed by washing of the galena particles in excess double deionised water to remove any collector molecules that may not have adsorbed on the galena surface. The wet mineral particles were immediately dried in a vacuum oven (100 mBar at 40°C) over a period of 4 days to drive off moisture until a constant mass was achieved. The same methodology was used by Prestidge and Ralston (1996) in their study to investigate the influence of ethyl xanthate coverage on the wettability of galena particles using contact angle measurements. They report that X-ray photoelectron spectroscopy (XPS) and Fourier-transform infrared spectroscopy (FTIR) have shown that this treatment has a negligible influence on the form and

surface coverage of xanthate collector. The chances of mineral surface oxidation were negligible because evacuation excludes both air and moisture.

3.6.2 Adsorption tests

The supernatant was analysed for the concentration of residual potassium amyl xanthate collector using Ultraviolet–visible spectrophotometry (UV-VIS) at the characteristic absorption wavelength of 301 nm. No residual xanthate collector was detected in the supernatant. This means that all the collector adsorbed onto the galena and realgar surfaces. A similar finding was made by Taguta et al (2017) who reported that the entire amount of collector dosed adsorbs onto the mineral surface at low collector concentrations equivalent to sub-pseudomonolayer coverages.

3.7 SOLUTION CALORIMETRY

All chemical, physical and biological reactions are exothermic or endothermic, viz accompanied by heat release or heat gain. Solution calorimetry is the measurement of the heat of solution of a solid immersed in a liquid. A calorimeter is defined as an instrument that enables the quantitative measurement of the heat released or gained in any process.

3.7.1 Description of the precision solution calorimeter

The Precision Solution Calorimeter is a single-position, semi-adiabatic (isoperibolic) calorimeter for high precision measurements of the heat generated or consumed when a solid or liquid sample is dissolved or diluted into a solvent. The Precision Solution Calorimeter is intended for use with the TAM III Thermostat up to 80°C. Supplied by TA instruments, the precision solution calorimeter was used in this study to determine the enthalpies of immersion at 30°C. The equipment has a liquid bath controlled to within 0.0001°C. The Precision Solution Calorimeter consists of three main parts, viz: the calorimetric unit, the calorimetric cylinder and the electronic functions. The calorimetric cylinder is mounted permanently in a thermostat and holds the calorimetric unit during the experiments. The calorimetric unit consists of a reaction vessel and a stirrer system. The reaction vessel is a thin-walled 100 mL or 25 mL Pyrex-glass reaction vessel fitted with a thermistor for sensing temperature and a heater for calibration and equilibration. The stirrer system consists of a motor and a gold stirrer. Apart from stirring, the gold stirrer also holds a glass, brittle ampoule containing the sample under investigation. The glass ampoule has a volume of 1.1 ml. The ampoule

is sealed with a silicone rubber and bees wax. During experiments, the stirrer system is inserted and locked onto the reaction vessel. The reaction between the sample and the wetting liquid is initiated by breaking the brittle, glass ampoule. Breaking of ampoules is achieved by pushing the entire stirrer system into the calorimetric cylinder. The calorimeter monitors the temperature change as a result of the reaction. Specifically, the precision solution calorimeter follows and monitors the reaction in real time by continuously observing the temperature offset as the reaction proceeds. The temperature offset is defined as the difference between the liquid bath temperature and the reaction vessel temperature. The glass ampoule, reaction vessel and the calorimetric unit are shown in Figure 3-2. The Precision solution calorimeter is equipped with a complete software package to control and analyse calorimetric experiments.

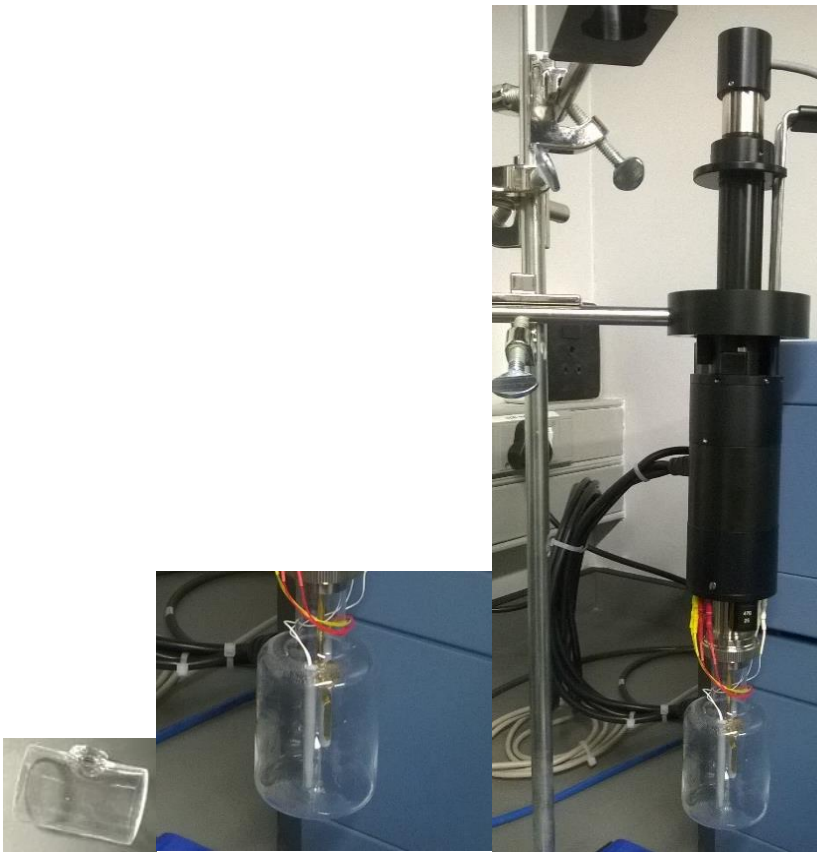

Figure 3-2 : Glass ampoule, pyrex reaction vessel and the calorimetric unit.

The calorimetric cylinder is mounted onto the thermostat which is part of the TAM III microcalorimeter. The TAM III microcalorimeter is shown in Figure 3-3.

Figure 3-3: The photograph of the TAM III microcalorimeter.

Precision solution calorimetry has been tested by Zimmerman et al. (1987) who measured the enthalpy of solution of CaF_2 in water as well as the enthalpies of immersion of different minerals in water. The results they got compared very well with those of previously published data. They further concluded that the calorimetric vessel is suitable for measuring enthalpies greater than 50 mJ. However, this value would depend on the sensitivity of the instrument used.

3.7.2 Calorimetry principles and energy balance

The heat release or gain accompanying a given process is observed by a temperature change in the calorimeter. Electrical calibration of the calorimeter is achieved by the introduction of a known quantity of electrical energy in a calibration experiment. The Precision Solution Calorimeter allows for the precise comparison between the calibration experiment and the actual experiment under investigation. The temperature changes accompanying both the calibration experiment and the actual experiment have to be as nearly identical as possible for accurate enthalpy of immersion measurements. The calorimetric software uses information obtained from the baseline temperature changes to mathematically adjust for the small heat changes due to mechanical stirring and exchange with the surroundings.

The calorimetric calculations are based on heat balance from the law of the conservation of energy. All the energy exchange with the surroundings and due to accumulation in the system must be accounted for according to equation 3-1:

$$-\frac{dQ}{dt} - \frac{dQ_F}{dt} = C\frac{dT}{dt} + k(T - T_S) \qquad \textit{Equation 3-1}$$

where $\frac{dQ}{dt}$ = heat flow due to the solution reaction or electrical calibration (W);

$\frac{dQ_F}{dt}$ = rate of energy dissipation caused by stirring or heating (W);

$C\frac{dT}{dt}$ = heat flow accumulated in the system (W);

$k(T - T_S)$ = rate of heat exchange between vessel and surroundings (W);

k = the heat exchange coefficient (W/K);

T_S = the temperature of the surroundings (K);

T = the temperature of the reaction solution (K);

C = the total heat capacity of the calorimetric vessel (J/K).

The precision solution calorimeter uses the heat balance in equation 3-1 to calculate the heat change due to the particular process under investigation.

3.7.3 Chemical validation of the precision solution calorimeter

Potassium chloride (KCl) dissolution has been extensively used as a standard test and validation reaction in solution calorimetry (Wadso & Goldberg, 2001). The assigned value of the enthalpy of dissolution of potassium chloride (NBS 1655) in distilled water with molality of 0.111 mol/kg at 25°C is 17.854 ± 0.017 kJ/mol (Wadso & Goldberg, 2001). Prior to the enthalpy of immersion measurements for the different pure minerals in this study, it was important to conduct chemical validation tests on the precision solution calorimeter to determine the suitability of the equipment. For a required molality of 0.111 mol/kg, ±300 g of KCl was dissolved in 100 mL double deionised water and the enthalpy of dissolution was measured at 30°C. For this purpose, 3 chemical calibration tests were conducted, and the results are presented in Section 4.3.

3.7.4 Enthalpy of immersion measurement procedure

The enthalpies of immersion measurements were determined using the precision solution calorimeter described above. The calorimeter was thermostated in a water bath, maintained at 30°C with a temperature precision of 0.0001°C. A glass ampoule

was weighed empty and the mass was recorded. Mineral sample was then loaded into the ampoule. The mineral sample was taken straight from the vacuum oven and adequate pre-cautions were taken to minimise exposure of the sample to air and moisture. The loaded ampoule was weighed. The mass of mineral sample loaded was the difference between the masses of the loaded and empty ampoule. The loaded glass ampoule was immediately sealed using a silicon rubber and melted beeswax. In the case of n-hexane, a silicon rubber seal and superglue were used to seal the ampoules as bees-wax was found to be soluble in n-hexane. The sealed ampoule was attached to the gold stirrer holder. All calorimetric experiments in this study were conducted using the 100 mL reaction vessel. 100 mL of wetting liquid was pipetted into the reaction vessel. As highlighted in Section 3.5.1, the wetting liquids were double-deionised water, formamide or n-hexane. Both n-hexane and formamide were dried over molecular sieves (3 A° porosity) prior the experiments in order to remove water. The stirrer was set at 300 rpm in all calorimetric experiments. The temperature offset was adjusted to be within ± 200 mK in all calorimetric experiments. This was achieved by either heating or cooling the reaction vessel. Once the required temperature offset was attained, the calorimeter was switched from the low-resolution mode to the high-resolution mode. The low-resolution mode is used for systems with relatively high heat change. Due to the very low energy associated with interfacial effects, the high-resolution mode was used in this study for better accuracy. The calorimetric unit was then mounted into the calorimetric cylinder. The system was allowed to equilibrate and stabilize before the start of a particular reaction. The criterion for initiating the reaction is that the baseline data should conform to the exponential baseline function. The standard deviation of the fit of the baseline data to the exponential temperature is calculated based on data from the previous 5 minutes of an ongoing experiment and should be ≤ 10 µK under the high-resolution mode. The energy input during calibration was 2 mJ and the duration of the immersion experiments was set at 10 minutes for all calorimetric experiments. Once the appropriate thermal baseline was achieved, the reaction was initiated by pressing down the calorimetric unit thereby breaking the ampoule. The SolCal software calculates the heat released or gained due to the reaction between the mineral powder and the wetting liquid. The heat change (mJ) due to the reaction was normalised relative to the surface area of the mineral sample thus yielding the enthalpy of

immersion per m^2 (mJ/m^2). Before the next experiment, the reaction vessel was cleaned by sucking out all the slurry and broken glass bits from broken glass ampoules by means of a vacuum pump. Double deionised water and a small amount of acetone was also used for cleaning the reaction vessel. The reaction vessel was rinsed as many times as possible to ensure it was clean.

3.7.5 Raw data output from precision solution calorimetry

The raw data output from the precision solution calorimeter experiment is a graph of the temperature offset as a function of time. A typical solution calorimeter response is shown in Figure 3-4 which shows the sequence of events in a typical calorimetric experiment. Electrical calibration was conducted before and after the particular reaction under investigation. It is seen from Figure 3-4 that the temperature offset drops immediately after the breaking of the glass ampoule, signifying the onset of the reaction. Furthermore, in this case the decrease in the temperature offset is indicative of an endothermic process taking place. The SolCal software uses the baseline and calibrations before and after the experiment to determine the heat change when a particular mineral powder is immersed in a particular wetting liquid. The SolCal software uses established heat balance equation to compute the heat change associated with a particular reaction from the temperature offset vs time graph (Section 3.7.2).

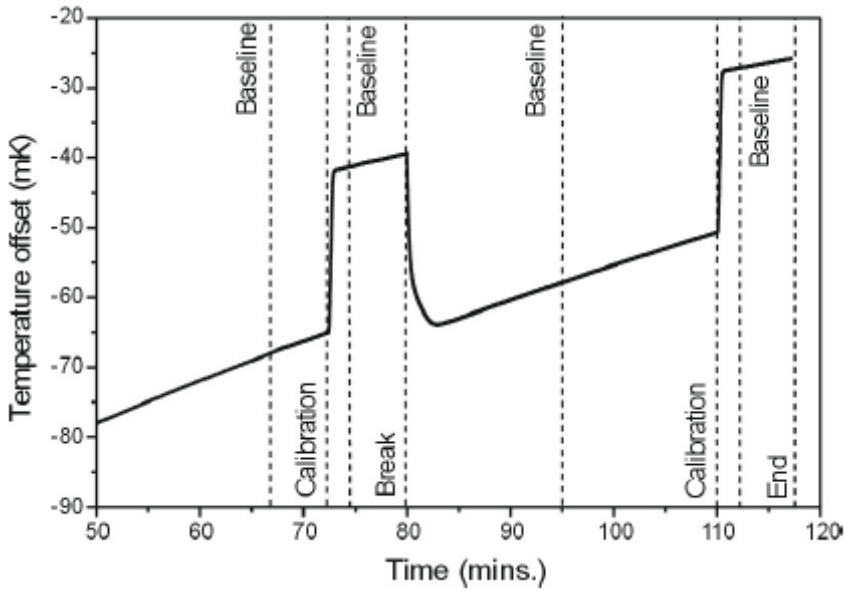

Figure 3-4: A plot of temperature offset as a function of time as a typical response of solution calorimeter experiments.

3.7.6 Important experimental considerations

Preliminary investigations have shown that the quality of the enthalpy of immersion measurements depends on a number of factors, viz: sample preparation, specific surface area of the mineral powder and dissolution of mineral surface ions.

3.7.6.1 Sample preparation

Preliminary investigations have shown that sample preparation has a considerable effect on the reproducibility and experimental success rates of the enthalpy of immersion measurements. Therefore, sample preparation should be as reproducible as possible. Pre-adsorbed moisture on mineral surfaces will obviously have an effect on the enthalpy of immersion measurements. Precautions were thus taken to minimise exposure of the mineral samples to air and moisture as much as possible prior to the enthalpy of immersion measurements. As highlighted in Section 3.4, all the mineral samples were evacuated for 4 days operating at a vacuum of 100 mBar and a temperature of 40°C. The mass of the samples was monitored as a function of time and it was found that after the 4 days, the mass of the samples remained constant. This implied that essentially all the pre-adsorbed water had been driven off, although it should be acknowledged that it is never possible to remove all the water from the mineral samples. It is important to note that the conditions of temperature and pressure for sample preparation used in this study were different from those used by Douillard et al. (2002) and Douillard et al. (2007) where talc and chlorite were stored under a vacuum of 10^{-3} Torr (1.3×10^{-3} mBar) at 150°C. Although the higher temperature is desirable in terms of ensuring that the samples were as dry as possible, there are important experimental considerations that led to the choice of this temperature. Sulphide minerals are not stable at high temperatures as they readily oxidise, and this alters their surface properties. Galena was shown to oxidise at a temperature as low as 52°C (Steger & Desjardins, 1980). For oxides, high temperatures are not problematic as their surface properties remain unaltered as temperature is increased. Furthermore, high temperatures lead to the decomposition of the xanthate collector and hence the choice of a temperature of 40°C. The rate of xanthate decomposition was shown to be 9.3×10^{-4} h^{-1} at 25°C; 1.7×10^{-2} h^{-1} at 50°C and 1.3×10^{-1} h^{-1} at 70°C (Shen et al., 2016). The choice of 40°C was also based on the sample preparation method of Prestidge and Ralston (1996) where they investigated the effect of ethyl xanthate coverage on the wettability of galena particles using contact angle

measurements. They reported that at such a temperature, the form and surface coverage of the adsorbed xanthate remained unaltered. This type of sample preparation method has been widely used for contact angle measurements, which is the traditional hydrophobicity measure for flotation minerals.

The focus of this study was to investigate the relationship between the enthalpy of immersion and the flotation response and to illustrate that the former parameter is a more robust indicator of wettability than contact angle. After evacuation at 100 mBars, there may be a small amount of residual air left on hydrophobic powders. However, the enthalpy of immersion, the flotation response and the contact angle measurements are subject to the same possibility of residual air, which allows comparisons and relationships to be formulated between these measurements. Furthermore, it could be argued that the presence of air represents a more realistic condition, in that in the real conditions under which minerals are treated there will be air present and so the enthalpy of immersion value measured provides a very good estimate of the relative wettability of an ore in an open, ambient system. The practical problem is that exposure to air is inevitable since irrespective of the magnitude of the vacuum, the mineral powder will still have to be transferred into the ampoule outside the vacuum system.

3.7.6.2 Surface area of mineral powder

Preliminary investigations also showed that a large specific surface area is required in order to obtain a considerable thermal effect in the calorimetric experiments. The larger the mineral surface area, the larger and better the calorimetric signal. Therefore, there was need to grind the mineral samples finer as indicated by the BET surface area shown in Table 3-1. It is assumed that the energy input occurring during fine grinding does not cause alterations or disruptions within the crystalline structure of the minerals. This is because the particle sizes obtained in this study are far larger than the crystalline size of the minerals and consequently the surface properties of the minerals are preserved during fine grinding. The maximum mass of mineral powder was loaded into the glass ampoule in order to have maximum possible surface area.

3.7.6.3 Dissolution of mineral surface ions

Preliminary experiments further showed that the dissolution of mineral surface ions greatly affects the enthalpy of immersion measurements. The raw data showed an

initial endothermic process followed by an exothermic process. The initial endothermic peak was attributed to the dissolution of the mineral surface ions. Thus, the measured enthalpy of immersion was the sum of the contributions from the dissolution process as well as the interaction of the mineral surface with water. For all enthalpy of immersion in water measurements, the wetting liquid was a saturated solution of the solid in water. This was done to suppress any contribution from the dissolution of mineral surface ions. In this case, the wetting liquid is always in equilibrium with a small amount of solid mineral phase, and hence the contribution of the enthalpy of dissolution of the solid is neglected. The same approach was employed by Zimmerman et al. (1987) and Douillard et al. (2002). To prepare the saturated solution of the solid in water, 20 g of the mineral was weighed out into a beaker and 200 mL of water was added to prepare a mineral slurry. The slurry was stirred overnight at 300 rpm to ensure that the water became saturated with mineral surface ions. The solids were allowed to settle, and the liquid phase was decanted out for use as wetting liquid. Preliminary tests using water as wetting liquid produced endothermic enthalpies of immersion, attributable to mineral surface ion dissolution. These endotherms disappeared when the saturated solution of the solids was used as wetting liquid.

3.7.7 Blank experiments

In a calorimetric experiment, there is heat release (or gain) associated with other sub-processes apart from the targeted mineral-wetting liquid interactions. These sub-processes include the breaking of glass ampoules and the vaporisation of the calorimetric liquid. Blank experiments were therefore conducted to determine the heat associated with these sub-processes. The procedure for the measurement of the enthalpy of immersion has been described in Section 3.7.4. The only exception was that empty ampoules were sealed, with no mineral present for the blank experiments. Thus, heat change accompanying the blank experiments accounted for the heat effects due to the breaking of the ampoules as well as vaporisation of the calorimetric liquid. The values of the enthalpy of immersion of different pure minerals reported in this thesis were corrected for the enthalpy of the blank experiments. This was done by subtracting the enthalpy of the blank experiments from the enthalpy change produced by the immersion of a particular mineral sample in a wetting liquid.

3.8 CONTACT ANGLE MEASUREMENTS

The Washburn capillary rise method was used to determine contact angles of the different mineral powders in this thesis. The contact angle has been extensively used as a conventional measure of hydrophobicity although it has many limitations as highlighted in Section 1.4.4.3. It was deemed logical to compare the enthalpies of immersion of different pure minerals in water to the corresponding powder contact angles as an intermediate step before the enthalpies of immersion measurements were compared to the flotation responses. Both the enthalpy of immersion and contact angle are thermodynamic parameters which are affected by the surface energy of the mineral surface. A comparison between the enthalpy of immersion and the powder contact angle would help in establishing the enthalpy of immersion as a robust surface characterisation tool for the wettability of minerals.

3.8.1 The Washburn method

The Washburn method is used to measure the contact angle of a mineral powder in this thesis (Washburn 1921; Crawford 1986; Studebaker & Snow 1955; Bruil & van Aartesen 1974). The method is based on measuring the rate at which the liquid is drawn into the bed of powder (Washburn, 1921). The liquid rises through the capillaries formed in between the particles within the tubing and the liquid penetration rate is computed by the equipment software. The method involves preparation of two homogeneous beds with identical and reproducible packing of particles. The principle is to first measure the rate of penetration of a probe liquid that is known to perfectly wet (0° contact angle) the particles into a loosely packed bed of powder. Short chain n-alkanes are generally used as the perfectly wetting liquids. The equipment software goes further to compute the material constant of the bed structure which is an essential parameter in the calculation of the contact angle according to the Washburn equation (equation 3-2). Using an identical bed of particles, the wetting process is repeated using the test liquid for which the contact angle is being measured and the rate of penetration is computed by measuring the mass of liquid adsorbed per unit time. The contact angle, Θ, is then calculated using the Washburn equation shown below:

$$cos\Theta = \left[\frac{\eta}{C\Upsilon\varsigma^2}\right]\left[\frac{m^2}{t}\right] \qquad \textit{Equation 3-2}$$

where t = time after contact;

η = viscosity of the liquid;

C = material constant of the solid bed structure;

ϱ= density of the liquid;

Y= surface tension of the liquid;

m = mass of liquid absorbed on solid.

The Washburn method is based on comparing the liquid penetration rates of the perfectly wetting liquid to that of the wetting liquid of interest. The advancing contact angles of the mineral powder against water is computed by direct comparison of the liquid penetration rates using equation 3-3 (Studebaker & Snow, 1955; Buckton 1990) as follows:

$$cos\,\theta = \left(\frac{gradient\ of\ the\ TL\ line}{gradient\ of\ the\ PWL\ line}\right) * \frac{\Upsilon_{PWL}}{\Upsilon_{TL}} * \frac{\eta_{TL}}{\eta_{PWL}} \qquad \textit{Equation 3-3}$$

where TL = test liquid

PWL = perfectly wetting liquid

3.8.2 Operating procedure for contact angle measurements

The Kruss contact angle equipment based on the Washburn method was used to determine the powder contact angles in this thesis. The equipment is embedded with an inbuilt software that computes the contact angle from the comparison of the liquid penetration rates of the perfectly wetting liquid and the test liquid of interest. It employs the principle of the Washburn method. A known weight of mineral powder was loaded into a capillary glass tube whose base is made up of porous paper. A narrow particle size range of 38-53 µm was chosen to maintain an essentially constant particle size. Homogenous, identical and reproducible beds of particles were prepared by centrifuging the loaded capillary tube at 4000 rpm for 10 minutes (Galet et al, 2010). Cyclohexane was used as the perfectly wetting liquid while double deionised water was used as the test liquid. Obtaining reproducible results using the Washburn method was an extremely tedious and time-consuming task. Multiple repeats were conducted to obtain reproducible contact angles of a particular mineral. Outliers among this data set were discarded. Average contact angles are reported in this thesis.

3.9 MICROFLOTATION

The microflotation technique is used in this study to determine the microflotation response of different mineral systems in this study. The technique is characterised by low energy input and thus provides a quiescent system of low turbulence in which the effect of surface properties such as hydrophobicity on the flotation response can be evaluated. This has been discussed in Section 1.2.5. Thus, the microflotation technique measures the extent of particle-bubble contact as measured by the recovery and kinetics of bubble-particle aggregates. There is no froth phase present, which may reject particles above a certain optimum hydrophobicity. All other parameters such as bubble size, energy input, particle properties (size, shape and density) are held constant, and thus the recovery and rate of flotation obtained in a microflotation experiment gives a direct indication of the hydrophobicity of the particle. The greater the hydrophobicity of the particle, the greater the recovery and the faster the rate of flotation. Thus, the microflotation technique is effectively a hydrophobicity meter. In the case of different mineral types, the effect of particle density on the sub-process of particle-bubble interaction was considered (Section 1.3.4).

3.9.1 Equipment description

A schematic of the UCT microflotation cell is shown in the Figure 3-5. The microflotation system consists of a bed of mineral particles maintained in a suspension by means of a peristaltic pump. The flow rate of the suspension is controlled by the pump speed of the peristaltic pump. A micro-litre needle is used to introduce synthetic air via an inlet located at the bottom of the cell. The large air bubbles are sheared and reduced in size by the circulating pulp producing a single stream of bubbles in the cell. The rising air bubbles attach to the sufficiently hydrophobic particles in the pulp forming stable particle-bubble aggregates. The rising particle-bubble aggregates hit the conical part at the top of the cell and get deflected in the process. As the air bubble burst, the mineral particles are released into the concentrate launder at the top of the cell. The concentrates and the tails are then collected for analysis.

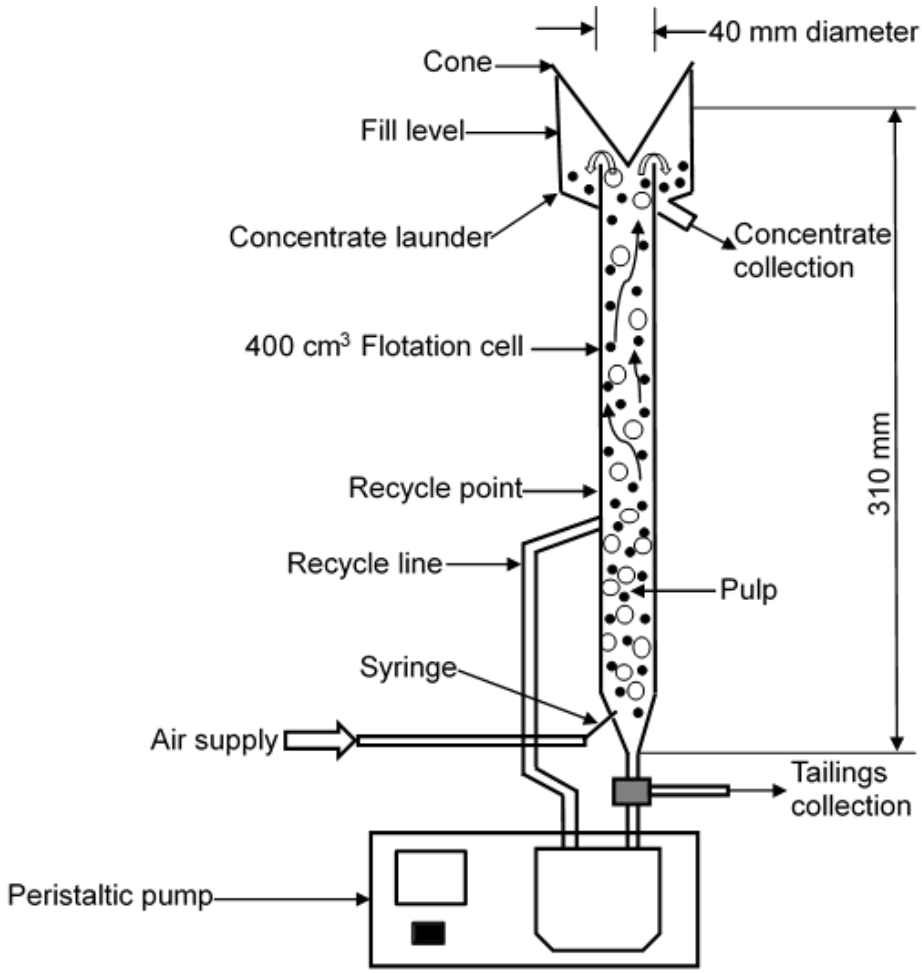

Figure 3-5: Schematic of the UCT microflotation rig

3.9.2 Operating procedure for microflotation tests

The UCT microflotation rig is used in this work to measure the hydrophobicity arising from the mineral-collector interactions (Bradshaw and O'Connor, 1996; Taguta et al, 2017). The microflotation cell has a volume of 400 cm^3 and is equipped with a recycle pump to keep mineral particles in a fine suspension. The UCT microflotation cell is shown in Figure 3-6.

A narrow particle size range of 38-53 µm was chosen to maintain an essentially constant particle size. The mass of the feed into the microflotation cell was 3 g. This was weighed into a beaker and 50 mL double-deionised water was added to make a slurry. This was followed by sonication of the pulp for 5 minutes to remove slimes, to destroy agglomerates and to disperse the slurry. The microflotation cell was filled with double deionised water up to the recycle point. The mineral slurry was then poured into the microflotation cell. The peristaltic pump was set at 130 rpm to circulate the

pulp. The microflotation cell was then topped up to the mark using double deionised water and the conical part was put in place.

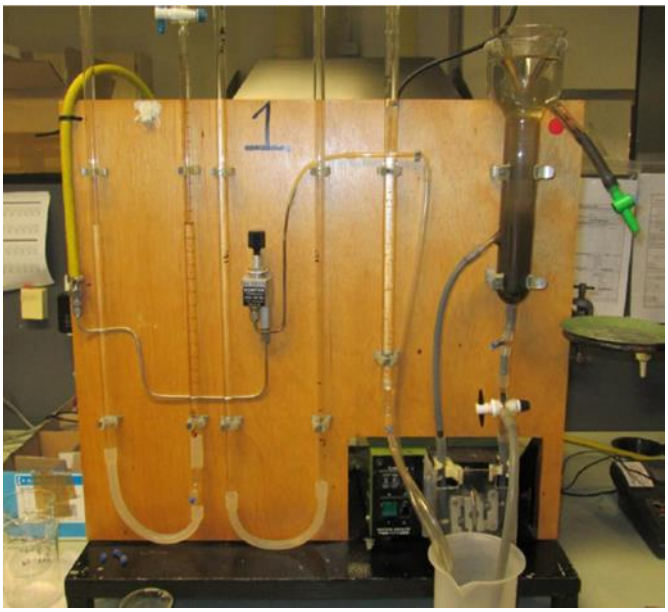

Figure 3-6: The UCT microflotation rig

Synthetic air was introduced through a syringe from the bottom of the cell at a constant rate of 10ml/min in all microflotation experiments. The rising air bubbles collected the hydrophobic particles from the pulp phase to the concentrates. The concentrates were collected at 2, 4, 6, 8 minutes intervals. The concentrates were dried at 60°C for 2 hours in an oven. The microflotation recoveries and rate of flotation were calculated using the dry mass of the concentrates and the tailings. All microflotation tests were conducted in duplicates and averages are reported in this thesis.

3.9.3 First-order flotation kinetics

This study required a detailed comparison of the hydrophobicities of different minerals as indicated by the microflotation recoveries and the first-order flotation rate constants. Preliminary flotation experiments showed that the flotation response of a number of the minerals and their collector-coated derivatives was almost 100% after 20 minutes of flotation time. Terminal recoveries, therefore, were not a suitable parameter for the cross-comparison of the hydrophobicity of the different minerals. For this reason, the first order rate constant was used as a comparative indicator of flotation performance. Recovery at 10 minutes was reported as a supporting parameter but is not a good indicator for the reasons given above. The recoveries after 10 minutes flotation time

for the different minerals were obtained by interpolation on the recovery-time graphs. In this thesis, the first-order flotation rate constants, k, were calculated using the first-order rate model shown in equation 1-2 from the recovery-time data.

$$R = R_{max}(1 - e^{-kt}) \qquad \textit{Equation 1-2}$$

A plot of *In{1-(R/Rmax)}* versus *t* gives a straight line whose gradient k, is the first-order flotation rate constant. The first-order flotation rate constants were normalised by fixing the maximum possible recovery, R_{max}, at 100%.

CHAPTER 4

4 RESULTS

4.1 INTRODUCTION

This chapter begins by presentation of the enthalpies of immersion of different pure minerals (in their natural form) in different probe liquids, viz: water, n-hexane and formamide. The corresponding contact angles and the subsequent microflotation response of the different pure minerals are also presented. The chapter goes further to present the surface energetics (surface energy and its components) of the different pure minerals calculated using the van Oss-Chaudhury-Good (VOCG) model. The chapter also presents the enthalpies of immersion in water and the corresponding surface energetics of a synthetic ore in the form of a binary mineral mixture. The chapter concludes by presenting the enthalpies of immersion in water, the Washburn powder contact angles and the microflotation response for different model systems. The model systems used in this thesis were galena and realgar mineral samples whose surfaces were coated to different surface coverages (hydrophobicities) using the amyl xanthate collector. Some of the results which were considered not critical to the major objective of this thesis are contained in the appendices.

4.2 CHEMICAL VALIDATION TESTS

The dissolution of potassium chloride (KCl) has been extensively used as a standard test and validation reaction in solution calorimetry (Wadso & Goldberg, 2001). Prior to the determination of the enthalpies of immersion of the different pure minerals in this study, it was important to conduct some chemical validation tests on the precision solution calorimeter to determine the accuracy of the equipment. For this purpose, ±300 mg of KCl (recommended molality = 0.111 mol/kg) was weighed into the glass ampoules and the calorimetric experiments were set up as previously described in Section 3.7.4. Double deionised water was used as the solvent and the dissolution experiments were conducted at 30°C. When the reaction was initiated, the KCl dissolved in the double deionised water. Experiments were conducted in duplicate and the enthalpy of dissolution of KCl in water was found to be 17.402 ± 0.028 kJ/mol, which is a relative standard error of 0.16%. The very low standard error validates the extremely good reproducibility of the precision solution calorimeter. The enthalpy of

dissolution ascribed to this test reaction is +17.584 ± 0.017 kJ/mol (Wadso & Goldberg, 2001). Therefore, there is a difference of 1.0% between the ascribed NBS value and the measured value. This proves the accuracy of the SolCal method and equipment.

4.3 REPRODUCIBILITY TESTS

Reproducibility tests were conducted in order to investigate the suitability of the different equipment as well as the reliability of different procedures employed in this thesis. The standard deviations of the various measured variables were calculated, and these were used to test the statistical significance of the various changes in the measured variables. The possible sources of error are discussed in this thesis. The standard error (SE) was calculated according to equation 4-1:

$$\mathrm{SE} = \frac{\mathrm{SD}}{\sqrt{\mathrm{n}}} \qquad \textit{Equation 4-1}$$

where *SD* = the standard deviation of the population size;

n = the population size, e.g. *n* = 2 for experiments conducted in duplicates.

4.3.1 Reproducibility of precision solution calorimetry

The enthalpy of immersion technique has seldom been applied in the mineral processing field, and therefore it was important to investigate the reproducibility of, not only the TAM III precision solution calorimeter but also the procedure used to measure the enthalpies of immersion in this thesis. The reproducibility tests provide the criterion against which differences in enthalpies of immersion from one mineral to another will be evaluated.

It must be emphasised that the solution calorimetry experiments in water were always performed in duplicate for all the different mineral samples in this thesis. On the other hand, single enthalpy of immersion experiments were performed in the case of n-hexane and formamide. This was because of the high costs associated with the SolCal experiments. For illustration purposes, the enthalpies of immersion of galena and talc in double deionised water were chosen to demonstrate how the reproducibility of the enthalpy of immersion was determined in this thesis. The procedure for the measurement of the enthalpies of immersion has been outlined in Section 3.7.4. The experiments were conducted in duplicate and averages were calculated. The standard

deviation associated with the enthalpies of immersion are reported in the tables and graphs. The results are shown in Table 4-1.

Table 4-1: Reproducibility tests of the enthalpy of immersion measurements.

Mineral Type	**Run**	**Enthalpy of immersion (mJ/m^2)**	**Average enthalpy of immersion (mJ/m^2)**	**Standard Deviation, SD (mJ/m^2)**	**Standard error, SE (mJ/m^2)**
Galena	1	-185.0	-175.6	13.2	9.4
	2	-166.3			
Talc	1	-77.3	-75.7	2.4	1.7
	2	-74.0			

The results in Table 4-1 show that the enthalpy of immersion measurements were adequately reproducible, with the relative standard error as low as 5.5% and 2.2% for both galena and talc respectively. In general, the relative standard error for most enthalpy of immersion experiments was lower than 10%. This implies that both the precision solution calorimeter and the procedure used for the enthalpy of immersion measurements were suitable to be used to measure the enthalpies of immersion of different minerals in this thesis. The sources of the small errors could be attributed to the heterogeneous nature of mineral surfaces.

4.3.2 Reproducibility of the Washburn method

The Washburn method was employed to determine the powder contact angles of different minerals in this thesis. The reproducibility of the Washburn method was investigated. As highlighted in Section 3.8.2, multiple repeats were conducted to obtain reproducible contact angles of a particular mineral. Outliers among this data set were discarded. The averages and standard deviations of these results are shown where the data is presented in the following sections. Obtaining reproducible results using the Washburn method was an extremely tedious and time-consuming task. As discussed in Section 1.4.4.3, there are a number of parameters that are difficult to control – surface roughness, chemical heterogeneity, particle size and shape (Denoyel et al, 2004; Gharabaghi and Aghazadeh, 2014).

4.3.3 Reproducibility of the microflotation cell

The reproducibility of the UCT microflotation cell as well as the microflotation procedure was also investigated. It must be emphasised that the microflotation experiments were always performed in duplicate for all the different mineral samples in this thesis. For illustration purposes, the natural (collector-less) flotation of galena and talc were chosen to demonstrate how the reproducibility of the microflotation tests were determined in this thesis. The microflotation procedure has been outlined in Section 3.9.2 and the microflotation recoveries after a flotation time of 10 minutes are shown in Table 4-2.

Table 4-2: Reproducibility tests of the UCT microflotation tests (microflotation recoveries).

Mineral Type	Run	Microflotation recovery (%)	Average microflotation recovery (%)	Standard Deviation, SD	Standard error, SE
Galena	1	24.8	25.5	0.98	0.69
	2	26.2			
Talc	1	74.0	76.5	3.54	2.50
	2	79.0			

The corresponding first-order microflotation rate constants calculated according to equation 1-2 are shown in Table 4-3.

Table 4-3: Reproducibility tests of the UCT microflotation tests (first-order flotation rate constants).

Mineral Type	Run	First-order flotation rate constant (%)	Average first-order flotation constant (%)	Standard Deviation, SD	Standard error, SE
Galena	1	0.029	0.029	0.0013	0.0009
	2	0.030			
Talc	1	0.135	0.145	0.0151	0.0107
	2	0.156			

The results in Table 4-2 and Table 4-3 show that the microflotation recoveries and the first-order flotation rate constants were adequately reproducible. In general, the relative standard error for most microflotation experiments was lower than 2%. This implies that both the UCT microflotation cell and the microflotation procedure were suitable to be used in this thesis. The sources of the small errors could be attributed to the heterogeneous nature of mineral surfaces.

4.4 CORRECTION FOR THE BLANK EXPERIMENTS

In all calorimetric experiments, there is need to correct for the enthalpy of the blank experiments. Blank experiments were therefore conducted to determine the enthalpy associated with ampoule breaking as well as the vaporisation of the calorimetric liquid. The ampoules were sealed, with no mineral present for the blank experiments. The enthalpy of the blank experiments was found to be -62.915 ± 0.28 mJ in this study. The values of the enthalpy of immersion of different pure minerals reported in this thesis were corrected for the enthalpy of the blank experiments. This was done by subtracting the enthalpy of the blank experiments from the enthalpy change produced by the immersion of a particular mineral sample in a wetting liquid. A sample calculation of the enthalpy of immersion of galena in water is shown in Table 4-4.

Table 4-4: Sample calculation of the enthalpy of immersion of galena in double deionised water. The BET specific surface area of the galena powder was measured to be 0.77 m^2/g.

Run	$h_{measured}$ (mJ)	h_{blank} (mJ)	$h_{corrected}$ (mJ)	Sample mass (g)	$h_{corrected}$ (mJ/g)	h_i (mJ/m^2)
1	-375.6	-62.9	-312.7	2.182	-143.3	-185.0
2	-320.0	-62.9	-257.1	1.996	-128.8	-166.3

The average enthalpy of immersion of 175.6 mJ/m^2 which was corrected for the blank experiment is the one that is reported in this thesis.

4.5 SINGLE MINERALS

The enthalpies of immersion, surface energetics, work of adhesion are presented in this section. The powder contact angles and the microflotation response (recoveries

and first-order flotation rate constants) for different minerals are also presented in this section.

4.5.1 Enthalpies of immersion of different minerals in water

The initial set of experiments investigated the enthalpies of immersion of different pure minerals in double deionised water. A total of 10 minerals were investigated. The enthalpies of immersion were normalised to 1 g and 1 m^2 of the mineral surface area and the results are shown in Table 4-5.

Table 4-5: Enthalpy of immersion of different minerals in water.

Mineral	h_i (mJ/m^2)	h_i (mJ/g)
Orpiment	-75 ± 14	320 ± 60
Talc	-76 ± 1.7	1477 ± 32
Realgar	-91 ± 15	437 ± 72
Graphite	-167 ± 7.2	1187 ± 52
Galena	-176 ± 9.4	136 ± 7
Albite	-202 ± 33	1171 ± 193
Mica	-306 ± 33	7342 ± 800
Diopside	-1225 ± 38	5819 ± 179
Wollastonite	-1241 ± 31	5308 ± 132

Table 4-5 shows the variation of the enthalpy of immersion by mineral type. Table 4-5 shows that all the minerals produced different enthalpies of immersion, and thus all the minerals showed different extents of wetting. This is not surprising since the minerals have different surface properties which will affect their wettability. The results in Table 4-5 show that the enthalpy of immersion technique was capable of distinguishing different mineral properties according to their wettabilities which is due to differences in their surface properties. The relatively small standard errors show that the enthalpies of immersion measurements were reproducible.

Table 4-5 shows that the wetting process of all the minerals in water was exothermic. The enthalpies of immersion became more exothermic in the following order: Orpiment < Talc < Realgar < Graphite < Galena < Albite < Mica < Diopside < Wollastonite. It follows that the magnitude of interaction of the different minerals with water increased

in the same order, with wollastonite being the most wettable while orpiment was least wettable. The silicate minerals produced more exothermic enthalpies of immersion than the metallic sulphide minerals, elemental minerals and talc. This finding indicates that the silicate minerals were more wettable than the sulphide and elemental minerals as well as talc.

4.5.2 The enthalpies of immersion of different minerals in different probe liquids

The enthalpies of immersion of different minerals in different probe liquids were measured and the results are shown in Table 4-6. As mentioned earlier, single experiments were performed for the enthalpies of immersion of the minerals in hexane and formamide. This was because of the high costs associated with the SolCal experiments and because the reproducibility of the technique had already been proven. The enthalpies of immersion of the different minerals in water were included again in Table 4-6 for ease of comparison. Only 6 of the 10 minerals were chosen for this investigation. It must be emphasised that the main objective for measuring the enthalpies of immersion of different minerals in different probe liquids was to characterise the surface energetics of the different minerals using the VOCG model (Section 1.6.2). Little attention was devoted to a detailed analysis of the molecular-level interactions between the different probe liquids and the different mineral surfaces.

Table 4-6: Enthalpy of immersion of different minerals in different probe liquids.

Mineral	h_i, water (mJ/m²)	h_i, n-hexane (mJ/m²)	h_i, formamide (mJ/m²)
Talc	-76	-26	-114
Realgar	-91	-42	-176
Galena	-176	-179	-164
Albite	-202	-81	-63
Mica	-306	-108	-113
Wollastonite	-1241	-280	-19

It is clear from Table 4-6 that a given mineral produced different enthalpies of immersion in the three different probe liquids. Furthermore, the different minerals

produced different enthalpies of immersion in the same wetting liquid. This is not surprising since the minerals have different surface properties which will affect their reactions with the different probe liquids.

Table 4-6 shows that the enthalpy of immersion depends on both the nature (mineralogy) of the mineral and the nature of the probe liquid. Based on the data presented in Table 4-6, it is evident that the enthalpy of immersion technique had adequate sensitivity to differentiate between the enthalpies of immersion of different minerals with the same probe and enthalpies of immersion of different probes with the same minerals.

The trend in the enthalpies of immersion of the different minerals in hexane was similar to that observed for water, with galena being the only outlier. However, the enthalpies of immersion in water were always higher than those of n-hexane for all the minerals. On the other hand, the enthalpies of immersion of the different minerals in formamide showed an opposite trend to that observed for water and n-hexane. The results suggest that the enthalpies of immersion in different probe liquids can provide a qualitative insight into the characteristics of the mineral surface.

4.5.3 The surface energetics of different minerals

The surface energy of minerals comprises of the Liftshitz-Van der Waals component *(H_s^{LW})*, the acidic (*H_s^+)* and the basic components (*H_s^-)*. By applying the VOCG model and its laws of exclusion, the enthalpies of immersion in different probe liquids were used to compute the surface energy components as well as the total surface energy of the different minerals. It must be noted that the values of the surface energy and its components calculated using the VOCG model are relative and not absolute. This is because the magnitude of the surface energetics depends strongly on the choice of the three probe liquids chosen for the experiments (Della Volpe & Siboni, 1997; Volpe & Siboni, 2000). The major limitation of the application of the VOCG model is that in some cases, the roots of the acidic and basic components are negative (Della Volpe & Siboni, 1997; Volpe & Siboni, 2000). However, this limitation can be ignored by working with the negative roots and the results obtained can be useful for the direct comparison of the surface energetics of different minerals (Volpe & Siboni, 2000). The surface energy components and the total surface energy were calculated according to equations 1-31 to 1-33 and the values are reported in Table 4-7.

Table 4-7 : The surface energy components and surface energy of different minerals.

Mineral	H_s^{LW}	H_s^{+}	H_s^{-}	H_s^{AB}	H_s^{T}
Talc	29.5	48.6	9.6	21.6	51.0
Realgar	41.8	107.5	0.016	1.3	43.2
Galena	265.5	4.3	95.4	20.3	285.9
Albite	84.9	19.8	432.8	92.6	177.6
Mica	125.9	21.6	742.1	126.5	252.4
Wollastonite	551.4	17573.0	2344.8	6419.1	6970.4

The results in Table 4-7 show that all the minerals are amphoteric (self-associated) as each of them was shown to contain both basic and acidic sites. The relative strength of the sites depends on the mineral type, viz whether metallic sulphide, silicate minerals and phyllosilicate minerals. It is clear from Table 4-7 that the silicate minerals (albite, wollastonite and mica) had a higher magnitude of the basic component (H_s^-) than the metallic sulphide minerals (realgar and galena) and talc. Thus, the silicate minerals were more basic than the sulphide minerals and talc. The same trend can be observed for the polar component of the surface energy. The same trend was further observed for the total surface energy of the minerals with galena being an outlier. It is generally accepted that the higher the total surface energy, the lower the hydrophobicity of the mineral. On the contrary, the lower the total surface energy, the higher the hydrophilicity of the mineral. Ali et al. (2013), using inverse gas chromatography (iGC) found that quartz (a known hydrophilic mineral) had a higher surface energy and a correspondingly lower recovery than galena (a hydrophobic mineral). These results are consistent with Yildirim (2001) who observed that the more hydrophobic the surface is, the lower the total surface energy. Thus, the trend in the total surface energy observed in this study is consistent with the known hydrophobic-hydrophilic nature of the different minerals.

On the contrary, there were no meaningful trends observed for the dispersion and the acidic components of the surface energy for the minerals. These results demonstrate that solution calorimetry is capable of characterising and distinguishing different minerals according to their acid-base characteristics. The significance of these will be discussed further in Section 5.5.

4.5.4 The interfacial energy of interaction between particle and bubbles immersed in water (ΔG_{pwb}) for different minerals

The interfacial energy of interaction of particles and bubbles immersed in water for different minerals, ΔG_{pwb}, was calculated using the surface energetics according to equation 1-35. The results are shown in Table 4-8.

Table 4-8: The interfacial energy of interaction of particles and bubbles in water, ΔG_{pwb} of different minerals at 30°C.

Mineral	ΔG_{pwb}
Talc	-42.0
Realgar	-24.0
Galena	111.3
Albite	198.0
Mica	307.0
Wollastonite	2363.5

The results in Table 4-8 shows that the ΔG_{pwb} parameter was less than zero for talc and realgar while it was greater than zero for the rest of the minerals (galena and the silicate minerals). Furthermore, the ΔG_{pwb} parameter for talc was more negative than it was for realgar. The results suggest that the process of particle-bubble interaction is spontaneous for talc and realgar. This should translate to better microflotation response for talc and realgar compared to galena and the silicate minerals.

4.5.5 Work of adhesion of different minerals

The work of adhesion, defined as a measure of the strength of the interaction between two materials quantifies the affinity of a particular mineral for a particular probe liquid. The work of adhesion between different minerals and the different wetting liquids were calculated using equation 1-38 and the values are shown in Table 4-9.

Table 4-9: Work of adhesion of different probe liquids on different minerals.

Mineral	W_{adh}, water (mJ/m²)	W_{adh}, n-hexane (mJ/m²)	W_{adh}, formamide (mJ/m²)
Talc	194	75	196
Realgar	209	90	258
Galena	294	227	246
Albite	320	129	145
Mica	424	156	195
Wollastonite	1359	328	101

It is clear from Table 4-9 that the work of adhesion values for all the probe liquids were different for all the 6 minerals. The work of adhesion for n-hexane was always lower than that for water. In the flotation context, it is the work of adhesion for water that is relevant since water is the medium for the flotation process. It is interesting to note that the trend in the work of adhesion for water coincides with the trend in the enthalpies of immersion in water previously reported in Table 4-5.

4.5.6 Powder contact angle of different minerals

The powder contact angles of all the different pure minerals were determined using the Washburn method. Cyclohexane was used as the perfectly wetting liquid while double deionised water was used as the test liquid. The powder contact angles of the silicate minerals were difficult to measure using the Washburn method as they could not be completely wetted using cyclohexane (Section 3.8.2) in order to determine the capillary constant. In fact, the difficulty experienced using the Washburn method further emphasizes the need for an alternative more rigorous method for determining the wettability of minerals. The powder contact angles of different minerals against water (in cases where it could be measured) are shown in Table 4-10.

Table 4-10: The Washburn contact angles of different minerals against water.

Mineral	Washburn contact angle against water (°)
Galena	40.9 ± 0.76
Graphite	54.0 ± 3.6
Realgar	65.0 ± 4.6
Talc	71.9 ± 4.8
Orpiment	72.1 ± 4.2

It is clear that the powder contact angles decreased in the order: orpiment ≈ talc > realgar > graphite > galena. Thus, the minerals showed different extents of wetting with water. This was expected since the minerals have different crystalline structures and surface chemistry and hence different surface properties. It is worth noting that the powder contact angles of orpiment and talc were very similar, around 72°. By referring to Table 4-10, it can again be seen that the enthalpies of immersion are good indicators of contact angle for those minerals where it was possible to determine the latter values. The relationship between the two measurements is discussed in more detail in Section 5.4.

4.5.7 Flotation response of different pure minerals in water

The UCT microflotation cell was used to investigate the collectorless flotation response of the different minerals investigated in this study. Since the system hydrodynamics (energy, air flow rate, bubble size) as well as physical properties of the particles (particle size and shape) were maintained constant in the microflotation experiments, any changes in flotation response are attributed to the changes in the hydrophobicities of the minerals in the pulp. Thus, recoveries and the first-order flotation rate constants from a microflotation cell are an indication of the extent of particle-bubble interaction and hence a good indicator of particle hydrophobicity. The microflotation recoveries and the first-order flotation rate constants of the different minerals are shown in Table 4-11.

Table 4-11: The first-order flotation rate constants and microflotation recoveries after 10 min of different minerals in the absence of collectors.

Mineral	First-order flotation rate constant (1/min)	Microflotation recovery after 10 min (%)
Orpiment	0.23 ± 0.013	94.0 ± 1.8
Talc	0.15 ± 0.007	75.0 ± 2.5
Realgar	0.06 ± 0.002	50.0 ± 0.5
Graphite	0.04 ± 0.001	37.5 ± 0.3
Galena	0.02 ± 0.000	25.0 ± 0.7
Albite	0.01 ± 0.000	9.5 ± 0.5
Mica	0.01 ± 0.000	7.5 ± 0.1
Diopside	0.01 ± 0.000	13.0 ± 1.4
Wollastonite	0.01 ± 0.000	7.5 ± 0.8

Table 4-11 shows the microflotation recoveries and first-order flotation rate constants as a function of mineral type. It is clear that different minerals produced different flotation responses. This was to be expected since the minerals have different surface properties, which dictate the wettability of the mineral surfaces. Table 4-11 shows that both the microflotation recoveries and the first-order flotation rate constants decreased in the following order: Orpiment > Talc > Realgar < Graphite > Galena > Albite ≈ Mica ≈ Diopside ≈ Wollastonite.

4.6 SYNTHETIC ORE (MINERAL MIXTURES)

The results presented so far have focussed on the enthalpies of immersion of isolated pure minerals. However, valuable minerals usually occur as combinations of liberated and composite particles associated with gangue minerals or other valuable minerals in a real ore. It follows that the results obtained for single mineral systems have limited value in developing an understanding of the wetting behaviour of real ores. Real ores consist of mixtures of fully and partially liberated minerals. Perfect liberation is rarely achieved during the grinding of a real ore (Meloy, 1984). Therefore, composite particles consisting of the valuable and gangue components are unavoidable in flotation. It was therefore necessary to investigate the effect of mineral composition on

the enthalpy of immersion of a synthetic ore, which for the present purposes is represented by a binary mineral mixture in water. For this investigation, a synthetic ore with well-controlled composition of metallic sulphide and silicate gangue minerals was formulated to simulate a real ore. There are no galvanic interactions between the sulphide minerals and the silicate gangue minerals. Realgar and albite were chosen as typical valuable metallic sulphides and silicate gangue minerals respectively. Since flotation is a surface controlled process, the surface area fraction was used in the calculation of the individual minerals making the binary mineral mixtures. The albite content of 0%, 25%, 50%, 75% and 100% were used in the formulation of realgar-albite binary mixtures. It should be emphasised that, although the behaviour of real mineral mixtures is a long-term goal of this research, it is not the central focus of this thesis. This part of the study represents a preliminary scoping study since the main focus remains on the single mineral studies.

4.6.1 Enthalpy of immersion of realgar-albite mixtures in water

The changes in the enthalpies of immersion of realgar-albite mixtures in water as a function of mineral composition are shown in Figure 4-1. The mineral composition was calculated based on the specific surface areas of both realgar and albite shown in Table 3-1.

Figure 4-1 shows the effect of increasing the albite content on the enthalpy of immersion of the realgar-albite mixtures. It is clear that the enthalpy of immersion became increasingly exothermic as the percentage of albite in the mineral mixture increased. The magnitude of the enthalpy of immersion increased from -90.7 mJ/m^2 for pure realgar to -202.3 mJ/m^2 for pure albite. There is a relatively good direct linear fit between the enthalpy of immersion and the albite content in the realgar-albite mixtures.

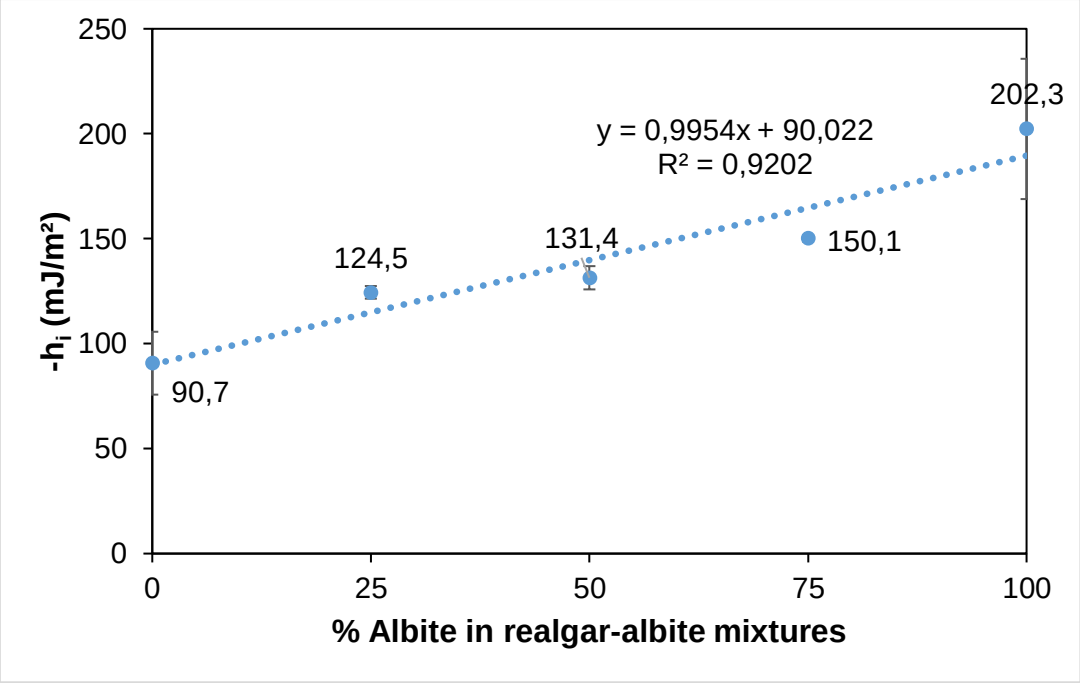

Figure 4-1: Changes in the enthalpy of immersion as a function of mineral composition for realgar-albite mixtures. The % represents the proportion of albite (hydrophilic phase) in the mineral mixture.

4.6.2 Surface energetics of the realgar-albite mixtures

The changes of the total surface energy and its components as a function of albite content of the realgar-albite mixtures were calculated using the VOCG model. The results are the shown in Figure 4-2.

It is clear from Figure 4-2 that the total surface energy and its components (the basic, polar, dispersive components) increased with the increase in the albite content in the mineral mixtures. The increase was more pronounced for the basic component for albite content above 50%. These results show that the enthalpy of immersion is capable of characterising the surface energy components of mineral mixtures. In order to attempt to relate surface energetics to a flotation response, the relative surface polarity of the synthetic ore as a function of the albite content was calculated from the surface energetics and this is discussed in Section 5.6.4.

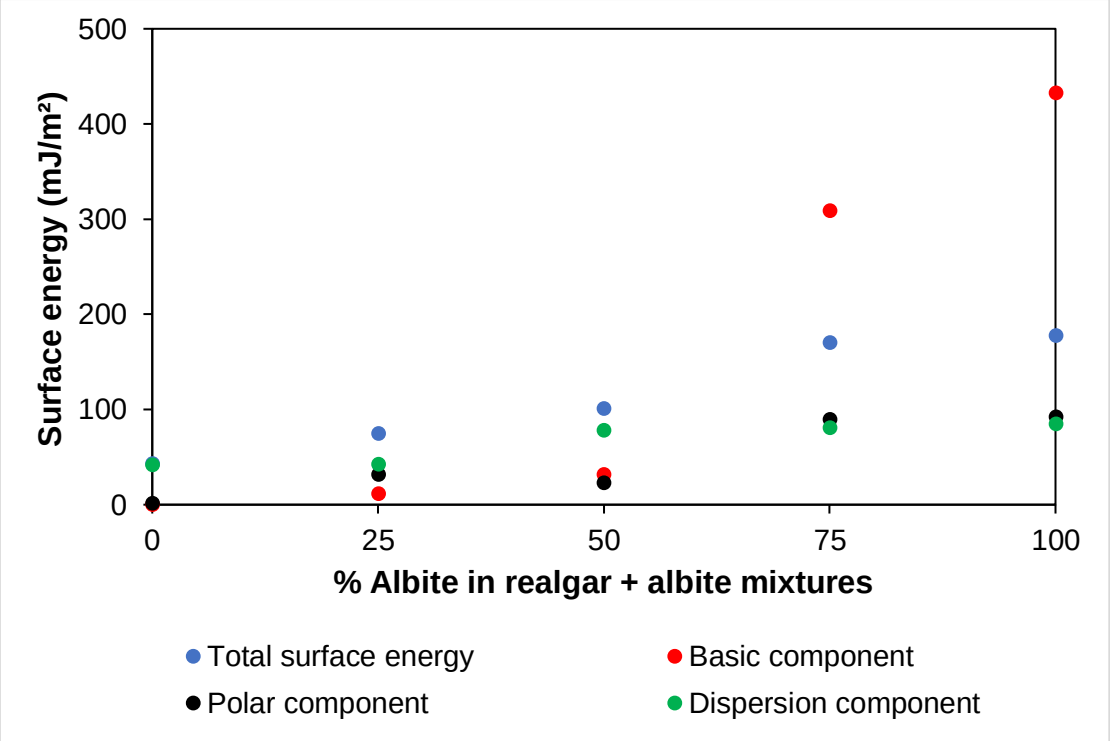

Figure 4-2: Changes of the total surface energy and its components as a function of the albite content in realgar-albite mixtures. The % represents the proportion of albite in the mineral mixtures.

4.7 MODEL SYSTEMS

A model system with well-controlled hydrophobicity is required for the proof of concept in order to assess the relationship between the enthalpy of immersion and the hydrophobicity of collector-coated minerals. For this purpose, the galena-xanthate system was considered as a model system. The realgar-xanthate system was also investigated to establish if the results obtained for the galena-xanthate system were not mineral specific.

4.7.1 Introduction

In the mineral processing context, hydrophobicity may be naturally arising from the mineralogical characteristics of the ore. Hydrophobicity may also be imparted by collectors. The results reported have so far focussed on pure minerals (single and binary mineral mixtures) in their natural form, without any surface treatment. However, the flotation process relies on the addition collectors to render the valuable mineral hydrophobic. It was therefore desirable to investigate whether the enthalpy of immersion method has the capacity to assess changes in surface chemical properties

of mineral samples. This would make the enthalpy of immersion method a more useful and relevant technique in flotation studies where collectors are extensively used. This chapter presents the enthalpies of immersion determined in water of samples of galena and realgar samples pre-treated with amyl xanthate.

4.7.2 Adsorption tests

Adsorption tests had been conducted to investigate the extent of adsorption of the xanthate onto the galena surface in a separate study (Taguta et al, 2017). Freshly ground galena particles were contacted with freshly prepared sodium isobutyl xanthate solutions for 8 minutes with stirring at 300 rpm. The collector concentrations spanned the range of sub-monolayer to multi-monolayer surface coverages. The supernatants were analysed for residual xanthate using UV-VIS at ʎ = 301 nm and the adsorption isotherm is shown in Figure 4-3.

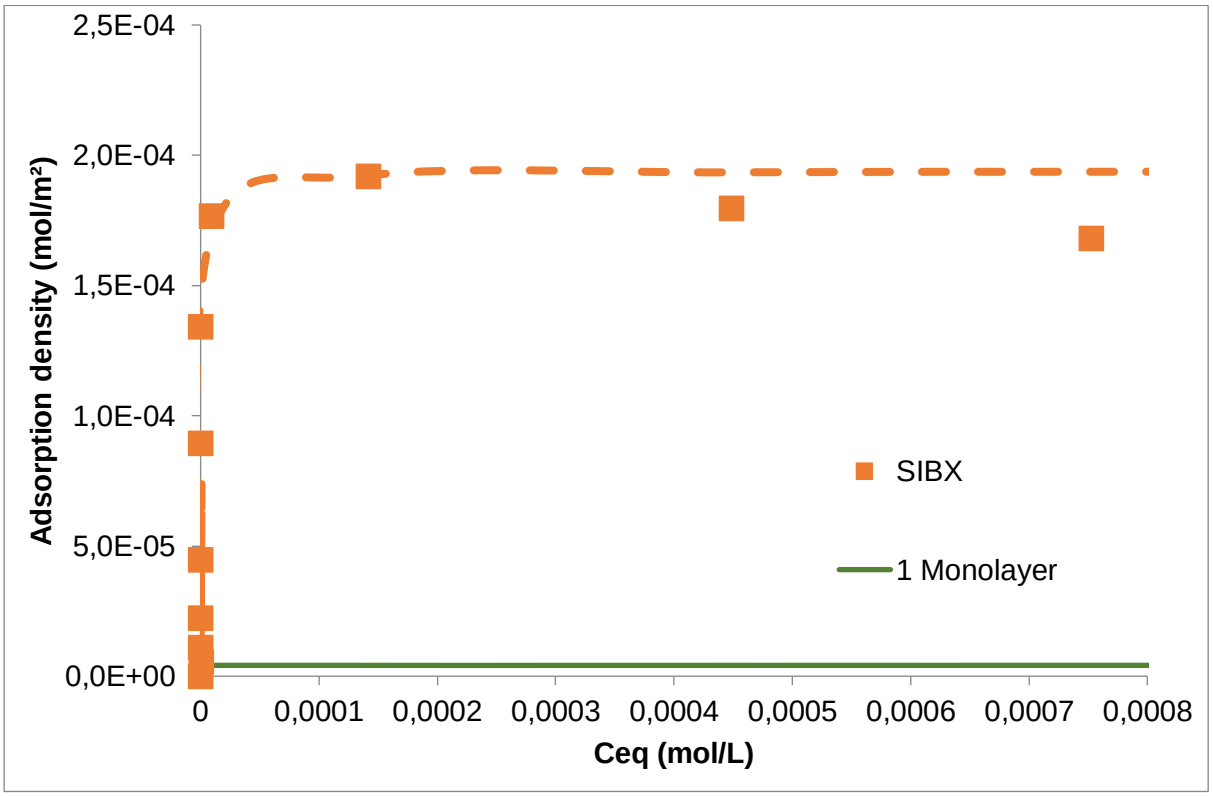

Figure 4-3: Adsorption isotherm of SIBX onto galena showing no residual collector left in solution until multiple monolayers have formed.

The results in Figure 4-3 shows that no residual collector was detected in solution until multiple monolayers of collector have been adsorbed onto the galena surface. This implies that at very low collector concentrations, equivalent to a single monolayer

investigated in this thesis, all the collector adsorbs onto the galena surface. This finding was also reported in a previous publication (Taguta et al, 2017). It can also be reasonably assumed that PAX adsorbs completely onto the galena and realgar surface at low xanthate concentrations since it has a greater affinity for the mineral surface than SIBX.

4.7.3 Enthalpy of immersion and collector coverage

The enthalpies of immersion of PAX-coated galena and realgar samples as a function of the surface coverage of PAX collector were determined and the results are shown in Figure 4-4.

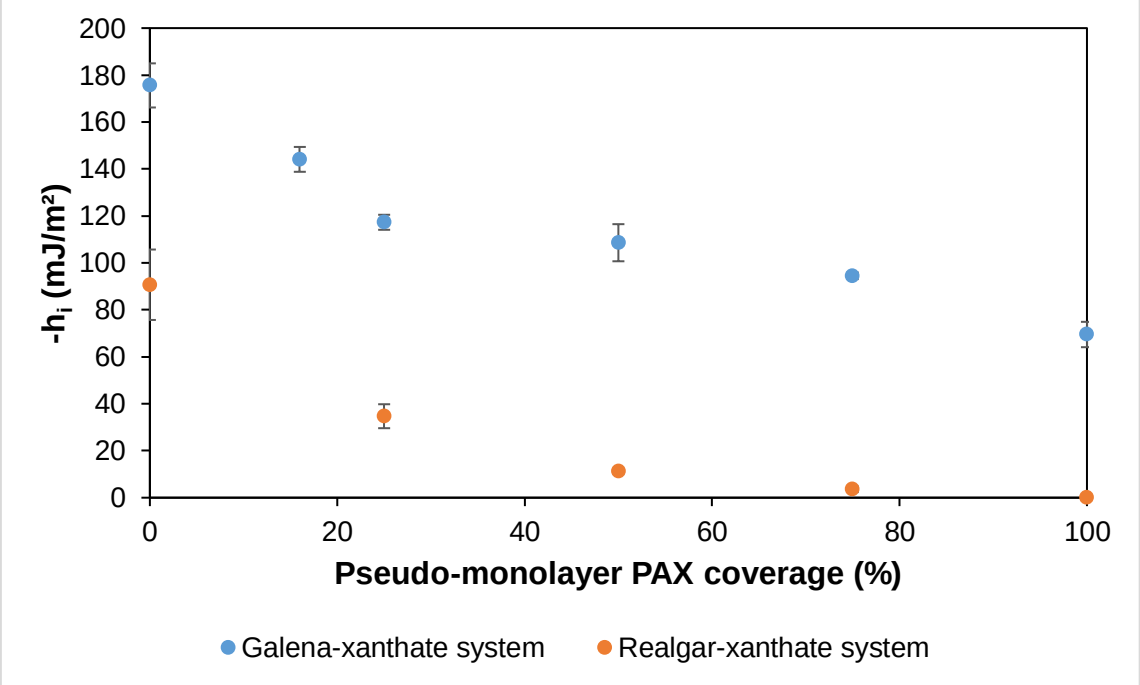

Figure 4-4: Enthalpy of immersion at different surface coverages of the PAX collector for the galena- and realgar-xanthate systems.

Figure 4-4 shows that the magnitude of the enthalpy of immersion was inversely related to the surface coverage of PAX on both galena and realgar. The higher the surface coverage of PAX, the less exothermic the enthalpy of immersion in water. The results show that the decrease in the magnitude of the enthalpy of immersion with increased PAX surface coverage does not appear to be mineral specific. This is in agreement with the earlier observation that the enthalpy of immersion becomes increasingly less exothermic as particle hydrophobicity increases. The decrease in the

enthalpies of immersion indicates significant changes in surface reactions with water as the PAX surface coverage increases. Figure 4-4 further shows that the enthalpies of immersion of the realgar-xanthate system were always less exothermic than that of the galena-xanthate system at all surface coverages of the PAX collector, suggesting that the xanthate-coated realgar was more hydrophobic than the galena-xanthate particles. It is clear from Figure 4-4 that the enthalpy of immersion method was able to assess the changes in the surface chemical properties of the galena surface resulting from collector adsorption.

4.7.4 Powder contact angle and collector coverage

The powder contact angles of the xanthate-coated galena and realgar were determined using the Washburn method and the results are shown in Table 4-12. Cyclohexane was used as the reference liquid while double-deionised water was used as the test liquid. It was difficult to measure the contact angles of the realgar samples with 75% and 100% pseudo-monolayer coverage of PAX. This is because the realgar particles were so hydrophobic that water could not penetrate the bed of particles.

Table 4-12: Washburn powder contact angles for the galena- and realgar-xanthate systems against water at different surface coverages of the PAX collector.

Pseudo-monolayer PAX coverage (%)	Contact angle, Galena (mJ/m²)	Contact angle, Realgar (mJ/m²)
0	40.9 ± 0.8	65.0 ± 4.6
16	56.6 ± 10	NM
25	58.2 ± 7.0	88.8 ± 1.3
50	60.1 ± 4.7	92.0 ± 5.8
75	66.8 ± 9.4	NM
100	76.0 ± 2.9	NM

NM – not measured in this study

Table 4-12 shows the powder contact angles of xanthate-coated galena and realgar mineral samples increased with the PAX coverage. The higher the surface coverage of PAX, the less wettable the mineral surface and the greater the contact angle. It is also clear that the powder contact angles of the realgar-xanthate system were always

higher than that of the galena-xanthate system for all the surface coverages of the PAX collector.

4.7.5 Flotation response and collector coverage

The microflotation recoveries and the first-order flotation rate constants for the flotation of the xanthate-coated galena and realgar samples are shown in Table 4-13 and Table 4-14 respectively. It was impossible to get a fine dispersion amenable to flotation of the realgar samples with 50%, 75% and 100% pseudo-monolayer coverage of PAX. This is because the realgar particles were so naturally hydrophobic that the particles settled at the air-water interface. The UCT microflotation cell was used to determine the flotation response of the galena samples and double-deionised water was used as the flotation medium.

Table 4-13: The first-order flotation rate constants and microflotation recoveries after 10 mins for the flotation of xanthate-coated galena.

Pseudo-monolayer PAX coverage (%	First-order flotation rate constant (1/min	Microflotation recovery after 10 min (%)
0	0.02 ± 0.000	25.0 ± 1.0
16	0.04 ± 0.002	42.0 ± 1.6
25	0.07 ± 0.000	52.0 ± 1.7
50	0.12 ± 0.004	67.0 ± 2.7
75	0.18 ± 0.002	83.0 ± 0.8
100	0.33 ± 0.030	98.0 ± 1.4

Table 4-14: The microflotation recoveries and the first-order flotation rate constants for the flotation of xanthate-coated realgar.

Pseudo-monolayer PAX coverage (%	Microflotation recovery (%)	First-order flotation rate constant (1/min
0	50.0 ± 0.5	0.06 ± 0.002
25	99.0 ± 0.1	0.32 ± 0.001

Table 4-13 and Table 4-14 show that the flotation response increased with PAX coverage. This was as expected as more collector coverage results in a greater hydrophobicity being imparted onto the mineral surface.

CHAPTER 5

5 DISCUSSION

5.1 INTRODUCTION

This section of the thesis discusses the results presented in Chapter 4 in relation to the major objective of this study, which was to investigate the relationship between the enthalpy of immersion and the flotation response in a microflotation cell. The Generalized Sutherland Equation (GSE) shows that the particle–bubble encounter efficiency is dependent on the particle and bubble sizes, the particle and liquid densities, and the liquid viscosity (Sutherland, 1948; Ralston & Dukhin, 1999). Since the particle properties (e.g. size, shape) and hydrodynamic factors (bubble size, air flow rate, and energy input) were maintained constant, any changes in the flotation response was attributed to changes in the wettability (hydrophobicity) of mineral surfaces as well as particle density.

The first section of this chapter focuses on relating the enthalpies of immersion in water, powder contact angles and the flotation of the different minerals to their surface properties as dictated by the crystalline structure of the minerals. Much attention was devoted to the discussion of the enthalpies of immersion of the different minerals in water since water is the medium in which flotation occurs. The chapter also discusses the enthalpy of immersion of xanthate-coated galena and realgar samples. The galena / amyl xanthate (PAX) system was investigated because galena is a simple mineral that has been widely studied in fundamental flotation research (Ralston, 1994; Prestidge and Ralston, 1996; Grano et al, 1997). The realgar-xanthate system was also investigated to establish if the results obtained for the galena-xanthate system were not mineral specific. The chapter further discusses the relationships between the enthalpy of immersion in water, powder contact angle and the microflotation response.

The chapter then discusses the acid-base characteristics and the relative surface polarity of different minerals and binary mineral mixtures. Special attention was given to the evaluation of the effect of mineral composition on the enthalpy of immersion of the synthetic ore in water. Finally, the chapter concludes by summarizing the major findings of this study.

5.2 THE EFFECT OF MINERAL SURFACE PROPERTIES ON THE ENTHALPY OF IMMERSION

The enthalpies of immersion of different minerals in water are central to the flotation process. Because water is balanced in terms of the acid-basic component (Table 3-2), the enthalpy of immersion in water is able to characterise different minerals according to their polarity or wettability. The enthalpy of immersion in water represents an average of all the contributions of the energetically different sites present on a given mineral surface to the wettability of the surface.

This section of the thesis discusses the effect of surface properties on the enthalpy of immersion for both pure minerals and the xanthate-coated galena and realgar samples. A model system with well-controlled hydrophobicity is required for the proof of the concept of the relationship between the enthalpy of immersion and the hydrophobicity or wettability of collector-coated minerals. The galena-xanthate system was considered to be an appropriate model system. The realgar-xanthate system was also investigated to investigate whether the results obtained for the galena-xanthate system were mineral specific.

5.2.1 Pure minerals

The enthalpies of immersion of different minerals in water have been reported in Table 4-5. The enthalpy of immersion became more exothermic in the following order: Orpiment < Talc < Realgar < Graphite < Galena < Albite < Mica < Diopside < Wollastonite. As discussed in Section 1.3.1.1.1, the reason for the natural hydrophobicity and subsequent floatability of sulphide minerals has also been attributed to the formation of the hydrophobic elemental sulphur (Gardner & Woods, 1979; Yoon & Luttrell, 1984; Acres, 2010). If sulphur is present on the mineral surface, wettability is low and hence less exothermic enthalpies of immersion of the metallic sulphide minerals in water are to be expected.

The enthalpy of immersion results obtained in this study are consistent with Ozcan (1992) who classified minerals according to their natural hydrophobicity using the critical surface tension of wetting, measured in a water/methanol system. The critical surface tension of wetting, γ_c is defined as that value of surface tension below which liquid wets the surface completely by spreading spontaneously. The lower the critical surface tension, the more hydrophobic the mineral.

Ozcan (1992) reported that talc, graphite, orpiment and realgar had very low critical surface tension of wetting values (26-35 dyne/cm), thus are naturally hydrophobic and can be easily be floated without a collector. Additionally, galena was reported to be partially or moderately hydrophobic with critical surface tension of wetting values between 35 and 49 dyne/cm. The actual values of γ_c reported by Ozcan (1992) are shown in Table 5-1.

Table 5-1: The critical surface tension of different minerals as reported by Ozcan (1992).

Mineral	**Critical surface tension of wetting, γ_c (dyne/cm)**
Orpiment	33.0
Talc	30.0-35.5
Realgar	33.0
Graphite	30.0-33.4
Galena	49.0

This classification of minerals according to their critical surface tension of wetting by Ozcan (1992) is consistent with the enthalpy of immersion measurements obtained in this study where galena is less hydrophobic than orpiment, realgar, talc and graphite. Table 5-1 shows that the critical surface tension method does not have adequate sensitivity to distinguish the wettabilities of realgar, orpiment, talc and graphite. However, the enthalpy of immersion method has been shown to have adequate sensitivity to distinguish the wettability of the same minerals in this study (Table 4-5).

The critical surface tension technique is labour-intensive and time-consuming. This is because the technique involves determining the wettability behaviour (contact angle) of a given mineral as a function of the surface tension of the water/alcohol system. An adhesion tension diagram would then be plotted from which the γ_c value is identified. Therefore, several tests have to be conducted to obtain a single value of γ_c as opposed to the enthalpy of immersion method where a single experiment is sufficient to infer into mineral surface wettability. Furthermore, the critical surface tension technique requires the measurement of the contact angles of the minerals. The limitations of the using contact angle as an indicator of wettability have been

extensively reviewed in Section 1.4.4.3. Moreover, an extensive review by Ozcan (1992) reveals major disagreements in the values of γ_c reported by different researchers for the same mineral. This was attributed to differences in the method used to determine both γ_c and the contact angles, differences in the liquids used as well as differences in the sample preparation method used.

The wettability of minerals is related, largely to their crystal structures as has been discussed in Section 1.3.1.1. (Gaudin, 1974). It is therefore important to relate wettability as indicated by the enthalpy of immersion of the different minerals in water to the crystalline structures of the minerals.

5.2.1.1 Elemental minerals

Graphite is an allotrope of carbon in which each carbon atom is covalently bonded to three other carbon atoms and these atoms are arranged in layers that can slide past one another. These layers are held together by weak Van der Waals forces which do not interact with water. This is consistent with the relatively less exothermic enthalpy of immersion of graphite in water. These results agree with the known hydrophobic nature of graphite (Morcos, 1970).

The enthalpy of immersion of graphite in water is further consistent with the absence of partial ionic character in these two minerals (Section 1.3.1.1). Graphite has been shown to have no partial ionic character and thus would be expected to have minimal interaction with water. However, once the bonds are broken during grinding, mineral surface oxidation may occur which leads to the presence of some hydrophilic species on the mineral surface. The oxidation products interact with water and this may be responsible for the relatively higher than expected exothermic enthalpy of graphite. Orpiment, talc and realgar all had less exothermic values than graphite, but this was consistent with both the contact angle and microflotation results, as will be discussed later.

5.2.1.2 Metallic sulphide minerals

It is clear from Table 4-5 that the metallic sulphide minerals produced less exothermic enthalpies of immersion in water than the silicate minerals. Thus, the results show that the metallic sulphide minerals were less wettable than the silicate minerals. These results can be explained in terms of the possible presence of elemental sulphur on the

surface of the metallic sulphide minerals, the crystalline structures of the metallic sulphide minerals, as well as the hydrophilic nature of the silicate mineral surfaces. To the best of our knowledge, there is very limited information in the open literature on the enthalpies of immersion of metallic sulphide minerals and hence it was not possible to compare the enthalpies of immersion of metallic sulphide minerals in water obtained in this study with any published data.

Metallic sulphide minerals consist of metallic atoms bonded to sulphur atoms in a crystalline structure. Realgar consists of ring molecules (As_4S_4) in which four sulphur and four arsenic atoms are bound together by covalent bonds. The ring molecules are held together by weak Van der Waals forces and therefore realgar has minimal interaction with water. This is consistent with the low exothermic enthalpy of immersion of realgar in water obtained in this study. Similarly, orpiment consists of superimposed As_2S_3 layers in which each arsenic atom is bonded to three sulphur atoms and each sulphur atom is bonded to two arsenic atoms. These layers are held together by weak Van der Waals forces which do not interact with water. Again, this is consistent with the low exothermic enthalpy of immersion obtained in this study. These results agree with Ozcan (1992) and Wills and Napier-Munn (2006) who classified both realgar and orpiment as naturally hydrophobic minerals which can be floated naturally without a collector.

Galena is a sulphide mineral in which the intra-molecular bonding of the lead and sulphur atoms is predominantly covalent. The covalently bonded molecules in galena are held together by Van der Waals forces which do not readily interact with water. This is consistent with the low exothermic enthalpy of immersion of galena in water obtained in this study. The results also agree with Ozcan (1992) and Wills and Napier-Munn (2006) who classified galena as a moderately hydrophobic mineral.

5.2.1.2.1 Effect of the metallic ion and sulphur content on the enthalpy of immersion of sulphide minerals

The enthalpies of immersion of the different metallic sulphide minerals (galena, realgar and orpiment) in water were compared to investigate the effect of the type of the metallic ion on the wettability of the sulphide minerals. Galena has the Pb^{2+} ion as the metallic ion while in both realgar and orpiment it is As^{4+}. Although the metal to sulphur bond in sulphide minerals is covalent in nature, the differences in the electronegativity

between the sulphur and the various metal atoms leads to an unequal sharing of electrons. This means that the sulphide minerals carry a certain degree of ionic character, which render the sulphide minerals wettable to different extents. The degree of interaction of the different metallic sulphide minerals with water depends on the magnitude of the difference in the electronegativity between the sulphur and the metallic atom. The partial ionic character of the Pb-S and the As-S bond has been calculated using the electronegativity values from Pauling (1960) to be 11.5% and 6.1% respectively (Section 1.3.1.2). Thus, the partial ionic character in galena (Pb-S bonds) is twice that of realgar and orpiment (As-S bonds). Therefore, galena is expected to be more wettable than the arsenic sulphides. As expected, the enthalpies of immersion in Table 4-5 show that galena produced a more exothermic enthalpy of immersion than the arsenic sulphides (-176 mJ/m^2 for galena, -91 mJ/m^2 for realgar and -75 mJ/m^2 for orpiment). This is consistent with the partial ionic characters of the minerals. Furthermore, orpiment, having less As-S bonds per molecule, should have a relatively lower partial ionic character than realgar. This is consistent with results presented in Table 4-5 where orpiment produced a less exothermic enthalpy of immersion than realgar.

The practical significance of this finding is that the enthalpy of immersion is able to rank sulphide minerals according to their wettability. It is clear from the preceding discussion that the low exothermic enthalpies of immersion of the elemental and sulphide minerals in water are consistent with their known hydrophobic properties.

5.2.1.3 Phyllosilicate minerals

It is clear from Table 4-5 that talc produced a less exothermic enthalpy of immersion in water than the silicate minerals. The enthalpy of immersion of talc in water was similar to that of orpiment. This means that talc was less wettable than the silicate minerals.

Talc is a trilayer phyllosilicate mineral with a structure consisting of an octahedral layer (brucite or gibbsite layer) sandwiched between two silica tetrahedral layers. The two silica tetrahedral layers have negative charges and the octahedral gibbsite layer has a neutralising positive charge. Each sheet of talc has a neutral net charge and van der Waals forces hold the trilayer sheets together. There is no tetrahedral substitution of silicon by aluminiun or magnesium which could affect the polarity of the talc. Because

of the low substitution and low polarity, talc is naturally hydrophobic (Yan et al., 2011; Yin et al., 2012). Thus talc reacts with water via weak van der Waals forces and this is consistent with the relatively low exothermic enthalpy of immersion obtained for talc in this study. XRD results presented in Table 3-1 have shown that the talc sample contained 12.2% dolomite and 3.3% quartz as impurities. Both dolomite and quartz are known hydrophilic minerals which interact readily with water. The presence of dolomite and quartz in the talc sample may have resulted in a more exothermic than expected enthalpy of immersion of talc in water. However, in general, the low enthalpy of immersion value (-76 mJ/m^2) was consistent with the known hydrophobic nature of talc.

Yildirim (2001) measured the enthalpies of immersion in water of different talc samples obtained from 5 different sources. The average enthalpy of immersion in water was -274 mJ/m^2 which is more exothermic than the -76 mJ/m^2 obtained in this study (Table 4-5). The difference in the enthalpies of immersion of talc in water is attributed to the changes in the wettability (hydrophobicity) of talc with the particle size. Yildirim (2001) found that the enthalpy of immersion in water became increasingly less exothermic as the particle size decreases. The BET specific surface area of the talc used in this study was 19.00 m^2/g while it was an average of 10.83 m^2/g for the 5 talc samples in the study by Yildirim (2001). Talc is an anisotropic mineral consisting of hydrophilic edges and hydrophobic basal planes. McHardy and Salman (1974) suggested that $Silo^-$ species are present at the hydrophilic edges and that the uncharged Si-O-Si are present at the hydrophobic basal planes. Yildirim (2001) asserts that grinding creates more hydrophobic basal plane surfaces of the talc. The aspect ratio (basal to edge ratio) increases as the talc is ground finer (decreasing particle size). This leads to a decrease in the hydrophilic: hydrophobic ratio as particle size decreases. Thus, talc particles become more hydrophobic as particle size decreases. The talc samples prepared in this study were therefore more hydrophobic than those used by Yildirim (2001) because of their smaller particle size. This explanation is consistent with the differences in the enthalpies of immersion of talc in water obtained in this study and that reported by Yildirim (2001).

5.2.1.4 Silicate minerals

It is clear from Table 4-5 that the silicate minerals produced more exothermic enthalpies of immersion in water than the metallic sulphide minerals. This means that these minerals were more wettable than the sulphide and elemental minerals. According to the partial ionic character of covalent bonds presented in Table 1-2, the Si-O bond in silicate minerals has a partial ionic character that is at least 5 times higher than that of the metal-sulphur bond in sulphide minerals. From this perspective, the silicate minerals are expected to interact more readily with water compared to the sulphide minerals. The enthalpies of immersion presented in Table 4-5 confirms this to be true. Most researchers have reported the enthalpies of immersion of silicate minerals in water. The literature values are compared to the enthalpies of immersion obtained in this study as shown in Table 5-2.

Table 5-2: Comparison of the enthalpies of immersion of silicate minerals in water surveyed in literature to those obtained in this study.

Literature values			**Values obtained in this study**	
Mineral Type	**h_i (mJ/m^2)**	**Reference**	**Mineral Type**	**h_i (mJ/m^2)**
Kaolinite	-422	Salles et al. (2006)	Albite	-202 ± 33
Serpentine	-300	Douillard et al (1997)	Mica	-306 ± 33
Green chlorite	-360	Salles et al. (2006)	Diopside	-1225 ± 38
Black chlorite	-900	Douillard et al. (2007)	Wollastonite	-1241 ± 32
Alumina	-775	Douillard et al. (2007)		
Illite	-700	Douillard (1997)		
Quartz	-400	Douillard (1997)		
Silica	-400	Douillard (1997)		

It is clear that the enthalpies of immersion of the silicate minerals measured in this study are comparable to the previously published data by other researchers. Naturally, it was not expected that enthalpy of immersion values should be the same as other studies, since all mineral samples will be unique. The relationship between the enthalpy of immersion to the structure of the silicate minerals is extensively discussed in the following paragraphs.

Mica, although a trilayer silicate mineral similar to talc, undergoes various degrees of lattice substitution whereby Al^{3+} substitute for the Si^{4+} in the tetrahedral layers. The result is a negative charge on the tetrahedral layer which is usually neutralised by potassium ions. However, the ion exchange capacity of mica is low as the potassium ions are fixed. When mica is cleaved during grinding, it is assumed that the surface carries a constant negative charge whose magnitude depends on the degree of lattice substitution (Yin et al., 2012). It follows that mica sheets are held together by ionic inter-layer bonds which render it hydrophilic. Thus mica is readility wettable in water and this is consistent with the highily exothermic enthalpies of immersion of mica in water (-306 mJ/m^2).

The highly exothermic enthalpies of immersion of wollastonite, albite and diopside are related to the structure of their surface, namely the hydroxyl cover. The hydroxyl surface groups have a high polarity and interact actively with water. Also, the process of dissociation of hydroxyl surface groups can also contribute to the enthalpy of immersion value.

Wollastonite is a calcium meta-silicate in which the Si-O tetrahedra group into chains. Dissolution tests on wollastonite showed that slurry pH changes quickly in the initial stages before reaching equilibrium at pH 9.5 (Prabhakar et al, 2005). The same phenomenon was observed by other researchers (Bailey & Reesman, 1971; Rimstidt & Dove, 1986). This was attributed to the exchange of protons from the aqeous media with calcium ions on the wollastonite surface. The release of calcium was found to be higher than that of silicon, thus wollastonite undergoes incongruent dissolution. Dissolution was more pronounced for finer size fractions. Calcium dissolution leaves behind a negative lattice and active SiOH and SiO^- sites. Auger electron spectroscopic analysis has shown that the exposed atoms on the cleavage surfaces of wollastonite are mainly Si and O and few calcium atoms. The resultant silica-rich surface (hydroxyl cover) is very hydrophilic, interacting strongly with water and hence the observed very highly exothermic enthalpies of immersion of wollastonite in water (-1241 mJ/m^2).

Incongruent initial dissolution was also reported for albite and diopside (Chou and Wollast, 1984; Blum and Lagasa, 1991; Wollast and Chou, 1992; Shmulovich et al, 2001). This again leaves behind a silica rich layer (hydroxyl cover) which render these minerals hydrophilic. This is consistent with the highly exothermic enthalpies of albite

and diopside in water, although the immersion data shows that the diopside has a far more hydrophilic surface (-1225 mJ/m^2) than the albite (-202 mJ/m^2).

In summary these results have shown that the enthalpy of immersion technique was able to classify all the different minerals according to their wettability. The enthalpies of the different minerals in water are also consistent with the known hydrophobic/hydrophilic nature of the minerals.

5.2.2 Collector-coated minerals

The enthalpies of immersion of xanthate-coated galena and realgar samples in water have been shown in Figure 4-4. The results have shown that the enthalpy of immersion is inversely related to the PAX surface coverage. The decrease in the enthalpy of immersion indicates significant changes in surface reactions with water as collector coverage increases. It is clear that the enthalpy of immersion method was able to assess the changes in the surface chemical properties of the galena and realgar surfaces as a result of collector adsorption and these results are consistent with the general observation that enthalpies of immersion will decrease as the particles become more hydrophobic.

Mineral surfaces are heterogeneous, that is they consist of a distribution of chemically different sites (hydrophobic and hydrophilic sites). Hydrophobic minerals have a higher proportion of hydrophobic sites and the inverse is also true. The PAX coating imparts a greater hydrophobicity to the natural galena. As expected, natural galena and realgar without any collector coating produced the most exothermic enthalpy of immersion, which would indicate that they have the highest concentration of hydrophilic sites which readily interact with water. When collector molecules are introduced, the collector ions displace the hydroxyl ions from the hydrophilic sites at the galena surface, as shown by McFadzean & O'Connor (2014), with the hydrocarbon chain length extending into the liquid phase. The hydrocarbon chain is hydrophobic and hence does not interact readily with water. As surface coverage of PAX increased, the galena and realgar surfaces will be increasingly covered with the hydrophobic amyl groups. The amyl moiety interacts with water via weak van der Waals forces and hence produces the lowest exothermic enthalpy of immersion.

The results agree with a number of studies in literature (Spagnolo et al, 1996; Yildirim, 2001; Goncharuk, 2015). Goncharuk (2015) measured the enthalpies of immersion of silica methylated to different surface coverages, which equates to different hydrophobicities, using hexamethyldisilazane and found that the enthalpy of immersion in water became increasingly less exothermic with increasing hydrophobicity. Spagnolo et al. (1996) also found that the enthalpy of immersion of fluorinated carbons in water decreased with increasing fluorine content (hydrophobicity). Furthermore, Yildirim (2001) found that the enthalpy of immersion of anatase in water decreased with increasing concentrations of hydroxamate collector.

5.3 RELATIONSHIP BETWEEN THE ENTHALPY OF IMMERSION AND THE FLOTATION RESPONSE

A major objective of this thesis was to investigate the relationship between the enthalpy of immersion and the mineral surface hydrophobicity as indicated by the flotation response in a microflotation cell. The aim is to be able to predict mineral floatability based on the enthalpy of immersion measurement. The enthalpy of immersion values were related to the corresponding first-order flotation rate constants of the minerals in a microflotation cell. Table 4-11 has shown that different minerals produced different flotation responses. This was expected as the minerals have different surface properties which dictate their wettability. The flotation response of the different minerals is related to the crystalline structures of the minerals and this has been extensively discussed in Section 5.2.1 with regards to the enthalpies of immersion.

The low flotation response obtained for the silicate gangue minerals (albite, diopside, wollastonite and mica) could be attributed to entrainment since these minerals are known not to be floatable. It is also worth noting that wollastonite has been shown to be readily entrained as a result of the needle-like shape of the particles (Wiese & O'Connor, 2016). The low flotation response of these minerals is related to their crystalline structure (Section 5.2.1). In a study of the flotation and surface interactions of the wollastonite/dodecyl amine system, Prabhakar et al, (2005) found the microflotation recovery of wollastonite to be as low as 20%.

Despite having significantly different enthalpies of immersion in water, the silicate gangue minerals showed similar slow flotation responses. This shows that although the wettabilities of the silicate gangue minerals are significantly different, they are all lower than the critical hydrophobicity required before flotation takes place (Blake & Ralston 1985; Crawford & Ralston 1988; Prestidge & Ralston 1996). Using atomic force microscopy, Shi et al. (2014) investigated the interaction of air bubbles in water with untreated and partially hydrophobised mica. It was observed that untreated, hydrophilic mica particles did not attach to the air bubble while the partially hydrophobised mica particles attached to the air bubbles. The fact that the flotation response of the silicate minerals were similar while enthalpies of immersion of the same minerals were significantly different shows that the enthalpy of immersion is a more sensitive tool to characterise the wettability of a mineral surface as opposed to the microflotation technique. The major limitation of the microflotation technique as far as characterising mineral surface wettability is that a certain critical contact angle (hydrophobicity) has to be achieved before mineral powders float. Immersion calorimetry has the ability to measure wettabilities below this critical level of hydrophobicity.

5.3.1 Pure minerals

The wettability of the different minerals as indicated by the enthalpy of immersion in water were compared to mineral surface hydrophobicity as indicated by the flotation response in the microflotation cell. Figure 5-1 is presented to highlight the relationship between the enthalpy of immersion and flotation rate constant.

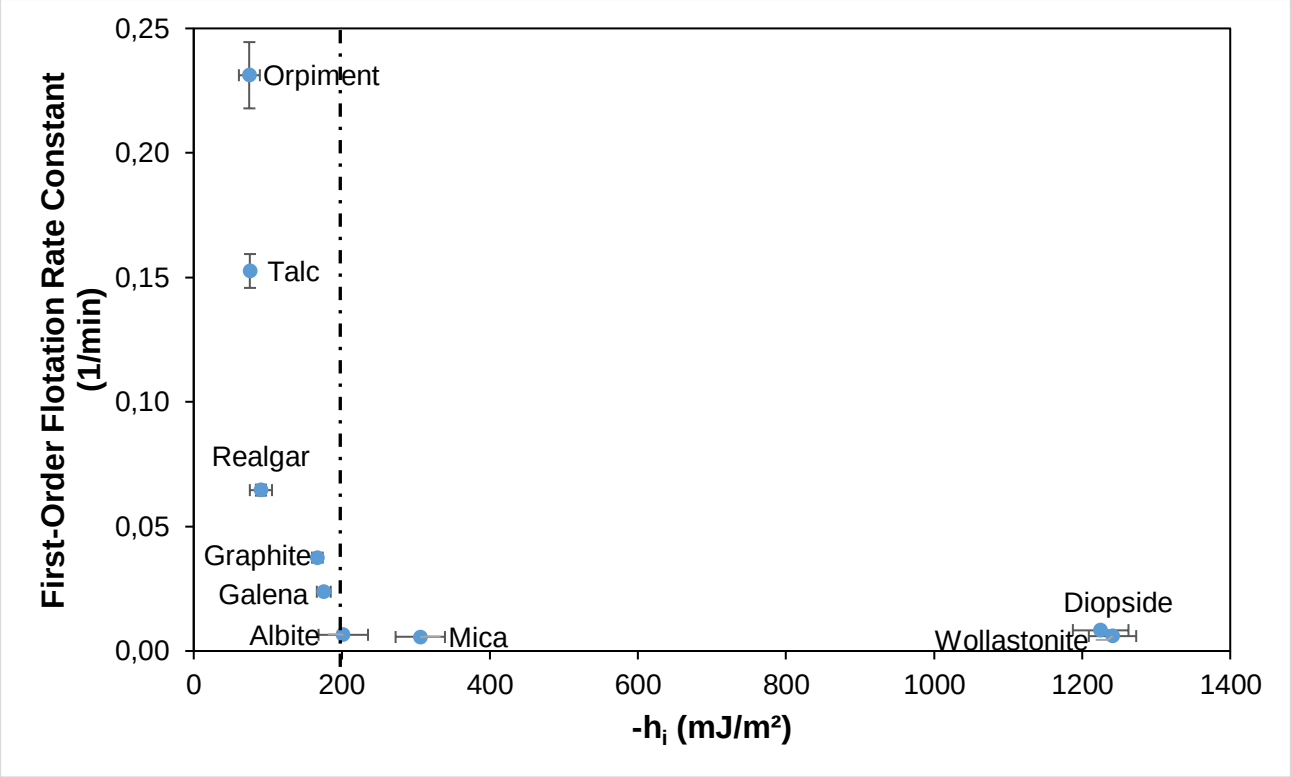

Figure 5-1: The relationship between the enthalpy of immersion and the first-order flotation rate constant for different minerals. The dotted line indicates the proposed critical enthalpy of immersion (CEI) (see text for details).

It is clear from Figure 5-1 that there are 2 distinct regions namely the floatable region (hydrophobic) to the left of the dotted line and the non-floatable (hydrophilic) region to the right of the dotted line. In the floatable region, the flotation rate constant decreases with the increasing magnitude of the enthalpy of immersion. The results agree with Melkus et al. (1987) who reported that the trend in the enthalpies of immersion coincided with trends of the floatability of different coals, concluding that the floatability is inversely related to the enthalpy of immersion. The non-floatable region is characterised by very low or no flotation response, independent of the enthalpy of immersion. Thus, the minerals do not have sufficient hydrophobicity to attach to the air bubbles in the pulp zone.

It is proposed that the enthalpy of immersion value or zone demarcating the floatable region from the non-floatable region be referred to as the critical enthalpy of immersion (CEI). The CEI was in the region of -200 to -300 mJ/m². Similar to the phenomenon of the critical contact angle proposed previously by Blake & Ralston (1985b), Crawford

& Ralston (1988) and Prestidge & Ralston (1996), the critical enthalpy of immersion is the value of the enthalpy of immersion below which no flotation occurs. Hence it is proposed that no flotation will occur in this system for minerals where the enthalpy of immersion is more exothermic than approximately -200 mJ/m^2. The CEI will vary for systems where parameters such as particle size, bubble size and energy input are different, but this has not yet been investigated.

The proposed value of the CEI is consistent with independent studies conducted by other researchers. A preliminary literature survey for the values of enthalpies of immersion of different hydrophobic materials, silicate minerals and oxides in water is summarised in Table 5-3.

Table 5-3: Values of the enthalpies of immersion of different materials and minerals in water surveyed in literature.

Material / Mineral	**Enthalpy of immersion, h_i (mJ/m²)**	**References**
Teflon	-6	(Chessick et al, 1956)
Graphon	-32	(Young et al., 1954)
Griseofulvin	-5.7	(Hansford et al, 1980)
Graphite	-47.5	(Arai, 1996)
Kaolinites	-422	Salles et al. (2006)
Serpentine	-300	Douillard (1997)
Green chlorite	-360	Salles et al. (2006)
Black chlorite	-900	Douillard et al. (2007)
Alumina	-775	Douillard et al. (2007)
Illite	-700	Douillard (1997)
Quartz	-400	Douillard (1997)
Silica	-400	Douillard (1997)

Teflon, graphon, graphite and griseofulvin are known to be very hydrophobic and hence very floatable. Their enthalpies of immersion are less exothermic than the critical enthalpy of immersion of -200mJ/m² obtained in this study. On the contrary, all the silicate minerals in Table 5-3 are known to be hydrophilic, and hence not floatable.

Their enthalpies of immersion are more exothermic than the critical enthalpy of immersion of -200mJ/m² obtained in this study. These results, hence, are consistent with the proposal of a CEI.

5.3.2 Model system

Increasing surface coverages of a xanthate collector will make a sulphide mineral surface increasingly hydrophobic. Figure 5-2 shows the relationship between the first-order flotation rate constant and enthalpy of immersion for different PAX coverages onto galena in order to emphasise the relationship between flotation kinetics and enthalpy of immersion. Because of the single data point, the relationship between the enthalpy of immersion and the flotation response was not graphically shown for the realgar-xanthate system.

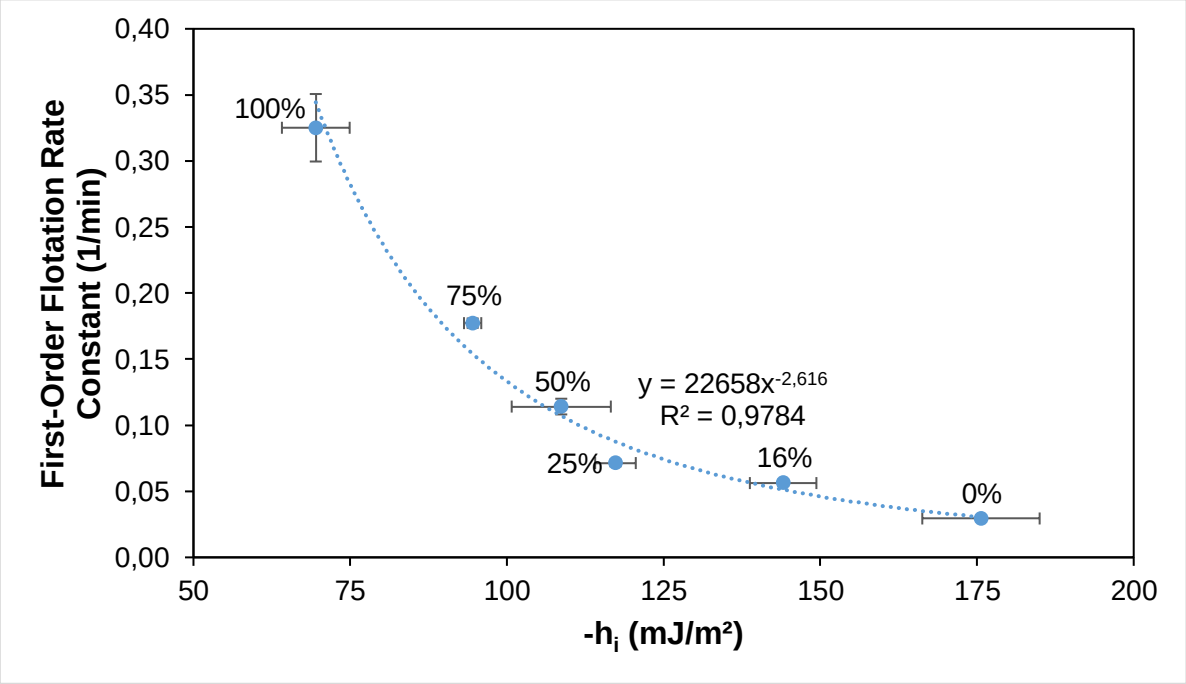

Figure 5-2: The relationship between enthalpies of immersion and flotation rate constant for galena – amyl xanthate model system. The percentage values indicate the extent of the PAX surface coverage on galena.

It is clear from Figure 5-2 that the flotation response decreases as the enthalpy of immersion becomes more exothermic. It is clear that the most floatable amyl xanthate-coated galena (equivalent to 100% surface coverage) produced the lowest enthalpy of immersion in water. The enthalpies of immersion became increasingly exothermic

as the amyl xanthate surface coverage decreased and the particles became less floatable. The results agree with Melkus et al. (1987) who reported similar results in a study of different coals. The inverse relationship between the enthalpy of immersion and the first-order flotation rate is sustained, even in the presence of collectors. The practical significance of these findings is that the enthalpy of immersion measurements provide a very good indication of the ability of the collectors to impart hydrophobicity to a mineral as indicated by the first order rate constant determined using microflotation. This relationship between floatability and hydrophobicity has traditionally been based on relationships between recovery and contact angle (e.g. Rao, 1982). However, as discussed above, the measurement of powder contact angles is frequently problematic. For example, it is not always possible to decide whether to use advancing or receding values and reproducibility is very difficult. The present measurements are consistent with the work of Zimmerman et al. (1987) who proposed that the enthalpy of immersion provides a reliable indicator of flotation behaviour.

5.3.3 Integrating pure minerals and the xanthate coated minerals

Two different mineral systems have been investigated in this study, viz: different pure minerals and a model system. The model system were galena samples whose surfaces were pre-treated to different levels of hydrophobicity using potassium amyl xanthate collector. For both systems, an inverse relationship has been observed between the enthalpy of immersion and the first-order flotation rate constant.

The enthalpies of immersion of different pure minerals in their natural form, those of the galena-xanthate model system and those of the realgar-xanthate system were compared. For ease of comparison, Figure 5-1 and Figure 5-2 were combined as shown in Figure 5-3. The non-floatable region was excluded in order to focus on the floatable region.

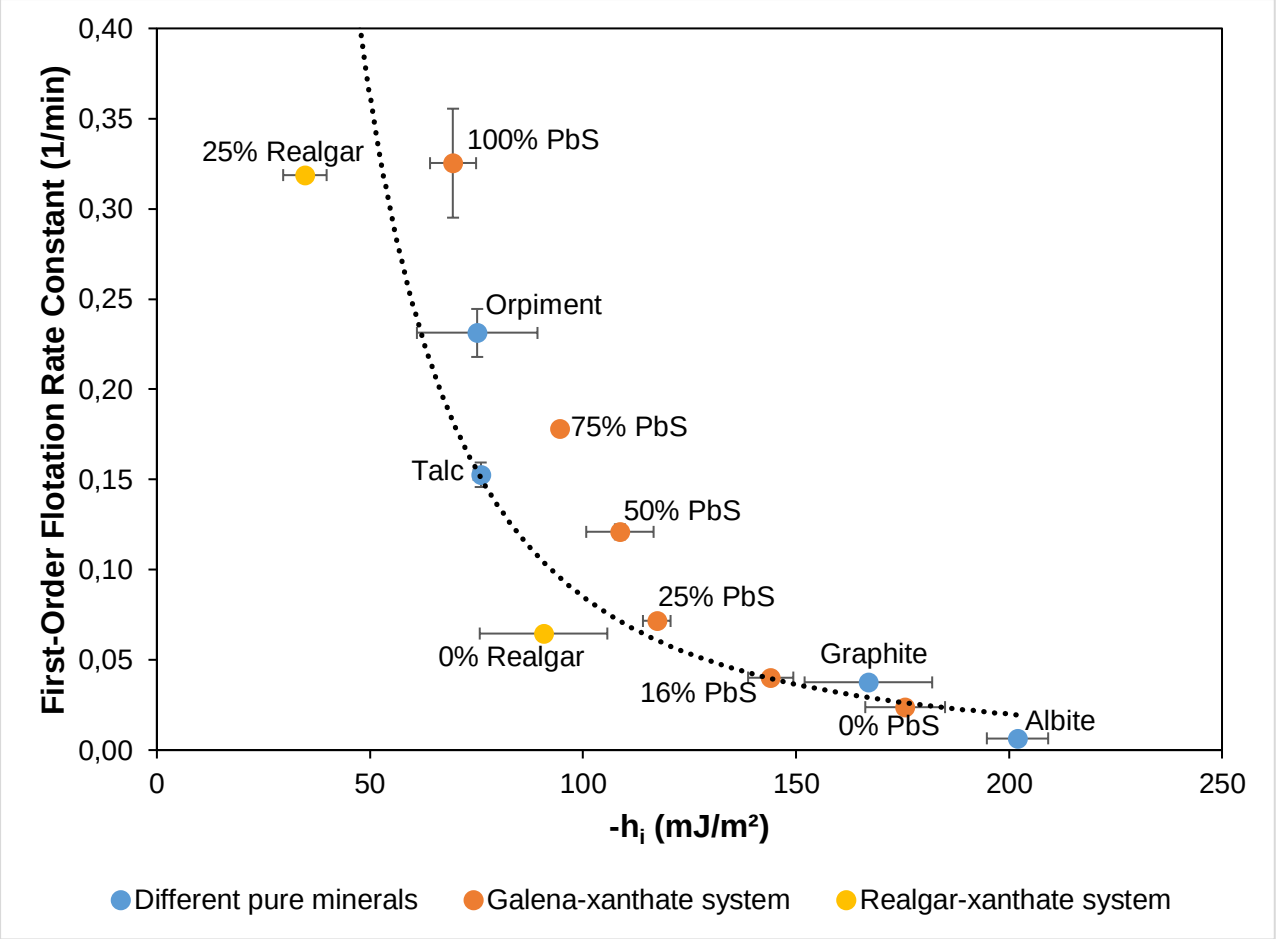

Figure 5-3: Combination of the enthalpy of immersion of the model system (galena / amyl xanthate system), realgar / xanthate system and different pure minerals in water – the floatable region. The line is a guide to the eye.

Figure 5-3 shows the relationship between the enthalpy of immersion and the first-order flotation rate constant for both different pure minerals and the model system. It is clear from Figure 5-3 that the proposal of a critical enthalpy of immersion (CEI) regime of around -200 mJ/m² was sustained, even in the presence of collectors. The dotted line is a power law fit inserted for ease of comparison. It is interesting to note that, as the enthalpy of immersion decreases, there is a sharp increase in the floatability of the minerals. Thus, for a small increase in hydrophobicity, there is a significant increase in floatability. Additionally, there was very good integration between enthalpies of immersion of the different pure minerals. This shows that the flotation response as measured by both the recovery and the flotation rate constant is highly dependent on the wettability of the mineral surface as measured by the enthalpy of immersion.

This validates the inverse relationship between the enthalpy of immersion and hydrophobicity as indicated by the first-order flotation rate constant. Figure 5-3 further reinforces the enthalpy of immersion as a robust indicator of mineral surface wettability, pre- and post-treatment of mineral surfaces with collectors. By measuring the enthalpy of immersion of a given mineral in water, it now appears to be possible to predict the floatability of the mineral by locating it in the floatable (hydrophobic) region.

5.3.4 Effect of particle density on the relationship between the enthalpy of immersion and hydrophobicity

There is need to decouple the effect of particle hydrophobicity from that of particle density on the relationship between the enthalpy of immersion and the first-order flotation rate constant. As highlighted in Section 3.9, particle size was maintained constant by choosing a narrow particle size range of 38 – 53 μm. The hydrodynamics (air flow rate, bubble size, energy) were also maintained essentially constant in all microflotation tests. By elimination, the only variable parameters in this study were particle hydrophobicity and particle density. Thus, the differences observed in the first-order flotation rate constants in Figure 5-3 are attributed to differences in both the particle hydrophobicity as well as particle densities. There is therefore a need to decouple the effects of particle hydrophobicity and particle density. The particle densities of the different minerals quoted from Battey and Pring (1997) are shown in Table 3-1.

The Generalized Sutherland Equation (GSE) shows that the particle–bubble encounter efficiency is dependent on the particle and bubble sizes, the particle and liquid densities, and the liquid viscosity (Sutherland, 1948; Ralston & Dukhin, 1999). In the present investigation these parameters were held constant except for the particle density. There are opposing forces at work, where an increase in density may increase the flotation response for smaller and intermediate particles due to increased inertial forces, which result in increased collision efficiencies. However, for larger particles an increase in density can result in an increase in detachment at higher energy inputs. Detachment has little influence in the microflotation cell, since it is a relatively quiescent environment. In order to correct for the effects of particle density, the rate constant was normalised using the density of each of the minerals as given in

Table 3-1. This is in keeping with the attachment model of Safari & Deglon (2018) given in equation 5-1.

$$k_a = d_p^{n1}(c_1 + c_2\varepsilon^{n2})(1 - cos\theta)^{n3} d_b^{n4} \rho_p^{n5} \qquad \textit{Equation 5-1}$$

where k_a = the attachment rate constant;

d_p = the particle diameter;

Θ = the contact angle;

d_b = the bubble diameter;

ρ_p = the mineral density;

c_x are empirical coefficients and n_x are empirical exponents.

According to Safari & Deglon (2018), the empirical exponent, *n5*, associated with the mineral density is given as 0.67 to 1 in the literature. Thus, the decision to normalise the rate constant by dividing by mineral density appears to be reasonable. Figure 5-4 shows the flotation rate constant as a function of the enthalpy of immersion on a log-log scale. The original data (red squares) shows some scatter, with an R^2 value of 0.87. After normalizing the rate constant with respect to the density of the minerals, the R^2 value improved to 0.96 (green triangles). This suggests that the scatter in the data may be due to the varying density of the minerals.

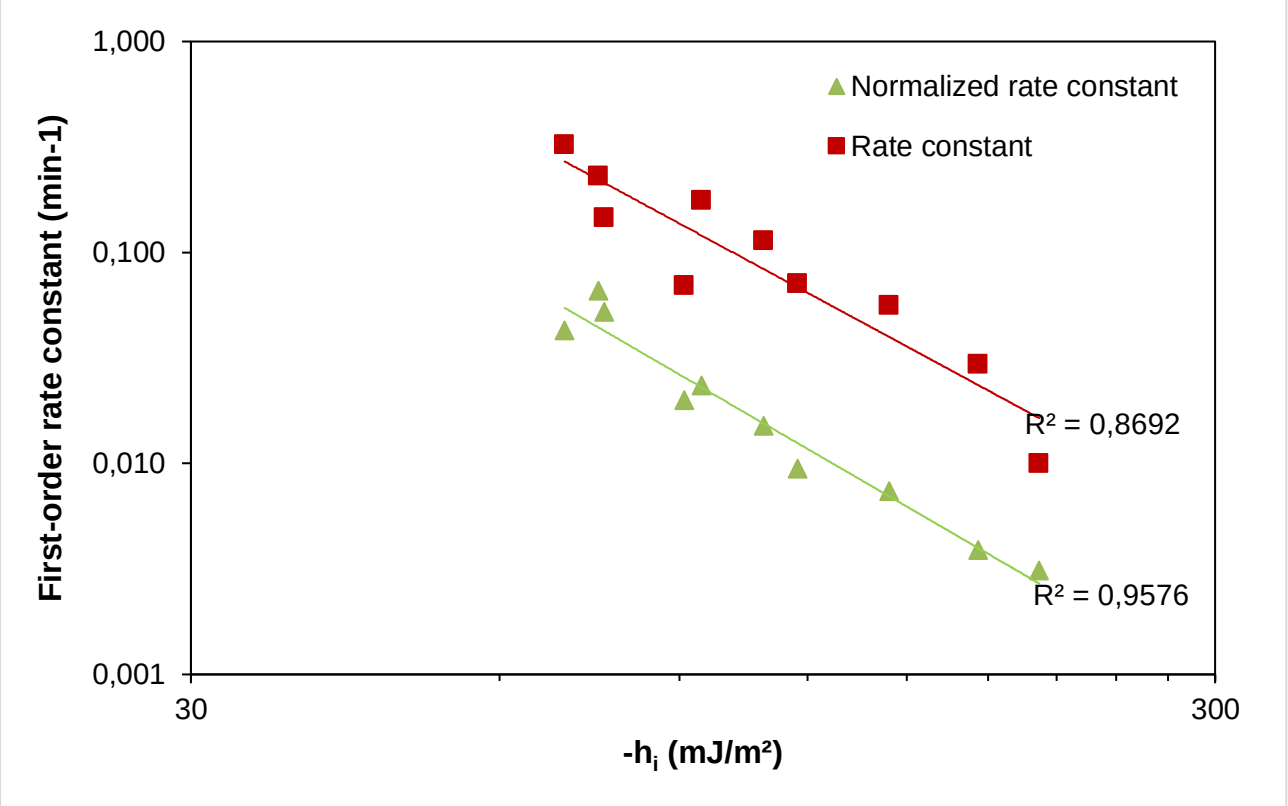

Figure 5-4: Rate constant and rate constant normalized relative to density as a function of the enthalpy of immersion. Note the log-log scale.

5.4 RELATIONSHIPS BETWEEN ENTHALPY OF IMMERSION, POWDER CONTACT ANGLE AND FLOTATION RESPONSE

The enthalpies of immersion of different minerals in water were also compared with the corresponding powder contact angle values. This was important in establishing the enthalpy of immersion as a wettability characterisation tool. The powder contact angle has been extensively used as a conventional measure of hydrophobicity, though its limitations have been discussed in Section 1.4.4.3. Nevertheless, the powder contact angle was compared to the enthalpy of immersion in order to test the robustness of the enthalpy of immersion method as a method to quantify wettability.

5.4.1 Enthalpy of immersion vs contact angle

Equation 1-15 in Section 1.5.4 shows the mathematical relationship between the enthalpy of immersion and the contact angle.

$$-h_i = T\Upsilon_{lv}\frac{dcos\theta}{dT} - \left(\Upsilon_{lv} - T\frac{d\Upsilon_{lv}}{dT}\right)cos\theta \qquad \textit{Equation 1-15}$$

This shows that there is a linear relationship between the enthalpy of immersion and the cosine of the contact angle. Using equation 1-15, it should be possible to determine the contact angle values from the enthalpy of immersion if γ_{lv}, $\delta\gamma_{lv}/\delta T$ *and* $\delta\cos\theta/\delta T$ are known. The first two parameters are usually available from literature. However, the temperature dependence of contact angle needs to be determined experimentally. The limitations of the contact angle have been extensively reviewed in Section 1.4.4.3. The relationship between the enthalpy of immersion and the cosine of the contact angle for the different minerals, the galena-xanthate system and the realgar-xanthate system was investigated and is summarised in Figure 5-5.

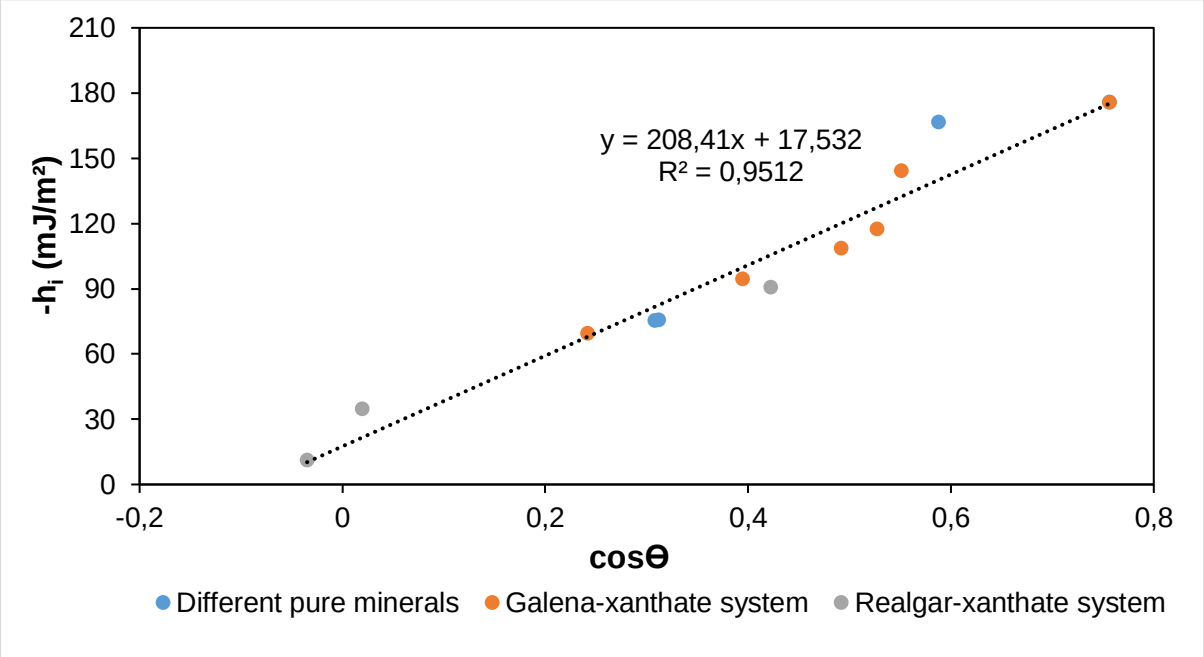

Figure 5-5: Variation of the enthalpy of immersion with the cosine of the powder contact angle of different pure minerals, the galena-xanthate system and the realgar-xanthate system.

Figure 5-5 shows an almost linear relationship between the enthalpy of immersion and the cosine of the contact angle. As discussed in Section 1.5.4, the $\delta\gamma_{lv}/\delta T$ and $\delta\cos\theta/\delta T$ terms are constants at a constant temperature and hence a linear relationship between the enthalpy of immersion and the cosine of the contact angle was expected.

To validate the relationship between the enthalpy of immersion and the contact angle, the $\delta\gamma_{lv}/\delta T$ term for water was calculated using slope of the line in Figure 5-5, given by equation 5-2.

$$-h_i = 208.41 cos\theta + 17.532 \qquad \textit{Equation 5-2}$$

The $\delta\gamma_{lv}/\delta T$ term was calculated to be -0.4575 mN/mK at 30°C. This was 3 times higher than the value of -0.1514 mN/mK reported in literature at 20°C. The discrepancy between the 2 values may be attributed to the poor reproducibility of the Washburn method and the differences in temperatures.

Equation 5-2 can be used to investigate certain boundary conditions. It must be emphasised that the parameters are temperature sensitive and in this study the experiments were conducted at 30°C. For a contact angle of 0° (cos Θ = 1), h_i is -226.0 mJ/m² by equation 5-2. This value is more exothermic than the proposed critical enthalpy of immersion (CEI) of around 200 mJ/m² (Section 5.3). The value of the CEI corresponds to a predicted contact angle of 20° for which flotation response is expected to be very poor. When h_i is more exothermic than -226.0 mJ/m², the mineral surface is very hydrophilic and should show poor flotation performance. However, when h_i is less exothermic than -226.0 mJ/m², the contact angle is greater than zero. When h_i is less exothermic than -17.5 mJ/m², the contact angle is greater than 90°. This agrees with the value calculated from equation 1-17, which is -20.9 mJ/m². The discrepancies in the 2 values may be attributed to the poor reproducibility of the Washburn method and the assumption made with regards to the derivation of equation 1-17 (Section 1.5.4). The least exothermic value for the enthalpy of immersion was measured for 100% xanthate-coated realgar and was -0.2 mJ/m^2.

For further validation, equation 5-2 was used to predict the contact angles of different materials whose enthalpies of immersion in water were determined from different literature sources. The comparison is summarised in Table 5-4 and it shows that the directly measured contact angles are similar to the predicted ones. The discrepancies between the predicted and the directly measured contact angles may be attributed to the poor reproducibility of the Washburn method. The references for the directly measured enthalpies of immersion are found in Table 1-5.

Table 5-4: Comparison between predicted and directly measured contact angles for different materials.

Material	h_i (mJ/m²)	Directly measured contact angles (°)	Predicted contact angles (°)
Teflon	-6	110	93.2
Graphon	-32	81	86.0
Griseofulvin	-5.7	101.9	93.3
Graphite	-47.5	86	81.7

While equation 1-17 can only be applied in cases where the enthalpy of immersion is less exothermic than -50 mJ/m² (only valid for hydrophobic surfaces), equation 5-2 is applicable to both hydrophilic and hydrophobic surfaces since the equation is defined for enthalpies of immersion that are less exothermic than -226.0 mJ/m². The practical significance of this finding is that the enthalpy of immersion can be used as a direct indication of wettability and one does not need to go through a correlation with a less rigorous parameter such as contact angle.

5.4.2 Powder contact angle vs the first-order flotation rate constants

The relationship between the powder contact angle and the first-order flotation rate constant for different minerals and the xanthate-coated minerals was investigated and is summarised in Figure 5-6. For the realgar-xanthate system, only 2 data points were shown because the contact angles and flotation responses of the 50%, 75% and 100% xanthate-coated realgar samples could not be measured.

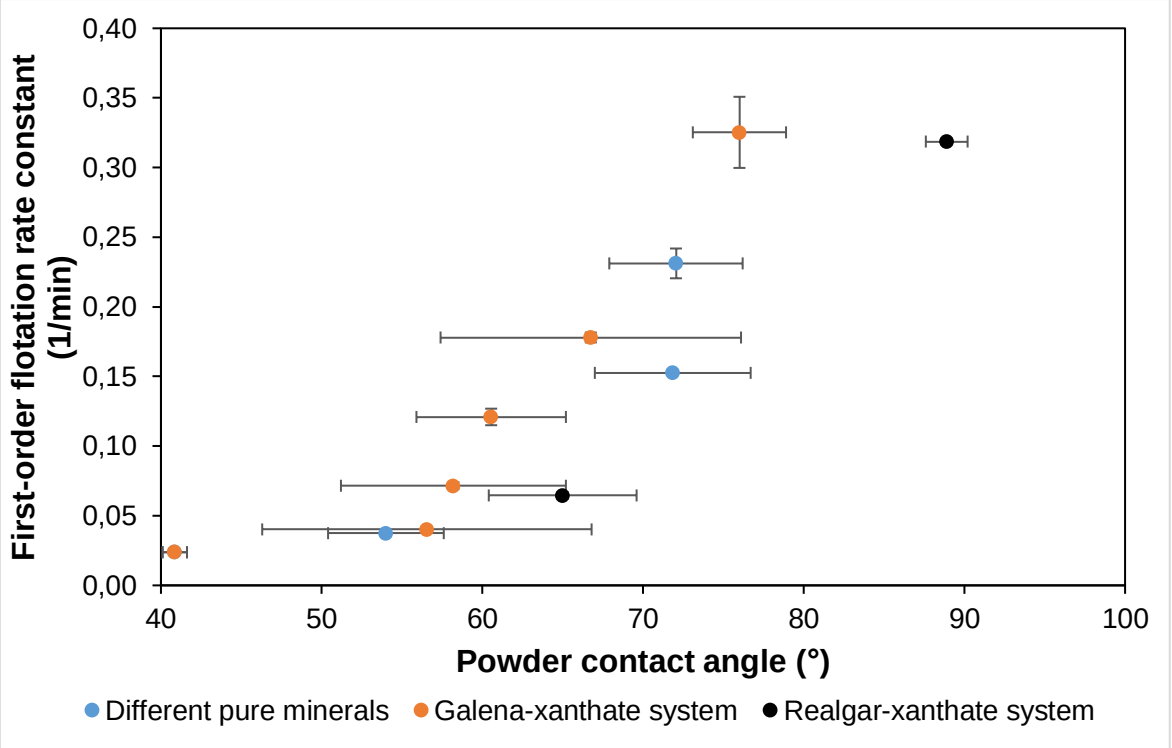

Figure 5-6: The relationship between the contact angle and the first-order flotation rate constant for the different pure minerals and the galena-xanthate system.

As expected Figure 5-6 shows that there is a direct correlation between the contact angle and the flotation response, i.e. the greater the contact angle the higher the rate of flotation. This was observed for both pure minerals and xanthate-coated sulphide minerals. The scatter in the data may be attributed to the poor reproducibility of the contact angle method and to differences in particle density as discussed in Section 5.3.4. This relationship is consistent with the findings made by other researchers that, above the critical contact angle, the flotation response increases significantly with contact angle (Blake and Ralston, 1985b; Crawford and Ralston, 1988; Prestidge and Ralston, 1996). The critical contact angle in this case, above which the flotation rate increases significantly, is about 55°. It is worth noting that the contact angles obtained in this study are lower than those obtained by Prestidge & Ralston (1996) which may be due to the fact that galena samples were possibly slightly oxidised. This is further reinforced by that fact that the collectorless recovery of galena was found to be 25.5% which was lower than expected (Table 4-11).

5.5 THE SURFACE ENERGETICS OF MINERALS

The surface energetics of the different minerals were calculated using the VOCG model and the results have been reported in Table 4-7. The enthalpies of immersion of the different minerals in different probe liquids have been presented in Table 4-6. It must be emphasised that the main objective behind measuring the enthalpies of immersion of different minerals in different probe liquids was to characterise the surface energetics of the different minerals using the VOCG model (Section 1.6.2). Little attention was devoted to a detailed analysis of the molecular-level interactions between the different probe liquids and the different mineral surfaces.

The results in Table 4-6 have shown that the enthalpies of immersion of the same mineral in the three probe liquids were different. Furthermore, the enthalpy of immersion of different minerals in the same probe liquid were significantly different. These results suggest that the enthalpy of immersion depends on both the nature of the mineral surface and the nature of the wetting liquid.

5.5.1 Relating the surface energetics to the crystalline structures of minerals

The results have shown that all the minerals were amphoteric containing both basic and acidic sites (Table 4-7). The table is reproduced here for ease of reference.

Table 4-7: The surface energy components and surface energy of different minerals.

Mineral	H_s^{LW}	H_s^{+}	H_s^{-}	H_s^{AB}	H_s^{T}
Talc	29.5	48.6	9.6	21.6	51.0
Realgar	41.8	107.5	0.016	1.3	43.2
Galena	265.5	4.3	95.4	20.3	285.9
Albite	84.9	19.8	432.8	92.6	177.6
Mica	125.9	21.6	742.1	126.5	252.4
Wollastonite	551.4	17573.0	2344.8	6419.1	6970.4

The strength of the acidic and basic sites was dependent on the type of the mineral. Silicate minerals (albite, wollastonite and mica) showed a higher basic component of the surface energy compared to the metallic sulphide minerals (realgar and galena) and talc. This implies that the silicate minerals were more basic than the sulphide

minerals and talc. It was also found that trends in the polar component and the total surface energy were similar to those observed for the basic component.

The amphoteric behaviour of the different minerals can be explained in terms of the Lewis acid/base theory. According to the theory, an acid is an electron acceptor while a base is an electron donor. Mineral surfaces are heterogeneous, containing a distribution of energetically different sites. The hydroxyl groups on the mineral surface can either accept or donate a proton in mineral suspensions. Therefore, sites on the mineral surface can act either as a Brønsted base (electron-rich) or Brønsted acid (electron-deficient). Oxygen atoms on the mineral surface with lone pairs of electrons can act as electron donors and thus act as basic sites. The silicate minerals (wollastonite and albite) are reported to undergo incongruent dissolution leaving behind a negative lattice and active SiOH and SiO^- sites (Bailey and Reesman, 1971; Chou and Wollast, 1984; Blum and Lagasa, 1991; Wollast and Chou, 1992; Weissbart and Rimstidt, 2000; Shmulovich et al, 2001; Swarna et al, 2003; Prabhakar et al, 2005). In light of this, silicate minerals behave as Lewis bases which donate electrons. This is consistent with the high basic components of albite and wollastonite.

Mica is reported to undergo various degrees of lattice substitution whereby Al^{3+} substitute for the Si^{4+} resulting in a negative charge on the tetrahedral layer (Yin et al., 2012). This is consistent with the highly basic component of mica. The basic nature of the silicates (mica, albite and wollastonite) is confirmed by the relatively low enthalpies of immersion of the silicate minerals in formamide as there is repulsion between the basic sites in silicate minerals and those in formamide.

On the other hand, Brønsted acidity depends on the electron attracting power (electronegativity) of the metal atoms bonded to the hydroxyl groups on the mineral surface. The electronegativity depends on the atomic size and the valence of the metal atom. If the metal atom is small and has a high positive valence, the proton will be less strongly bonded to the oxygen in the hydroxyl group. This translates to a higher acidity of the hydroxyl group and consequently the mineral surface. The results in Table 4-7 have shown no trends for the dispersion and the acidic components as a function of mineral type.

The results in Table 4-7 have further shown that talc has the lowest total surface energy compared to the rest of the silicate minerals. This is consistent with the known hydrophobic nature of talc and the hydrophilic nature of the other silicate minerals. Similar results have been reported by Douillard et al. (1994, 1997) where talc was shown to have a lower total surface energy than chlorites. The results have also shown that although talc is an oxide mineral, it has the lowest basic component compared to other silicate minerals. This is attributed to the structure of talc in which each sheet of talc is held together by the weak Van der Waals forces with no tetrahedral substitution of silicon by aluminium or magnesium which could affect the polarity of the talc (Yan et al., 2011; Yin et al., 2012). Because of the low substitution and low polarity, there are no OH groups at the external surface of the crystal and hence the low magnitude of the basic and polar components of the talc as opposed to the other silicate minerals. The talc surface appears acidic (Table 4-7), which can be attributed to the positive partial charge of the Si atoms in the crystallographic external layer. Similar results on the acidity of talc were reported by Douillard et al. (1994) and Douillard et al. (1997). It is interesting to note the magnitude of the total surface energy of talc obtained in this study (51 mJ/m^2) is comparable to those obtained by Yildirim (2001) (26–51 mJ/m^2).

The results in Table 4-7 further showed that the sulphide minerals (realgar and galena) had relatively small magnitudes of the basic and polar components of the surface energy compared to the silicate minerals. This is consistent with the hydrophobic nature of these minerals (Ozcan, 1992; Wills and Napier-Munn, 2006). Because of low polarity, there are relatively few OH groups on the surface and hence the observed low magnitude of basic and polar components of surface energy.

The acid-base characteristics of the minerals, measured by solution calorimetry, can give a detailed insight into the different surface energies of mineral types and may be useful in optimising processing strategies.

5.5.2 Important wettability parameters derived from the enthalpy of immersion

5.5.2.1 Relative surface polarity of minerals

The relative surface polarities of the different minerals were calculated using equation 1-34 are shown in Table 5-5. The total surface energy and its components for the different minerals have been shown in Table 4-7.

Table 5-5: The relative surface polarities as a function of mineral type.

Mineral type	Relative surface polarity (%)
Realgar	3.1
Galena	7.1
Talc	42.3
Mica	50.1
Albite	52.2
Wollastonite	92.2

The relative surface polarity increased in the following trend: realgar < galena < talc < albite < mica < wollastonite. It is clear from Table 5-5 that the sulphide minerals (realgar and galena) had major contributions from the non-polar component while the silicate minerals had major contributions from the polar component. Therefore, the metallic sulphide minerals, together with talc are predominantly hydrophobic as their surfaces contained more hydrophobic (non-polar) sites than hydrophilic (polar) sites. These results are consistent with known hydrophobic nature of realgar, galena and talc (Ozcan, 1992; Wills & Napier-Munn, 2006; Yan et al., 2011; Yin et al., 2012). Realgar has a lower relative surface polarity than galena, suggesting that realgar is the more hydrophobic of the two. These results agree with Ozcan (1992) who, using the critical surface tension of wetting classified realgar as naturally hydrophobic while galena was classified as moderately hydrophobic. The trend in the relative surface polarities of the sulphide minerals is similar to the trend in the percentage partial ionic character of the minerals presented in Table 1-2. The partial ionic character of the As-S bond in realgar is 6.1% while that of the Pb-S bond in galena is 11.5% respectively. It is interesting to note that both the relative surface polarity and the percentage ionic character of galena were twice that of realgar.

Talc, although a naturally hydrophobic mineral, has an unusually high relative surface polarity. Both the enthalpies of immersion in water and the powder contact angle in Table 4-5 and Table 4-10 respectively have shown that talc was more hydrophobic than galena. However, the relative surface polarities showed the opposite trend. This discrepancy is explained in terms of the structure of talc as well as its mineralogical composition as determined by the XRD results presented in Table 3-1. The

comparison of talc to the metallic sulphide minerals (realgar and galena) is difficult as these minerals have different crystalline structures. Talc is anisotropic, comprising of both the hydrophobic basal planes as well as the hydrophilic edges (Yan et al., 2011; Yin et al., 2012). The aspect ratio (basal to edge ratio) determines the hydrophobic-hydrophilic ratio. Talc has Mg-O and Si-O bonds which have very high partial ionic characters of 74.4% and 53.4% respectively (Table 1-2). McHardy and Salman (1974) reports that the SiO^- species dominate the hydrophilic edges while the uncharged Si-O-Si dominates the hydrophobic basal planes. The very high relative surface polarity of talc observed in this study may be due to the contribution of the hydrophilic edges. Mineralogical characterisation showed that talc contained 12.2% dolomite as well as 3.3% quartz (Table 3-1). Both dolomite and quartz are known to be hydrophilic minerals and hence these minerals increase the relative surface polarity of the talc sample.

The rest of the silicate minerals (albite, mica and wollastonite) had the polar component as the major contributor to the total surface energy. Wollastonite had the highest contribution from the polar contributions (92%). These results are consistent with the known hydrophilic nature of these minerals. Wollastonite, mica and albite are primarily hydrophilic due to a silica rich surface resulting from the non-uniform dissolution of the silicate minerals in water (Bailey and Reesman, 1971; Chou and Wollast, 1984; Blum and Lagasa, 1991; Wollast and Chou, 1992; Weissbart and Rimstidt, 2000; Shmulovich et al, 2001; Swarna et al, 2003; Prabhakar et al, 2005).

These results provide a firm foundation for the investigation of the wettability of mineral mixtures, composite particles and real ores using the enthalpy of immersion technique. The wettability of mineral mixtures is discussed in Section 5.6 while the wettability of real ores is beyond the scope of this thesis. The relatively high surface polarity of the silicate minerals suggests a higher affinity for water and should consequently translate to poor flotation response. On the contrary, the very low relative surface polarity of the sulphide minerals should translate to better flotation performance.

5.5.2.2 Work of adhesion of different minerals

It is important to note that it is the work of adhesion for water that is relevant in the flotation process. This is because water is used as the medium in the flotation process. The work of adhesion for water increased in the following order: realgar < talc < galena

< albite < mica < wollastonite. A comparison of Table 4-5 and Table 4-9 shows that the enthalpies of immersion and the work of adhesion for water followed similar trends. Similar to the enthalpies of immersion in water, these results show that the sulphide minerals and talc had a higher work of adhesion than the rest of the silicate minerals. This means that the silicate minerals had a higher affinity for water than the sulphide minerals and talc. Therefore, the silicate minerals should exhibit poor flotation performance compared to the sulphide minerals and talc. These results are consistent with the known hydrophobic-hydrophilic character of the minerals as described previously in Section 1.3.1.1. The results of the work of adhesion are consistent with Ali et al. (2013) who found that galena (moderately hydrophobic) had a lower work of adhesion than quartz (a hydrophilic oxide mineral).

5.5.2.2.1 Work of adhesion vs powder contact angle

In the flotation context, it is the work of adhesion to water that is of interest as the interaction between a mineral particle and an air bubble in an aqueous medium is necessary for the separation. Work of adhesion of the minerals to water is a direct indicator of wettability and directly related to the contact angle (equation 1-36). The higher the work of adhesion to water, the greater the affinity to water (more hydrophilic surface) and hence the lower the contact angle. On the contrary, the lower the work of adhesion to water, the lower the affinity to water and hence the greater the contact angle. The Washburn method was used to measure the contact angles of different minerals in this study, using cyclohexane as the perfectly wetting liquid. For ease of comparison, the work of adhesion and the corresponding contact angles are shown in Table 5-6. As explained earlier on in Section 4.5.6, the contact angles of the silicate gangue minerals were difficult to measure as they could not be perfectly wetted using cyclohexane. The powder contact angles for the mica and wollastonite in Table 5-6 were quoted from literature.

Table 5-6: Relating the powder contact angles and work of adhesion of different minerals with water.

Mineral	Contact angle (°)	Work of adhesion in water (mJ/m²)
Talc	72.6 ± 4.8	194
Realgar	70.3 ± 3.1	212
Galena	40.9 ± 0.76	347
Mica	10*	543
Wollastonite	11*	2600

**literature values - mica* (Bryant, Bowman & Buckley, 2006) *and wollastonite* (Hou et al., 2013).

The results show that there is an inverse relationship between the work of adhesion and the contact angle. This was expected since a hydrophobic mineral with a higher contact angle has little interaction with water. On the contrary, a hydrophilic mineral with a lower contact angle has more interaction with water. Thus, the work of adhesion values for the minerals with water are consistent with contact angle values. The most hydrophobic talc had a correspondingly lowest work of adhesion and vice versa. As already mentioned wollastonite, albite and diopside are reported to undergo incongruent dissolution (Bailey and Reesman, 1971; Chou and Wollast, 1984; Blum and Lagasa, 1991; Wollast and Chou, 1992; Weissbart and Rimstidt, 2000; Shmulovich et al, 2001; Swarna et al, 2003; Prabhakar et al, 2005). This leaves a silica rich surface which interacts readily with water and hence relatively high work of adhesion.

5.5.2.2.2 Work of adhesion in water vs the flotation response

The work of adhesion between the minerals and water, being a more concrete parameter than the contact angle for the evaluation of wettability of minerals, was related to the first order flotation rate constant. Work of adhesion of the minerals to water is a direct indicator of wettability and directly related to the contact angle (equation 1-36) and surface free energy (equation 1-37). There has been some work relating contact angle to flotation response (Crawford & Ralston, 1988) and by extension the work of adhesion is related to the flotation response. The higher the work of adhesion in water, the greater the affinity to water (more hydrophilic surface) and consequently the less floatable the minerals.

The relationship between the work of adhesion in water and the first order flotation rate constant of the different minerals is shown in Figure 5-7. The flotation rate constant was calculated using the first-order kinetic model, based on collector-less flotation. As expected, the most hydrophilic mineral had the highest value of the work of adhesion. Equally, the most hydrophobic mineral had the lower value of the work of adhesion. As the work of adhesion decreases (i.e. wettability decreases), the flotation response increases. The most hydrophobic mineral produced the least work of adhesion and consequently improved flotation response. The results are consistent with Ali et al. (2013) who found that galena, with a lower work of adhesion produced a higher recovery as opposed to quartz, which had a higher work of adhesion, but a lower recovery. Thus, there is an inverse relationship between the work of adhesion and the flotation response.

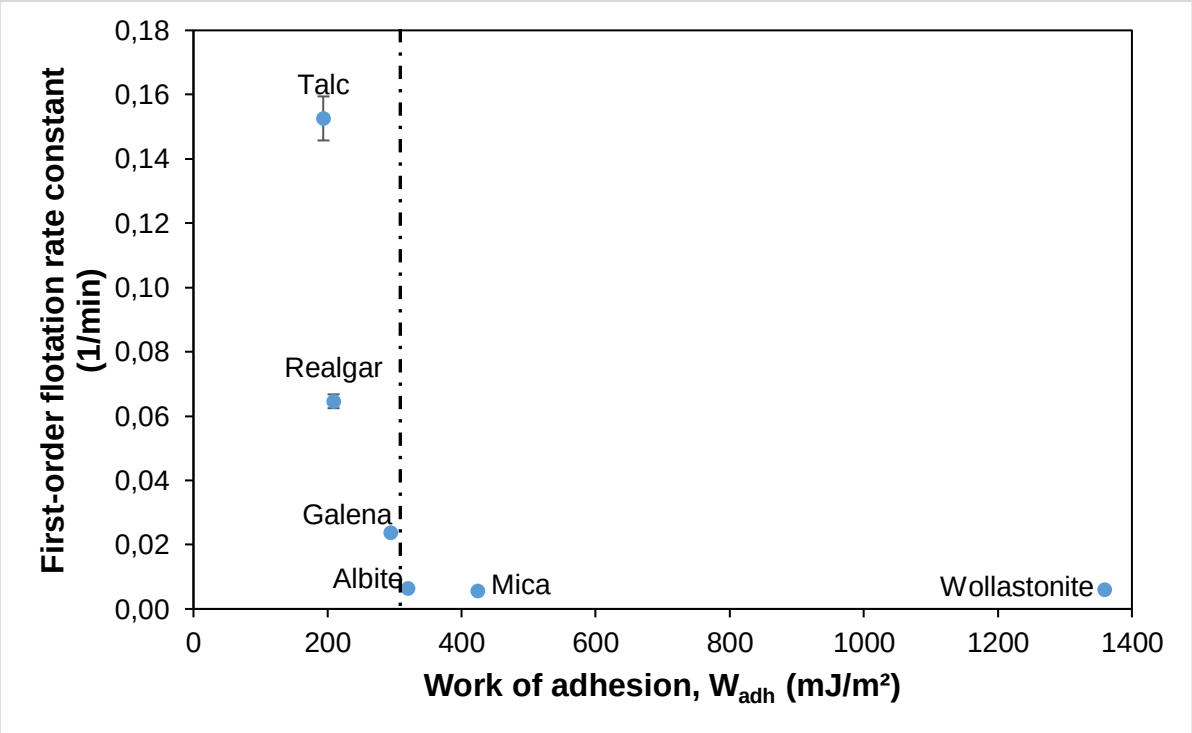

Figure 5-7: The relationship between the work of adhesion and the first order flotation rate constant.

Figure 5-7 further shows that there are two distinct regions namely the floatable region and the non-floatable region. In the floatable region, the work of adhesion is inversely related to the first-order flotation rate constant and flotation rate increases significantly with small decreases in the work of adhesion. In the non-floatable region, the first order

flotation rate constant is very low and independent of the work of adhesion. This proposal of the floatable and non-floatable region was observed for the enthalpies of immersion in water in Figure 5-1. This critical work of adhesion, demarcating the floatable region from the non-floatable region, is approximately 320 mJ/m^2.

5.5.2.3 The interfacial energy of interaction of particles and bubbles immersed in water (ΔG_{pwb}) vs flotation response

The interfacial energy of interaction of particles and bubbles immersed in water, ΔG_{pwb} has been shown in Table 4-8. The results have shown that the value of ΔG_{pwb} became more positive in the following order: talc > realgar > galena > albite > mica > wollastonite. The results in Table 4-8 have shown that ΔG_{pwb} was negative for talc and realgar while it was positive for the rest of the minerals. The ΔG_{pwb} gives information on whether the attachment of a particle to a bubble in water is thermodynamically feasible. If $\Delta G_{pwb} < 0$, bubble-particle attachment occurs spontaneously. Therefore, the results suggest that the process of particle-bubble interaction is spontaneous for talc and realgar, while it is not spontaneous for the rest of the minerals. The values of ΔG_{pwb} are consistent with the well-known hydrophobic-hydrophilic nature of the different minerals. Talc is well known to be hydrophobic (Yan et al., 2011; Yin et al., 2012). Realgar is also well known to be hydrophobic (Ozcan, 1992; Wills and Napier-Munn, 2006). These minerals therefore readily interact with super hydrophobic air bubbles via strong hydrophobic forces of attraction and hence the negative value of ΔG_{pwb} parameter. The silicate minerals, on the other hand are well known to be hydrophilic (Section 1.3.1.1.4), should interact less readily with air bubbles and hence the more positive value of ΔG_{pwb} parameter. Thus, the relative values of ΔG_{pwb} parameter indicate the relative wettabilities of the surfaces. The more negative the value of ΔG_{pwb}, the more hydrophobic the mineral. On the contrary, the less negative the value of ΔG_{pwb}, the more hydrophilic the mineral.

The relationship between ΔG_{pwb} parameter and the flotation response of the minerals was investigated and the results are shown in Figure 5-8.

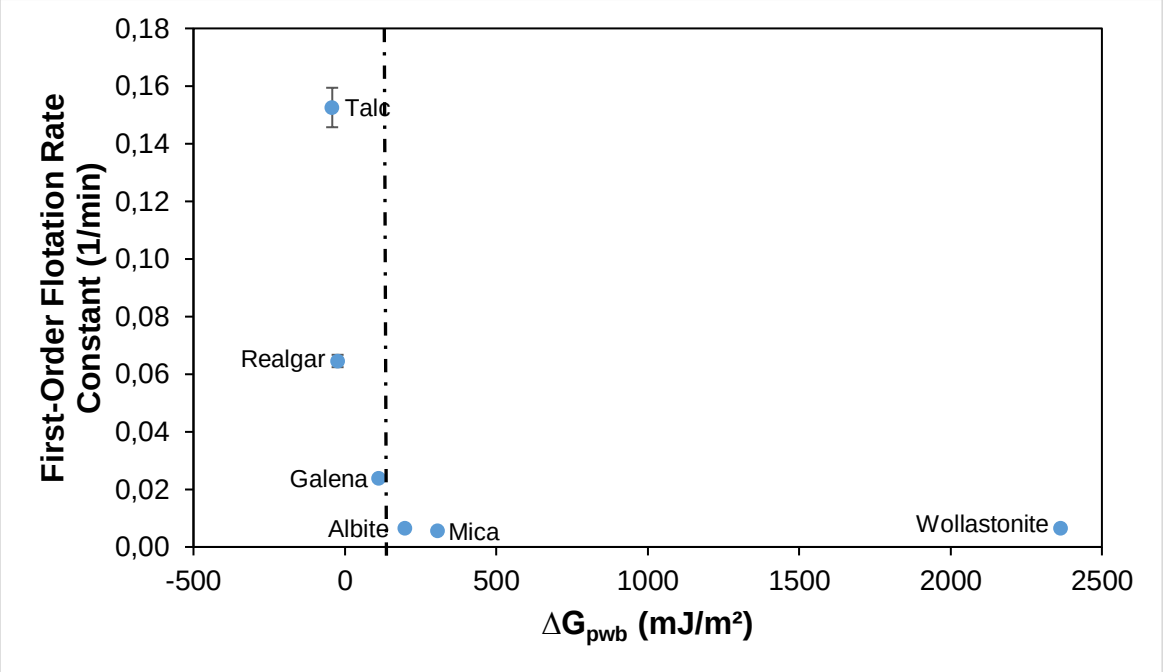

Figure 5-8: The relationship between the interfacial energy of interaction between particles and bubbles in water (ΔG_{pwb}) and the first order flotation rate constant.

Figure 5-8 shows that there are two distinct regions namely the floatable region and the non-floatable region. In the floatable region, the interfacial energy of interaction of particles and bubbles immersed in water is inversely related to the first-order flotation rate constant. This was expected as the more negative the value of ΔG_{pwb}, the stronger the hydrophobic force and consequently the greater the probability of bubble-particle attachment in water. This then translates to improved flotation response in a quiescent system where particle-bubble detachment is negligible.

In the non-floatable region, the first order flotation rate constant is very low and independent of the interfacial energy of interaction. This proposal of the floatable and non-floatable region was observed for the enthalpies of immersion in water in Figure 5-1. Again, we have called the value of the interfacial energy of interaction demarcating the floatable region from the non-floatable region as the critical interfacial energy of interaction and it is in the region of 200 mJ/m^2.

5.6 SYNTHETIC ORE (MINERAL MIXTURES)

5.6.1 Enthalpy of immersion of the synthetic ore in water

The enthalpies of immersion in water of a synthetic ore comprising of realgar and albite of varying proportions have been determined and the results have been presented in

Figure 4-1. The results have shown that the magnitude of the enthalpy of immersion in water linearly increased with the albite content in the synthetic ore. The magnitude of the enthalpy of immersion became more exothermic from -90 mJ/m² for pure realgar to -202.3 mJ/m² for pure albite. The results in Table 4-5 have shown that realgar is more hydrophobic than albite. The increase in the magnitude of the enthalpy of immersion with the albite content is explained in terms of the increase in the overall polarity of the synthetic ore as albite content increases. Hence the synthetic ore interacts more strongly with water as the albite content increases. It is clear from the results that the overall hydrophobicity of the synthetic ore decreased as the albite content increased. The results clearly show that wettability of the synthetic ore depended on the proportion of the minerals in the synthetic ore. This finding is consistent with Qi et al. (1992) who reported that the overall hydrophobicity of composite particles depends on the proportion, type of both valuable (hydrophobic phase) and gangue minerals (hydrophilic phase) present in the composite particles. It is clear from Figure 4-1 that the enthalpy of immersion method is capable of investigating the wettability of mineral mixtures with very good reproducibility.

The results in Figure 4-1 are consistent with the findings made by Wang and Fornasiero (2009) who found that the powder contact angle of lead borate-methylated quartz mixtures increased with increasing the content of the methylated quartz. The contact angle increased from 28° to 90° for pure lead borate and pure methylated quartz respectively. The results in Figure 4-1 also agree with Yildirim (2001) who found that the enthalpy of immersion in water became increasingly less exothermic as the particle size decreases. As talc is ground finer, the amount of the hydrophilic material decreases and thus talc becomes increasingly hydrophobic. Correspondingly, the contact angle of talc increased with decreasing particle size.

The results in Figure 4-1 show that the presence of the gangue mineral reduces the overall hydrophobicity of the synthetic ore. The more the quantity of the hydrophilic gangue associated with the valuable mineral, the more wettable it is. These results have negative implications on the flotation process in which the bubble-particle attachment depends strongly on hydrophobicity (Section 1.3). In the mineral processing context, the presence of the hydrophilic phase (gangue mineral) in association with the hydrophobic phase (valuable mineral) may be a result of

incomplete liberation, mineral surface oxidation or slimes coating. All these have the negative effect of lowering the wettability (hydrophobicity) of the synthetic ore. This ultimately leads to the loss of valuable minerals in the tailings in flotation concentrators. The loss is reported to be more pronounced in the coarse size fraction and this is attributed to both the destabilisation of the bubble-particle aggregates in high turbulent conditions and the low hydrophobicity of the of the coarse particles (Schubert, 1999; Pyke et al, 2003).

The concept of the mineral mixture may represent different amounts of two fully liberated minerals or different amounts of two incompletely liberated minerals. Concerning the latter, the synthetic ore with 0% albite (100% realgar) represents fully liberated valuable minerals (hydrophobic phase). Since complete liberation is rarely achieved during grinding (Meloy, 1984), the degree of mineral liberation dictates the mineralogical composition of the composite particles. The increase in the albite content corresponds to a decrease in the degree of liberation. The practical significance of these results is that the degree of liberation has an effect on the wettability of the composite particles. The lower the degree of liberation, the more the amount of gangue and the higher the wettability. On the contrary, the higher the degree of liberation, the less the amount of gangue and the lower the wettability.

5.6.2 Predicting the enthalpy of immersion for mineral mixtures

It was further investigated to establish whether it is possible to predict the enthalpy of immersion of binary mineral mixtures in water. For this purpose, the experimentally determined enthalpies of immersion of the realgar-albite mixtures were compared to the predicted (weighted) enthalpies of immersion of the pure samples and the results are shown in Figure 5-9. The enthalpies of immersion of pure albite and pure realgar in water were -202.3 mJ/m² and -90.7 mJ/m² respectively (Table 4-5). The predicted enthalpies of immersion were calculated based on the proportion by surface area of realgar and albite in the binary mineral mixtures as follows:

$$h_{pred} = (X_A * -202.3) + \big((1 - X_A) * -90.7\big) \qquad \textit{Equation 5-3}$$

where h_{pred} = predicted enthalpy of immersion of the mineral mixture (mJ/m^2);

X_A = the proportion of albite in the albite-realgar mixture.

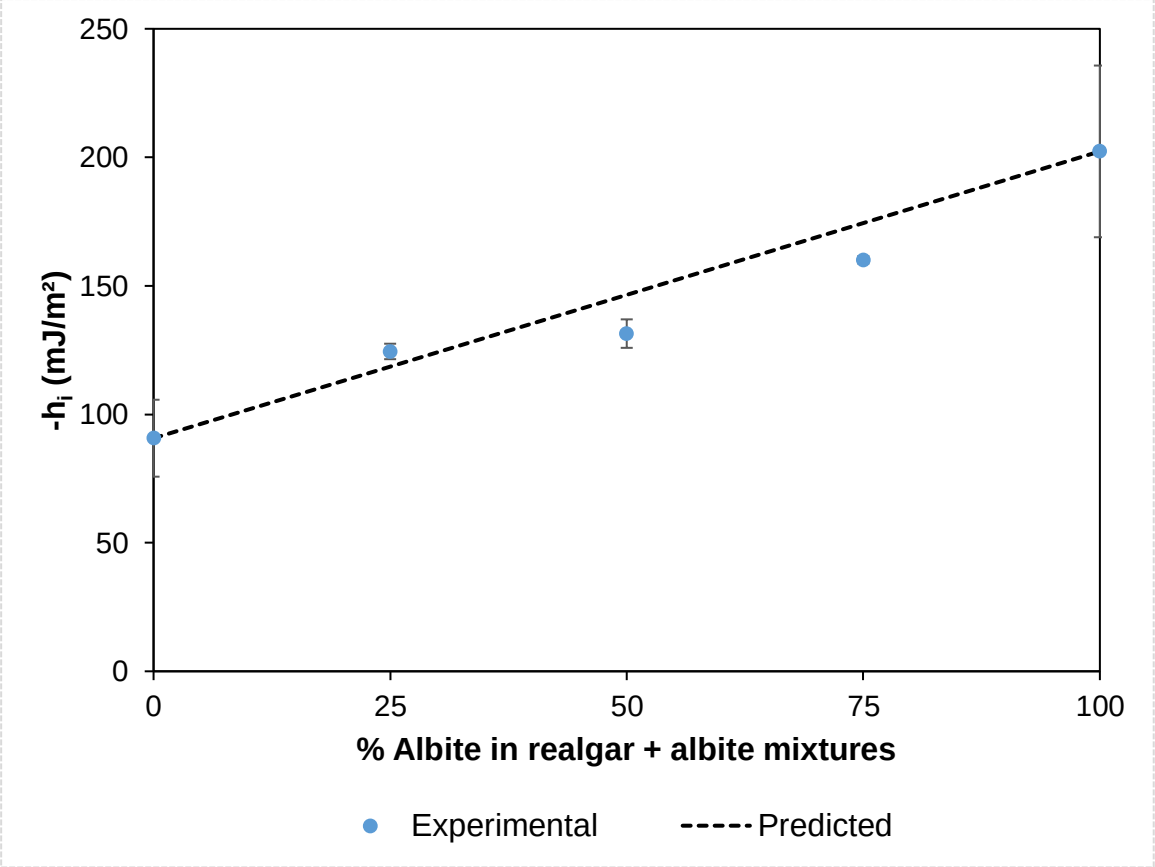

Figure 5-9: Comparison of the predicted enthalpies of immersion to the experimentally determined enthalpies of immersion for albite-realgar mixtures. The % represents the proportion of albite in the mineral mixture.

Figure 5-9 shows that the experimentally determined enthalpies of immersion were in excellent agreement with the predicted (weighted) enthalpies of immersion for the synthetic ore. This implies the enthalpies of immersion of mineral mixtures are additive in nature. Thus, in the present case, the enthalpy of immersion of a synthetic ore was found to be the weighted sum of the enthalpies of immersion of the individual minerals making up the ore. These results also suggest that there are no interactions between the sulphide minerals and the silicate gangue minerals which affect the enthalpy of immersion.

It is interesting to note that equation 5-3 used for calculating the predicted the enthalpies of immersion of the mineral mixtures takes the form of the Cassie equation shown in equation 1.9 (Section 1.4.4). The Cassie equation has been applied in various studies to calculate the contact angle of mixtures of particles of different wettability (Cassie, 1948; Oliver et al, 1980; Crawford et al, 1987). The proportion as

well as the contact angles of the individual phases in the mixture must be known. The results in Figure 5-9 are consistent with Wang and Fornasiero (2009) who found that the calculated contact angle (using the Cassie equation 1-9) agreed with the experimentally determined contact angles for the lead borate-methylated quartz mixtures. The similarity of the variation of both the enthalpy of immersion (in this study) and contact angles (Wang and Fornasiero, 2009) with mineral composition for the mineral mixtures reinforces the enthalpy of immersion as a robust indicator of mineral surface wettability, even for mineral mixtures. Therefore, the Cassie equation (equation 1-9) can be theoretically extended to the enthalpy of immersion measurements for determining the enthalpy of immersion of mineral mixtures containing *n* mineral phases as follows:

$$h_{pred} = \sum_{n=1}^{n} f_m h_i^m \qquad \textit{Equation 5-4}$$

where h_{pred} = the predicted enthalpy of immersion of the mineral mixture (mJ/m^2);

n = the number of different mineral phases in the mineral mixture;

f_m = the proportion of mineral phase *m* in the mineral mixture where $f_1+f_2+..f_n = 1$. This would be determined using quantitative evaluation of minerals by scanning electron microscopy (QEMSCAN);

$h^m{}_i$ = the enthalpy of immersion of individual mineral phase *m*.

Therefore, it is possible to calculate the enthalpy of immersion of a synthetic ore (mineral mixtures) from the knowledge of the proportion and the enthalpy of immersion in water of the individual minerals making the synthetic ore. The practical significance of this finding is that the enthalpy of immersion could be used to predict the wettability of composite particles and real ores. These results suggest that it is possible to start building models to be used in more complex systems. However, this was beyond the scope of this thesis.

5.6.3 Surface energetics of the synthetic ore

The surface energetics of the realgar-albite mixtures have been reported in Figure 4-2. The results have shown that as the albite content increases, all the surface energy components (dispersion, acidic, basic, polar components) and the total surface energy polar component of the realgar-albite mixture increase. The increase was more

pronounced for the polar component for albite content above 50%. Similarly, the work of adhesion was found to linearly increase with the albite content.

Both the enthalpies of immersion results presented in Table 4-5 and the flotation responses presented in Table 4-11 have shown that realgar is hydrophobic while albite is hydrophilic. Therefore, increasing the albite content increases the overall polarity of the synthetic ore. Thus, the overall wettability of the synthetic ore increases. This explains the increase in the surface energy components, especially the polar component as well as the total surface energy with increasing albite content. As the albite content increases, the interaction of the realgar-albite mixtures with water becomes increasingly stronger. Therefore, the bond formed between water and the synthetic ore becomes increasingly stronger, hence the observed increase in the work of adhesion with increasing albite content.

5.6.4 The relative surface polarity of the synthetic ore

The relative surface polarities, defined as the ratio of the polar component to the total surface energy, of the synthetic ore with varying albite content were calculated using equation 1-34 and the results are shown in Table 5-7. The variation of total surface energy and its components with albite content has been shown in Figure 4-1.

Table 5-7: The relative surface polarities as a function of the albite content in the synthetic ore.

Albite content (%)	Relative surface polarity (%)
0	3.1
25	42.8
50	22.9
75	52.4
100	52.2

The graph in Figure 5-10 shows the calculated mass recovery based on the flotation recoveries of the individual realgar and albite recoveries. These are plotted against both an experimental and a calculated relative surface polarity. The calculated relative surface polarity is based on a weighted sum from the individual polar and total surface energies of the pure realgar and pure albite. This data shows that there is a

relationship between the mass recovery and the calculated relative surface polarity, based on the individual polar and total surface energies. As the relative surface polarity increases, there is a significant decrease in the mass recovery after a relative surface polarity of about 0.4.

The experimental data for the relative surface polarities are based on the polar and total surface energies that were measured for each mineral mixture. It can be seen that, particularly the 50:50 mixture of realgar and albite (polarity 23%), lies off the calculated curve. Since each measured relative surface polarity is based on three enthalpy of immersion values from different probe liquids, there is greater accumulated error in these values. This is certainly an area that deserves further attention and has the potential to be used to predict the floatability potential of mineral mixtures. This work should be extended to other mineral mixtures, with careful measurement and calculation of the surface energetics of these mixtures.

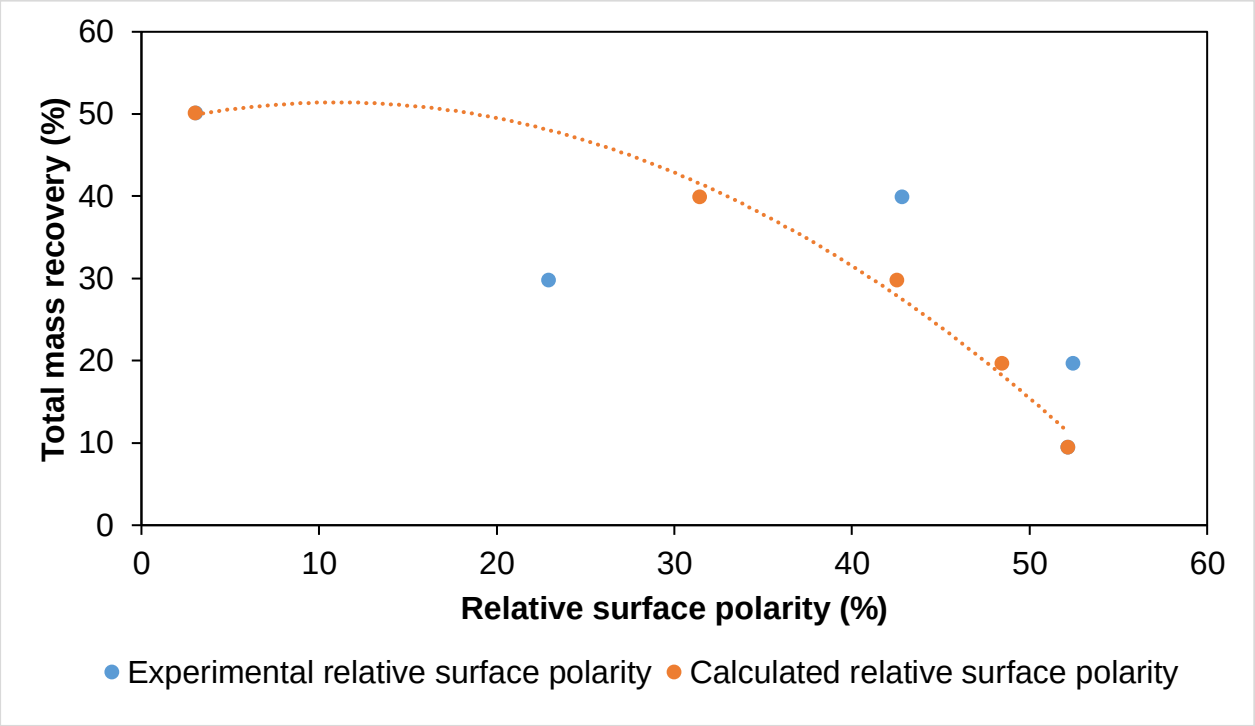

Figure 5-10: Variation of the total mass recovery with the experimental and measured relative surface polarity for realgar-albite mineral mixtures of different compositions.

CHAPTER 6

6 CONCLUSIONS, RECOMMENDATIONS AND FUTURE WORK

6.1 Conclusions

The main objective of this work was to investigate the use of the enthalpy of immersion to characterise mineral surface hydrophobicity and to relate this to flotation performance. Hydrophobicity may naturally occur as a result of the mineralogical characteristics of the ore or may be imparted by collectors. In the present study the enthalpies of immersion of different pure minerals were measured in their natural form as well as after treatment with collectors. Specifically, xanthate-coated galena and realgar samples were investigated. The relationship between the wettability of different minerals as characterised by the enthalpy of immersion and the flotation recovery and the first-order flotation rate constant in a quiescent system typical of a microflotation cell, was investigated. As an intermediate step, the enthalpy of immersion values of different minerals in water were compared to the corresponding powder contact angle values. This intermediate step was important in order to confirm that the enthalpy of immersion is a good measure of mineral surface hydrophobicity, which has previously been determined using the contact angle.

The other objective of this work was to systematically characterise the surface energetics of different minerals as well as binary mineral mixtures (synthetic ore). This was achieved by the measuring the enthalpies of immersion of the minerals in different probe liquids (water, formamide and n-hexane) and applying the van Oss-Chaudhury-Good (VOCG) model with its laws of exclusion. The calculated acid-base characteristics and the relative surface polarity of the minerals were then related to the flotation response of the minerals.

The other objective of this work was to assess whether enthalpy of immersion is able to differentiate between the amounts of minerals of different wettabilities in a mineral mixture. The effect of mineral composition on the enthalpy of immersion of binary mineral mixtures was investigated. It should be emphasised that, although the behaviour of real mineral mixtures is a long-term goal of this research, it is not the central focus of this thesis. This part of the study represents a preliminary scoping study since the main focus remains on the single mineral studies.

It has been found that the enthalpy of immersion technique was capable of distinguishing differences in the wettabilities of different minerals and these differences were explained in terms of the solid state properties of the minerals. The enthalpy of immersion method was also able to assess the changes in the surface chemical properties of the galena and realgar surfaces resulting from collector adsorption. The magnitude of the enthalpy of immersion was inversely related to the surface coverage of PAX on both galena and realgar. The higher the surface coverage of PAX, the less exothermic the enthalpy of immersion in water. The enthalpy of immersion measurements correlated with powder contact angle measurements, with the enthalpy of immersion measurements being found to be more reproducible and sensitive than the contact angle. It has also been shown that the enthalpy of immersion is more widely applicable measure of hydrophobicity of mineral particles typical of that used in the flotation process as opposed to the contact angle. It is therefore concluded that the enthalpy of immersion is a most useful indicator of the extent to which minerals are hydrophobic or hydrophilic either in their natural form or after treatment with a collector.

A linear relationship was confirmed between the enthalpy of immersion and the cosine of the powder contact angle for minerals in their natural form and in the presence of collectors as predicted by equation 5-2. The equation for the linear relationship was used to establish boundary conditions, which showed that the enthalpy of immersion would be less exothermic than -226.0 mJ/m² and -17.5 mJ/m² for contact angles greater than 0° and 90°, respectively. These results were consistent with the observed floatability of the minerals and the well-known floatability characteristics based on contact angle.

Furthermore, it was found that there was a strong inverse relationship between the enthalpy of immersion of the minerals studied and their flotation performance as indicated by recoveries and rates of flotation in a microflotation cell. The strong inverse relationship has potential to be used in pulp phase flotation models, although this was not the focus of this thesis. In addition, a critical enthalpy of immersion (CEI) value was observed above which no flotation occurred. The CEI was in the region of -200 mJ/m². At values less exothermic than the CEI, the flotation response was found to be inversely related to the enthalpy of immersion. At values more exothermic than the

CEI, no flotation occurs. The significance of this finding is that for any mineral whose flotation behaviour is unknown, the measurement of the enthalpy of immersion appears to be able to predict the flotation response of the mineral. The variance in the linear relationship between enthalpy of immersion and rate of flotation became much less (R^2 of 0.87 increased to 0.96) when the data was normalized with respect to particle density which was the only variable in the flotation studies with respect to particle-bubble encounter efficiency. This robust relationship has great potential for the modelling of mineral flotation behaviour.

The enthalpy of immersion was shown to depend on both the nature (mineralogy) of the mineral and the nature of the probe liquid. It was evident that the enthalpy of immersion technique had adequate sensitivity to differentiate between the enthalpies of immersion of different minerals with the same probe liquid and enthalpies of immersion of different probe liquids with the same minerals. The relative strength of the acid-base sites was shown to depend on the mineral type, viz whether metallic sulphide, silicate minerals and phyllosilicate minerals. Silicate minerals (albite, wollastonite and mica) had a higher magnitude of the basic component than the metallic sulphide minerals (realgar and galena) and talc. Thus, the silicate minerals were more basic than the sulphide minerals and talc. It was also found that trends in the polar component and the total surface energy were similar to those observed for the basic component. It was observed that the higher the total surface energy, the lower the hydrophobicity of the mineral. The surface energetics obtained in this study were consistent with the hydrophobic-hydrophilic nature of these minerals. The acid-base characteristics of the minerals, measured by solution calorimetry, can give a detailed insight into the different surface energies of mineral types and may be useful in optimising processing strategies.

The relative surface polarity, defined as the ratio of the polar component to the total surface energy, was calculated for the different minerals. It was observed that the silicate minerals had higher relative surface polarity than the metallic sulphide minerals and talc. Thus, the silicate minerals were predominantly hydrophilic while the metallic sulphide minerals and talc were predominantly hydrophobic. The relative surface polarity was inversely related to both the powder contact angle and the mineral surface

hydrophobicity as indicated by the microflotation recoveries and the first-order flotation rate constants. These results were consistent with the known hydrophobic-hydrophilic nature of the minerals. The results demonstrate that the relative surface polarity is a robust indicator of the hydrophobicity or hydrophilicity of a given mineral surface and has potential to be used in optimising mineral processing strategies.

The interfacial free energy of interaction between mineral particles and bubbles immersed in water as well as the work of adhesion, a fundamental parameter in wettability studies, were calculated using the surface energetics of the different minerals. In the flotation context, it is the work of adhesion for water that is relevant since water is the medium for the flotation process. It was interesting to note that the trends in both the energy of interaction between particles and bubbles immersed in water and the work of adhesion for water coincided with the trend in the enthalpies of immersion of the different minerals in water. Similarly, to the enthalpies of immersion in water, these results show that the sulphide minerals and talc had a lower energy of interaction between particles and bubbles immersed in water as well as a lower work of adhesion than the rest of the silicate minerals. This means that the silicate minerals had a higher affinity for water than the sulphide minerals and talc. These results are consistent with the known hydrophobic-hydrophilic character of the minerals. The work of adhesion was found to be inversely related to the powder contact angle. Similarly, to the enthalpy of immersion in water, a critical interfacial energy of interaction between particles and bubbles immersed in water (ΔG_{pwb}) and a critical work of adhesion for water values in the region of 200 mJ/m² and 500 mJ/m² respectively were observed, above which no flotation occurs. At values less than the critical values, both the energy of interaction and the work of adhesion were inversely related to the first-order flotation rate constant. The flotation rate constants increased significantly with small decreases in the energy of interaction and the work of adhesion. It is therefore concluded that both the energy of interaction and the work of adhesion for water are important parameters providing useful information concerning the floatability of different minerals.

The enthalpy of immersion was able to differentiate between the amounts of minerals of different wettabilities in a mineral mixture. The enthalpy of immersion became

increasingly exothermic as the percentage of albite in the mineral mixture increased. A relatively good direct linear fit between the enthalpy of immersion and the albite content in the realgar-albite mixtures was observed. The experimentally determined enthalpies of immersion in water were in excellent agreement with the weighted enthalpies of immersion for the realgar-albite mixtures. This implies the enthalpies of immersion of mineral mixtures are additive in nature. Therefore, it is possible to calculate the enthalpy of immersion of a synthetic ore (mineral mixtures) from the knowledge of the proportion and the enthalpy of immersion in water of the individual minerals making the synthetic ore. This is an extension of the Cassie equation for contact angles of composite particles. In terms of the surface energetics, the total surface energy and its components (the basic, polar, dispersive components) increased with the increase in the albite content in the mineral mixtures. The increase was more pronounced for the basic component for albite content above 50%. The surface energetics of the synthetic ore showed that there is a relationship between the mass recovery and the calculated relative surface polarity, based on the individual polar and total surface energies. As the relative surface polarity increases, there is a significant decrease in the mass recovery after a relative surface polarity of about 0.4. Thus, the enthalpy of immersion has the potential to be used to predict the wettability and the floatability potential of mineral mixtures. This work should be extended to other mineral mixtures, with careful measurement and calculation of the surface energetics of these mixtures.

6.2 Recommendations and future work

As highlighted in the scope, the behaviour of mineral mixtures was not the central focus of this thesis. This part of the study was a brief scoping foray into this area of research and the main focus remains on the single mineral studies. Thus, this work presents an opportunity for further study to investigate the use of the enthalpy of immersion to characterise the wettability of real ores and relate this to their flotation behaviour.

Most metallurgical plants are recycling process water in response to water scarcity challenges. The recycled process water contains a number of ions which are reported to have an effect on the efficiency of the flotation process. It is therefore recommended

to investigate the effect of water quality on the enthalpy of immersion and the floatability of the different minerals.

Furthermore, the results obtained in this study only hold for low energy systems with no froth phase present. It would be useful to investigate whether these findings are sustained when the froth phase is introduced and in a high energy (turbulent) system. It therefore recommended that a batch flotation cell be used to determine the flotation response of the different minerals.

Most pulp phase flotation models have the contact angle as an input parameter. This thesis has demonstrated that enthalpy of immersion is more reproducible, sensitive and widely applicable measure of hydrophobicity of mineral particles typical of that used in the flotation process than the contact angle. Therefore, further work is required to incorporate the enthalpy of immersion in the pulp phase flotation models. This is beneficial in the design of mineral processing flow sheets as well predicting and optimising the flotation process.

CHAPTER 7

7 REFERENCES

Ackerman, P.K., G.H. Harris, R.R. Klimpel and Aplan, F.F. (1987): Evaluation of flotation collectors for copper sulfides and pyrite, III. Effect of xanthate chain length and branching. *International Journal of Mineral Processing*, 21 (1-2):141–156.

Acres, R.G. (2010): Advanced Synchrotron Spectroscopy Studies of Homogeneous and Heterogeneous Metal Sulfide Surface Chemistry. *PhD Thesis.* Ian Wark Research Institute, University of South Australia.

Adamson, A.W., and Ling, I. (1964): The Status of Contact Angle as a Thermodynamic Property. *Advances in Chemistry*, 43, Chapter 3: 57–73.

Ali, S.S.M., Heng, Y.Y.J., Nikolaec, A.A. and Waters, K.E. (2013): Introducing inverse gas chromatography as a method of determining the surface heterogeneity of minerals for flotation. *Powder Technology*, 249: 373–377.

Allison S.A., L.A. Goold, M.J. Nicol and Granville, A. (1972): A determination of the products of reaction between various sulfide minerals and aqueous xanthate solution, and a correlation of the products with electrode rest potentials. *Metallurgical Transactions* 3: 2513-2618.

Allen, T. and Patel, R.M. (1968): Determination of specific surface using the flow microcalorimeter. *Powder Technology,* 2: 111-120.

Arai, Y. (1996). *Chemistry of Powder Production*

Ata, S., Ahmed, N. and Jameson, G.J. (2002): Collection of hydrophobic particles in the froth phase. *International Journal of Mineral Processing*, 64(2-3): 101–122.

Ata, S., Ahmed, N. and Jameson, G.J. (2003): A study of bubble coalescence in flotation froths. *International Journal of Mineral Processing*, 72(1-4): 255–266.

Bailey, A. and Reesman, A. L. (1971): A survey study of the kinetics of wollastonite dissolution in H_2O-CO_2 and buffered systems at 25 degrees. *American Journal of Science*, 271: 464–472.

Bartell, F.E. and Merrill, E.E. (1931): Determination of adhesion tension of liquids against solids. A microscopic method for the measurement of interfacial contact

angles. *Journal of Physical Chemistry*, 36: 1178.

Battey, M. H. and Pring, A. (1997): *Mineralogy for students third edition.*

Blake, P. and Ralston, J. (1985a): Controlled methylation of quartz particles. *Colloids and Surfaces*, 15: 101–118.

Blake, P. and Ralston, J. (1985b): Particle size, surface coverage and flotation response. *Colloids and Surfaces*, 16: 41-53.

Blum, A. E. and Lagasa, A. C. (1991): The role of surface speciation in the dissolution of albite. *Geochim. Cosmochim. Acta*, 55: 2823–2830.

Bolis, V., Fubini, B., Marchese, L, Martra, G. and Costat, D. (1991): Hydrophilic and Hydrophobic Sites on Dehydrated Crystalline and Amorphous Silicas. *J. Chem. Soc. Faraday Trans*, 87(3): 497–505.

Bradshaw, D.J. and O'Connor, C.T. (1996): Measurement of the sub-process of bubble loading in flotation. *Minerals Engineering*, 9(4), pp.443–448.

Brito, S., Abreu, E. and Skinner, W. (2011a): Predicting the surface chemistry contribution to the flotation recovery of chalcopyrite by ToF-SIMS. *Minerals Engineering*, 24(2): 160–168.

Brito, S., Abreu, E. and Skinner, W. (2011b): ToF-SIMS-derived hydrophobicity in DTP flotation of chalcopyrite: Contact angle distributions in flotation streams. *International Journal of Mineral Processing*, 98(1-2): 35–41.

Bruil, J.G. and van Aartesen, J.J. (1974): The determination of contact angles of aqueous surfactant solutions on powders. *Colloid and Polymer Science*, 252: 32–38.

Bryant, E. M., Bowman, R. S. and Buckley, J. S. (2006): Wetting alteration of mica surfaces with polyethoxylated amine surfactants. *Journal of Petroleum Science and Engineering*, 52(1–4): 244–252.

Buckton, G. (1990): Contact angle, adsorption and wettability - a review with respect to powders. *Powder Technology*, 61(3): 237–249.

Bulatovic, S.M. (2007): Handbook of Flotation Reagents: Chemistry, Theory and Practice: Flotation of Silfide Ores. *Elsevier Science & Technology Books.*

Cassie, A. B. D. (1948): Contact angles. *Discussions of the Faraday Society*, 3: 11–16.

Chau, T.T., Bruckard, J.W., Koh, P.T.L. and Nguyen, A.V. (2009): A review of factors that affect contact angle and implications for flotation practice. *Advances in Colloid and Interface Science*, 150(2): 106–115.

Chelgani, S.C. and Hart, B. (2014): TOF-SIMS studies of surface chemistry of minerals subjected to flotation separation - A review. *Minerals Engineering*, 57: 1–11.

Chessick, J. J., Healey, F. H. and Zettlemoyer, A. C. (1956): Adsorption and heat of wetting studies of teflon. *The Journal of Physical Chemistry*, 60(10): 1954–1956.

Chibowski, E. and Perea-Carpio, R. (2002): Problems of contact angle and solid surface free energy determination. *Advances in Colloid and Interface Science*, 98: 245–264.

Chou, L. and Wollast, R. (1984): Study of the weathering of albite at room temperature and pressure with a fluidized bed reactor. *Geochim. Cosmochimica. Acta,* 48(11): 2205–2217.

Crawford, J. (1986): Particle Size, Hydrophobicity and Flotation Response. *MSc Thesis.* Swirnburne Institute of Technology.

Crawford, R., Koopal, L. K. and Ralston, J. (1987): Contact Angles on Particles and Plates. *Colloids and Surfaces*, 27: 57–64.

Crawford, R. and Ralston, J. (1988): The influence of particle size and contact angle in mineral flotation. *International Journal of Mineral Processing*, 23(1-2): 1–24.

Dai, Z.; Dukhin, S; Fornasiero, D. and Ralston, J. (1998): The Inertial Hydrodynamic Interaction of Particles and Rising Bubbles with Mobile Surfaces. *The Journal of Colloid and Interface Science*, 197: 275–292.

Dai, Z., Fornasiero, D. and Ralston, J. (1999): Particle-bubble attachment in flotation. *Journal of Colloid And Interface Science,* 217: 70–76.

Della Volpe, C. and Siboni, S. (1997): Some reflections on acid-base solid surface free energy theories. *Journal of Colloid and Interface Science,* 195(1): 121–136.

Della Volpe, C and Siboni, S. (2000): Acid-base surface free energies of solids and the definition of scales in the Good-van Oss-Chaudhury theory. *Journal of Adhesion Science and Technology,* 14(2): 235–272.

Denoyel, R., Beurroies, I. and Lefevre, B. (2004): Thermodynamics of wetting : information brought by microcalorimetry. *Journal of Petroleum Science and*

Engineering, 45: 203–212.

Dooby, G. S. and Finch, J. (1987): Particle size dependence in flotation derived from a fundamental model of the capture process. *International Journal of Mineral Processing,* 21(3–4): 241–260.

Douillard, J. M., Malandrini, H. and Clauss, F. Zoungrana, T. and Partyka, S. (1994): Surface tension of talc and talc-chlorite mixtures. *Journal of Thermal Analysis*, 41: 1205–1210.

Douillard, J. M., Malandrini, H., Clauss, F. and Partyika, S. (1997): Interactions between talc particles and water and organic solvents. *Journal of Colloid and Interface Science,* 194(1): 183–93.

Douillard, J. M., Salles, F., Henry, M., Malandrini, H. and Clauss, F. (2007): Surface energy of talc and chlorite : Comparison between electronegativity calculation and immersion results. *Journal of Colloid and Interface Science,* 305: 352–360.

Douillard, J. M. (1997): Concerning the Thermodynamic Consistency of the "Surface Tension Components" Equations. *Journal of Colloid and Interface Science*, 515(188): 511–515.

Douillard, J. M., Zajac, J., Malandrini, H. and Clauss, F. (2002): Contact Angle and Film Pressure : Study of a Talc Surface. *Journal of Colloid and Interface Science*, 255: 341–351.

Douillard, J. M., Zoungrana, T. and Partyka, S. (1995): Surface Gibbs free energy of minerals: some values. *Journal of Petroleum Science and Engineering*, 14: 51–57.

Douillard, J.M. and Zajac, J. (2006): Enclopedia of surface and colloid science. pp.1514–1524.

Drelich, J., Boinovich, L., and Ziqi, S. (2017): Editorial [Surface Innovations, Volume 6 Issue 1–2, March 2018]. *Surface Innovations*, *6*(1-2): 1-3.

Duan, J.; Fornasiero, D. and Ralston, J. (2003): Calculation of the flotation rate constant of chalcopyrite particles in an ore. *International Journal of Mineral Processing*, 72(1-4): 227–237.

Fielden, M. L., Hayes, R. A. and Ralston, J. (1996): Surface and Capillary Forces Affecting Air Bubble−Particle Interactions in Aqueous Electrolyte. *Langmuir*, 12:

3721–3727.

Finkelstein, N. and L. Goold (1972): The reaction of sulphide minerals with thiol compounds. *National Institute for Metallurgy*, Project C.33/62: Project Report No. 14.

Fowkes, F.M. (1972): Attractive forces at interfaces. *Industrial and Engineering Chemistry*, 56: 40-52.

Fowkes, F. M. (1968): Calculation of work of adhesion by pair potential summation. *Journal of Colloid and Interface Science*, 28: 493-505.

Fowkes, F.M. (1972): Donor-acceptor interactions at interfaces . *Journal of Adhesion*, 4: 155-159.

Fox, H. W. and Zisman, W. A. (1952a): The spreading of liquids on low energy-surfaces. II. Modified tetrafluoroethylene polymers. *Journal of Colloid Science*, 7: 109-121.

Fox, H. W. and Zisman, W. A. (1952b): The spreading of liquids on low-energy surfaces. III. Hydrocarbon surfaces. *Journal of Colloid Science,* 7: 428-442.

Fuerstenau, D.W. (2005): A Century of Developments in the Chemistry of Flotation. *Centenary of Flotation Symposium*: 13.

Galet, L., Patry, S. and Dodds, J. (2010): Determination of the wettability of powders by the Washburn capillary rise method with bed preparation by a centrifugal packing technique. *Journal of Colloid And Interface Science*, 346(2): 470–475.

Gardner, J. R. and Woods, R. (1979): An electrochemical investigation of the natural flotability of chalcopyrite. *International Journal of Mineral Processing*, 6(1): 1–16.

Gaudin, A. M. (1957): Flotation, 2nd Edition, McGraw Hill Co., New York.

Gaudin, A. (1974): The role of oxygen in flotation. *Journal of Colloid and Interface Science*, 47(2): 309–314.

Gharabaghi, M. and Aghazadeh, S. (2014): A review of the role of wetting and

spreading phenomena on the fl otation practice. *Current Opinion in Colloid & Interface Science*, 19(4): 266–282.

Goncharuk, O. V. (2015): The heat of immersion of modified silica in polar and nonpolar liquids. *Journal of Thermal Analysis and Calorimetry*, 120: 1365–1373.

Grano, S. R., Prestidge, C. A. and Ralston, J. (1997): Solution interaction of ethyl xanthate and sulphite and its effect on galena flotation and xanthate adsorption. *International Journal of Mineral Processing,* 52(2–3): 161–186.

Groszek, A.J. (1958): A Calorimeter for Determination of Heats of Wetting. *Nature*, 182(4643): 1152–1153.

Groszek, A.J. (1998): Flow Adsorption Microcalorimetry. *Thermochimica Acta*, 312: 133–143.

Hamilton, I.C. and R. Woods (1979): Effect of alkyl chain length on the aqueous solubility and redox properties of symmetrical dixanthogens. *Australian Journal of Chemistry*, 32(10): 2171 - 2179.

Hammer, M.U., Anderson, T.H., Chaimovich, A., Shell, S.M. and Israelachvilli, J. (2010): The search for the hydrophobic law. *Faraday Transactions,* 146: 299-308.

Hansford, D.T., Grant, D.J.W. and Newton, J.M. (1980): Surface Energetics of the Wetting of a Hydrophobic Powder. *Journal of Chemical Society, Faraday Transactions*, 76: 2417–2431.

Hewitt, D., Fornasiero, D. and Ralston, J. (1995): Bubble-particle attachment. *Journal of Chemical Society, Faraday Transactions,* 91(13): 1997–2001.

Ho, R., Hinder, S.J., Watts, J.F., Dilworth, S.E., Williams, D.R., Heng, J.Y.Y. (2010): Determination of surface heterogeneity of d -mannitol by sessile drop contact angle and finite concentration inverse gas chromatography. *International Journal of Pharmaceutics*, 387: 79–86.

Hou, X., Ding, H., Liang, Y., Zheng, Y.X., Yang, Z.D. and Luo, H.N. (2013): Mechanism of surface hydrophobicity modification of wollastonite powder. *Materials Research Innovations,* 17: 260–266.

Jameson, G.J. (2012): The effect of surface liberation and particle size on flotation rate constants. *Minerals Engineering*, 36-38: 132–137.

Jańczuk, B., Wójcik, W., Zdziennicka, A. and González-Caballero, F. (1992): Components of surface free energy of galena. *Journal of Materials Science*, 27(23): 6447–6451.

Jańczuk, B., Wójcik, W. and Zdziennicka, A. (1993): Determination of surface-free energy components of synthetic chalcocite from contact angle measurements. *Powder Technology,* 76(3): 233–239.

Johansson, G. and Pugh, R.J. (1992): The influence of particle size and hydrophobicity on the stability of mineralized froths. *International Journal of Mineral Processing*, 34(1-2): 1–21.

Jones, J. B. and Adamson, A. W. (1968): Temperature dependence of contact angle and of interfacial free energies in the naphthalene-water-air system. *The Journal of Physical Chemistry*, 72(2): 646–650.

Kelebek, S. (1984): Surface properties and selective flotation of inherently hydrophobic minerals. *PhD Thesis.* McGill University.

Kim D.S., S.E. Kuh and Moon, K.S. (2012): Characteristics of Xanthates Related to Hydrocarbon Chain Length Characteristics of Xanthates Related to Hydrocarbon Chain Length. *Geosystem Engineering*, 3(1): 30–34.

Klimpel, R. R. (1984): Froth flotation: The kinetic approach. *Proceedings of Mintek 50, Johannesburg, South Africa.*

Kohad, V.P. and Mines, Z. (1998): Flotation of Sulphide Ores - HZL Experience. *Froth Flotation: Recent trends @ IIME, Jamshedpur*, pp.18–41.

Krasowska, M., Terpilowski, K., Chibowski, E. and Malysa, K. (2006): Apparent contact angles and time of the three phase contact formation by the bubbles colliding with teflon surfaces of different roughness. *Physicochemical problems of mineral processing,* 40: 293–306.

Krasowska, M., Zawala, J. and Malysa, K. (2009): Air at hydrophobic surfaces and kinetics of three phase contact formation. *Advances in Colloid and Interface Science,* 147-148: 155-169.

Kraus, G. (1955): The heat of immersion of carbon black in water, methanol and n-hexane. *The Journal of Physical Chemistry*, 59: 343–345.

Kumar, G. and Prabhu, K.N. (2007): Review of non-reactive and reactive wetting of liquids on surfaces. *Advances in Colloid and Interface Science*, 133(2): 61–89.

Kwok, D.Y. and Neumann, A.W.U. (1999): Contact angle measurement and contact angle intepretation. *Journal of Colloid and Interface Science*, 81: 167-249.

Laskowski, J. and Kitchener, J. A. (1969): The hydrophilic-hydrophobic transition on silica. *Journal of Colloid and Interface Science,* 29(4): 670–679.

Li, Z. and Yoon, R. (2013): Thermodynamics of hydrophobic interaction between silica surfaces coated with octadecyltrichlorosilane. *Journal of Colloid and Interface Science*, 392(1): 369-375.

Makrides, A.C. and Hackerman, N. (1952): Heats of immersion. I. The system silica-water. *The Journal of Physical Chemistry*, 63: 594–598.

McFadzean, B. and O'Connor, C.T. (2014): A thermochemical study of thiol collector surface reactions on galena. *Minerals Engineering,* 65: 54–60.

McHardy, J. C. and Salman, T. (1974): Some aspects of the surface chemistry of talc flotation. *Trans. IMM.,* 83: 25–30.

Melkus, T.G.; Chiang, S.H. and Wen, W.W. (1987): An experimental study of heat of immersion of coal. *Colloids and Surfaces*, 28: 109–121.

Meloy, T.P. (1984): Liberation theory - Eight, modern, usable theorems. *International Journal of Mineral Processing,* 13(4): 313–324.

Melrose, J.C. (1965): On the thermodynamic relations between immersional and adhesional wetting. *Journal of Colloid Science*, 20(8): 801–821.

Mishchuk, N., Ralston, J. and Fornasiero, D. (2002): Influence of dissolved gas on van der Waals forces between bubbles and particles. *Advances in Colloid and Interface Science*, 106(4): 689-696.

Mohammadi-Jam, S.; Burnett, D.J. and Waters, K.E. (2014): Surface energy of minerals - Applications to flotation. *Minerals Engineering*, 66: 112–118.

Mohammadi-Jam, S. and Waters, K.E. (2014): Inverse gas chromatography applications: A review. *Advances in Colloid and Interface Science*, 212: 21–44.

Morcos, I. (1970): On contact angle and dispersion energy of the cleavage graphite/water system. *Journal of Colloid And Interface Science,* 34(3): 469–471

Muganda, S.; Zanin, M. and Grano, S.R. (2011a): Benchmarking fl otation

performance : Single minerals. *International Journal of Mineral Processing*, 98: 182–194.

Muganda, S.; Zanin, M. and Grano, S.R. (2011b): Influence of particle size and contact angle on the flotation of chalcopyrite in a laboratory batch flotation cell. *International Journal of Mineral Processing*, 98: 150–162.

Nakamoto, H. and Takahashi, H. (1982): Hydrophobic natures of zeolite ZSM-5. *Zeolites*, 2(2): 67–68.

Neumann, A.W. (1974): Contact angles and their temperature dependence: Thermodynamic status, measurement, interpretation and application. *Advances in Colloid and Interface Science*, 4: 105–191.

Nguyen, A.V., Nalaskowski, J., Miller, J.D. and Butt, H.J. (2003): Attraction between hydrophobic surfaces studied by atomic force microscopy. *International Journal of Mineral Processing,* 72(1-4): 215-225.

Nguyen, C. M., Nguyen, A. V. and Miller, J. D. (2006): Computational validation of the Generalized Sutherland Equation for bubble-particle encounter efficiency in flotation. *International Journal of Mineral Processing,* 81: 141–148.

Nguyen, P. T. and Nguyen, A. V (2009): Validation of the Generalised Sutherland Equation for bubble-particle encounter efficiency in flotation: Effect of particle density. *Minerals Engineering,* 22: 176–181.

Oliver, J. P., Huh, C. and Mason, S. G. (1980): An experimental study of some effects of solid surface roughness on wetting. *Colloids and Surfaces,* 1(1): 79–104.

Owens, D.K. and Wendt, R.C. (1969): Estimation of the surface energy of polymers. *Journal of Applied Polymer Science*, 13(13): 1741-1747.

Ozcan, O. (1992): Classification of minerals according to their critical surface tension of wetting values. *International Journal of Mineral Processing,* 34(3): 191–204.

Pan, L., Jung, S. and Yoon, R. H. (2012): A fundamental study on the role of collector in the kinetics of bubble-particle interaction. *International Journal of Mineral Processing,* 106–109: 37–41.

Park, J. H. and Aluru, N. R. (2009): Temperature-dependent wettability on a titanium dioxide surface. *Molecular Simulation,* 35(1–2): 31–37.

Partyka, S. (1993): Measurements of hydrophobic and hydrophilic surface sites by

flow microcalorimetry. *Langmuir*, 9: 2721–2725.

Pauling, L. (1960): The Nature of the chemical bond and the structure of molecules and crystals, 3rd Edition, Cornell Univ. Press.

Peng, H., Hampton, M.A. and Nguyen, A.V. (2013): Nanobubbles do not sit alone at the solid-liquid interface. *Langmuir*, 20:6123-6130.

Prabhakar, S., Hanumantha Rao, K. and Forsling, W. (2005): Dissolution of wollastonite and its flotation and surface interactions with tallow-1,3-diaminopropane (duomeen T). *Minerals Engineering,* 18(7): 691–700.

Prestidge, C.A. and Ralston, J. (1996): Contact angle studies of ethyl xanthate coated galena particles. *Journal of colloid and interface science*, 184: 512–8.

Prestidge, C.A. and Ralston, J. (1996): Contact angle studies of particulate sulphide minerals. *Minerals Engineering*, 9(1): 85–102.

Puri, B.R.; Singh, D.D. and Sharma, L.R. (1953): The heat of immersion of charcoal as a function of its oxygen complexes. *The Journal of Physical Chemistry*, 62: 756–758.

Pyke, B. (2004): Bubble-particle capture in turbulent flotation systems. *PhD Thesis.* University of South Australia.

Pyke, B., Fornasiero, D. and Ralston, J. (2003): Bubble particle heterocoagulation under turbulent conditions. *Journal of Colloid and Interface Science,* 265: 141–151.

Qi, W. Q., Parentich, A., Little, L. H. and Warren, L. J. (1992): A QEM*SEM study of the flotation of composite particles. *International Journal of Mineral Processing,* 34(1–2): 71–82.

Rabinovich, Y.I. and Yoon, R.H. (1994): Use of atomic force microscope for the measurements of hydrophobic forces. *Colloids and Surfaces A: Physicochemical and Engineering Aspects,* 93: 263–273.

Raichur, A. M., Wang, X. H. and Parekh, B. (2001): Estimation of surface free energy of pyrite by contact angle measurements. *Minerals Engineering,* 14(1): 65–75.

Ralston, J. (1994): The chemistry of galena flotation: Principles & practice. *Minerals Engineering,* 7(5–6): 715–735.

Ralston, J. (1999): Controlled flotation processes: Prediction and manipulation of

bubble- particle capture. *The Journal of The South African Institute of Mining and Metallurgy,* 27–34.

Ralston, J. and Dukhin, S. S. (1999): The interaction between particles and bubbles. *Colloids and Surfaces A: Physicochemical and Engineering Aspects,* 151(1–2): 3–14.

Ralston, J., Fornasiero, D. and Mishchuk, N. (2001): The hydrophobic force in flotation - a critique. *Colloids and Surfaces A*, 192 (1-3): 39-51.

Rao, S.R. (1982): Surface chemistry of froth flotation, Fundamentals, 1st edition. Kluwer Academic / Plenum Publishers, New York.

Rao, S.R. and Leja, J., (2004): Surface chemistry of froth flotation Volume 2: Reagents and mechanisms. 2nd edn. Plenum Publishers.

Rimstidt, J. D. and Dove, P. M. (1986): Mineral/solution reaction rates in a mixed flow reactor: wollastonite hydrolysis. *Geochim. Cosmochim. Acta,* 50: 2509–2516.

Rudolph, M. and Hartmann, R. (2017): Specific surface free energy component distributions and flotabilities of mineral microparticles in flotation - An inverse gas chromatography study. *Colloids and Surfaces A: Physicochemical and Engineering Aspects,* 513: 380–388.

Safari, M. and Deglon, D. (2018): An attachment-detachment kinetic model for the effect of energy input on flotation. *Minerals Engineering,* 117: 8–13.

Salles, F., Henry, M. and Douillard, J. (2006): Determination of the surface energy of kaolinite and serpentine using PACHA formalism - Comparison with immersion experiments. *Journal of Colloid and Interface Science,* 303: 617–626.

Schubert, H. (1999): On the turbulence-controlled microprocesses in flotation machines. *International Journal of Mineral Processing,* 56(1-4): 257–276.

Schultz, J., Lavielle, L. and Martin, C. (1987): The role of the interface in carbon fibre-epoxy composites. *The Journal of Adhesion,* 23(1): 45-60.

Schwarz, S. and Grano, S. (2005): Effect of particle hydrophobicity on particle and water transport across a flotation froth. *Colloids and Surfaces A: Physicochemical and Engineering Aspects*, 256(2-3): 157–164.

Sharma, P. K. and Hanumantha Rao, K. (2002): Analysis of different approaches for evaluation of surface energy of microbial cells by contact angle goniometry.

Advances in Colloid and Interface Science, 98: 341–463.

Shen, Y., Nagaraj, D.R., Farinato, R. and Somasundaran, P. (2016): Study of xanthate decomposition in aqueous solutions. *Minerals Engineering.* 93:10–15.

Shi, C., Chan, D.Y.C., Liu, Q. and Zeng, H. (2014): Probing the Hydrophobic Interaction between Air Bubbles and Partially Hydrophobic Surfaces Using Atomic Force Microscopy. *The Journal of Physical Chemistry,* 118: 25000−25008.

Shi, Y. and Fornasiero, D. (2003): Effects of particle size, density and turbulence on flotation recovery. *in Engineering Our Future: Are We up to the Challenge?*: 27-30 September 2009, Burswood Entertainment Complex, p. 528.

Shmulovich, K., Graham, C. and Yardley, B. (2001): Quartz, albite and diopside solubilities in H_2O-NaCl and H_2O-CO_2 fluids at 0.5-0.9 GPa. *Contributions to Mineralogy and Petrology,* 141(1): 95–108.

Spagnolo, D.A.; Maham, Y. and Chuang, K.T. (1996): Calculation of Contact Angle for Hydrophobic Powders Using Heat of Immersion Data. *Journal of Physical Chemistry*, (100): 6626–6630.

Steger, H.F. and Desjardins, L.E. (1980): Oxidation of sulphide minerals. V. Galena, sphalerite and chalcocite. *Canadian Mineralogist.* 18:365–372.

Studebaker, M.L. and Snow, W, C. (1955): The influence of ultimate composition upon the wettability of carbon blacks. *American Chemical Society*, 79: 973-976.

Sun, C. and Berg, J. C. (2002): Effect of moisture on the surface free energy and acid – base properties of mineral oxides. *Journal of Chromatography A*, 969: 59–72.

Sutherland, K. L. (1948): Physical chemistry of flotation. XI: Kinetics of the flotation process. *Journal of Physical and Colloid Chemistry,* 52(2): 394–425.

Swarna, P., Forsling, W. and Rao, H. K. (2003): Flotation and Surface Interactions of Wollastonite / Dodecylamine System. *In: Lorenzen, L., Bradshaw, D., Proceedings of the 22nd International Mineral Processing Congress (IMPC),* Cape Town South Africa, (2003): 764–773.

Taguta, J., O'Connor, C.T. and McFadzean, B. (2018): The relationship between the enthalpy of immersion and flotation response. *Colloids and Surfaces A: Physicochemical and Engineering Aspects,* 558: 263-270.

Taguta, J., O'Connor, C. T. and McFadzean, B. (2017): The effect of the alkyl chain

length and ligand type of thiol collectors on the heat of adsorption and floatability of sulphide minerals. *Minerals Engineering,* 110: 145-152.

Templer, C.E. (1972): A modified flow microcalorimeter for the determination of heats of adsorption on evacuated adsorbents. *Nature physical science*, 235: 158-160.

Ticknor, K. V and Saluja, P.P.S. (1990): Determination of surface areas of mineral powders by adsorption calorimetry 1. *Clays and Clay Minerals*, 38(4): 437–441.

Tsutsumi, K. and Takahashi, H.: (1969): A study of the nature of active sites on zeolites by the measurement of heat of immersion. 1. Electrostatic field of calcium-substituted Y zeolite. *The Journal of Physical Chemistry*, 74(13): 2710–2713.

van Oss, C. J., Chaudhury, M. K. and Good, R. J. (1988): Interfacial Lifshitz-van der Waals and Polar Interactions in Macroscopic Systems. *Chem Rev,* 88: 927–941.

van Oss, C. and Giese, R.F. (1995): The hydrophilicity and hydrophobicity of clay minerals. *Clays and Clay Minerals*, 43(4): 474-477.

van Oss, C. J. (2003): Long-range and short-range mechanisms of hydrophobic attraction and hydrophilic repulsion in specific and aspecific interactions. *Journal of Molecular Recognition*, 16: 177–190.

van Oss, C. J., Giese, R. F. and Docoslis, A. (2005): Hyperhydrophobicity of the water - air interface. *Journal of Dispersion Science ad Technology*, 26: 585–590.

Wadso, I. and Goldberg, R.N. (2001): Standards in isothermal microcalorimetry (IUPAC Technical Report). *Pure and Applied Chemistry*, 73(10): 1625–1639.

Wang, J., Yoon, R. H. and Morris, J. (2013): AFM surface force measurements conducted between gold surfaces treated in xanthate solutions. *International Journal of Mineral Processing,* 122: 13–21.

Wang, N., Sasaki, M., Yoshida, T. and Kotanigawa , T. (1998): Estimation of coal hydrophilicity by flow microcalorimetry. *Colloids and Surfaces A: Physicochemical and Engineering Aspects,* 135: 11-18.

Wang, W. and Fornasiero, D. (2009): Hydrophobicity of composite particles. Paper presented at the CHEMECA 2009 Engineering Our Future: Are we up to the challenge?

Wark, E.E. and Wark, I.W. (1932): The Physical Chemistry of Flotation III. The relationship between contact angle and the constitution of the collector. *Journal*

of Physical Chemistry, 37(1): 805–814.

Washburn, E.W. (1921): The Dynamics of Capillary Flow. *Physical Review Letters, Physical Review, and Reviews of Modern Physics*, 17(3): 273.

Weissbart, E. J. and Rimstidt, J. D. (2000): Wollastonite: Incongruent dissolution and leached layer formation. *Geochim. Cosmochimica. Acta*, 64(23), 4007–4016.

Wiese, J. G. and O'Connor, C. T. (2016): An investigation into the relative role of particle size, particle shape and froth behaviour on the entrainment of chromite. *International Journal of Mineral Processing,* 156: 127–133.

Wills, Barry A. and T.J. Napier-Munn (2006): Mineral processing technology. 7th edition. Elsevier Science & Technology Books.

Wollast, R. and Chou, L. (1992): Surface reactions during the early stages of weathering albite. *Geochim. Cosmochim. Acta,* 56: 3113–3131.

Wu, S. (1971): Calculation of interfacial tension in polymer system. *Journal of Polymer Science C*, 34: 19-30.

Wu, S. (1973): Polar and non-polar interactions in adhesion. *Journal of Adhesion*, 5: 39-55.

Xing, Y., Gui X., Karakas, F. and Cao, Y. (2017): Role of collectors and depressants in mineral flotation: A theoretical analysis based on extended DLVO theory. *Minerals*, 7(223): 1-14.

Yan, L., Englert, A.H., Masliyah, J.H. and Xu, Z. (2011): Determination of anisotropic surface characteristics of different phyllosilicates by direct force measurements. *Langmuir,* 27(21): 12996–13007.

Yan, N.; Maham, Y.; Masliyah, J.H.; Gray, M. R. and Mather, A.E. (2000): Measurement of Contact Angles for Fumed Silica Nanospheres Using Enthalpy of Immersion Data. *Journal of Colloid and Interface Science*, 228, pp.1–6.

Yildirim, I. (2001): Surface free energy characterisation for powders. *PhD Thesis.* Virginia Polytechnic Institute and State University.

Yin, X., Gupta, V., Du, H., Wang, X. and Miller, J.D. (2012): Surface charge and wetting characteristics of layered silicate minerals. *Advances in Colloid and Interface Science.* 179–182:43–50.

Yoon, R.-H. and Mao, L. (1996): Application of extended DLVO theory, IV: Derivation

of flotation rate equation from first principles. *Journal of Colloid and Interface Science,* 181: 613–626.

Yoon, R. H. (2000): The role of hydrodynamic and surface forces in bubble-particle interaction. *International Journal of Mineral Processing,* 58: 129–143.

Yoon, R. H. and Yordan, J. L. (1991): Induction time measurements for the quartz-amine flotation system. *Journal of Colloid And Interface Science,* 141(2): 374–383.

Yoon, R. and Luttrell, G. H. (1984): Surface studies of the collectorless flotation of chalcopyrite. *Colloids and Surfaces,* 12: 239–254.

Young, G.J.; Chessick, J.J.; Healey, F.H. and Zettlemoyer, A.C. (1954): Thermodynamics of the adsorption of water on graphon from heats of immersion and adsorption data. *The Journal of Physical Chemistry*, 58: 313–315.

Zettlemoyer, A.C.: (1968): Hydrophobic surfaces. *Journal of Colloid and Interface Science*, 38(3/4): 343–369.

Zhang, L., Zhang, X., Fan, C., Zhang, Y. and Hu, J. (2009): Nanoscale multiple gaseous layers on a hydrophobic surface. *Langmuir,* 25(16): 8860-8864.

Zimmerman, R.; Wolf, G. and Scheneider, H.A. (1987): Calorimetric measurements of the heat of solution and immersion of minerals in water using a new calorimetric vessel. *Colloids and Surfaces*, 22: 1–7.

CHAPTER 8

8 APPENDICES

APPENDIX A: XRD traces

Graphite

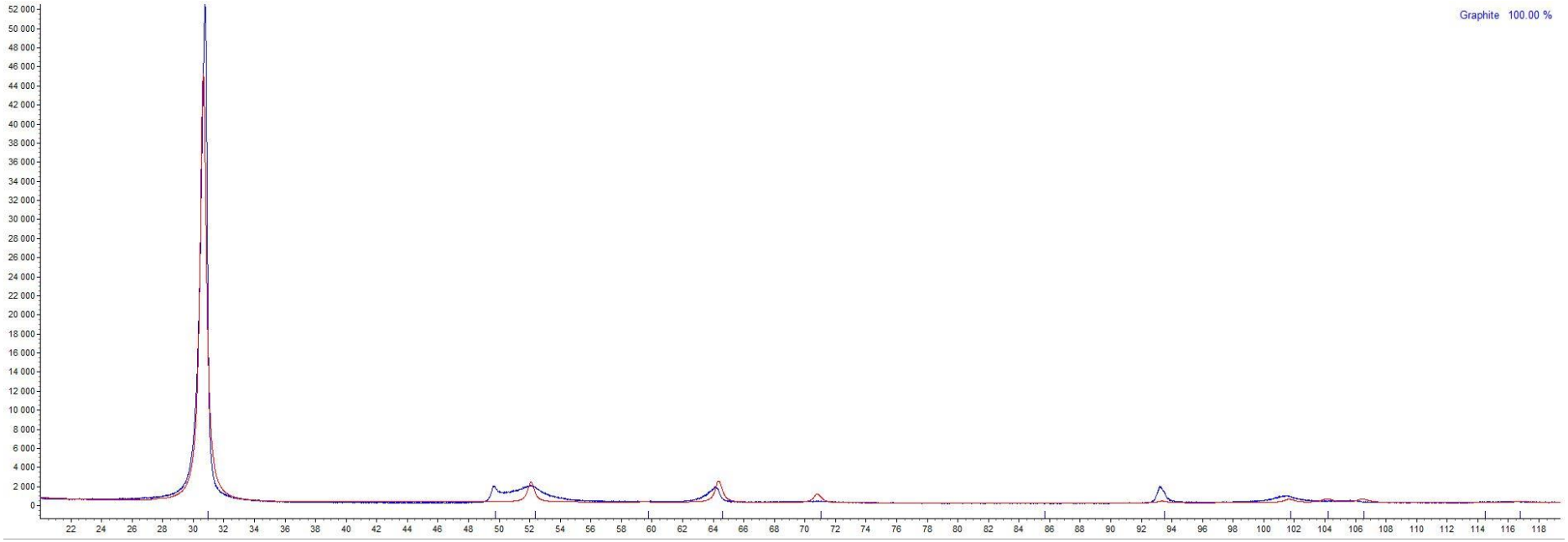

Galena

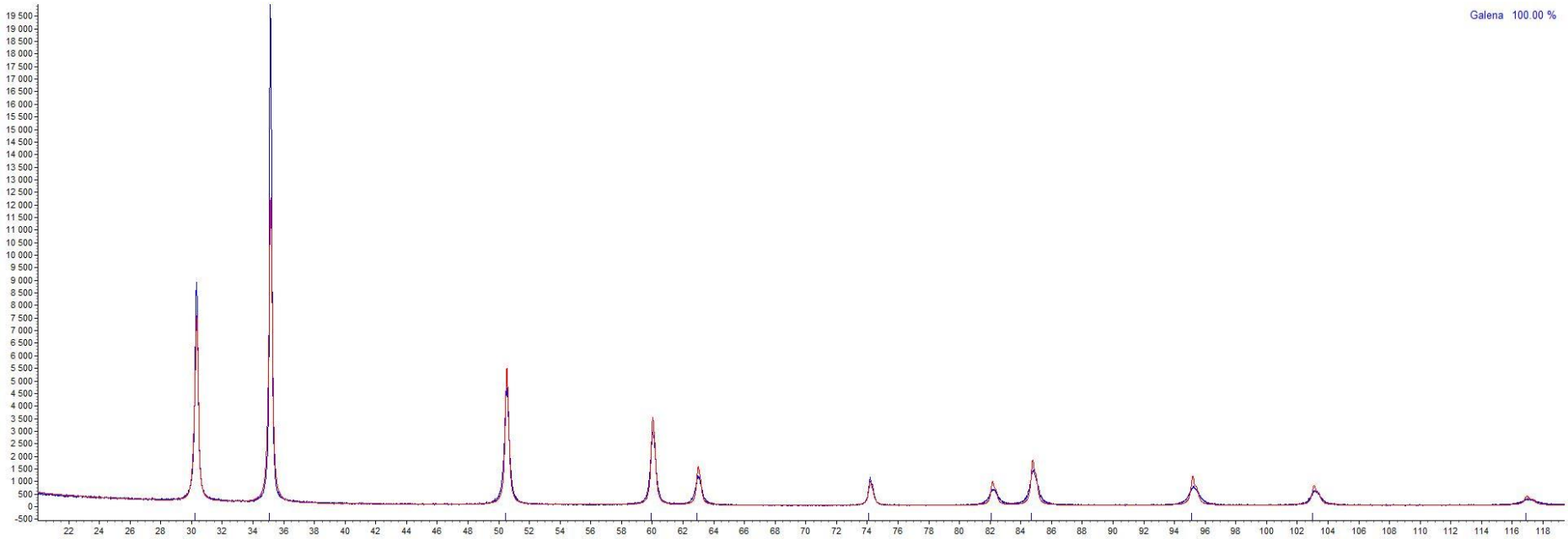

Realgar

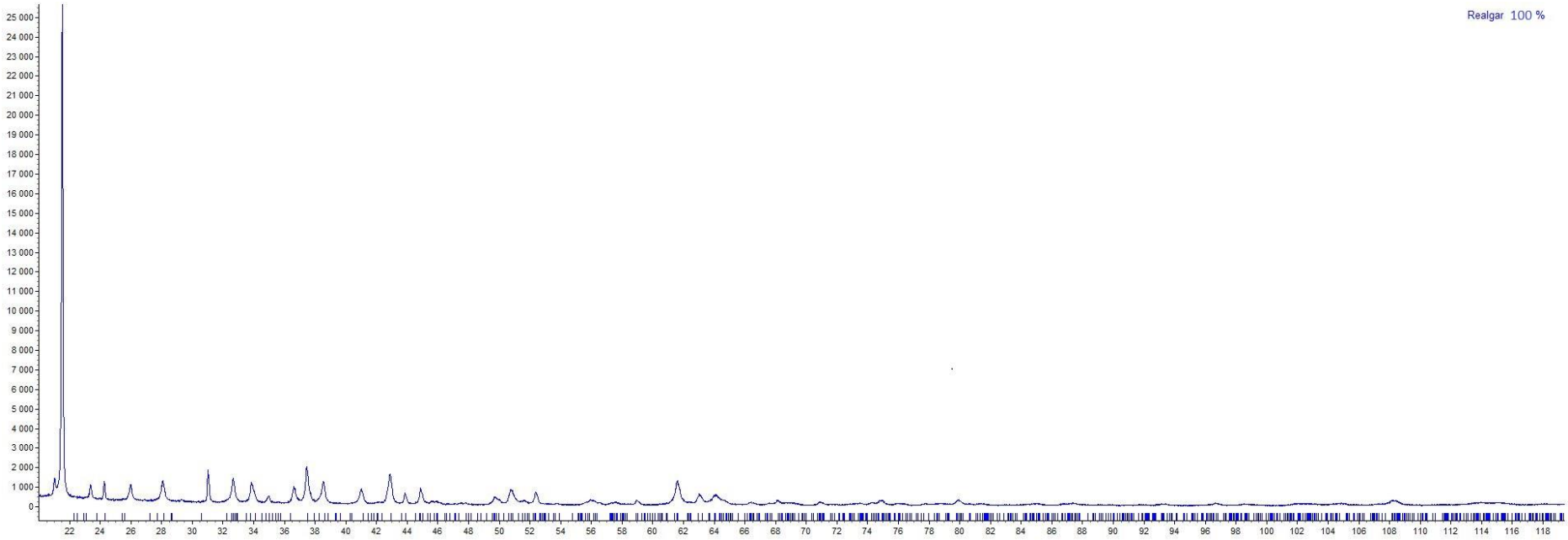

Orpiment

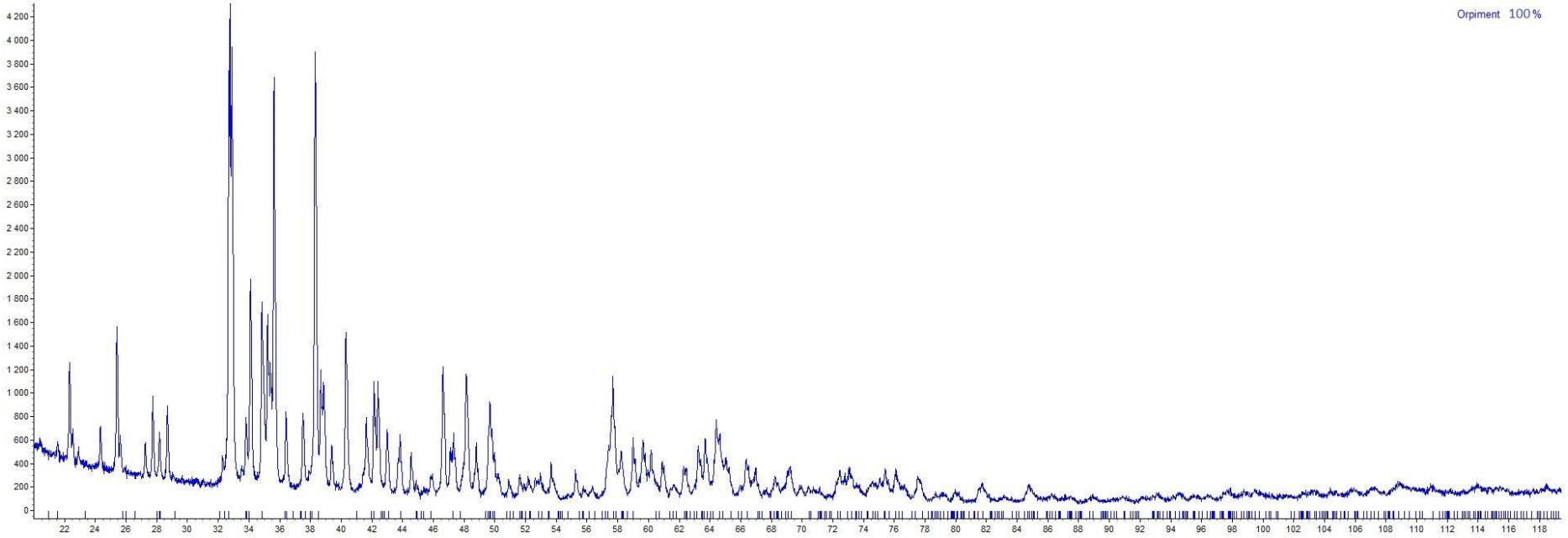
Orpiment 100 %
4 200
4 000
3 800
3 600
3 400
3 200
3 000
2 800
2 600
2 400
2 200
2 000
1 800
1 600
1 400
1 200
1 000
800
600
400
200
0
22 24 26 28 30 32 34 36 38 40 42 44 46 48 50 52 54 56 58 60 62 64 66 68 70 72 74 76 78 80 82 84 86 88 90 92 94 96 98 100 102 104 106 108 110 112 114 116 118

Albite

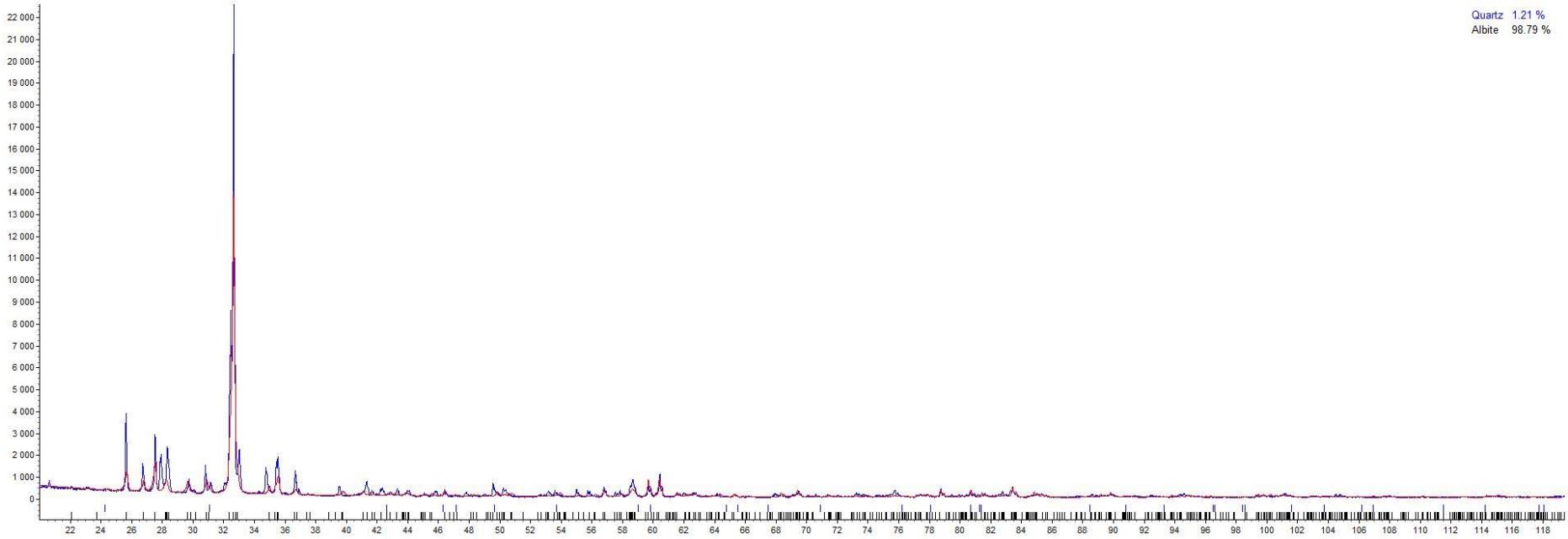

Diopside

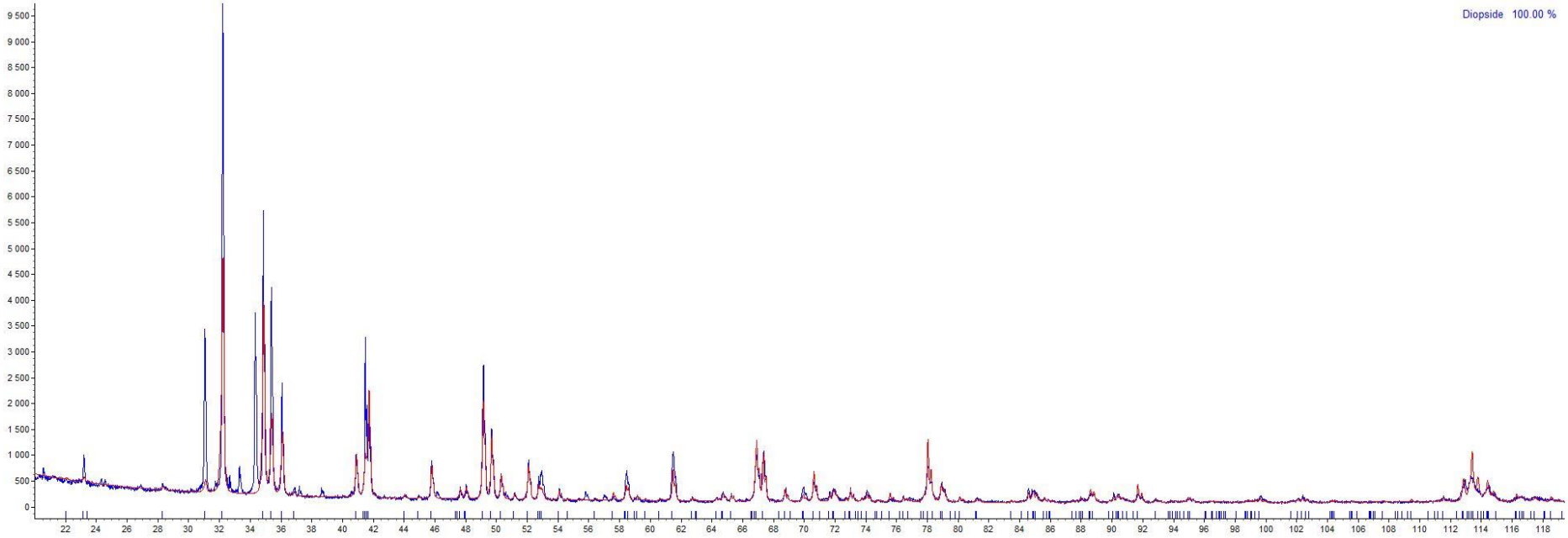

Talc

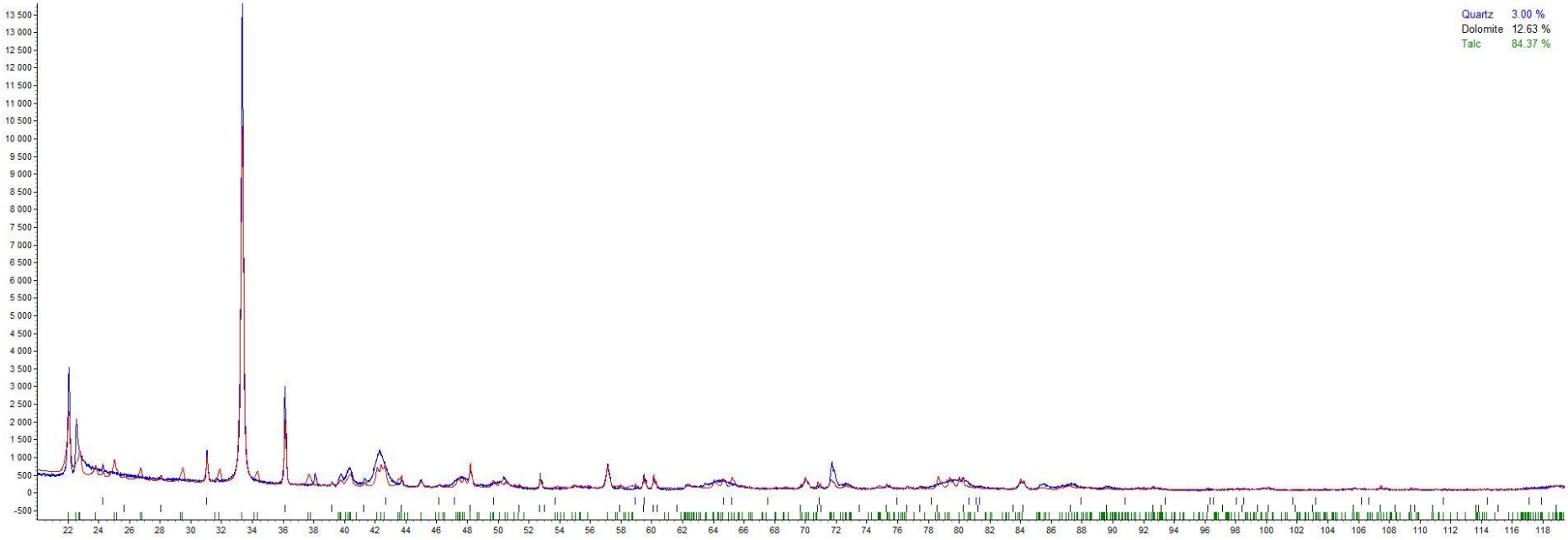

Mica

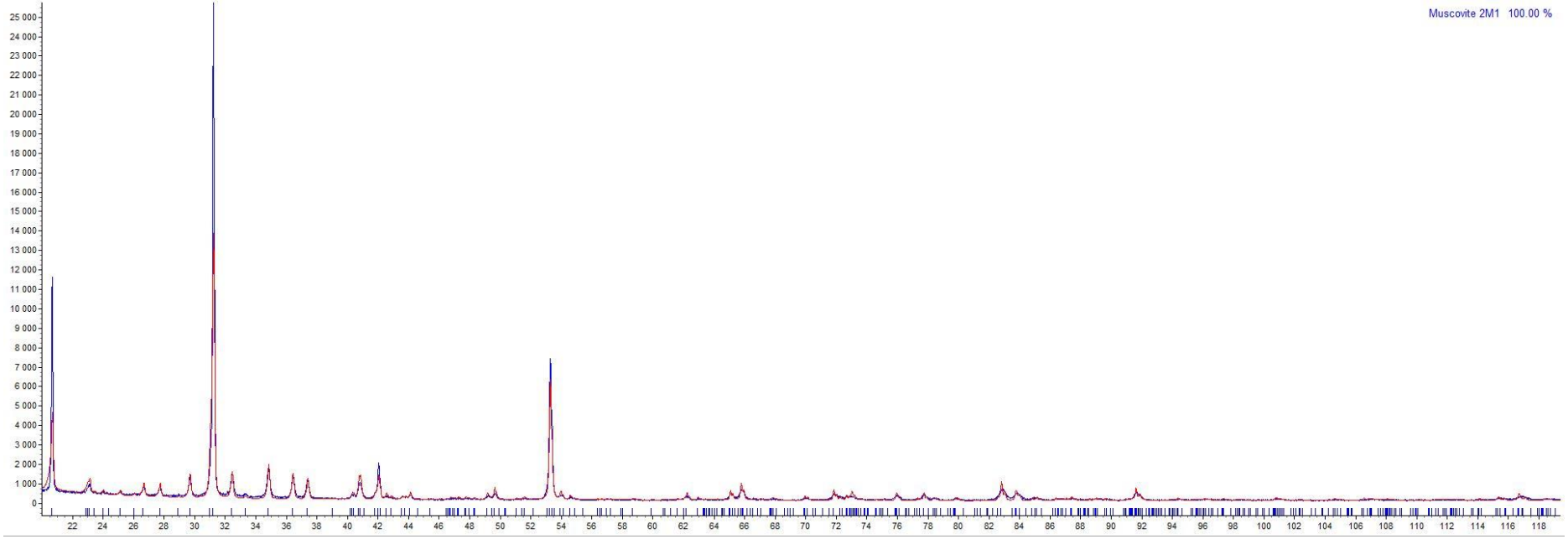

APPENDIX B: Enthalpies of immersion of different minerals in water.

Mineral	BET SSA (m^2)	Run	$-h_{measured}$ (mJ)	$-h_{blank}$ (mJ)	$-h_{corrected}$ (mJ)	Sample mass (g)	$-h_{corrected}$ (mJ/g)	$-h_i$ (mJ/m^2)	Avg $-h_i$ (mJ/m^2)	SE
Orpiment	4.2607	1	455.6	62.9	392.7	1.0318	380.6	89.3	75.2	14.2
		2	321.3	62.9	258.4	0.9936	260.0	61.0		
Realgar	4.8117	1	416.7	62.9	353.8	0.9702	364.6	75.8	90.7	15.0
		2	511.8	62.9	448.9	0.8825	508.7	105.7		
Talc	19.5136	1	1066	62.9	1003.1	0.6647	1509.1	77.3	75.7	1.7
		2	1033	62.9	970.1	0.6717	1444.2	74.0		
Graphite	7.1236	1	491.1	62.9	428.2	0.3772	1135.3	159.4	166.6	7.2
		2	534.1	62.9	471.2	0.3807	1237.8	173.8		
Galena	0.7747	1	375.6	62.9	312.7	2.182	143.3	185.0	175.6	9.4
		2	320.0	62.9	257.1	1.996	128.8	166.3		
Albite	5.7863	1	721.5	62.9	658.6	0.6737	977.5	168.9	202.3	33.4
		2	955.3	62.9	892.4	0.6542	1364.1	235.8		
Mica	24.0038	1	3699	62.9	3636.1	0.5558	6542.1	272.5	305.9	33.3
		2	4468	62.9	4405.1	0.5410	8142.5	339.2		

Mineral	**BET SSA (m^2)**	**Run**	**$-h_{measured}$ (mJ)**	**$-h_{blank}$ (mJ)**	**$-h_{corrected}$ (mJ)**	**Sample mass (g)**	**$-h_{corrected}$ (mJ/g)**	**$-h_i$ (mJ/m^2)**	**Avg $-h_i$ (mJ/m^2)**	**SE**
Diopside	4.7511	1	4926	62.9	4863.1	0.8109	5997.1	1262.3	1224.7	37.5
		2	4873	62.9	4810.1	0.8528	5640.3	1187.2		
Wollastonite	4.2762	1	3845	62.9	3782.1	0.6953	5439.5	1272.0	1241.2	30.8
		2	3540	62.9	3477.1	0.6718	5175.8	1210.4		

APPENDIX C: Enthalpies of immersion of different minerals in formamide (F) and n-hexane (n-H)

Mineral	BET SSA (m^2)	Run	$-h_{measured}$ (mJ)	$-h_{blank}$ (mJ)	$-h_{corrected}$ (mJ)	Sample mass (g)	$-h_{corrected}$ (mJ/g)	$-h_i$ (mJ/m^2)
Realgar	4.8117	F	852.4	62.9	789.5	0.9302	848.7	176.4
		n-H	249.2	62.9	186.3	0.9307	200.2	41.6
Talc	19.5136	F	1348	62.9	1285.1	0.5775	2225.3	114.0
		n-H	355.5	62.9	292.6	0.5593	523.1	26.7
Galena	0.7747	F	336.1	62.9	273.2	2.499	127.1	164.0
		n-H	365.2	62.9	302.3	2.183	138.5	178.7
Albite	5.7863	F	272.7	62.9	209.8	0.5744	365.2	63.1
		n-H	376.6	62.9	313.7	0.6737	465.6	80.5
Mica	24.0038	F	1586	62.9	1523.1	0.5628	2706.3	112.7
		n-H	1405	62.9	1342.1	0.5175	2593.4	108.0
Wollastonite	4.2762	F	114.2	62.9	51.3	0.6450	79.5	18.6
		n-H	782.9	62.9	720	0.6024	1195.2	279.5

APPENDIX D: Collector coverage calculations.

Galena

	Enthalpy of immersion measurements	Washburn contact angle measurements	Microflotation tests
Mass of galena (g)	10	70	10
Surface area of mineral (m^2/g)	0.7747	0.2575	0.2575
Specific surface area of mineral (m^2)	7.747	18.025	2.575
One molecule collector head (m^2)	2.88E-19	2.88E-19	2.88E-19
Number of molecules required for 100% coverage	2.69E+19	6.26E+19	8.94E+18
Number of moles required for 100% coverage	4.47E-05	1.04E-4	1.48E-05
Number of moles of PAX in 0.5 mL	4.47E-05	1.04E-4	1.48E-05
Number of moles of PAX in 10mL	8.93E-04	2.08E-03	2.97E-04
Active mass of PAX used (g) in 10 mL	0.1778	0.4236	0.0591
PAX purity (%)	0.982	0.982	0.982

	Enthalpy of immersion measurements	**Washburn contact angle measurements**	**Microflotation tests**
Total mass of PAX (g) for 100% coverage in 10 mL	0.1810	0.4136	0.060
Total mass of PAX (g) for 75% coverage in 10 mL	0.1358	0.3102	0.045
Total mass of PAX (g) for 50% coverage in 10 mL	0.0905	0.2068	0.030
Total mass of PAX (g) for 25% coverage in 10 mL	0.0453	0.1034	0.015
Total mass of PAX (g) for 16% coverage in 10 mL	0.0290	NM	NM
Total mass of PAX (g) for 8% coverage in 10 mL	0.0145	NM	NM

NM – not measured in this study.

Realgar

	Enthalpy of immersion measurements	**Washburn contact angle measurements**	**Microflotation tests**
Mass of realgar (g)	10	50	10
Surface area of mineral (m^2/g)	4.812	1.319	1.319
Specific surface area of mineral (m^2)	48.12	65.96	13.19
One molecule collector head (m^2)	2.88E-19	2.88E-19	2.88E-19
Number of molecules required for 100% coverage	1.67E+20	2.29E+20	4.58E+19
Number of moles required for 100% coverage	2.78E-04	3.80E-04	7.61E-05
Number of moles of PAX in 0.5 mL	2.78E-04	3.80E-04	7.61E-05
Number of moles of PAX in 10mL	5.55E-03	7.61E-03	7.61E-03
Active mass of PAX used (g) in 10 mL	1.104	1.513	1.513
PAX purity (%)	0.982	0.982	0.982
Total mass of PAX (g) for 100% coverage in 10 mL	1.1243	1.541	1.541

	Enthalpy of immersion measurements	**Washburn contact angle measurements**	**Microflotation tests**
Total mass of PAX (g) for 75% coverage in 10 mL	0.8432	1.135	1.135
Total mass of PAX (g) for 50% coverage in 10 mL	0.5621	0.757	0.757
Total mass of PAX (g) for 25% coverage in 10 mL	0.2811	0.378	0.378

APPENDIX E: Enthalpies of immersion of xanthate-coated sulphide minerals in water

Galena

BET specific surface area of galena = 0.7747 m^2/g

PAX surface coverage (%)	Run	$-h_{measured}$ (mJ)	$-h_{blank}$ (mJ)	$-h_{corrected}$ (mJ)	Sample mass (g)	$-h_{corrected}$ (mJ/g)	$-h_i$ (mJ/m^2)	Avg $-h_i$ (mJ/m^2)	SE
0	1	375.6	62.9	312.7	2.182	143.3	185.0	175.6	9.4
	2	320.0	62.9	257.1	1.996	128.8	166.3		
16	1	315.4	62.9	252.5	2.182	115.7	149.4	144.1	5.3
	2	300.6	62.9	237.7	2.211	107.5	138.8		
25	1	261.9	62.9	198.9	2.251	88.4	114.1	117.3	3.2
	2	268.6	62.9	205.7	2.202	93.4	120.6		
50	1	263.0	62.9	200.1	2.215	90.3	116.6	108.7	7.9
	2	245.9	62.9	183.0	2.344	78.1	100.8		
75	1	220.3	62.9	157.4	2.131	73.9	95.3	94.5	1.4
	2	219.0	62.9	156.1	2.194	71.2	91.9		
	3	233.2	62.9	170.3	2.280	74.7	96.4		
100	1	176.5	62.9	113.6	1.957	58.0	74.9	69.5	5.4
	2	151.7	62.9	88.8	1.788	49.7	64.1		

Realgar

BET specific surface area of realgar = 4.8117 m^2/g

PAX surface coverage (%)	Run	$-h_{measured}$ (mJ)	$-h_{blank}$ (mJ)	$-h_{corrected}$ (mJ)	Sample mass (g)	$-h_{corrected}$ (mJ/g)	$-h_i$ (mJ/m^2)	Avg $-h_i$ (mJ/m^2)	SE
0	1	416.7	62.9	353.8	0.9702	364.6	75.8	90.7	15.0
	2	511.8	62.9	448.9	0.8825	508.7	105.7		
25	1	205.0	62.9	142.1	0.9952	142.8	29.7	34.7	5.1
	2	260.5	62.9	197.6	1.0317	191.5	39.8		
50	1	114.8	62.9	51.9	1.0417	49.8	10.3	11.2	0.9
	2	122.7	62.9	59.7	1.0293	58.0	12.1		
75	1	73.9	62.9	11.0	1.0417	10.6	2.2	3.4	1.2
	2	85.2	62.9	22.3	1.0293	21.7	4.5		
100	1	64.4	62.9	1.44	1.1633	1.2	0.3	0.2	0.1
	2	63.4	62.9	0.51	1.137	0.4	0.1		

APPENDIX F: Enthalpies of immersion of a realgar-albite synthetic ore in water

Refer to Appendix B for 0% albite (realgar) and 100% albite.

	25% Albite		50% Albite		75% Albite	
	Run 1	**Run 2**	**Run 1**	**Run 2**	**Run 1**	**Run 2**
mass of realgar (g)	0.6072	0.6007	0.4034	0.3984	0.2002	0.1926
SSA of realgar (m^2/g)	4.8117	4.8117	4.8117	4.8117	4.8117	4.8117
Total SA of realgar (m^2)	2.9217	2.8904	1.9410	1.9170	0.9633	0.9267
mass of albite (g)	0.1973	0.2029	0.400	0.4038	0.5923	0.6049
SSA of albite (m^2/g)	5.7863	5.7863	5.7863	5.7863	5.7863	5.7863
Total SA of albite (m^2)	1.1416	1.1740	2.3145	2.3365	3.4272	3.5001
Total mass in ampoule (g)	0.8045	0.8036	0.8034	0.8022	0.7925	0.7975
Total SA in ampoule (m^2)	4.0633	4.0644	4.2556	4.2535	4.3905	4.4269
% albite by weight	24.5	25.2	49.8	50.3	74.7	75.8
% albite by surface area	28.1	28.9	54.4	54.9	78.1	79.1
Enthalpy of immersion (mJ)	562.6	587.1	645.8	598.5	705.1	743.1
less enthalpy of blank (mJ)	62.9	62.9	62.9	62.9	62.9	62.9
net enthalpy of immersion (mJ)	499.7	524.2	582.9	535.5	642.2	680.1

net enthalpy of immersion (mJ/g)	621.1		652.3	725.6		667.6	810.3	852.8
net enthalpy of immersion (mJ/m²)	123.0		129.0	137.0		125.9	146.3	153.6
Average enthalpy of immersion (mJ/m²)		126.0			131.4			150.0
Standard deviation		4.2			7.8			5.2
Standard error		3.0			5.5			1.4

APPENDIX G: Surface energetics, relative surface polarity, the work of adhesion for water and energy interaction between particles and bubbles immersed in water.

Talc

The enthalpy of immersion of talc in different probe liquids.

	Enthalpies of immersion		
Mineral	**Water**	**n-Hexane**	**Formamide**
Talc	75.673	26.68709	114.03613

The surface energy components of the different probe liquids used in this study.

Liquid	H_L^{LW}	H_L^+	H_L^-	H_L
n-Hexane	48.4	0	0	48.4
Water	36	41	41	118
Formamide	55.2	3.23	56	82.1

Equation 1-31 given below is used to compute the surface energetics of talc:

$$-h_i = -H_l + 2\left[\left(\sqrt{H_s^{LW} H_l^{LW}}\right) + \left(\sqrt{H_s^+ H_l^-}\right) + \left(\sqrt{H_s^- H_l^+}\right)\right] \qquad \textit{Equation 1-31}$$

Non-polar component of the surface energy

n-Hexane

Substituting the enthalpy of immersion of talc in n-hexane and the surface energy components.

$H_S^+ \text{ x } H_l^- = 0;$

$H_S^- \text{ x } H_l^+ = 0$

$$26.687 = -48.4 + 2\left[\left(\sqrt{H_s^{LW} \text{x } 48.4}\right) + 0 + 0\right]$$

$H_S^{LW} = 28.824$ mJ/m².

Acid-base component of the surface energy

Water

Substituting the enthalpy of immersion of talc in water and the surface energy components of water.

$$114.036 = -118 + 2\left[\left(\sqrt{28.824 \text{ x } 36}\right) + \left(\sqrt{H_s^+ \text{ x } 41}\right) + \left(\sqrt{H_s^- \text{ x } 41}\right)\right]$$

$$\sqrt{H_S^+} + \sqrt{H_S^-} = 10.092 \ldots\ldots\ldots\ldots\ldots\ldots\ldots \text{ (1)}$$

Formamide

Substituting the enthalpy of immersion of talc in formamide and the surface energy components of formamide.

$$75.673 = -82.1 + 2\left[\left(\sqrt{28.824 \text{ x } 55.2}\right) + \left(\sqrt{H_s^+ \text{ x } 56}\right) + \left(\sqrt{H_s^- \text{ x } 3.23}\right)\right]$$

$$\sqrt{H_S^+ \text{ x } 56} + \sqrt{H_S^- \text{ x } 3.23} = 58.179 \ldots\ldots\ldots\ldots\ldots\ldots\ldots \text{ (2)}$$

Solving equations (1) and (2) simultaneously:

H_S^+ = 49.588 mJ/m².

H_S^- = 9.306 mJ/m².

Polar component of the surface energy

$$H_s^{AB} = \sqrt{(H_s^+ H_s^-)} \qquad \textit{Equation 1-32}$$

$$= \sqrt{(49.588 \text{ x } 9.306)}$$

= 21.482 mJ/m².

Total surface energy

$$H_s^T = H_s^{LW} + H_s^{AB} \qquad \textit{Equation 1-33}$$

$$= 28.824 + 21.482$$

= 50.306 mJ/m².

Relative surface polarity, k_{rsp}

$$k_{rsp} = \frac{H_S^{AB}}{H_S^T} \qquad \textit{Equation 1-34}$$

$$= \frac{21.482}{50.306} \text{ x } 100\%$$

= 42.7%

Calculating the energy of interaction (ΔG_{pwb}) between talc particles and bubbles in immersed water.

$$\Delta G_{pwb} = \left(\sqrt{H_p^{LW}} - \sqrt{H_b^{LW}}\right)^2 - \left(\sqrt{H_p^{LW}} - \sqrt{H_w^{LW}}\right)^2 - \left(\sqrt{H_b^{LW}} - \sqrt{H_w^{LW}}\right)^2 +$$

$$2\left[\sqrt{H_w^+}\left(\sqrt{H_p^-} + \sqrt{H_b^-} - \sqrt{H_w^-}\right) + \sqrt{H_w^-}\left(\sqrt{H_p^+} + \sqrt{H_b^+} - \sqrt{H_w^+}\right) - \sqrt{H_p^+ H_b^-} - \sqrt{H_p^- H_b^+}\right]$$

Equation 1-35

Air bubbles are super hydrophobic and the following parameters for the air bubbles are quoted from (van Oss et al, 2005).

Fluid	H^{LW}	H^+	H^-
Water	36	41	41
Bubble	0	0	0

$$\Delta G_{pwb} = \left(\sqrt{28.824} - \sqrt{0}\right)^2 - \left(\sqrt{28.824} - \sqrt{36}\right)^2 - \left(\sqrt{0} - \sqrt{36}\right)^2$$
$$+ 2\left[\sqrt{41}\left(\sqrt{9.306} + \sqrt{0} - \sqrt{41}\right) + \sqrt{41}\left(\sqrt{49.588} + \sqrt{0} - \sqrt{41}\right) - \sqrt{0} - \sqrt{0}\right]$$

= -42 mJ/m².

Calculating the work of adhesion of talc for water

$$W_{adh} = -h_i + H_l \qquad \textit{Equation 1-38}$$

$$= -(-75.673) + 118$$

= 194.0 mJ/m².

APPENDIX H: Recovery-time data

Different pure minerals

Albite

	Time (min)	Run 1	Run 2	Avg	SD	SE
C0	0	0	0	0	0	0
C1	2	2.7	3.9	3.3	0.867	0.613
C2	6	6.2	5.8	6.0	0.262	0.185
C3	12	10.0	9.0	9.5	0.691	0.488
C4	20	13.4	12.1	12.7	0.892	0.631

Wollastonite

	Time (min)	Run 1	Run 2	Avg	SD	SE
C0	0	0	0	0	0	0
C1	2	3.3	2.9	3.1	0.283	0.200
C2	6	4.1	3.8	4.0	0.212	0.150
C3	12	10.0	7.0	8.5	2.121	1.500
C4	20	11.9	11.3	11.6	0.424	0.300

Diopside

	Time (min)	Run 1	Run 2	Avg	SD	SE
C0	0	0	0	0	0	0
C1	2	3.1	3.7	3.4	0.424	0.300
C2	6	8.1	8.3	8.2	0.141	0.100
C3	12	14.9	12.2	13.6	1.954	1.382
C4	20	15.2	15.7	15.5	0.354	0.250

Mica

	Time (min)	Run 1	Run 2	Avg	SD	SE
C0	0	0	0	0	0	0
C1	2	2.6	2.9	2.7	0.247	0.175
C2	6	5.0	5.4	5.2	0.283	0.200
C3	12	7.6	7.3	7.5	0.208	0.147
C4	20	11.9	10.7	11.3	0.849	0.600

Talc

	Time (min)	Run 1	Run 2	Avg	SD	SE
C0	0	0	0	0	0	0
C1	2	15.1	13.9	14.5	0.849	0.600
C2	6	54.5	58.1	56.3	2.546	1.800
C3	12	82.0	79.8	80.9	1.556	1.100
C4	20	94.2	95.9	95.1	1.202	0.850

Graphite

	Time (min)	Run 1	Run 2	Avg	SD	SE
C0	0	0	0	0	0	0
C1	2	7.0	8.1	7.6	0.778	0.550
C2	6	22.4	24.8	23.6	1.697	1.200
C3	12	41.6	43.3	42.5	1.202	0.850
C4	20	50.4	52.7	51.6	1.626	1.150

Orpiment

	Time (min)	Run 1	Run 2	Avg	SD	SE
C0	0	0	0	0	0	0
C1	2	20.0	19.6	19.8	0.283	0.200
C2	6	79.2	81.6	80.4	1.697	1.200
C3	12	97.6	95.7	96.7	1.344	0.950
C4	20	98.9	98.4	98.7	0.354	0.250

Galena-xanthate system

Collectorless flotation (0%)

	Time (min)	Run 1	Run 2	Avg	SD	SE
C0	0	0	0	0	0	0
C1	2	6.2	3.9	5.1	1.620	1.145
C2	6	13.2	16.1	14.7	2.051	1.450
C3	12	27.3	29.7	28.5	1.697	1.200
C4	20	38.3	36.0	37.1	1.602	1.133

16%

	Time (min)	Run 1	Run 2	Avg	SD	SE
C0	0	0	0	0	0	0
C1	2	6.2	8.9	7.6	1.909	1.350
C2	6	21.4	25.8	23.6	3.111	2.200
C3	12	47.7	48.5	48.1	0.566	0.400
C4	20	50.3	55.1	52.7	3.394	2.400

25%

	Time (min)	Run 1	Run 2	Avg	SD	SE
C0	0	0	0	0	0	0
C1	2	13.0	11.6	12.3	1.047	0.740
C2	6	32.2	29.1	30.6	2.191	1.550
C3	12	64.1	56.8	60.4	5.137	3.632
C4	20	74.4	75.8	75.1	0.990	0.700

50%

	Time (min)	Run 1	Run 2	Avg	SD	SE
C0	0	0	0	0	0	0
C1	2	11.7	11.1	11.4	0.420	0.297
C2	6	42.0	40.6	41.3	0.971	0.687
C3	12	77.5	75.0	76.3	1.768	1.250
C4	20	91.0	89.5	90.3	1.061	0.750

75%

	Time (min)	Run 1	Run 2	Avg	SD	SE
C0	0	0	0	0	0	0
C1	2	20.0	20.5	20.3	0.356	0.252
C2	6	66.2	67.6	66.9	0.985	0.696
C3	12	86.6	89.1	87.8	1.717	1.214
C4	20	97.2	96.8	97.0	0.288	0.203

100%

	Time (min)	Run 1	Run 2	Avg	SD	SE
C0	0	0	0	0	0	0
C1	2	29.0	27.7	28.4	0.915	0.647
C2	6	86.0	86.0	86.0	0.052	0.037
C3	12	97.1	98.5	97.8	0.988	0.699
C4	20	99.7	99.9	99.8	0.141	0.100

Realgar-xanthate system

Collectorless (0%)

	Time (min)	Run 1	Run 2	Avg	SD	SE
C0	0	0	0	0	0	0
C1	2	9.4	10.3	9.8	0.645	0.456
C2	6	30.2	28.5	29.4	1.202	0.850
C3	12	55.1	59.4	57.3	3.041	2.150
C4	20	70.3	72.1	71.2	1.273	0.900

25%

	Time (min)	Run 1	Run 2	Avg	SD	SE
C0	0	0	0	0	0	0
C1	2	80.0	79.2	79.6	0.566	0.400
C2	6	93.2	95.4	94.3	1.556	1.100
C3	12	99.8	99.8	99.8	0.000	0.000
C4	20	99.8	99.8	99.8	0.000	0.000

Combined recovery-time data

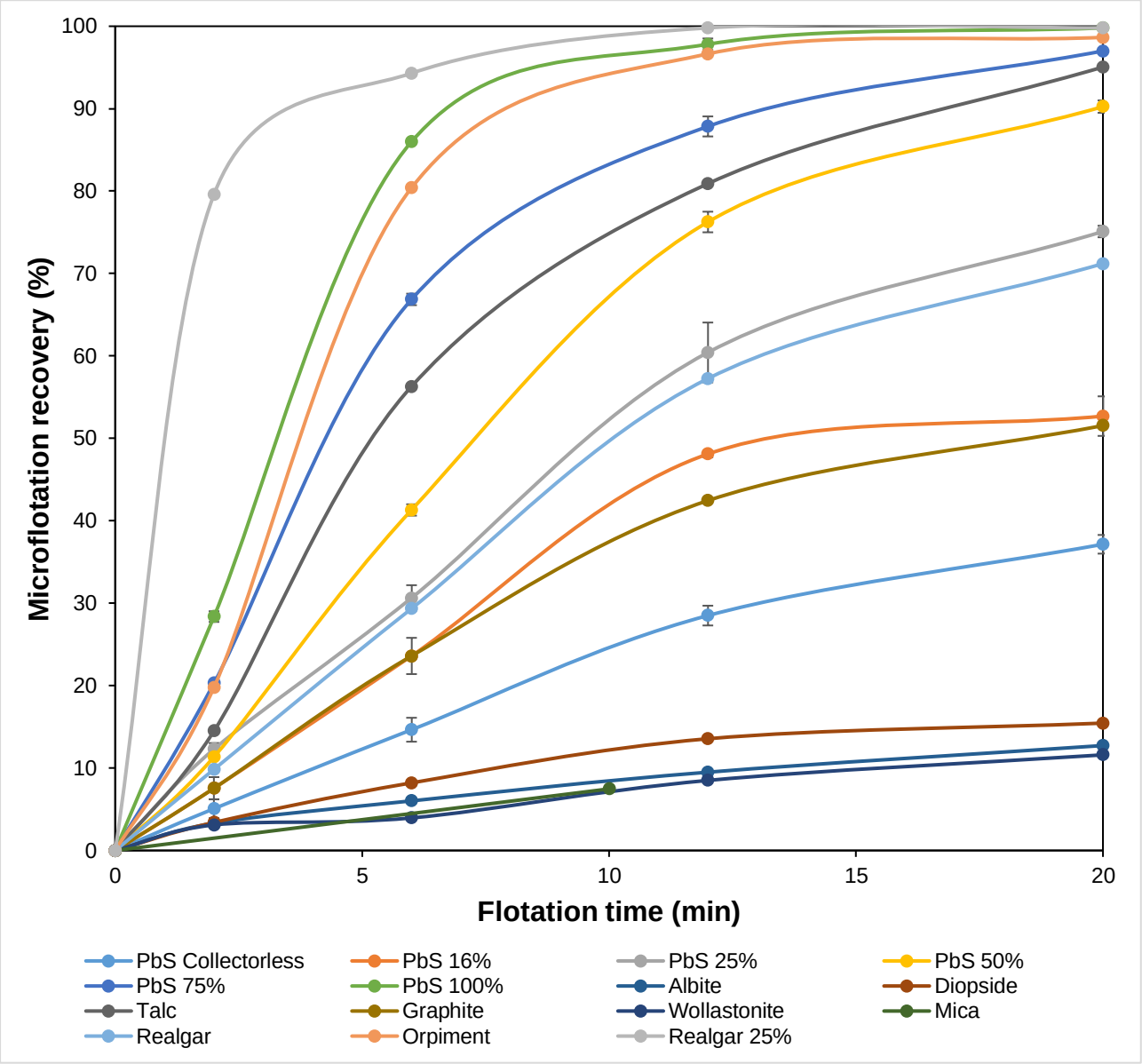

Sample calculation of the first-order flotation rate constant

Talc

The first-order flotation rate constants, k, were calculated using the first-order rate model shown in Equation 1-2. The recovery-time data has been shown in the tables above.

$$R = R_{max}(1 - e^{-kt}) \qquad \textit{Equation 1-2}$$

A plot of In{1-(R/Rmax)} versus t gives a straight line whose gradient k, is the first-order flotation rate constant. The first-order flotation rate constants were normalised by fixing the maximum possible recovery, R_{max}, at 100%.

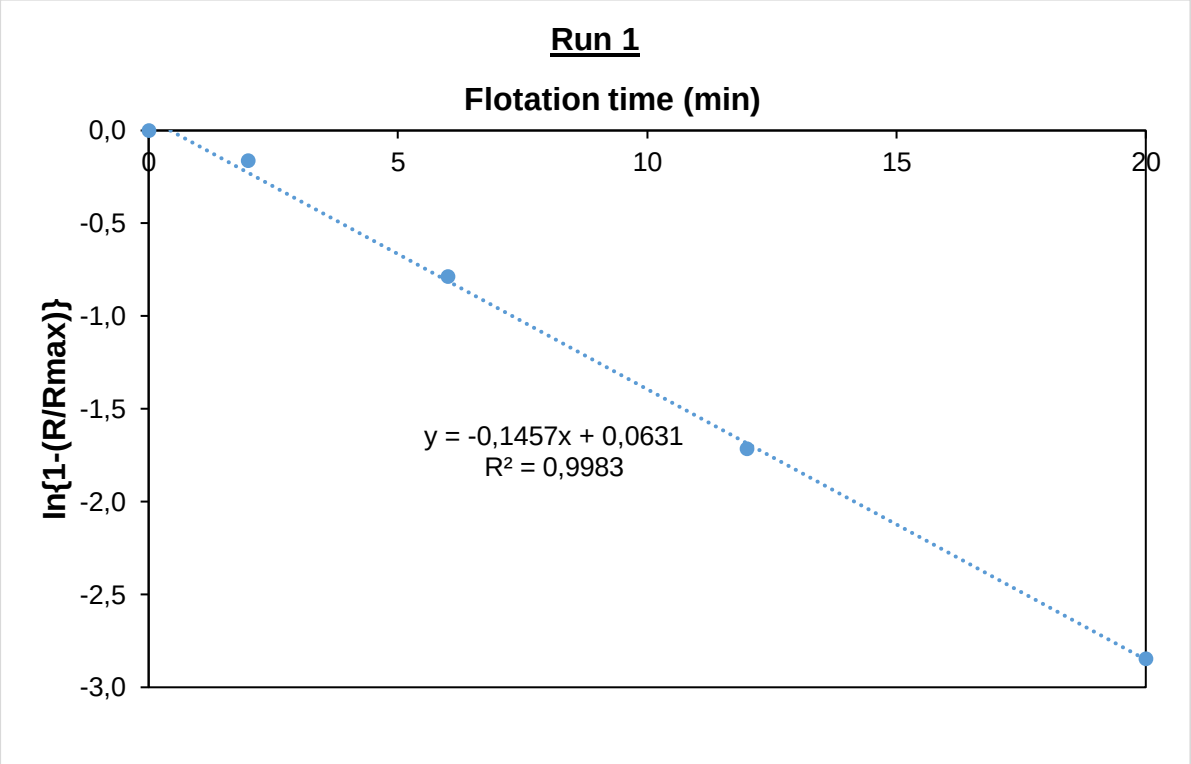

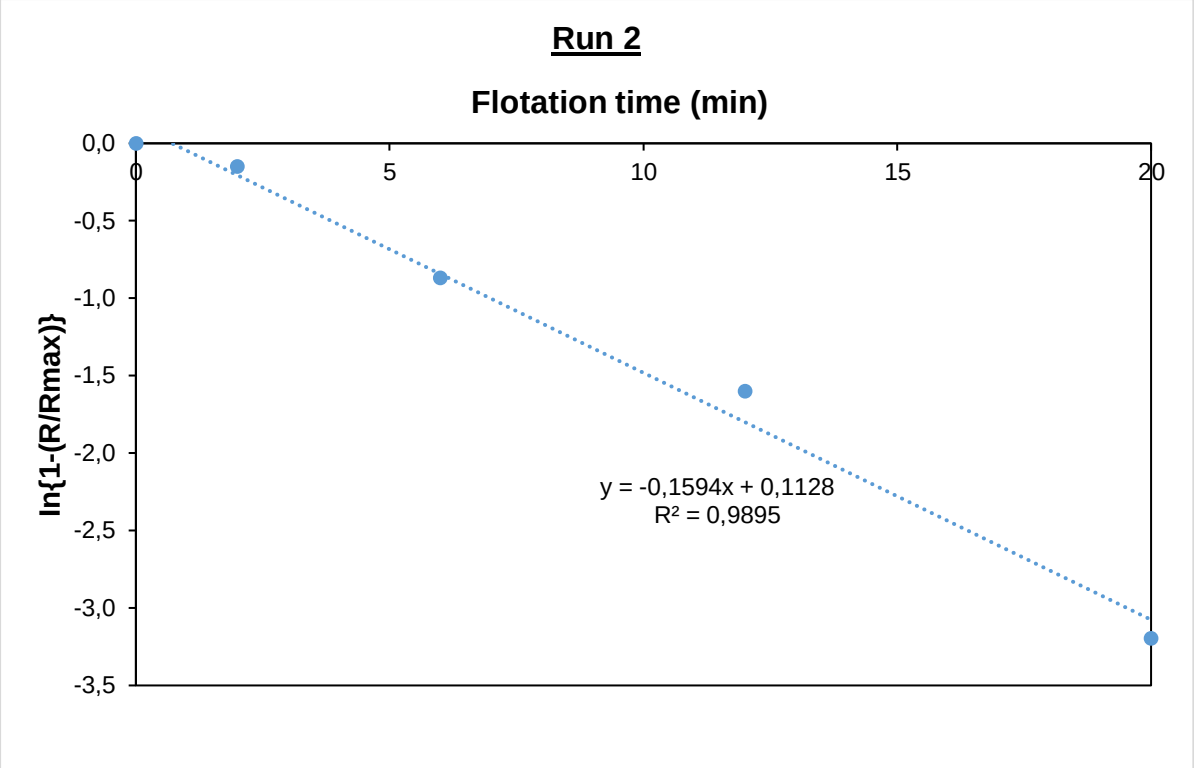

First-order flotation rate constant

Mineral type	Run 1	Run 2	Avg	STD	SE
Talc	0.1457	0.1594	0.1526	0.0097	0.0067

APPENDIX G: The Lambert-beer linearity plot and spectrogram for SIBX adsorption onto galena.